LIÈGE université
Gembloux
Agro-Bío Tech

Université de Lille

Evaluating inulin and chicory-induced gut health outcomes in weaning piglets via *in vivo* and complex *in vitro* models

Tushar Kulkarni

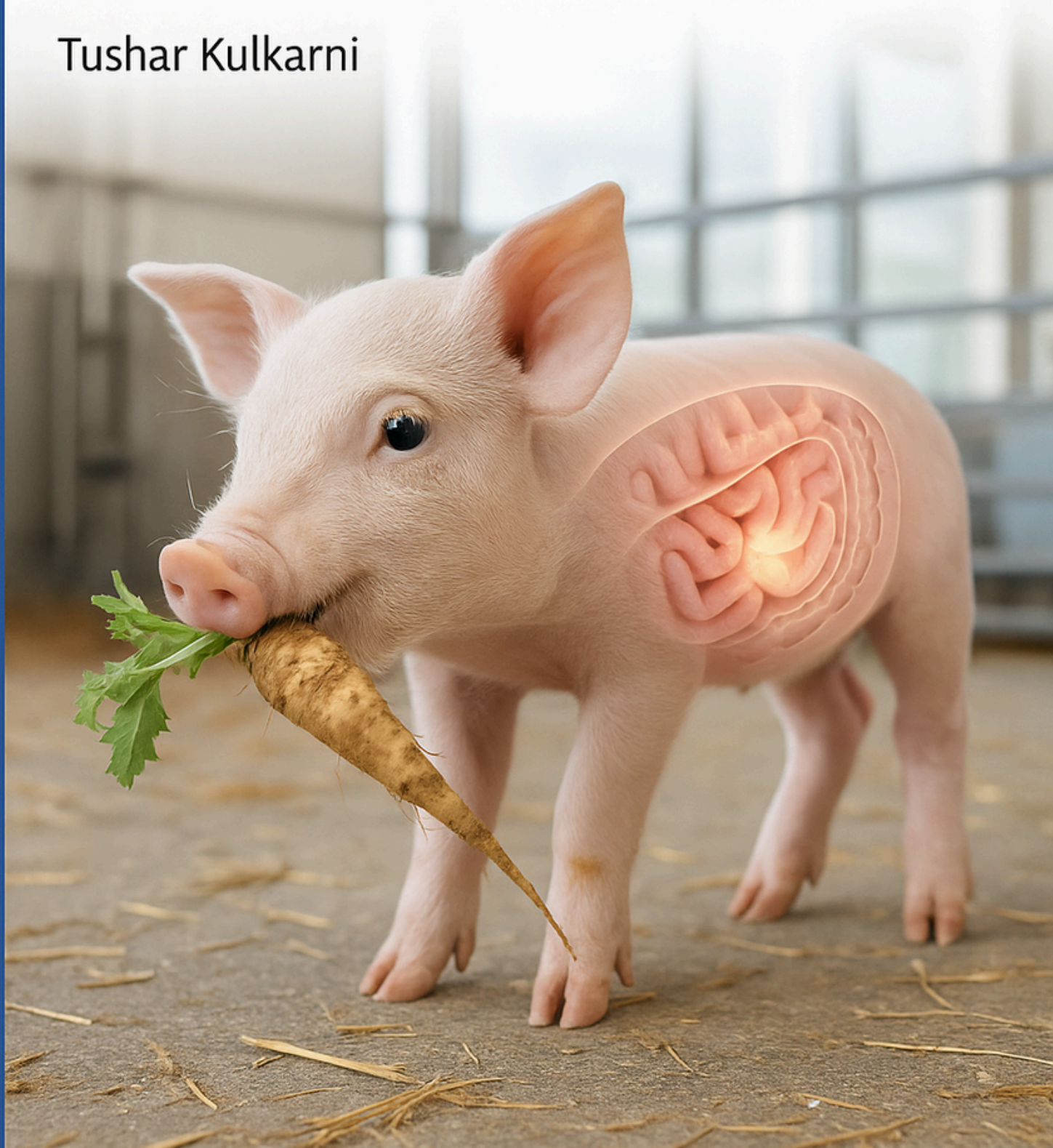

UNIVERSITÉ DE LILLE – SCIENCES ET TECHNOLOGIES
École Doctorale Sciences de la Matière, du Rayonnement, et de l'Environnement, FRANCE

AND

COMMUNAUTÉ FRANÇAISE DE BELGIQUE
UNIVERSITÉ DE LIÈGE – GEMBLOUX AGRO-BIO TECH, BELGIUM

Cotutelle Doctoral Thesis

Evaluating inulin and chicory-induced gut health outcomes in weaning piglets via *in vivo* and complex *in vitro* models

(Évaluation des effets de l'Inuline et de la Chicorée sur la santé intestinale de porcelets en sevrage par l'utilisation de modèles *in vivo* et *in vitro*)

Thèse préparée et soutenue publiquement par

Tushar Sanjay KULKARNI

12/05/2025

Pour obtenir le grade de docteur en sciences agronomiques et ingénierie biologique (ULiège) & biotechnologies agroalimentaires, sciences de l'aliment, physiologie (ULille)

UMR-T 1158, BioEcoAgro

President: Prof. Laurent DUBUQUOY
Composition of Jury:
Prof. Muriel THOMAS (Reporter; INRAE, France)
Prof. Claude KNAUF (Reporter; INSERM Université Paul Sabatier, France)
Prof. Laurent DUBUQUOY (Member; University of Lille France)
Prof. Jeroen DEGROOTE (Member; University of Ghent, Belgium)
Prof. Jérôme BINDELLE (Member; University of Liège, Belgium)
Prof. Kristin VERBEKE (Member; K U Leuven, Belgium)
Prof. Rozenn RAVALLEC (Promoter; University of Lille, France)
Prof. Martine SCHROYEN (Promoter; University of Liège, Belgium)

This thesis was co-promoted by:

Prof. Nadia EVERAERT

K U Leuven, Belgium.

Copyright

Abstract

The gastrointestinal (GI) tract is essential for nutrient absorption and serves as a barrier against harmful substances. However, weaning often disrupts this balance in piglets, leading to intestinal permeability, dysbiosis, and inflammation. Inulin, a prebiotic extracted from *Cichorium intybus*, promotes gut health but is costly to extract and during extraction bioactive compounds like polyphenols and sesquiterpene lactones are lost. To address these challenges, this study first aimed to compare the effects of purified inulin and crude chicory flour on intestinal permeability, inflammation, and microbiota in weaning piglets **(Chapter 3)**. Additionally, the study sought to develop advanced *in vitro* methods combining digestion, absorption, fermentation, and a triple cell culture model **(Chapter 4 & 5)** to evaluate the effects of these bioactives under physiologically relevant conditions.

Two sequential dose-dependent experiments (E1 and E2) were conducted, each involving 80 castrated male piglets weaned at 21 days of age and allocated to three groups with *ad libitum* feed: control (Ctrl), inulin (INU), and crude chicory flour (CHI). In E1, CHI exhibited a lower average daily calorie intake only at week 3 (W3), whereas in E2, it consistently remained lower than Ctrl and INU throughout the study. In E2, CHI supplementation resulted in an improved villus-to-crypt ratio and reduced diarrhoea incidence compared to Ctrl and INU. Both supplemented groups in E2 demonstrated higher butyrate production and reduced D-xylose permeability at W3 relative to Ctrl. Notably, CHI in E2 showed a greater impact on increasing the abundance of health-promoting genera such as *Catenisphaera* and *Butyricicoccus* while reducing harmful genera like *Erysipelotrichaceae_UCG-002* and *Turicibacter*. At W3, CHI and INU downregulated several inflammatory target genes (*CXCL10*, *IL18*, *TNFα*) and signalling pathway genes (*MyD88*, *NFκB1*) in the ileum. In the colon, both CHI and INU reduced the expression of inflammatory signalling and target genes (*NFκB1*, *DEFβ4A*, *TLR2*, and *IFNα*), highlighting their anti-inflammatory effects. These findings suggest that crude chicory flour, which is approximately three times less expensive than extracted inulin, may serve as a cost-effective alternative supplement to enhance gut health in weaned piglets.

To address ethical and economic concerns of *in vivo* research, an innovative *in vitro* approach was developed using digestion-dialysis-fermentation protocols and a triple cell culture model comprising Caco-2 (epithelial), HT-29-MTX (goblet), and U937 (immune) cells. To create a more comprehensive model, human cell lines were used, due to similarities between human and piglet GI physiology. The experiment had 5 groups: Inulin equated (Inu eq.), Chicory equated (Chi eq.), Feed (F), Feed+2% Chicory (F2C), Feed+2% Inulin (F2I). After digestion and 24-hour (h) dialysis, samples were fermented using a weaned piglet faeces inoculum. Gas volume was measured for 48 h, and fermentation broth (FB) collected at 12 h. Differentiated Caco-2/HT-29-MTX in the apical part were pre-treated with LPS (-ctrl), 6 hr prior to, and during incubation with FB from 12 h timepoint for 24 h. Cytokine levels were analysed in the basolateral media with differentiated U937 (macrophages), gene expression was measured in the apical cells, and permeability was assessed by Lucifer Yellow after 24 h of treatment. Inu eq. produced more gas and short chain fatty acids (SCFA) than Chi eq. while F2C had higher levels of butyrate than F2I. Chi eq. and F2C showed a higher α-diversity than Inu eq. and F2I. Compared to Inu eq., Chi eq. increased the abundance of beneficial microbiota such as *Lactobacillus*, *Bifidobacterium*, *Butyricicoccus* & *Ruminococcus.* After 24 h exposure of LPS and fermentation

supernatant, Inu eq. and Chi eq. downregulated pro-inflammatory cytokines IL1β, IL8, and TNFα (4-8-fold) as well as *MAPK14*, *MyD88*, and *AKT1* genes. Interestingly, F2C showed a more significant effect than F2I. Chi eq. had a 3-fold increase in *MUC2*, while Inu eq. upregulated *JAMB* expression. F2I had a higher permeability than F2C. In conclusion, cost-effective Chi eq. and F2C showed greater benefits in enhancing gut health.

Additionally, the study highlighted the critical impact of digestion and dialysis on fermentation outcomes. Digested-dialyzed (DD) samples displayed significantly altered fermentation patterns, including increased butyrate production, improved microbial diversity, and reduced substrates favouring opportunistic microbes compared to non-digested samples.

In conclusion, crude chicory flour, enriched with bioactives, demonstrated either similar or superior effects over inulin in improving gut health, offering a cost-effective and sustainable dietary supplement for weaning piglets. The integration of *in vitro* digestion, fermentation, and cell culture techniques provides a robust platform for studying bioactives' effects, bridging the gap between *in vivo* and *in vitro* approaches while addressing ethical and economic challenges in research.

Keywords: Weaning, chicory, inulin, inflammation, microbiota, permeability.

Resumé

Le tractus gastro-intestinal (GI) est essentiel pour l'absorption des nutriments et sert de barrière contre les substances nocives. Cependant, le sevrage perturbe souvent cet équilibre chez les porcelets, entraînant une perméabilité intestinale, une dysbiose et une inflammation. L'inuline, un prébiotique extrait de *Cichorium intybus*, favourise la santé intestinale, mais sa production est coûteuse et l'extraction entraîne la perte de composés bioactifs tels que les polyphénols et les lactones sesquiterpéniques. Pour relever ces défis, cette étude visait tout d'abord à comparer les effets de l'inuline purifiée et de la farine de chicorée brute sur la perméabilité intestinale, l'inflammation et le microbiote chez des porcelets en cours de sevrage **(Chapter 3)**. En outre, l'étude a cherché à développer des méthodes *in vitro* avancées combinant la digestion, l'absorption, la fermentation et un modèle de culture cellulaire triple **(Chapter 4 & 5)** afin d'évaluer les effets de ces bioactifs dans des conditions physiologiques pertinentes.

Deux expériences séquentielles dose-dépendantes (E1 et E2) ont été menées, chacune impliquant 80 porcelets mâles castrés sevrés à l'âge de 21 jours et répartis en trois groupes avec une alimentation *ad libitum* : contrôle (Ctrl), inuline (INU) et farine de chicorée brute (CHI). Dans le groupe E1, l'apport calorique quotidien moyen de la CHI n'a diminué qu'à la semaine 3 (W3), alors que dans le groupe E2, il est resté inférieur à celui du groupe Ctrl et de l'INU pendant toute la durée de l'étude. Dans l'étude E2, la supplémentation en CHI a permis d'améliorer le rapport villosités/cryptes et de réduire l'incidence de la diarrhée par rapport au Ctrl et à l'INU. Les deux groupes supplémentés en E2 ont montré une production plus élevée de butyrate et une réduction de la perméabilité au D-xylose à W3 par rapport au Ctrl. Notamment, CHI dans E2 a montré un impact plus important sur l'augmentation de l'abondance des genres favourables à la santé tels que *Catenisphaera* et *Butyricicoccus* tout en réduisant les genres nuisibles tels que *Erysipelotrichaceae_UCG-002* et *Turicibacter*. A W3, CHI et INU ont régulé à la baisse plusieurs gènes cibles inflammatoires (CXCL10, IL18, TNFα) et des gènes de signalisation (*MyD88, NFκB1*) dans l'iléon. Ces résultats suggèrent que la farine de chicorée brute peut servir de complément alternatif rentable pour améliorer la santé intestinale des porcelets sevrés.

Pour répondre aux préoccupations éthiques et économiques de la recherche *in vivo*, une approche *in vitro* innovante a été développée en utilisant des protocoles de digestion-dialyse-fermentation et un modèle de culture cellulaire triple comprenant des cellules Caco-2 (épithéliales), HT-29-MTX (gobelet) et U937 (immunitaires). Pour créer un modèle plus complet, des lignées cellulaires humaines ont été utilisées, en raison des similitudes entre la physiologie gastro-intestinale de l'homme et celle du porc. L'expérience comprenait 5 groupes Inulin equated (Inu eq.), Chicory equated (Chi eq.), Feed (F), Feed+2% Chicory (F2C), Feed+2% Inulin (F2I). Après digestion et dialyse de 24 h, les échantillons ont été fermentés en utilisant un inoculum de fèces de porcelets sevrés. Les Caco2/HT-29-MTX différenciés dans la partie apicale ont été prétraités avec du LPS (-ctrl), 6 heures avant, et pendant l'incubation avec 12 heures de FB pendant 24 heures. Inu eq. a induit la production de plus de gaz et d'acides gras à chaîne courte que Chi eq. mais F2C a permis d'obtenir des niveaux plus élevés de butyrate qu'avec F2I. Les fermentations obtenues avec Chi eq. et F2C ont montré une plus grande diversité α que Inu eq. et F2I. Par rapport à Inu eq., Chi eq. a augmenté l'abondance d'un microbiote bénéfique tel que *Lactobacillus*, *Bifidobacterium*, *Butyricicoccus* et *Ruminococcus*. Après une

exposition de 24 heures au LPS et au surnageant de fermentation, Inu eq. et Chi eq. ont régulé à la baisse les cytokines pro-inflammatoires IL1β, IL8, TNFα et les gènes *MAPK14, MyD88, AKT1*. Il est intéressant de noter que F2C a montré un effet plus significatif que F2I. Chi eq. a multiplié par 3 l'expression de MUC2, tandis que Inu eq. a augmenté l'expression de JAMB. La perméabilité cellulaire dans la condition F2I était plus élevée que celle avec F2C. En conclusion, Chi eq. et F2C se sont révélés plus bénéfiques pour la santé intestinale. En outre, l'étude a mis en évidence l'impact de la digestion et de la dialyse sur les résultats de la fermentation. Les échantillons digérés-dialysés (DD) ont présenté des schémas de fermentation significativement modifiés, notamment une production accrue de butyrate, une diversité microbienne améliorée et une réduction des substrats favourisant les microbes opportunistes par rapport aux échantillons non digérés.

En conclusion, la farine de chicorée brute, enrichie en bioactifs, a démontré une efficacité supérieure à celle de l'inuline dans l'amélioration de la santé intestinale, offrant un complément alimentaire rentable et durable pour les porcelets en cours de sevrage. L'intégration des techniques de digestion *in vitro*, de fermentation et de culture cellulaire fournit une plateforme solide pour étudier les effets des bioactifs, comblant ainsi le fossé entre les approches *in vivo* et *in vitro* tout en répondant aux défis éthiques et économiques de la recherche.

Mots-clés: Sevrage, chicorée, inuline, inflammation, microbiote, perméabilité.

Acknowledgements

The journey of completing this PhD has been both challenging and rewarding, and I feel incredibly fortunate to have had the support of so many wonderful people along the way.I would like to express my heartfelt gratitude to **Rozenn Ravallec**, my thesis promoter from the University of Lille, and **Martine Schroyen** from the University of Liège. Rozenn, your unwavering support and belief in my abilities made this journey not only possible but profoundly enriching. Martine, your constant guidance, kindness, and expertise have been invaluable at every stage of this PhD but more specifically during *in vivo* experimental work.

You both allowed me to take ownership of this research and the freedom you gave me to steer its course have been truly transformative, instilling in me a sense of confidence and independence that I will carry forward in my career.

I am deeply grateful to **Nadia Everaert**, my co-promoter, for her insightful suggestions and constructive feedback, which played a pivotal role in shaping this work. Nadia, your initiative in conceptualizing and building this fascinating project deserves special thanks, as it laid the foundation for what was accomplished. A special thanks to **Benoit Cudennec,** whose guidance and *'instant problem-solving skills'* were a lifeline whenever I found myself stuck. Benoit, your patience, and ability to simplify the complex gave me the clarity I needed at time and again.

I owe immense gratitude to **Sylvie Mabile,** our exceptional lab technician, for her invaluable assistance in the lab and during animal experiments. Sylvie, your dedication, especially in completing the analysis while I was in India for a medical emergency, is something I will always be profoundly thankful for. I am equally grateful to **Pawel Siegen** and **Pauline Lemal** for their readiness to step in and assist during animal experiments, often at inconvenient hours. I thank you for your commitment, generosity, and teamwork.

To my labmates at the University of Lille — **Allane, Pauline, Sandy, Camille**, **Hairati, Elodie** and **Morgan** — thank you for creating such a supportive and enjoyable environment. Each of you contributed in your own unique way, making the lab a place I looked forward to being every day. A special mention goes to **Melissa,** whose consistent readiness to lend a hand or an ear whenever I needed it was a source of great comfort. A sincere thanks to Jimmy Vandel for his expertise in statistical integration. Jimmy, your support added depth and precision to my research, and I am grateful for your patience and collaboration.

I would also like to acknowledge the members of my thesis committee, who guided me year after year with their thoughtful advice and constructive feedback. Your guidance was crucial in shaping this work and keeping it on the right track. Last but by no means least, to my family and friends: thank you for your unwavering support, encouragement, and belief in me. You were my source of strength during tough times, and your faith in my abilities gave me the courage to keep going. To everyone, thank you from the bottom of my heart. This PhD would not have been possible without your support, and I am forever grateful. Thanks!

Contents

List of Figures

List of Tables

List of Abbreviations

A: Maximum Gas Volume
ACTB: Actin B-
AJ: Adherent Junctions
ADCI: Average Daily Calorie Intake
ADF: Acid Detergent Fibre
ADFI: Average Daily Feed Intake
ADG: Average Daily Gain
AGDS: Artificial gastric digestive system
AKT1: A- d serine/threonine-protein kinases
AMP: Antimicrobial Peptide
ANOVA: Analysis of variance
ARCOL: Artificial Colon
ASV: Amplicon Sequence Variant
ATCC: American Type Culture Collection
ATP: Adenosine Triphosphate
BCFA: Branch Chain Fatty Acid
BMI: Body mass index
CASP: Caspase
CCK-8: Cell Counting Kit-8
CCK: Cholecystokinin
CGA: Chlorogenic Acid
CHO: Carbohydrate
CL: Chloride
CLDN: Claudin
COX2: Cyclooxygenase 2
CRF: Corticotropin-Releasing Factor
DAPI: 4',6-Diamidino-2-Phenylindole
DC: Dendritic Cells
DCQA: Dicaffeoylquinic Acids
DEFβ: Defensin B-
DGM: Dynamic Gastric Model
DGSM: Dynamic Gastric Simulation Model
D/I: Dexamethasone/Indomethacin
DIVHS: Near real dynamic *in vitro* human stomach system
DMEM: Dulbecco's Modified Eagle's Medium
DM: Dry Matter
DNA: Deoxyribonucleic Acid
DP: Degree of Polymerization
DP_n: Average number degree of polymerization
DP_w: Average weight degree of polymerization
EDTA: Ethylenediaminetetraacetic Acid
EFSA: European Food Safety Authority
ELISA: Enzyme-Linked Immunosorbent Assay
ETEC: Enterotoxigenic *E. coli*
ESIN: Engineered Stomach and Small Intestinal
EU: European Union
FA: Fatty Acids
FBS: Fetal Bovine Serum
FCR: Feed Conversion Ratio
FOS: FructoOligoSaccharides
FWER: Family Wise Error Rate
GALT: Gut-Associated Lymphoid Tissue
GAPDH: Glyceraldehyde-3-Phosphate Dehydrogenase
GC: Gas Chromatography
GDS: Gastric Digestion Stimulator
GIT: Gastrointestinal Tract
GLM: General Linear Model
GLP: Glucagon like Peptide
GM: Genetically Modified
GM-CSF: Granulocyte-macrophage colony-stimulating factor
GOS: Galactooligosaccharides
GPR43: G protein coupled receptor 43
HCl: Hydrochloric Acid
HCO_3: Bicarbonate
HGS: Human Gastric Stimulator
HMVEC-d: Human Microvascular Endothelial Cells
HPLC: High performance Liquid Chromatography
HPRT1: Hypoxanthine Phosphoribosyltransferase
HPSEC: High Performance Size-Exclusion Liquid Chromatography
IFN: Interferon
IgA: Immunoglobulin A
IgG: Immunoglobulin G
IHGS: Improved Human Gastric Simulator
Ikkβ: Inhibitor of Nuclear Factor Kappa-B Kinase B-
IL: Interleukin
ILRN1: Interleukin-1 Receptor Antagonist
JAM: Junctional Adhesion Molecule
kDa: KiloDalton

LAB: Lactic Acid bacteria

LBP: Lipopolysaccharide Binding Protein

LC-MS: Liquid Chromatography-Mass Spectrometry

LPS: Lipopolysaccharide

LY: Lucifer yellow

MAPK14: Mitogen-Activated Protein Kinase 14

MCQA: Monocaffeoyllquinic acids

M_n: Number-Average Molecular Weight

MCT1: Monocarboxylate Transporter

M cells: Microfold Cells

MLCK: Myosin Light Chain Kinase

mRNA: Messenger Ribonucleic Acid

MTX: Methotrexate

MUC: Mucin

M_w: Weight-Average Molecular Weight

MyD88: Myeloid Differentiation Primary Response 88

NADH: Nicotinamide adenine dinucleotide

NCBI: National Centre for Biotechnology Information

NDF: Neutral Detergent Fibre

NFκB: Nuclear Factor-Kappa B

NLR: Nucleotide-Binding Oligomerisation Domain-Like Receptor

NO: Nitric Oxide

NOD1: Nucleotide-Binding Oligomerisation Domain-Containing Protein 1

P_{app}: Apparent Permeability

PBMC: Peripherial Blood Mononuclear Cells

PBS: Phosphate Buffer Saline

PCA: Principal Component Analysis

PCR: Polymerase Chin Reaction

PMA: Phorbol 12-myristate 13-acetate

POS: Pectin Oligo Saccharides

PP: Peyer's Patches

PPARγ: Peroxisome Proliferator-Activated Receptor Gamma

PPIA: Peptidylprolyl Isomerase A

PPM: Parts Per Million

PWD: Post-weaning Diarrhoea

qPCR: Quantitative PCR

QIIME: Quantitative Insights into Microbial Ecology

RGCCA: Regularized Generalized Canonical Correlation Analysis

R_{max}: Maximum Rate of Gas Production

RNA: Ribonucleic Acid

RPMI: Roswell Park Memorial Institute

ROS: Reactive Oxygen Species

RS: Resistant Starch

RT: Real Time

SCFA: Short Chain Fatty Acid

SHIME: Simulator of the Human Intestinal Microbial Ecosystem

SPIME: Simulator of the Porcine Intestinal Microbial Ecosystem

SDS: Sodium Dodecyl Sulphate

SEM: Standard Error of the Mean

SPF: Specific Pathogen Free

STL: Sesquiterpene Lactones

TEER: Transepithelial Electrical Resistance

TGF: Transforming Growth Factor

TJ: Tight juctions

TNFα: Tumour Necrosis Factor-A-

T_{reg}: Regulatory T Cell

TLR: Toll Like Receptor

VFA: Volatile Fatty Acid

V:C: Villus: Crypt Ratio

WHO: World Health Organization

YWHAZ: Tyrosine 3-Monooxygenase/Tryptophan 5-Monooxygenase Activation Protein Zeta

ZnO: Zinc Oxide

ZO: Zonula Occlude

1

State of the Art

Weaning represents a pivotal transition in the life of a piglet, marked by the shift from a milk-based diet to solid feed. This abrupt dietary change often induces nutritional stress, resulting in reduced feed intake and subsequent weight loss. Moreover, weaning is commonly associated with digestive disturbances, including diarrhoea, which further compromise the piglet's health and growth performance (Moeser *et al.,* 2017a). The GI tract plays a central role in maintaining overall health, functioning as a sophisticated defence system. This system is comprised of the intestinal epithelium (mechanical barrier), antimicrobial peptides, mucus layer (physical and chemical barrier), immune cells (immune barrier), and a diverse community of commensal bacteria (microbial barrier) (Tang *et al.,* 2022; Zihni *et al.,* 2016). The delicate interplay between epithelial cells, immune cells within the lamina propria, and the microbiota is critical for sustaining mucosal integrity. Disruption of this balance can result in a "leaky gut," allowing harmful substances to translocate into the bloodstream. This phenomenon can provoke systemic immune responses, potentially contributing to the development of inflammation (Bischoff *et al.,* 2014; Mu *et al.,* 2017a). Given the GI tract's essential role in health and its susceptibility to disruption during weaning, an in-depth review of the digestive physiology of weaning piglets is presented in **Section 1.1.** This review aims to provide a foundation for understanding these challenges and guiding the development of sustainable, evidence-based solutions.

For over five decades, antibiotics and heavy metals, particularly zinc oxide, have been extensively used during the weaning period to mitigate health and growth challenges in piglets. However, new EU regulations (Regulations (EU) 2019/6 and 2022/4) restrict the use of in-feed antibiotics and limit therapeutic zinc oxide to 150 ppm. These changes highlight the urgent need for alternative strategies, with a growing focus on the potential of bioactive molecules derived from plant sources. Prebiotics have demonstrated positive effects on gut homeostasis and intestinal health. Among these, inulin—a widely studied prebiotic commonly extracted from chicory roots—has shown promising benefits in promoting gut integrity. Chicory, beyond being a source of inulin, contains a diverse array of bioactive compounds, known for their antioxidant and anti-inflammatory properties (Pouille *et al.,* 2022a). Consequently, **Section 1.2** of this chapter delves into the bioactives previously studied for gut health in weaning piglets, with a particular emphasis on the composition of chicory and its documented effects on inflammation and gut integrity.

In 2019, approximately 82,819 pigs were used for research purposes within the EU (European Animal Research Association, 2024). However, the use of laboratory animals has been increasingly questioned due to ethical considerations, rising costs, and scientific limitations. This highlights the necessity of developing alternative *in vitro* methods that can accurately mimic *in vivo* environments, particularly GI tract, to reduce and eventually replace animal experimentation. Numerous *in vitro* techniques have been developed to study intestinal functions, including models focusing on digestion, fermentation, gut integrity, and cellular responses. While each method comes with unique advantages, none are without limitations. Importantly, systematic comparisons of *in vitro* models with *in vivo* results remain scarce, leaving significant room for improvement in their predictive accuracy. To address this, **Section 1.3** of this chapter reviews the existing literature on *in vitro* GI tract models, highlighting their current applications, limitations, and the scope for refinement to bridge the gap between *in vitro* and *in vivo* studies.

1.1. GI physiology and functionality during weaning

The GI barrier is a dynamic, multilayered system that protects the host from harmful substances while allowing nutrient absorption. Comprising structural, chemical, microbial, and immune components, it plays a vital role in maintaining gut homeostasis. However, during weaning, piglets experience profound physiological, environmental, and dietary changes that disrupt these barriers, increasing their susceptibility to infections, malabsorption, and inflammation.

1.1.1. Structural and Chemical Adaptations

1.1.1.1. Anatomy and morphological changes

The GI tract, a complex and highly specialized system extending from the mouth to the intestines, plays a pivotal role in digestion, nutrient absorption, and defence. Within this system, the stomach serves as a critical organ for both protective and digestive functions. During weaning, however, its physiology undergoes significant changes that compromise its ability to maintain these roles. In pre-weaning piglets, lactic acid produced from the fermentation of lactose by lactic acid bacteria plays a crucial role in lowering gastric pH; however, post weaning a reduction in lactic acid production leads to elevated stomach pH, which compromises gastric acid secretion, impairs protein digestion and enzyme activation, and increases the risk of gastrointestinal infections (Heo *et al.,* 2013). Furthermore, gastric motility slows, and reduced emptying rates contribute to bacterial overgrowth and post-weaning diarrhoea. Sudden dietary shifts, such as the transition from a milk-based to a wheat-based diet, further disrupt stomach function by temporarily altering gastric emptying (Guérin, *et al.,* 2004; Snoeck *et al.,* 2004). These changes extend beyond the stomach to also influence the overall pH of the intestinal digesta, a key indicator of intestinal health and microbial activity. Maintaining an optimal pH becomes increasingly difficult during weaning due to reduced hydrochloric acid production, dietary modifications, and environmental stressors, thereby exacerbating the risk of post-weaning complications (Heo *et al.,* 2013; Nyachoti *et al.,* 2006; Partanen and Mroz, 1999).

The small intestine in piglets is a highly specialized organ divided into duodenum, jejunum, and ileum. In adult pigs, these regions constitute approximately 4–4.5%, 88–91%, and 4–5% of the small intestine, respectively, with similar proportions observed in newborns despite less distinct boundaries between the jejunum and ileum (Pluske *et al.,* 2018a). Structurally, the small intestine comprises four layers: the tunica serosa, tunica muscularis, tunica submucosa, and tunica mucosa. The tunica serosa is the outermost layer, consisting of connective tissue housing blood vessels and nerves, and is involved in forming the mesentery. The tunica muscularis features two layers of muscle fibers which facilitate GI motility. The tunica submucosa contains connective tissue, blood and lymphatic vessels, and nerves, with the duodenum uniquely possessing Brunner's glands. These glands secrete alkaline mucus rich in bicarbonate to neutralize stomach acid and activate intestinal enzymes (Modina *et al.,* 2021). This contributes to buffering and pH regulation, primarily through the secretion of HCO_3^- ions by the crypt epithelium. Additionally, the secretion of Cl^- plays a role in maintaining fluid balance and, together with bicarbonate, supports mucosal hydration and the flushing of pathogens during stress or infection (Moeser and Blikslager, 2007).

The **tunica mucosa**, the innermost layer, consists of:

1. **Muscularis mucosa**, a thin muscle layer that forms transient intestinal folds.
2. **Lamina propria**, connective tissue with blood vessels, neurons, lymphocytes, and Peyer's patches (in the ileum), supporting the epithelial layer.
3. **Epithelium**, a single-cell layer forming the luminal surface of the intestine.

The mucosa forms finger-like projections called villi **(Figure 1)**, significantly increasing the surface area for absorption and digestion. Each villus is covered with microvilli, which further amplify the absorptive capacity by 15–40 times and are coated with a glycocalyx layer containing digestive enzymes (Sumigray *et al.,* 2018). At the base of the villi are structures called crypts, tubular glands that open into the intestinal lumen and serve as regions of active cell proliferation. In mammals, cell division and renewal within the small intestine are confined to the crypts at the base of the villi (Cheng and Leblond, 1974). While the villi are primarily composed of mature enterocytes, goblet cells, and enteroendocrine cells, the crypts function as reservoirs for stem cells, undifferentiated proliferative cells, and specific secretory cells such as Paneth cells, which play a critical role in maintaining gut health. Paneth cells near the crypt base contribute to gut immunity by secreting antimicrobial substances such as lysozymes and defensins (van der Hee *et al.,* 2018; Verdile *et al.,* 2019).

Villus morphology and crypt depth vary along the intestinal tract, reflecting functional adaptations, such as longer villi in the mid-jejunum for maximal nutrient absorption. The intestinal tract is a continuously regenerating tissue, with its structural and functional stability hinging on a finely tuned equilibrium between the proliferation of mucosal epithelial cells and their programmed apoptosis (Cai *et al.,* 2016; Tang *et al.,* 2022; Tang and Xiong, 2022). The epithelial layer consists of a single layer of intestinal epithelial cells, including absorptive enterocytes, mucus-producing goblet cells, enteroendocrine cells Intraepithelial Lymphocytes (IEL), and antimicrobial paneth cells located at the crypt base.

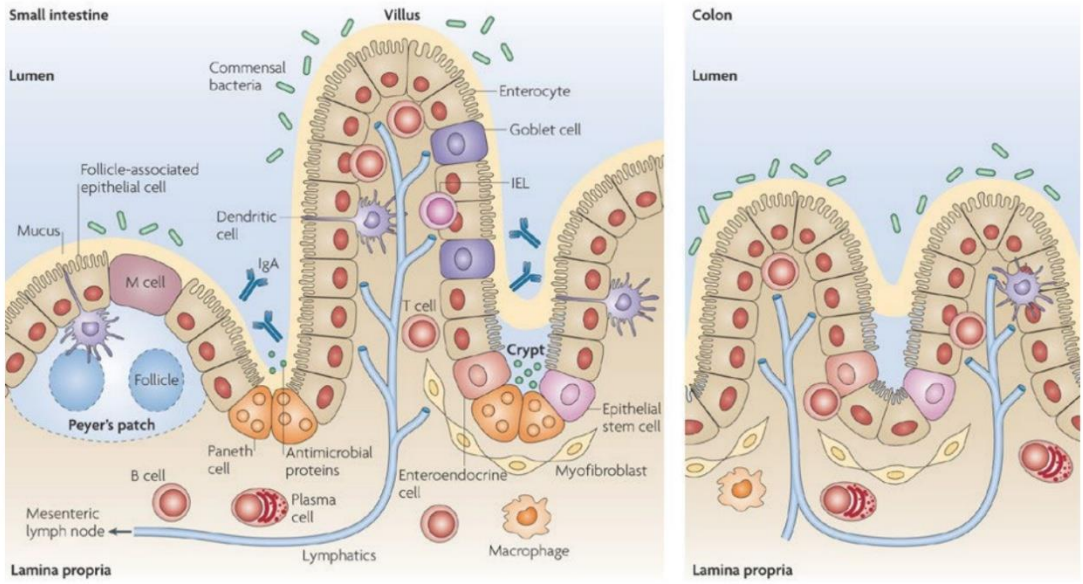

Figure 1. Schematic representation of intestinal epithelium cells and their localisation (Adapted from Abreu *et al.,* 2010)

The mechanical barrier is composed of a monolayer, that acts as the primary interface between the host and the external environment. Cell types within the villi include:

- **Enterocytes** (90-94%), responsible for nutrient absorption. Enterocytes mature as they migrate from the crypt base to the villus tip. Their enzymatic activity, reflecting digestive functions, begins in the basal third of the villus axis. Absorption begins at the mid to upper villus and peaks at the tip, where enterocytes are fully mature. These cells are continuously renewed, maintaining the villus's functional integrity through ongoing cellular turnover. (Zhu *et al.,* 2021).

- **Goblet cells** (5-8%), secreting mucus to protect the epithelium. Goblet cells, located between enterocytes, are specialized for secreting viscous mucus. Their number increases progressively from the proximal jejunum to the distal ileum, enhancing mucus production and contributing to the protective barrier and lubrication of the intestinal lining. The main constituents of intestinal mucus are mucins, which are high molecular weight glycosylated proteins that are mostly produced by goblet cells (Birchenough *et al.,* 2015; Paone and Cani, 2020; Sicard *et al.,* 2017). As the initial line of defence, this mucus layer keeps intestinal homeostasis intact by shielding intestinal epithelial cells from infections and preventing their colonization (Kim and Ho, 2010). Based on their structure and location, mucins are divided into two categories: membrane-bound mucins (e.g., MUC1, MUC3, MUC4, MUC13, MUC17) and gel-forming secretory mucins (e.g., MUC2, MUC5, MUC6). The main mucin in intestinal mucus, MUC2, is crucial for intercellular communication, lubrication, and pathogen protection (Ma *et al.,* 2018; Sharpe *et al.,* 2018; Tang *et al.,* 2022).

- **Enteroendocrine cells** (1%), located along the villi, secrete various gut hormones such as GLP-1 and CCK that not only regulate gastrointestinal motility and secretion but also play a key role in appetite regulation via the gut-brain axis (Gribble and Reimann, 2019; Crooks *et al.,* 2021).

This structural complexity underscores the small intestine's critical role in digestion, nutrient absorption, and maintaining gut health. To further add to this complexity, monolayer of cells is connected further by the apical junctional complex, which contains tight junctions (TJs), adherens junctions (AJs), and desmosomes **(Figure 2).** This structure preserves cellular polarity, limits intercellular space, and selectively permits nutrition absorption while preventing pathogen and toxin penetration (Catalioto *et al.,* 2011; Tang *et al.,* 2022; Usuda *et al.,* 2021). TJs, which are predominantly made up of transmembrane proteins such as Claudin, Occludin, and JAM-A, as well as cytoplasmic proteins like ZO-1, ZO-2, and ZO-3, play an important role in regulating intestinal permeability and the mechanical barrier (Cai *et al.,* 2016; Montagne *et al.,* 2007a, 2007b; Turner, 2009; Vancamelbeke and Vermeire, 2017).

Transport across the small intestinal epithelium can be divided into paracellular and transcellular pathways. Paracellular transport occurs between adjacent epithelial cells through tight junctions and allows passive diffusion of water, ions, and small solutes. In contrast, transcellular transport involves the movement of substances through the enterocytes themselves and includes several mechanisms: passive diffusion of lipophilic molecules, facilitated diffusion, and active transport. Facilitated transport, a form of passive transport, relies on specific membrane proteins—such as carrier or channel proteins—to assist the movement of hydrophilic molecules like glucose, amino acids, and ions along their concentration gradient, without requiring energy. Key transporters involved include sodium-glucose linked transporter 1 (SGLT1) and glucose transporter 2 (GLUT2). Active transport, on the other hand, requires ATP to move molecules against their gradient and plays a critical role in nutrient absorption. Together, these tightly regulated pathways ensure selective permeability and maintain intestinal barrier integrity. (Pácha, 2000; Zheng *et al.,* 2021a)

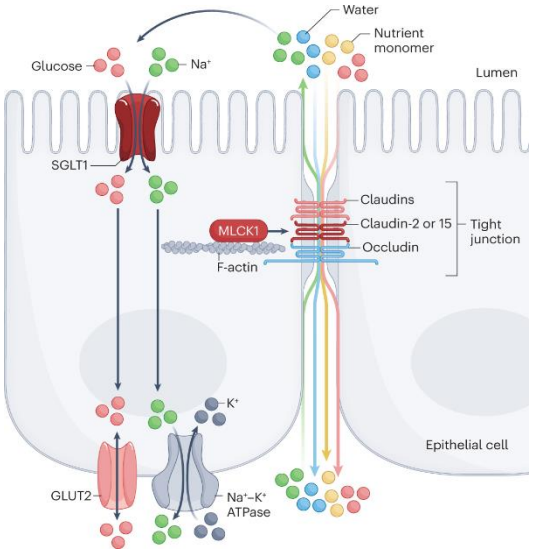

Figure 2. Schematic representation of transcellular and paracellular transport (Adapted from Horowitz *et al.,* 2023).

The figure shows transcellular transport driven by Na+ gradient via SGLT. The tight junction proteins occludin, claudin-2, zonula occludens 1 (ZO-1), and other members of the claudin family mediate the paracellular trafficking between cells. (SGLT1: Sodium-Glucose Linked Transporter 1; GLUT2: Glucose Transporter Type 2; MLCK1: Myosin Light Chain Kinase 1; F-actin: Filamentous Actin

The large intestine, comprising the caecum, colon, and rectum, serves critical roles in fluid and electrolyte absorption and as a physical barrier against microbial invasion. These functions are vital for maintaining gut health, and their disruption can contribute to the pathophysiology of post-weaning diarrhoea (PWD). Unlike the small intestine, the large intestine lacks villi, with its mucosal surface lined by crypts. During the prenatal, neonatal, and weaning phases, the GI tract of piglets' experiences notable morpho-functional changes that are intimately associated with significant changes in the microbial ecology. An outline of these significant alterations and their effects on gut health and function will be given in the sections that follow.

1.1.1.1.1. Preweaning development

The preterm phase, which starts a few weeks prior to birth, is a time of accelerated development for the small intestine. Intestinal villi begin to form in the jejunum by the sixth week of pregnancy, and by the third month, epithelial cells undergo differentiation into enterocytes, goblet cells, and enteroendocrine cells. Large cytoplasmic vacuoles seen in fetal enterocytes are necessary for the digestion and transportation of macromolecules, as well as for the passive transfer of immunity through colostrum. The vacuoles shrink as these fetal cells are replaced by mature enterocytes after birth. Structural changes include crypt formation and differentiation of the muscular tunic by the third month of gestation (Modina *et al.,* 2021; Sangild *et al.,* 2000).

The small intestine develops more quickly in the last stages of pregnancy due to high cellular turnover. The crypts' stem cells develop into specialized cell types such as enterocytes that absorb nutrients, goblet cells that secrete mucus, and enteroendocrine cells that produce hormones. With enterocytes aiding in the absorption of nutrients, goblet cells growing in density toward the ileum to improve mucus production, and enteroendocrine cells regulating GI activity, these cells migrate upward along the villus axis. Fully developed cells are released into the lumen at the villus tip, guaranteeing the intestinal lining's ongoing regeneration (Wong and Wright, 1999).

The intestinal volume rises by around 70% in the last three weeks of pregnancy, mostly due to increased mitotic activity and a decrease in apoptosis **(Figure 3)**. Through continuous renewal, stem cell proliferation in the crypts and enterocyte migration to the villus tips preserve epithelial integrity. To maintain intestinal function, apoptosis makes sure that old or damaged cells are eliminated, and enterocytes have a quick turnover of 48 to 72 h. After birth, the intestine is ready for effective nutrient absorption and immunological function thanks to

autophagy, a lysosome-mediated recycling process that promotes tissue growth and homeostasis (McPherson *et al.,* 2004; Willemen *et al.,* 2013; Darwich *et al.,* 2014; Godlewski *et al.,* 2005; Yen and Wright, 2006).

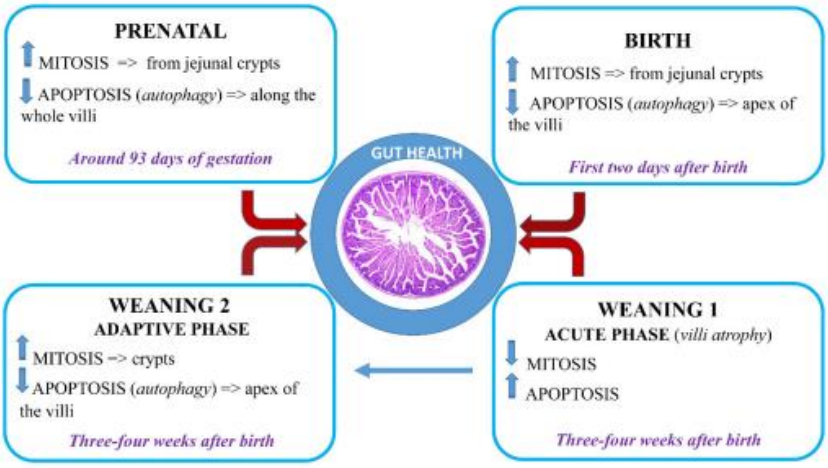

Figure 3. Timing of cellular turnover during gut development: apoptosis and mitosis (Adapted from Modina *et al.,* 2021) The effect of the weaning transition can be divided in to two periods: an acute period (Weaning 1) which takes place immediately after the piglets is taken away from the sow and then followed, after 1 week, by an adaptive and maturational phase (Weaning 2).

The intestinal permeability significantly decreases with the small intestine's subsequent rapid growth and functional maturation following birth (Skrzypek *et al.,* 2005). Within just three days, its weight doubles, and its length increases by around 30%, reflecting the substantial demands of neonatal growth. During this time, structural changes such as lengthened villi, deeper crypts, and a thicker mucosa all contribute to a greatly expanded absorptive surface area, particularly in the duodenum and jejunum (Sangild *et al.,* 2002). This transformation is largely driven by colostrum, an essential early source of bioactive compounds. Colostrum provides both immunological benefits and stimulatory effects on epithelial proliferation in the intestinal crypts, especially in the jejunum. During this time, mitosis peaks, while apoptosis becomes more restricted to the villus tips as cell turnover stabilizes. This balance between cell proliferation and programmed cell death facilitates efficient tissue remodelling and maintenance of the intestinal barrier (Everaert *et al.,* 2017; Modina *et al.,* 2021). Although the precise mechanisms underlying this early postnatal development remain unclear, it is thought to be influenced by genetic programming, microbial colonization, and the initiation of feed intake. Most animals achieve substantial epithelial barrier maturation within the first two to three weeks of life (Mackey *et al.,* 2016; Moeser *et al.,* 2017b).

1.1.1.1.2. Post-weaning changes

Piglets are highly susceptible to weaning stress due to physiological, environmental, and social challenges, which disrupt the balance between proliferation and apoptosis in intestinal mucosal epithelial cells. This results in significant challenges to the intestinal health of piglets, marked by disruptions in barrier function, increased susceptibility to infections and inflammation, compromised digestion, biochemical functions and gut integrity (Souza *et al.,* 2005; Tang *et al.,* 2021; Yan *et al.,* 2018).

Changes in intestinal morphology

The structure of the intestine, reflected in features like villus height, crypt depth, provides essential insights into its overall ability to absorb nutrients effectively. However, several studies have reported the negative effect of weaning on these features **(Table 1).** During weaning, one of the most noticeable changes is the shrinking of the villi, known as villus atrophy, which is often paired with an increase in the size of the crypts as the intestine attempts to compensate. For instance, Bomba *et al.* (Bomba *et al.,* 2014a) reported a significant reduction in villus height and the villus height-to-crypt depth ratio in the ileum of piglets five days post-weaning (33 days of age) compared to pre-weaning levels (28 days of age). Similarly, Hu *et al.* (2013a) observed deterioration in villus height and the villus height-to-crypt depth ratio significantly reduced on days 3 and 7 post-weaning. The villi, which play a crucial role in nutrient absorption, shrink during this period due to an imbalance between cell loss (apoptosis) and cell renewal (mitosis). This shrinkage causes structural damage to the intestine and significantly reduces its ability to absorb nutrients, adding to the challenges faced during this critical stage (Su *et al.,* 2022; Tang *et al.,* 2022; Zhu *et al.,* 2014). These changes are most pronounced in the duodenum, the region of the intestine most exposed to dietary changes (Budiño *et al.,* 2005; Marion *et al.,* 2002). In the jejunal cells of weaned pigs, there is also evidence of an increase of genes linked to apoptosis and a decrease in genes related to proliferation and differentiation (Cai *et al.,* 2016; Wang *et al.,* 2008; Zhu *et al.,* 2014). Insufficient feed intake is known to contribute to villus atrophy in the small intestine (Lalles *et al.,* 2004). Approximately 10% of piglets do not consume feed within the first 48 h after weaning, and those that do show little consumption, according to multiple studies conducted during the weaning process (Brooks *et al.,* 2001; van der Meulen *et al.,* 2010).

Table 1. Morphological changes in the small intestine of weaned piglets (Adapted from Zheng *et al.,* 2021).

Weaning age (day)	Intestinal section	Results
21	Small intestine	Decreased villus height and increased crypt depth during day 11 post-weaning
21 or 35	Jejunum	Decreased villus height during day 3 post-weaning when weaned at 21 or 35 days
14	Small intestine	Decreased villus height to crypt depth ratio at day 7 post-weaning
28	75% of small intestine	Increased crypt depth at day 5 post-weaning
26	Small intestine	Decreased villus height at day 2 and 4, and decreased villus height to crypt depth ratio at day 2 and 4 post-weaning
29	Jejunum	Decreased villus height from day 2 post-weaning, with minimal length observed at day 3 post-weaning and increased crypt depth at day 5 post-weaning
21	Jejunum	Decreased villus height from day 2 post-weaning and increased crypt depth from day 5 post-weaning

The table explains effect of weaning on the morphology irrespective of the weaning age. Focusing on the villus height, crypt depth and its ratio as it can be directly correlated to the absorption capacity and the intestinal health.

The small intestine's villus height can drop by up to 75% within 24 h of weaning as compared to its pre-weaning state, mostly because of decreased crypt cell proliferation and increased epithelial cell loss (Liu *et al.,* 2016). Mature enterocytes, which are essential for effective nutrition absorption, are lost because of this villus

atrophy and decreased crypt cell formation (Hampson, 1986). The intestine's ability to digest and absorb nutrients during the post-weaning phase is further compromised by the shortening of villi, which is also linked to a decrease in the activity of brush-border enzymes like lactase and peptidases as well as a loss in nutrient transporter activities (Tsukahara *et al.,* 2013). These structural and functional alterations underline the significant challenges piglets face in maintaining intestinal health immediately after weaning. However, recovery begins within days, with crypts becoming deeper and mitotic activity increasing to restore the epithelium (Budiño *et al.,* 2005; Marion *et al.,* 2002). Weaning has also been shown to decrease crypt density and increase the mitotic index in the caecum of piglets (Castillo *et al.,* 2007).

Effect on physical barrier

The intestines perform a dual role, acting both as the primary site for nutrient digestion and absorption and as a selective barrier that prevents harmful substances from entering the bloodstream while allowing essential nutrients, electrolytes, and water to pass through (Lallès *et al.,* 2007; Tang *et al.,* 2022). However, the weaning process imposes significant stress on this physical barrier. Studies have shown that weaning in pigs causes a breakdown in intestinal barrier function, evidenced by a marked decline in transepithelial electrical resistance and increased permeability to paracellular probes, as observed in Ussing chamber experiments (Hu *et al.,* 2013c; Moeser and Blikslager, 2007).

Weaning leads to compromised paracellular barrier function, characterized by increased intestinal epithelial permeability (Kim *et al.,* 2019; Zheng *et al.,* 2021; Hu *et al.,* 2013a; Boudry *et al.,* 2004). Research has demonstrated that pigs weaned at 26 days of age exhibit disrupted intestinal barrier integrity, particularly during the first week post-weaning. Fortunately, this disruption typically resolves within two weeks, returning to pre-weaning levels (Montagne *et al.,* 2007; Verdonk *et al.,* 2007). This loss of barrier function is most prominent during the first week post-weaning but typically returns to pre-weaning levels within two weeks. Older weaning age is associated with enhanced barrier function both short- and long-term, likely due to the advanced maturation of the small intestine at weaning (Smith *et al.,* 2010). The loss of intestinal barrier integrity during weaning facilitates the translocation of pathogenic bacteria and allergenic compounds from the intestinal lumen into the body, triggering heightened inflammatory responses (Arrieta, 2006a; Zheng *et al.,* 2021a).

However, following weaning, endocytosis, which transports macromolecules across cells, tends to improve. Notably, in contrast to the proximal and distal jejunum, where nutrient absorption is most crucial, the ileum's paracellular barrier function is mostly intact. This implies that the loss of barrier function in these areas is largely caused by a decreased luminal food supply brought on by poor feed intake. The expression of tight junction proteins is a critical marker for evaluating the integrity of the intestinal mechanical barrier. Weaning has been shown to disrupt these proteins, potentially through the activation of mitogen-activated protein kinase (MAPK) and transforming growth factor-β1 (TGF-β1) signalling pathways (Hu *et al.,* 2013a; Xiao *et al.,* 2014), leading to impaired tight junction structures and increased intestinal permeability.

Evaluating intestinal barrier function and absorption in weaned pigs primarily involves *ex vivo* methods, such as Ussing chambers, and *in vivo* techniques, including sugar marker tests. In Ussing chamber studies, intestinal mucosa is placed between two compartments, with marker probes added to the mucosal side. The movement of these probes to the serosal side reflects the permeability of the intestinal barrier, largely determined by tight junctions between epithelial cells. Changes in transepithelial electrical resistance (TEER) indicate alterations in paracellular permeability: higher TEER suggests reduced permeability, while lower TEER implies increased permeability. This method provides localized measurements but requires tissue samples, necessitating the sacrifice of animals and limiting insights into regional differences along the intestine (Boudry *et al.,* 2004;

Wijtten *et al.,* 2011). In contrast, orally administered sugar markers provide a non-invasive way to evaluate intestinal permeability. Non-metabolized sugars, such as lactulose, L-rhamnose, and mannitol, are absorbed across the intestinal epithelium and detected in the blood or urine. The dual sugar test, a common approach, involves administering a disaccharide like lactulose, which crosses tight junctions, and a monosaccharide such as L-rhamnose or mannitol, which diffuses *via* aqueous pores or tight junctions. The ratio of these sugars in urine reflects permeability: an increased lactulose-to-rhamnose ratio indicates compromised barrier, while a decreased ratio suggests improvement. However, this method is influenced by premucosal factors (gastric emptying and transit time) and postmucosal factors (renal function and urinary collection efficiency), potentially affecting accuracy (Bjarnason *et al.,* 1995).

Effect on mucus composition and functionality

The intestinal chemical barrier, essential for maintaining gut integrity, is primarily composed of a mucus layer formed by mucins (MUCs) secreted by goblet cells, along with antimicrobial peptides produced by epithelial cells (Ge *et al.,* 2020; Johansson and Hansson, 2011). Early weaning has been associated with compromised barrier function due to reduced mucin secretion, often linked to impaired differentiation of goblet cells (Wang *et al.,* 2020). Adequate mucin secretion is crucial for preserving the functionality of this barrier, as a thinner mucus layer resulting from reduced mucin levels allows easier penetration by harmful bacteria and weakens the gut's defence mechanism (Birchenough *et al.,* 2015); MUC2 is particularly important as its oligosaccharide chains provide adhesion sites for probiotics, immunoglobulin A (IgA), and antimicrobial peptides within the gut microbiota, reinforcing its barrier function (Johansson *et al.,* 2013). Additionally, early weaning alters mucin glycosylation patterns, further compromising barrier integrity. A significant decrease in MUC2 gene expression, a key marker for mucin production, has also been reported in weaned piglets (Hedemann *et al.,* 2007).

The mucus layer not only acts as a shield against infections but also contributes to intestinal health by supporting microbial homeostasis and supplying intestinal juice. Goblet cells are primarily responsible for mucus secretion, but enterocytes also play a role, with a 70-kg piglet producing approximately 6 litres of intestinal juice daily (Gribble and Reimann, 2019). During weaning, the composition of mucus undergoes notable changes, including a shift from neutral mucins to more acidic mucins. This alteration is particularly evident in the ileum, making this region more vulnerable to stress during the dietary transition. While these changes are necessary for adaptation to a solid-feed diet, they temporarily weaken the gut's defences, increasing susceptibility to microbial imbalances and inflammation (Deplancke and Gaskins, 2001; Forder *et al.,* 2007; Jha and Berrocoso, 2016).

Alteration in digestive enzyme activity

Absorptive epithelial cells in the small intestine secrete a variety of digestive enzymes, including disaccharidases, peptidases, and alkaline phosphatase, which play a crucial role in nutrient breakdown and absorption (Benoit *et al.,* 2010). During the first three weeks after birth, piglets experience rapid digestive system development fueled by adequate nutrition from sow's milk. This leads to significantly increased activities of enzymes such as lactase, protease, and lipase, which are essential for digesting milk nutrients (Jensen-Waern *et al.,* 1998). However, the weaning transition introduces significant challenges to enzymatic activity, primarily due to intestinal morphological changes and dietary shifts. Early weaning is associated with a transitional shift in digestive enzyme activity, reflecting the dietary switch from milk to solid feed. While the activity of lactase, a milk-specific enzyme, typically declines, the activity of enzymes required for digesting solid feed—such as maltase, sucrase, and various peptidases—generally increases (Lallès *et al.,* 2004a; Ma *et al.,* 2021). However, this enzymatic adaptation may be delayed or insufficient in early-weaned piglets, leading

to temporary digestive inefficiency and contributing to post-weaning challenges. (Boudry, Péron, *et al.,* 2004; Lallès *et al.,* 2004b; Marion *et al.,* 2005; Montagne *et al.,* 2007; Tang *et al.,* 2022; Xiong *et al.,* 2019a). The decline in lactase activity after weaning significantly impairs carbohydrate absorption and contributes to diarrhoea in piglets (Hedemann *et al.,* 2003). Similarly, alkaline phosphatase, a key enzyme involved in ATP generation, is notably reduced during early weaning (Yang *et al.,* 2014). In addition to disaccharidases, the enzymatic activity of peptidases, such as aminopeptidase N and dipeptidylpeptidase IV, also decreases shortly after weaning. This decline may result from villus atrophy or insufficient feed intake, both of which inhibit endogenous enzyme secretion (Tang *et al.,* 2022).

Enzyme activity typically reaches its lowest levels 3–5 days post-weaning but gradually recovers as feed intake increases. Studies suggest that nutrient availability plays a critical role in this recovery, with pigs receiving a continuous nutrient supply exhibiting higher enzyme activity (Pluske *et al.,* 1997). As enzymatic activity adapts post-weaning, distinct patterns emerge. Enzymes suited for milk digestion, such as lactase, naturally decline, while those required for starch and protein digestion, including amylase and proteases, increase to meet the demands of a solid-feed diet (Cera *et al.,* 1990; Lindemann *et al.,* 1986). However, lipase activity often decreases due to the lower fat content of weaning diets compared to sow's milk and the limited feed intake during early weaning. This decline may also stem from enzyme depletion when secretion rates exceed synthesis. Despite these adaptations, a temporary reduction in nutrient digestibility is common immediately after weaning, often leading to reduced feed efficiency and growth setbacks if the intestinal adjustments are inadequate (Le Dividich and Sève, 2000). For instance, as the neonatal diet becomes less milk-dependent, lactase activity decreases while sucrase and maltase levels increase to accommodate carbohydrate-rich feeds (Modina *et al.,* 2021). While these enzymatic shifts are necessary for dietary adaptation, the timing and adequacy of the transition are critical for minimizing digestive challenges and ensuring optimal growth and development in piglets.

Effect of weaning age

Piglets' intestinal barrier function is significantly impacted by the age at which weaning takes place **(Figure 3)**. In comparison to pigs weaned later at 28 days, it has been demonstrated that early weaning, such as at 21 days of age, dramatically increases intestinal permeability and electrogenic ion transport responses within just 24 h after weaning. Lower permeability levels are the outcome of gradually improving the intestinal barrier by delaying the weaning age from as early as 15 days to 28 days. Surprisingly, these gains last for as long as nine weeks after weaning, highlighting the long-term advantages of postponing weaning for gut health and function (Moeser *et al.,* 2007; Smith *et al.,* 2010).

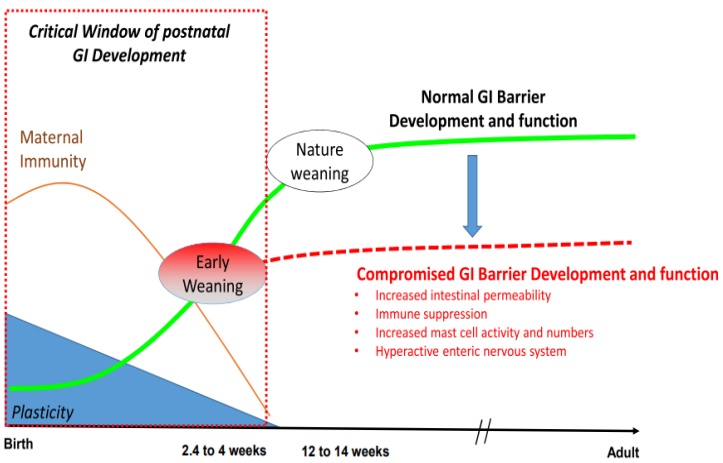

Figure 3. Weaning age and post-weaning complications (Adapted from Moeser *et al*., 2017)

Piglets GI systems grow significantly throughout the first 12 weeks of postnatal life. First, sow's milk and colostrum offer vital growth and immunological components as well as passive (maternal) immunity. In the natural weaning (shown by the green line), the immunological and enteric nervous systems, the epithelial barrier, and transport functions all mature during this postnatal phase, which is almost complete by 12 to 14 weeks of age.

Early weaning also leads to lasting GI disturbances, including impaired barrier integrity and immune function, with these effects extending into adulthood (Moeser *et al.,* 2017b; Pohl *et al.,* 2017). One important component of these disruptions is the corticotropin-releasing factor (CRF) system. Shortly after weaning, early weaned pigs exhibit elevated serum CRF levels, which are associated with increased intestinal permeability. Meanwhile, cortisol levels continue to be elevated for the duration of the post-weaning period (Moeser *et al.,* 2007). Chronic CRF elevation contributes to barrier dysfunction by downregulating intestinal CRF receptor expression and increasing jejunal glucocorticoid receptor expression (Smith *et al.,* 2010). These findings underscore the critical influence of weaning age on the long-term health of the GI system, emphasizing the importance of optimizing weaning practices to mitigate barrier dysfunction, reduce stress-induced disruptions, and promote better gut health and overall resilience in pigs.

1.1.2. Microbial Dynamics

The mammalian GI tract hosts a vast and diverse community of microorganisms that are integral to various physiological functions, including nutrient digestion, intestinal barrier maintenance, immune regulation, and endocrine signalling (Beaumont *et al.,* 2020). Research has identified *Firmicutes*, *Proteobacteria*, *Bacteroidetes*, *Tenericutes*, and *Spirochaetes* as the five predominant bacterial phyla present in the intestinal tract of piglets, irrespective of their weaning status (Li *et al.,* 2018). Mucosa-associated microbiota serves as a critical defence mechanism against pathogens and plays a key role in modulating host immune responses. By stimulating the mucosal immune system, the microbiota induces IgA production, which is secreted into the lumen to limit bacterial colonization and prevent bacterial penetration through the epithelial barrier (Brandtzaeg, 2007; Mayer *et al.,* 2015; Zheng *et al.,* 2021a).

Additionally, the fermentation of dietary components by gut bacteria plays a pivotal role in gut health. Microbes ferment carbohydrates and proteins, producing short-chain fatty acids (SCFA) such as acetate, propionate, and butyrate. These SCFA not only serve as an energy source for intestinal cells but also help maintain a healthy gut environment by lowering pH levels, which enhances mineral absorption and inhibits the growth of harmful bacteria. Research has also demonstrated that SCFA enhance the expression of key tight junction proteins, such as occludin, claudin-1, and ZO-1, thereby strengthening the intestinal barrier in weaned piglets (Diao *et al.,* 2019). Moreover, SCFA contribute to intestinal barrier integrity by stimulating the secretion of interleukin-18 (IL18), antimicrobial peptides, and mucins *via* the G-protein-coupled receptor 43 (GPR43). Butyrate supports the repair and renewal of the intestinal lining, strengthening the gut barrier. Commonly found genus *Alloprevotella,* which has been linked to the production of succinate and acetate, or *Oscillibacter* species which are known to produce butyrate, a key metabolite that enhances intestinal barrier integrity and exhibits anti-inflammatory properties (Christensen and Huber, 2022; Upadhaya and Kim, 2021). Weaning stress-induced changes in intestinal microbiota are closely associated with the microbial-driven production of SCFA, which play a pivotal role in re-establishing intestinal homeostasis post-weaning. For example, *Erysipelotrichaceae* and *Lachnospiraceae* which are also found commonly in the piglet's gut are inversely correlated to butyrate production and directly proportional to upregulation of proinflammatory genes (Dinh *et al.,* 2015; Kaakoush, 2015a; Zhong *et al.,* 2019). These findings suggest that alterations in intestinal microbiota can disrupt the microbial-driven SCFA production, increase permeability and trigger inflammation (Jha and Berrocoso, 2016; Modina *et al.,* 2021; Topping and Clifton, 2001).

Beyond short-chain fatty acids, the gut microbiota produces a wide array of other bioactive molecules that contribute significantly to host physiology. Among these, microbial-derived lipids and peptides have gained

increasing attention for their roles in modulating immune responses, enhancing gut barrier integrity, and influencing metabolic signaling pathways. These compounds represent an additional layer through which the microbiota can exert beneficial—or sometimes detrimental—effects on host health. In addition to SCFAs, microbial metabolism of dietary components generates various bioactives that contribute to gut barrier integrity. Tryptophan is catabolized by indole-producing microbes like *Clostridium sporogenes* into indole derivatives, which act as ligands for the aryl hydrocarbon receptor (AhR), promoting immune responses via IL-22 and enhancing epithelial junctional protein expression (Teresa *et al.*, 2013; Shimada *et al.*, 2013; Ghosh *et al.*, 2021). Similarly, microbial synthesis of conjugated fatty acids, such as conjugates linoleic acid and conjugated linolenic acid isomers, modulates barrier function and inflammation by regulating tight junction proteins and cytokine expression (Schoeler and Caesar, 2019; Roche *et al.*, 2001; Chen *et al.*, 2019). Polyamines like spermidine, produced by gut microbes such as *E. coli* and *Bacteroides*, enhance E-cadherin-mediated adhesion via intracellular Ca^{2+} signaling, contributing to reduced permeability (Michael AJ, 2016; Liu *et al.*, 2009). Together, these microbial products represent important modulators of gut homeostasis beyond SCFAs.

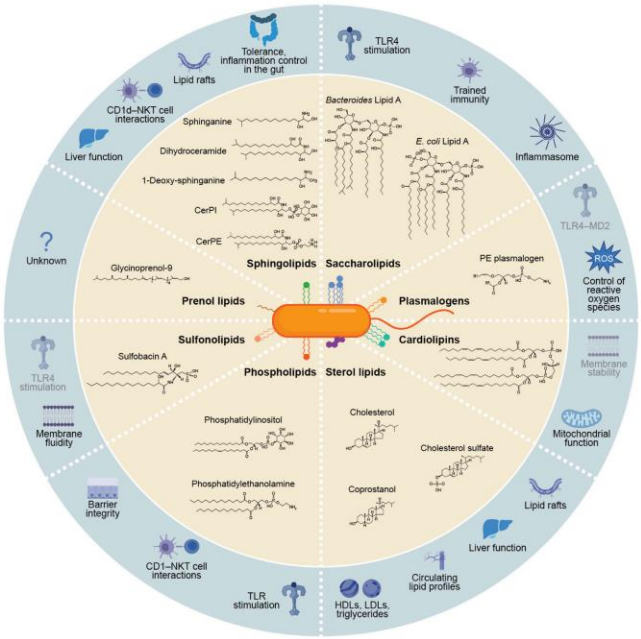

Figure 4. Membrane lipids biosynthesized by the gut microbiome and their known host signalling functions (Adapted from Brown *et al.*, 2023)

The inner beige ring displays representative structures of each lipid, while the outer blue ring illustrates their proposed host functions. Functions supported by limited experimental evidence are indicated in a lighter shade of blue. TLR4 stands for Toll-Like Receptor 4, HDL and LDL refer to High-Density Lipoprotein and Low-Density Lipoprotein respectively, and CD1-NKT refers to Cluster of Differentiation 1-restricted Natural Killer T cells.

1.1.2.1. Pre-weaning Microbial colonization

While the gut is sterile at birth, microbial colonization begins immediately, shaping intestinal health and function from their environment, feed, and oral-fecal transmission. (Siggers *et al.*, 2007). The initial colonization of the neonatal gut begins at birth, as the newborn passes through the maternal genital tract, ingesting bacteria from the cervix, vagina, and skin. Postnatally, further colonization occurs during suckling, where neonates acquire bacteria from the sow's skin and ingest both bacteria and oligosaccharides in milk, which are considered prebiotics. Additionally, maternal licking facilitates the transfer of oral bacteria to the neonate (Chen *et al.*, 2018; Dominguez-Bello *et al.*, 2011; Mackie *et al.*, 1999). Pigs' gut microbiota primarily develops with age while weaning being a critical period (Karasova *et al.*, 2021), but the development of this microbiota is also influenced by factors such as intestinal pH, substrate availability, mucus secretion, peristalsis, and transit time (O'Sullivan *et al.*, 2005). Interestingly, within the first three days of life, piglets exhibit a consistent microbiota composition irrespective of their breed or nursing mother. As suggested by Chen *et al.*, (2017) the initial gut colonization of newborn piglets predominantly involves bacteria from the *Clostridiaceae*, *Enterobacteriaceae*,

Fusobacteriaceae, and *Bacteroidaceae* families. While at phyla level, the intestinal microbiota of pre-weaned and weaned piglets is predominantly composed of Firmicutes (51%), Bacteroidetes (25%), and Proteobacteria (16%) (Bian *et al.,* 2016a; Cremonesi *et al.,* 2022).

The consumption of colostrum and milk from the sow affects this first colonization, while full microbial colonization occurs in about two days as facultative and obligate anaerobes increasingly replace aerobic bacteria as the gut environment changes. Initially, the stomach and upper small intestine host fewer bacteria due to rapid transit, with *Lactobacillus*, *Streptococcus*, and *Helicobacter* spp. dominating in the acidic stomach environment (Sun *et al.,* 2019; Wei *et al.,* 2021; Jensen *et al.,* 2006). Due to the acidic environment and peristalsis, bacterial presence in the stomach and duodenum remains minimal. However, bacterial abundance increases progressively along the intestinal tract, with the highest load and diversity observed in the cecum and colon (Lawley and Walker, 2013). In contrast, the large intestine supports a diverse microbial population, dominated by strict anaerobes like *Bacteroides* and *Clostridium* spp., due to slower digesta transit (Gaskins, 2000).

1.1.2.2. Post-weaning transition

The GI tract hosts distinct microbial populations that vary based on physicochemical conditions and diet (Zhao *et al.,* 2015). During the suckling period, this microbiota remains relatively stable, but the transition to solid feed during weaning introduces significant changes **(Figure 4)**. For example, initially, it is adapted to the degradation of milk carbohydrates and dominated by families such as *Bacteroidaceae* and *Lactobacillaceae*. Following weaning, these microbes are progressively replaced by carbohydrate-fermenting bacteria, which play a key role in producing SCFA like acetate, propionate, and butyrate (Chen *et al.,* 2017). These dietary shifts lead to a more diverse microbial community, which, while necessary for long-term gut health, can temporarily destabilise the intestinal environment (Modina *et al.,* 2021). During this period of destabilization, a reduction in α-diversity is commonly observed which is accompanied by diminishing variability of the microbiota among individual piglets (Koo *et al.,* 2021; Oliphant *et al.,* 2021; Quast *et al.,* 2012; Shu *et al.,* 2022). Furthermore, reduction in microbial diversity in piglets can lead to increased degradation of glycans within the mucus layer by symbiotic bacteria. This process releases monosaccharides such as mannose, galactose, and fucose, which may inadvertently promote the growth of pathogenic bacteria (Bäumler and Sperandio, 2016). Notably, fucose can be utilized by enterohemorrhagic *E. coli* to activate the gene expression of its type III secretion system. This mechanism allows certain pathogenic bacteria to sense and adhere to intestinal epithelial cells (IEC) (Tran *et al.,* 2018).

The growth of harmful bacteria can further also disrupt the balance of the beneficial gut microbiota and its metabolites (Castillo *et al.,* 2007; Gresse *et al.,* 2021; Kubasova *et al.,* 2018). For instance, in the ileal mucosa of weaned pigs infected with *Salmonella typhimurium*, a decrease in beneficial bacteria, such as *Bifidobacterium* and *Lactobacillus*, and an increase in harmful bacteria, such as *Citrobacter* was observed (Argüello *et al.,* 2018). Additionally, a consistent reduction in *Lactobacilli* levels is another hallmark of post-weaning microbial disruption. Profound microbial shifts occur post-weaning, with significant reductions in *Lactobacilli* (e.g., *Lactobacillus sobrius*, *Lactobacillus acidophilus*, and *Lactobacillus reuteri*) and increases in coliforms and *E. coli* across the GIT. This disruption, characterized by a decline in milk-utilizing bacteria and an overgrowth of potentially pathogenic bacteria such as enterotoxigenic *ETEC*, heightens the piglet's susceptibility to gut infections during the weaning transition (Heo *et al.,* 2013; Konstantinov *et al.,* 2006a).

This post-weaning dysregulation and translocation of the intestinal microbiota contributes to intestinal cell apoptosis, physical barrier disruption, and immune dysfunction, all of which adversely affect intestinal health in animals (Allam-Ndoul *et al.,* 2020; Takiishi *et al.,* 2017; Usuda *et al.,* 2021). Disruptions in intestinal

microbiota after weaning are also strongly associated with diarrhoea and pathogenic infections (Gresse *et al.,* 2017a; Lallès *et al.,* 2007). Research by Yang *et al.* (2019) revealed that diarrheic piglets experience disrupted competition between *Prevotella* and *Escherichia* before weaning, alongside lower abundances of critical nutrient-metabolizing genera such as *Bacteroides*, *Ruminococcus*, *Bulleidia*, and *Treponema* post-weaning, compared to healthy counterparts. Similarly, Sun *et al.* (2019) reported that diarrheic piglets exhibited lower relative abundances of *Bacteroidales* compared to their non-diarrheic counterparts during the weaning period.

Weaning stress has a large impact on the relative abundance of specific families and genera within key bacterial phyla, but it has no discernible effect on the species composition of these phyla. The relative abundances of the two leading bacterial families, *Erysipelotrichaceae* and *Lachnospiraceae*, increased considerably during the first week after weaning (Y. Li *et al.,* 2018; Zhong *et al.,* 2019). Several studies have also reported significant shift from the dominant genus *Bacteroides* to *Prevotella* due to abrupt dietary and environmental changes associated as weaning progresses (Adhikari *et al.,* 2019; Gresse *et al.,* 2017b; Macpherson *et al.,* 2005; Rios *et al.,* 2016; Zheng *et al.,* 2021a). The marked increase in the relative abundance of *Prevotella* is likely attributed to the well-documented ability of this genus to metabolize plant-derived non-starch polysaccharides into SCFA (Flint and Bayer, 2008). This aligns closely with previous findings that highlight *Prevotella* as a key player in the typical post-weaning microbiota, alongside other prominent genera such as *Roseburia*, *Faecalibacterium*, *Ruminococcus*, *Lachnospira*, *Dorea*, *Blautia*, and *Subdoligranulum* (Guevarra *et al.,* 2018, 2019; Kim *et al.,* 2011; Luise, *et al.,* 2021; Ramayo-Caldas *et al.,* 2016; Saladrigas-García *et al.,* 2021; Slifierz *et al.,* 2015). Dietary changes and the stress associated with weaning trigger intestinal inflammation, which can be further exacerbated by enteric infections. This inflamed state creates an environment conducive to the expansion of *Enterobacteriaceae*. During inflammation, the host's immune response generates reactive species such as nitric oxide (NO), which exhibits antimicrobial properties. However, NO released into the intestinal lumen is rapidly converted into nitrate (Bäumler and Sperandio, 2016; Zeng *et al.,* 2017). The nitrate-enriched environment of the inflamed gut provides a growth advantage to *E. coli* strains equipped with nitrate reductase genes, a feature absents in species belonging to *Clostridia* or *Bacteroidia*. Furthermore, the increased oxygen availability in the inflamed intestine, resulting from heightened blood flow, favours the proliferation of facultative anaerobes like members of the *Enterobacteriaceae* family (Spees *et al.,* 2013; Winter *et al.,* 2013a).

The levels and sources of dietary proteins and fibers significantly influence the diversity and composition of the gut microbiome in weaning piglets (Pieper *et al.,* 2015; Rist *et al.,* 2013). For example, diets enriched with pectin or soybean meal have been shown to reduce the relative abundance of *Lactobacillus* while increasing *Prevotella* populations in the colon (Tian *et al.,* 2017). Additionally, the inclusion of fish protein as a dietary source has been associated with a notable expansion of the *Escherichia/Shigella* group (Cao *et al.,* 2016). These alterations in gut microbial composition and activity are strongly associated with an increased risk of pathogenic infections following weaning (Konstantinov *et al.,* 2006b; Zheng *et al.,* 2021a). In conclusion, the weaning transition disrupts gut microbiota balance, promotes inflammation, and increases pathogen susceptibility. Bioactive compounds, such as prebiotics, probiotics, and plant-derived metabolites, offer a promising approach to alle*via*te these stresses. Their role in supporting gut health will be discussed further in the nutritional strategies section.

1.1.3. Immune modulation and responses

The intestinal mucosa and submucosa collectively house approximately 70% of the body's immune cells, making the gut the most extensive immunological organ in animals (Zheng *et al.,* 2021b). This sophisticated intestinal immune system includes various components such as intraepithelial lymphocytes, lamina propria lymphocytes, neutrophils, macrophages, and secreted factors like antimicrobial peptides, immunoglobulins, and cytokines, which together form a well-developed immunological barrier (Gou *et al.,* 2022; Wells *et al.,* 2017). The intestinal immune system plays a crucial role in recognizing exogenous antigens, preventing allergic reactions, and maintaining epithelial homeostasis through the secretion of immune mediators, including antimicrobial peptides, interferons (IFNs), interleukins (ILs), and immunoglobulins (Yin, 2016).

Immune cells such as macrophages, dendritic cells, T cells, and B cells recognise antigens entering the lamina propria (Allaire *et al.,* 2018; Chi *et al.,* 2023). The gut-associated lymphoid tissue (GALT), comprising Peyer's patches and mesenteric lymph nodes, serves as a central component of immune defence. Microfold cells (M cells) initiate antigen presentation, while immune regulation—particularly immunoglobulin A (IgA) production—occurs in the lamina propria, which is rich in myeloid cells. Additionally, Paneth cells in the intestinal epithelium play a pivotal role in bacterial recognition by activating toll-like receptors (TLRs). TLR2, TLR4, and TLR5 specifically recognise peptidoglycan, lipopolysaccharides, and bacterial flagellin, respectively (Kayama *et al.,* 2020). Once activated, signalling pathways such as the nuclear factor kappa B (NFκB) pathway, mediated by myeloid differentiation factor 88, lead to the overexpression of pro-inflammatory cytokines, including IL1β, IL6, IL8, and tumor necrosis factor α- (TNFα), which can result in intestinal inflammation (Jang *et al.,* 2013; Wang *et al.,* 2017). TLRs and nucleotide-binding oligomerization domain (NOD)-like receptors, allow immune cells to distinguish between harmful and beneficial substances. These PRRs also activate NFκB, as well as mitogen-activated protein kinase (MAPK), and peroxisome proliferator-activated receptor gamma (PPARγ), to modulate immune responses and inflammation. Furthermore, secretory antibodies, primarily IgA and IgM, produced by epithelial cells in the intestinal crypts, collaborate with innate immune mechanisms to maintain gut protection (Bron *et al.,* 2012; O'Flaherty *et al.,* 2010).

Birth and weaning are critical periods in the development of the immune system, requiring significant adaptations to microbial colonization and dietary antigens. The rapid establishment of an effective epithelial barrier, coupled with immune modulation by exogenous and endogenous factors, helps suppress unnecessary immune activation during these stages. However, the intestinal immune system in pigs remains immature until approximately the seventh week of life. Consequently, early weaning at 3 to 4 weeks poses a significant challenge, as it increases the susceptibility of piglets to diseases. The weaning process induces profound changes in diet and environment, which in turn disrupt the mucosal immune response and compromise intestinal homeostasis (Artis, 2008; Mabbott *et al.,* 2013; Zheng *et al.,* 2021a).

1.1.3.1. Immune Development Pre-Weaning

Maternal milk plays a pivotal role by delivering immunoglobulins (e.g., IgA), leukocytes, and glycans that neutralize intestinal microbes, along with anti-inflammatory cytokines and peptides that suppress neonatal TLRs and inflammatory cytokine responses (Newburg and Walker, 2007). Neonates are also born with limited lymphocytes and co-stimulatory molecule expression, maintaining an immunosuppressive state until lymphocyte development progresses structurally and functionally several weeks post-birth (Nguyen *et al.,* 2010; Upham *et al.,* 2006) **(Table 2)**. Nursing piglets reach a stable lymphocyte count around 6 weeks of age (Blikslager *et al.,* 1997).

Table 2. Summary of Mucosal Immune System Development in Piglets (Adapted from Bauer *et al.,* 2006).

Time	Development
Birth	• Low numbers of macrophages and granulocytes in the villous and crypt regions, indicating functional immaturity. • Peyer's patches consist of primordial follicles with few surrounding T cells. • Very low numbers of CD4+ and CD8+ T cells. • Intestinal MHC class II+ cells are present in low numbers. • Ig-containing cells are rare or absent.
1-2 Weeks	• The intestine becomes colonized with lymphoid cells that express the CD2 surface marker but lack CD4 and CD8 expression. • Peyer's patches begin to organise, achieving a relatively mature architecture by 10–15 days of age.
2-4 Weeks	• CD4+ cells colonize the mucosa, particularly in the lamina propria. • CD8+ cells are still largely absent at this stage. • Small populations of B cells appear, predominantly expressing IgM.
5 Weeks Onwards	• CD8+ cells begin to appear in the intestinal epithelium. • IgA+ B cells emerge, with IgA becoming predominant isotype. • The intestinal architecture reaches a mature structure comparable to that of an adult pig by approximately seven weeks.

IgA stands for Immunoglobulin A, and CD8 refers to Cluster of Differentiation 8, a marker for cytotoxic T lymphocytes.

1.1.3.2. Immune Dysregulation Post-weaning

Weaning impacts both innate and adaptive immunity, primarily due to the cessation of milk intake. The immune system of pigs matures to an adult-like structure by 7 weeks of age, but weaning typically occurs at 3–4 weeks, a time when cytotoxic T (CD8+) cells are still largely absent. This period is characterized by underdeveloped immune barrier having upregulation of pro-inflammatory cytokines, which disrupt intestinal barrier function and increase epithelial permeability, increasing their susceptibility to diseases (Capaldo and Nusrat, 2009; Sido *et al.,* 2017; Stokes *et al.,* 2004; Zheng *et al.,* 2021a).

In early weaned piglets face numerous pathogenic and non-pathogenic challenges due to physiological and psychological stress, which affects immune cells, such as T lymphocytes and mast cells, leading to transient gut

inflammation. Early weaned piglets (weaned at 19 days) show higher intestinal mast cell numbers within 24 h of weaning and sustained hyperplasia at 7, 9, and even 20 weeks post-weaning compared to late-weaned piglets (Tang *et al.,* 2022). During the first two days post-weaning, intestinal inflammatory T cells and matrix metalloproteinase levels were found to rise significantly, while the CD4+/CD8+ T lymphocyte ratio decreases, signalling temporary gut inflammation (McCracken *et al.,* 1999; Spreeuwenberg *et al.,* 2001). Administration of the mast cell stabilizer sodium cromolyn has been shown to prevent weaning-induced increases in intestinal permeability and short-circuit current changes (Moeser *et al.,* 2007b). Both *in vivo* and *ex vivo* studies demonstrate that CRF receptor activation triggers mast cell degranulation, releasing proteases and TNFα, which increase intestinal permeability (Overman *et al.,* 2012; Smith *et al.,* 2010). Collectively, these findings highlight mast cells' central role in driving gut barrier disturbances in early weaned pigs.

Weaning stress further activates the immune system, triggering the production of pro-inflammatory cytokines such as TNFα, IFNγ, IL1β, IL6, and IL8 causing intestinal dysfunction. NFκB is a pivotal transcription regulation factor that triggers the release of inflammatory mediators, including IL-1, IL6, TNFα, COX-2, and iNOS, regulating cellular inflammatory responses. Butyrate has been shown in other studies to inhibit NFκB1 activation and upregulate other cytoplasmic inhibitors of NFκB1, thereby reducing inflammation (Segain, 2000; Tedelind *et al.,* 2007).

Additionally, microbial invasion during weaning induces the secretion of immunoglobulin A (sIgA) and defensins in the jejunum, supporting the restoration of intestinal barrier function (ASadi, 2009; Groot *et al.,* 2021; Hu *et al.,* 2013a; Lallès *et al.,* 2004a). Early weaned pigs demonstrate a suppressed immune response compared to late-weaned pigs. Specifically, reduced IL6, IL8, and neutrophil responses to an *E. coli* challenge suggest compromised mucosal innate immunity in early weaned pigs. Additionally, a study comparing 14-day and 21-day weaned pigs showed higher lymphocyte concentrations in 21-day weaned pigs after mixing and resorting stress at 37 days post-weaning, while no such changes were observed in 14-day weaned pigs. These findings indicate that weaning age induces lasting alterations in both peripheral and mucosal immune cell profiles (Davis *et al.,* 2006; Moeser *et al.,* 2017b). Following weaning the tissue concentration of the anti-inflammatory cytokine and growth factor TGF-β (β1 isoform) was shown to transiently decrease in villi and to increase in crypts of the duodenum and jejunum (Mei and Xu, 2005). Thus, weaning marks profound disruptions in immune and intestinal barrier function due to stress, dietary changes, and microbial colonization. The interplay between the microbiota and immune system is pivotal during this transition, as microbial exposure not only triggers pro-inflammatory responses but also facilitates the maturation of mucosal immunity. These findings underscore the delicate balance required to mitigate weaning stress, support immune development, and restore intestinal homeostasis.

1.2. Nutritional Approaches

Enhancing intestinal development is vital for boosting nutrient absorption and strengthening disease resistance in weaned piglets, ultimately improving their survival rates. While the precise mechanisms underlying these benefits remain unclear, growing evidence points to the promising role of dietary approaches in supporting intestinal health. This section delves into the latest insights on nutritional strategies, focusing on the impact of prebiotics and bioactive compounds from chicory in fostering gut development and resilience in weaned piglets, highlighting the pressing need for further mechanistic investigations in this area.

1.2.1. Restricted Interventions

Zinc Oxide

Zinc oxide (ZnO), a heavy metal used as a feed additive, has long been a common tool for preventing and managing post-weaning disorders in piglets. To achieve its performance-enhancing effects, ZnO must be administered in doses significantly exceeding the physiological needs of piglets, —often as high as 2000–4000 ppm. These levels far surpass the dietary zinc requirements and result in low absorption rates, with only about 20% bioavailability (European Commission, 2003). The remaining unabsorbed zinc accumulates in manure, contributing to significant environmental contamination. Recognizing these concerns, European legislation has already restricted total dietary zinc levels in piglet feed to 150 mg/kg, with further reductions under consideration (Morales *et al.,* 2012). An increasing number of countries are implementing restrictions on the use of medical levels of ZnO in swine diets, prompting the need to explore alternative strategies. While high doses of ZnO have been shown to suppress the growth of *E. coli* and other coliform bacteria in piglets (Walk *et al.,* 2015; Wang *et al.,* 2019), there is growing evidence of its adverse effects. Studies have highlighted potential drawbacks, such as a reduction in beneficial intestinal bacteria and increased environmental zinc emissions (Højberg *et al.,* 2005; Wu *et al.,* 2019). These findings underscore the urgency to identify and adopt effective alternatives as reliance on ZnO in piglet feed diminishes (Wei *et al.,* 2020).

Antibiotics Growth promoters (AGP)

The weaning transition is a critical period that frequently results in GI infections such as colibacillosis diarrhoea, which are responsible for the loss of approximately 17% of piglets born in Europe (Gresse *et al.,* 2021; Schokker *et al.,* 2018a). The widespread use has significantly contributed to the emergence of antimicrobial-resistant pathogens, posing severe risks to both animal and human health. For instance, some bacterial families, such as Enterobacteriaceae, have developed resistance to nearly all available antibiotics, including those considered last-resort options. In response to this global health concern, the European Union gradually phased out the use of in-feed antibiotics as growth promoters (Gross, 2013). Consequently, AGPs no longer have a place in sustainable animal farming, as their use accelerates the development of antibiotic resistance, threatening the effectiveness of vital drugs for both veterinary and human medicine.

Sodium Saccharin

Sodium saccharin, a flavoring agent in animal feed, has raised concerns due to its environmental and safety risks. European Food Safety Authority (EFSA) evaluations found potential groundwater contamination from sodium saccharin or its degradation product, 4-hydroxysaccharin, exceeding the safety threshold of 0.1 µg/L. The additive's use was restricted to suckling and weaned piglets at 5 mg/kg feed, but environmental safety

remains unresolved. A safe use level to prevent groundwater contamination would be as low as 0.022 mg/kg feed, far below the proposed limit. Further research is needed to address these concerns and evaluate safer alternatives (Bampidis *et al.,* 2023).

1.2.2. Non-Prebiotic Alternatives

The weaning phase is a critical period characterized by a delicate balance between stress-induced intestinal damage and growth-driven recovery. During this time, the intestine must adapt quickly to a less digestible, plant-based diet, which can lead to changes in gut structure, motility, enzyme activity, and microbial composition. Additionally, this transition places considerable strain on the host's immune system as it works to maintain intestinal stability. To support gut health and optimize the productivity of weaned pigs, various nutritional strategies have been explored **(Table 3)**.

Table 3. Effects of feed additives on weaning piglet growth and intestinal health.

Feed Additive	Effect of Weaned Piglet	References
Protein hydrolysates	↑ growth, barrier and immune function ↑ nutrient digestibility ↑ LAB ↓ ADG and ↓ serum cortisol ↑ growth performance ↓ diarrhoea	(Peace *et al.,* 2011) (Yuan *et al.,* 2017) (Roh *et al.,* 2015) (Kim *et al.,* 2010)
Emulsifiers	Improved fat digestibility ↑ ADG, digestibility, ↓ triglyceride conc.	(Xing *et al.,* 2004) (Zhao *et al.,* 2015)
Probiotics	↑ feed intake, ↑ digestibility of N and P ↑ ADG and FCR Reduced PWD Protected piglets from intestinal pathogens such as *Salmonella* and *E. coli* colonization ↑ SCFA production **Limitations:** Strain specific effect	(Huang *et al.,* 2004) (Tang *et al.,* 2019) (Lodemann *et al.,* 2006) (Zhang *et al.,* 2017) (Gresse *et al.,* 2021)
Postbiotics	Products of *Saccharomyces* has overall positive effect on intestinal health	(Weedman *et al.,* 2011)
Enzymes	Xylanase: ↑ ADG and digestibility. ↓ inflammation Phytase: ↑ ADG, ADFI, digestibility Protease: ↓ fecal score, ammonia nitrogen, volatile FA, *E.coli*. ↑ *Lactobacillus*	(Chen *et al.,* 2020 ; Duarte *et al.,* 2019 ; Shen *et al.,* 2011) (Kies *et al.,* 2006) (Wang *et al.,* 2011 ; Zuo *et al.,* 2015)
Nucleotides	↑ growth performance and digestibility of dry matter and nitrogen. ↓ blood creatinine and fecal ammonia ↑ ADFI and ADG Positively affected villus structure. ↑ final body weight, growth efficiency and digestibility of dry matter and energy	(Tactacan *et al.,* 2016) (Jang and Kim, 2019) (Weaver and Kim, 2014)

Organic Acids (Citric, Propionic, Latic, fumaric acid)	↑ ADG, FCR, and intestinal morphology Altered microbiota and ↓ inflammatory cytokines and *E. coli* count in faeces, ↓ PWD. ↑ digestibility of nutrients acetic and propionic acid conc ↑ *Lactobacillus* **Limitations:** Lack of efficiency towards ETEC K88 challenge	(Li *et al.,* 2018) (Long *et al.,* 2018) (Gong *et al.,* 2008) (Bae and Lee, 2017)
Essential Oils (Thymol, Cinnaldehyde)	Increased ADFI Reduced ileum total microbial mass and increased the Lactobacilli: Enterobacteria ratio ↓ *E. coli* and total coliforms **Limitations:** No effect in few studies on *S.typhimuriium* Mode of action unclear Concerns regarding toxicity (lipophilic nature) Favour emergence of resistant *E. coli* strain	(Manzanilla *et al.,* 2004) (Fairbrother *et al.,* 2017) (Winter and Bäumler, 2014) (Trevisi *et al.,* 2007) (Ambrosio *et al.,* 2017) (Nerio *et al.,* 2010)
Supplemented milk	↑Cell proliferation, cell growth ↑ SCFA conc. Softer faeces ↓ *E. coli* ↓ jejunal pro-inflammatory genes **Limitations:** Does not provide same bioactives as sow milk. Not very cost effective	(de Greeff *et al.,* 2016; Huting *et al.,* 2021; Shi *et al.,* 2018)
Functional Amino Acids	L-Arginine: Enhance growth and reduced negative effect in young pigs. Proline: Improved mucosal proliferation, intestinal morphology, TJ protein and potassium channel expression Glutamine**:** Prevent intestinal atrophy, increase enzyme activity, and promote growth performance	(Hernandez *et al.,* 2009; Wang *et al.,* 2015; Guoyao. Wu *et al.,* 1996)
Phytochemical Extract	Pepper or capsicum oleoresin, curcumin: ↑ TJs expression, ↓ *E. coli* Garlic Extract: ↓ inflammation Extracts from oregano, thyme, ginger, fennel, pepper, clove, basil, cinnamon, garlic, mint: ↑ antioxidant activities Pomegranate extract: Anti-inflammatory	(Frankič *et al.,* 2010a, 2010b; Lang, 2004; Liu *et al.,* 2014; Yuan *et al.,* 2017)

ADG: Average Daily Gain; ADFI: Average Daily Feed Intake; PWD: Post-Weaning Diarrhoea, FCR: Feed Conversion Ratio, and LAB stands: Lactic Acid Bacteria; TJ: Tight Junction

1.2.3. Prebiotics

Overall, the weaning phase represents a delicate balance between stress-induced damage and recovery-driven growth, therefore the intestine must rapidly adapt to a less digestible, plant-based diet, which triggers modifications in gut morphology, motility, enzyme activity, and microbial composition. The concept of prebiotics was first introduced in 1995 by Gibson and Roberfroid, who defined them as "non-digestible food ingredients that beneficially affect the host by selectively stimulating the growth and/or activity of specific bacteria in the colon, thereby enhancing host health." However, the definition has since evolved. According to the 2017 consensus statement by the International Scientific Association for Probiotics and Prebiotics (ISAPP), a prebiotic is now defined as *"a substrate that is selectively utilized by host microorganisms conferring a health benefit."* (Gibson *et al.,* 2017). This updated definition emphasizes the requirement for selective utilization, distinguishing true prebiotics from other non-digestible carbohydrates that may undergo non-selective fermentation (Bamigbade *et al.,* 2022; Davani-Davari *et al.,* 2019).

1.2.3.1 Fructans

Fructans, a class of prebiotics, include inulin and fructo-oligosaccharides (FOS), also known as oligofructose. Structurally, they consist of linear chains of fructose molecules linked by β (2→1) bonds, often terminating with glucose units connected *via* similar β (2→1) linkages. The degree of polymerization (DP) differentiates inulin and FOS: inulin has a DP of up to 60, while FOS typically has a DP of less than 10. Studies have shown that both chain length and dietary concentration of inulin play a crucial role in its prebiotic effect (Herosimczyk *et al.,* 2020) **(Table 4)**. Notably, approximately 90% of inulin reaches the colon undigested, where it undergoes fermentation by gut bacteria, contributing to its prebiotic effect (Louis *et al.,* 2016) **(Figure 5).**

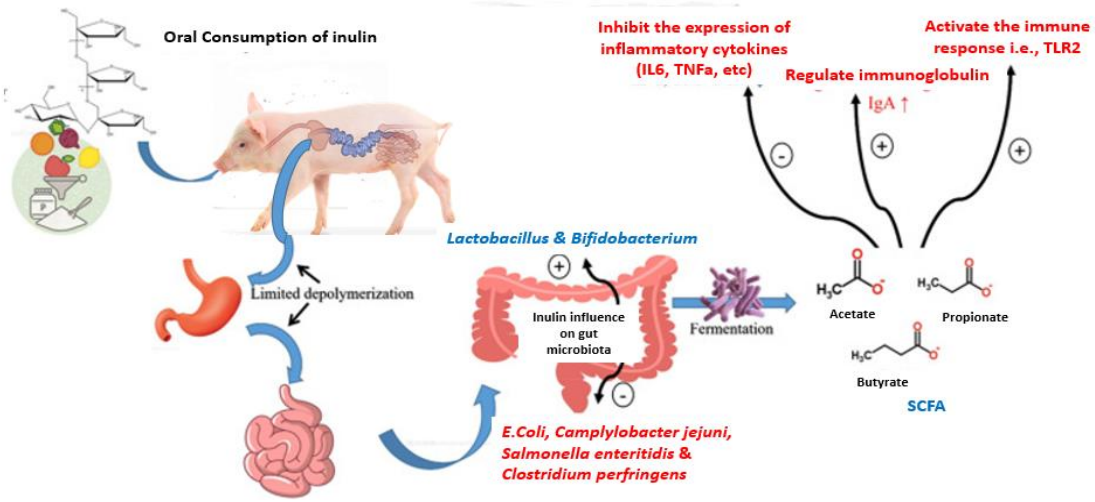

Figure 5. Effect of inulin supplementation on the gut health of the weaning piglet Adapted from: (Tawfick *et al.,* 2022)
(IL6: Interleukin-6; TNFa; Tumor Necrosis Factor-alpha; TLR2;Toll-Like Receptor 2; SCFA;Short-Chain Fatty Acids)

Table 4. Inulin dosage and its effects on weaning piglets in various studies.

FOS Dosage	Weaning Age	Other Points	Conclusion	Reference
2% of *ad libitum* diet	25-28th day	No mention about Average Feed intake	-↑ diversity with fermentable carbohydrates -*Clostridium* and *Ruminococcus* associated with fibers -Microbiota shifts immediately after weaning	(Konstantinov, 2003)
0.5% of DFI Days 0-7: 1.35g Days 7-14:2.2g Days 14-21: 3g	18th day	Daily Feed Intake: (Only 0.5% FOS) Days 0-7: 271g Days 7-14: 451g Days 14-21:616g	-FOS and *Bifidobacteria* improve growth W1 - *B. longum* boosts growth, FOS reduces it. -FOS lowers IGF-I, B. longum increases it.	(Estrada *et al.,* 2001)
1.2g/kg body weigh/day	7th day	Combination of GOS, milk fat globule membrane, and FOS	-GMF improves growth and microbiota diversity. -Enhances intestinal barriers and SCFA levels. -Supports neonatal development through microbiota.	(Wu *et al.,* 2020)
0.5% of feed 3.15g/day	21st day	-	-FOS relieves soybean antigen-induced anaphylaxis. -Modulates gut microbes, increasing Lactobacillus. -Enhances immune function *via* IgG/IgE.	(Chang *et al.,* 2018)
4g/day	28th day	Treated for 4 weeks	-FOS enhances *L. plantarum* growth and stress tolerance. -Combination of FOS and *L. plantarum* improves growth performance and nutrient digestibility. -Boosts beneficial microbiota and immune response.	(Wang *et al.,* 2019)
1-1.2g/day	21.5th day	Started treatment from 7th day to 35th day	-scFOS boosts weight and reduces mortality. -Minimal effect on gut morphology and immunity. - Mechanisms of scFOS benefits need clarification	(Ayuso *et al.,* 2020a)

0.5/kg/day	21.5th day	Started treating from 1st to 37th	- scFOS promotes *Bifidobacterium* except during weaning. -Effects on non-bifidobacteria vary with age. -HFA piglets model prebiotics' human impact	(Shen *et al.,* 2010)
5g/day	NA	Treatment from 1st to 14th day Incidental vomiting of the piglets in the first week	-FOS enhances bifidogenic effects in the colon. -Jejunal gene expression and structure improve. -Mechanisms behind FOS effects remain unclear	(Schokker *et al.,* 2018b)
1.2g/d	20th day	*Ad libitum* diet (7.30am and 2pm) Prestarter (20-40), Starter (41-64), pregrowing (65-103), growing (104-148), Finishing (148-slaughter	-scFOS enhances sow colostrum quality and IgG. - Improves piglet growth and reduces feeding time. -Increases influenza IgG levels in piglets.	(Apper *et al.,* 2016a)
8g/l rafitlose		3-10-Chain length No mention of how much was consumed or if its *ad libitum*	-FOS increases cecal polyamine production. -Bifidobacterium spp. not the main polyamine producer. -No significant effect on gut maturation.	(Sabater-Molina *et al.,* 2011a)
1.9g/d	33rd day	*Ad libitum* diet average daily intake 474g 5 times feed / day FOS mixed with the diet	-FOS and antibiotics improve FCR, diarrhoea. -Increased VFA concentrations in cecum, faeces. -FOS enhances villi height, goblet cells. -No effect on crypt depth, serum protein levels	(Xu *et al.,* 2005)

FOS: Fructooligosaccharides; GOS: Galactoologosaccharides; FCR: Feed Conversion Ratio, IGF-1: Insulin-like Growth Factor 1; IgG: Immunoglobulin G; IgE:Immunoglobulin E.

Inulin has demonstrated significant gut health benefits across various species, including rodents, humans, and pigs **(Figure 5)**. Jensen *et al.* (Jensen *et al.,* 2011) observed an increased abundance of *Bifidobacterium* in the ileum of piglets fed a diet containing 30% chicory, which is rich in inulin. Despite this microbial change, no diarrhoea was observed in any treatment group, consistent with findings by (Hossain *et al.,* 2016). No diarrhoea developed in any group. Similarly, (Halas *et al.,* 2010), administered diets containing 4% or 8% inulin to weaners but observed PWD only sporadically, making it challenging to assess the impact of inulin. Moreover, no significant effects on ileal morphology were detected. In another study, (Chen *et al.,* 2020) added 1% inulin

to the diet fed the first two weeks post-weaning and found no effect on the incidence of diarrhoea. Several studies have shown that inulin at different dosages **(Table 4)** can reduce pro-inflammatory processes, enhance intestinal integrity, maintain healthy gut morphology, and support the growth and composition of beneficial intestinal microbiota. These properties highlight its potential as a powerful prebiotic in promoting gut health and overall well-being (Apolinário *et al.,* 2014; Cani *et al.,* 2009; Chen *et al.,* 2017a; Liu *et al.,* 2016; Mensink *et al.,* 2015).

1.2.3.2. Galactooligosaccharides

Galactooligosaccharides (GOS) are non-digestible carbohydrates consisting of 3–10 or more galactose units linked to a terminal glucose molecule. They are typically synthesized using glycoside hydrolase enzymes, with lactose serving as the primary substrate, resulting in a mixture of GOS with varying degrees of polymerization (Panesar *et al.,* 2018). GOS are well-known for their ability to promote the growth of beneficial gut bacteria, particularly *Bifidobacteria* and *Lactobacilli*. In infants, higher populations of *Bifidobacteria* have been linked to the inclusion of GOS in their diet. Although GOS can also stimulate other bacterial groups, such as *Bacteroides* and members of the phylum *Firmicutes*, their effect on these bacteria is less pronounced compared to their impact on probiotics like *Bifidobacteria* (Louis *et al.,* 2016).

1.2.3.4. Other Oligosaccharides

Pectin, a polysaccharide, serves as a precursor to produce specific oligosaccharides known as pectin oligosaccharides (POS). These oligosaccharides are derived from the structural extensions of galacturonic acid (homogalacturonan) or rhamnose (rhamnogalacturonan I). The carboxyl groups within the POS structure may undergo methyl esterification, leading to acetylation at carbon positions 2 or 3. Additionally, the side chains of POS can incorporate various sugars, such as arabinose, galactose, and xylose, or ferulic acid, contributing to their diverse structural properties. The structural diversity of POS largely depends on their source, which influences the specific arrangement of their chemical groups and side chains. This variability plays a critical role in determining their functional properties and potential health benefits (Davani *et al.,* 2019; Gullón *et al.,* 2013; Panesar *et al.,* 2018).

1.2.3.5. Non-Carbohydrate Prebiotics

In addition to carbohydrate-based prebiotics, certain non-carbohydrate compounds also align with the prebiotic definition. These are referred to as non-carbohydrate oligosaccharides. A notable example is flavanols derived from cocoa, which have been investigated in both *in vivo* and *in vitro* studies for their ability to promote the growth of lactic acid bacteria (LAB). Dietary polyphenols, such as flavanols, have been shown to interact with gut microbiota, selectively stimulating or inhibiting the growth and proliferation of specific microbial populations. These findings highlight the broader scope of prebiotics, extending beyond carbohydrates to include other bioactive compounds with selective microbiota-modulating properties (Bamigbade *et al.,* 2022; Davani *et al.,* 2019; Tzounis *et al.,* 2011).

1.2.4. Chicory: A Functional Ingredient

Crude chicory consists of a blend of linear oligomers and polymers with chain lengths ranging from 2 to 60 units. Oligofructose, comprising approximately 10% of total INU (Degree of Polymerization (DP) <10) while 90% are long length INU fractions (DP=11 to 60), with an average DP of around 25 (Niness, 1999a). Crude chicory, in addition to containing inulin and oligofructose, is a rich source of diverse bioactive compounds. These include phenolic compounds, sesquiterpene lactones (e.g., lactucin, lactucopicrin, and 8-deoxy lactucin), guaianolid glycosides, and various caffeic acid derivatives such as chicoric acid, chlorogenic acid, isochlorogenic acid, and dicaffeoyl tartaric acid. Other notable components include hydroxycoumarins, flavonoids, alkaloids, steroids, terpenoids, volatile compounds, vitamins, β-carotene, and zeaxanthin. (Carazzone *et al.,* 2013) identified 64 compounds, including hydroxycinnamic acid derivatives such as eight mono- and dicaffeoylquinic acids, three tartaric acid derivatives, 31 flavonol glycosides, two flavone glycosides, ten anthocyanins, and multiple isomers of caffeic acid derivatives.

Collectively, these bioactives have been linked to a wide array of beneficial effects, including anti-inflammatory and antioxidant activities, modulation of lipid metabolism, inhibition of pathogenic growth, enhancement of growth performance, and potential anticancer properties (Karioti *et al.,* 2008; Pouille *et al.,* 2022b; San Andres *et al.,* 2019; Schumacher *et al.,* 2011). Other bioactive components of chicory, such as fructose, chlorogenic acid (CGA), and sesquiterpene lactones (STL), have been associated with various beneficial effects. These include promoting SCFA production, exhibiting psychobiotic properties, and supporting the growth of bacteria with hypolipidemic, hepatoprotective, and hypotensive roles (Pouille *et al.,* 2022b).

In addition to their scientific relevance and functional application in nutrition, inulin and related non-digestible carbohydrates have also been evaluated from a regulatory standpoint within the European Union. According to the European Commission Regulation No. 575/2011, fermentable carbohydrates naturally found in cereal grains and roots are recognised as raw feed materials and are approved for use in animal nutrition. This regulatory endorsement underscores their accepted role in promoting gastrointestinal function, especially in monogastric animals. Furthermore, the European Food Safety Authority (EFSA), under Regulation (EC) No. 1924/2006, has supported a health claim highlighting the beneficial effect of fructo-oligosaccharides (FOS) from inulin in reducing post-prandial glycaemic responses. This is attributed to their resistance to enzymatic hydrolysis and absorption in the small intestine, allowing them to modulate metabolic responses in a beneficial manner. Together, these regulatory assessments emphasize not only the nutritional but also the health-promoting potential of inulin-type fructans, aligning well with their use in strategies aimed at improving gut health and metabolic outcomes.

While the current thesis primarily focuses on scientific aspects, it is important to consider the broader regulatory and sustainability contexts when evaluating the applicability of chicory as a prebiotic. The cultivation of chicory in Europe is increasingly challenged by climate variability, fluctuating yields, and mounting regulatory pressures, particularly regarding pesticide use. These factors introduce year-to-year variability in chicory availability, which could limit its long-term scalability and consistent market presence. Although hydroponic chicory can be produced year-round, its production is still sensitive to environmental conditions and economic pressures. Recent reports from Belgium—a key chicory-producing region—highlight supply shortages due to extreme weather, increased production costs, and the phasing out of essential phytosanitary products, underscoring the fragility of chicory production systems. Such constraints must be considered in future research and commercialization strategies, especially given the growing demand for sustainable and locally produced prebiotics (Fresh Plaza Newsletter, Feb 2024). Additionally, changing climatic conditions, such as

drought and cold stress, can significantly affect the growth, photosynthetic efficiency, and the composition of secondary metabolites like carotenoids and tocopherols in chicory (Delfine *et al.,* 2022; Devacht *et al.,* 2009). While these environmental stresses may lead to reduced biomass and photosynthetic activity, they can also enhance the accumulation of protective antioxidant compounds.

1.3. *In vitro* models

The GI tract is a highly dynamic and complex system, essential for feed digestion, nutrient absorption, and the regulation of the delicate balance between host and microbiota. Digestion begins in the mouth, where mechanical and enzymatic processes initiate the breakdown of food. In the stomach, gastric acid and proteolytic enzymes further process the feed into chyme, which then moves to the small intestine for enzymatic digestion and nutrient absorption. Remaining undigested components pass into the colon, where microbial fermentation takes over, producing metabolites such as SCFA. These metabolites are crucial for gut health and epithelial integrity, influencing intestinal barrier function, immune responses, and metabolic pathways (Alminger *et al.,* 2014; Durcan *et al.,* 2024; McQuilken, 2021).

In vivo studies have traditionally been used to explore the effects of bioactive compounds and their interactions with these digestive processes. However, *in vitro* models have emerged as a cost-effective, ethical, and sustainable alternative, allowing for detailed and sustainable investigation into the mechanisms of bioactive compounds and their impact on gut health. The subsequent sections will explore the wide variety of GI models developed to replicate the digestion and fermentation processes, ranging from simple static systems to sophisticated multi-compartmental and dynamic models.

1.3.1. Digestion and absorption models

Static Models

INFOGEST Model

The INFOGEST and its successor, INFOGEST 2.0 **(Figure 6)** are an internationally recognised protocols designed to mimic the human GI system, focusing on the digestion processes occurring in the mouth, stomach, and small intestine (Minekus *et al.,* 2014; Brodkorb *et al.,* 2019). This *in vitro* digestion model standardizes key parameters such as pH, enzyme activity, bile salt levels, mechanical forces, and incubation times to ensure uniformity and reproducibility across laboratories. By simulating the composition of digestive fluids—including saliva, gastric, and intestinal secretions—this model provides a robust framework for studying nutrient release and bioavailability.

Its reproducibility has been validated through interlaboratory studies using skim milk powder as a standard, demonstrating the method's reliability in assessing digestion processes (Egger *et al.,* 2017). The model excels in determining nutrient release kinetics, such as peptides, amino acids, fatty acids, and simple sugars, and has been instrumental in evaluating diverse food matrices and dietary components. The model has demonstrated strong correlations with *in vivo* studies, particularly in protein hydrolysis and fatty acid release, establishing its relevance for bridging *in vitro* and *in vivo* findings (Bohn *et al.,* 2018; Egger *et al.,* 2019). With its high reproducibility, adaptability, and proven correlation with *in vivo* data, the INFOGEST method remains a cornerstone for advancing our understanding of human digestion, nutrient bioavailability, and gut health.

Despite its widespread use, the static INFOGEST model has limitations, such as its inability to replicate the dynamic physiological changes during digestion, including fluctuating gastric pH and enzyme activity over time (Mat *et al.,* 2018). To address these challenges, a semi-dynamic version was developed, incorporating features like progressive acidification, gradual enzyme and fluid addition, and gastric emptying to simulate real-life GI conditions more accurately (Mulet-Cabero *et al.,* 2020).

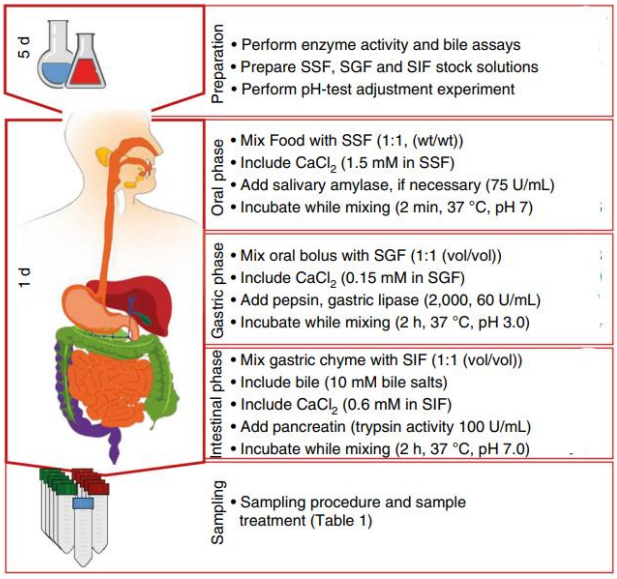

Figure 6. INFOGEST 2.0 protocol (Adapted from Brodkorb *et al.,* 2019)

The expected time (left) and the sequential stages with corresponding steps (right) divided into different phases are shown. SGF (simulated gastric fluid), SIF (simulated intestinal fluid), and SSF (simulated salivary fluid) can be made 1 week prior to the actual *in vitro* digestion process. ($Cacl_2$: Calcium Chloride)

Dialysis Digestion and Absorption Model

In the dialysis digestion model, the intestinal and stomach digestive processes are reproduced in a dialysis membrane bag. The feed is digested with pepsin in an acidic environment in the stomach and then with pancreatin in the intestines using body-temperature buffers. To maintain dynamic conditions, the system uses a circulation pump and a water bath. Following digestion, the bag's content is lyophilized to create fermentation substrates. This model provides a method for modelling the phases of digestion that is both regulated and reproducible (Lo *et al.,* 2022). Another approach can be followed to mimic intestinal absorption in the small intestine. After *in vitro* digestion, the digesta is subjected to dialysis using cellulose membranes for 24 hours under continuous stirring, with periodic water renewal. The dialyzed residues are then freeze-dried for further analysis (Uerlings, *et al.,* 2020).

Dynamic models

Near real dynamic *in vitro* human stomach system (DIVHS)

Based on earlier designs, the near-real dynamic *in vitro* human stomach (DIVHS) system is a sophisticated model. A temperature-controlled environment, a silicone stomach vessel in the shape of a J that resembles the size and shape of a human stomach, and mechanisms for secretion, contraction, and gastric emptying are all part of this system. Motors, rollers, and eccentric wheels are used to simulate contractions; an additional roller system improves the decomposition of food. Tilting angles regulate the exponential model of gastric emptying rates for both solids and liquids, which takes into consideration a lag phase in solids but not in liquids. This model offers a thorough simulation of the movements of the human stomach (Wang *et al.,* 2019).

Engineered Stomach and Small Intestinal (ESIN) system

The ESIN system is a dynamic *in vitro* model which simulates realistic food boluses and mimics differential gastric emptying of liquids and solids, as seen *in vivo*. The system includes six vessels representing the stomach and segments of the small intestine (duodenum, jejunum, and ileum), as well as a meal reservoir and salivary container. Food enters the stomach gradually, where solid particles larger than 2 mm remain for further digestion, while smaller particles and liquids pass into the next compartment through a specialized opening. Two peristaltic pumps simulate gastric emptying based on an exponential model, with solids incorporating a 30-minute lag phase. *In vivo* data are used to replicate temperature, pH variations, secretion flow rates, retention times, and nutrient absorption, enhancing its physiological relevance (Guerra *et al.*, 2016).

Dynamic Gastric Model (DGM)

The Dynamic Gastric Model (DGM) **(Figure 7)**, developed at the Institute of Food Research (Norwich, UK), is a computer-controlled system designed to replicate the stomach's physiological conditions (Wickham *et al.,* 2012; Dupont *et al.,* 2019). It processes real-size chewed meals and simulates key gastric processes, including mixing, meal transit, and the forces exerted in the stomach.

The model mimics three stages of gastric digestion:

1. **Proximal stomach**: Ingestion and rhythmic massaging; acid and enzyme secretions
2. **Antrum**: Simulating physiological shear and grinding forces.
3. **Duodenum**: Representing the first part of the small intestine (Bornhorst and Singh, 2012).

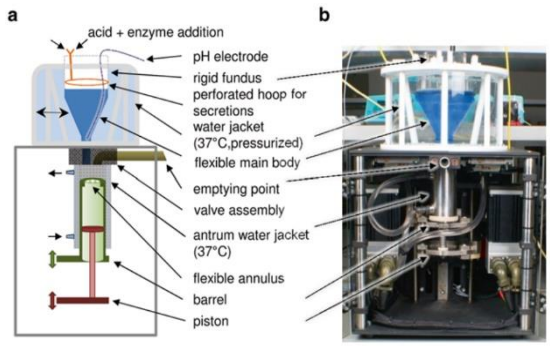

Figure 7. The dynamic gastric model (DGM). (a) Main components (b) DGM image (Adapted from Verhoeckx *et al.,* 2015))

Food disintegration is achieved through a stationary outer tube and a mobile inner tube. Parameters such as temperature, transit time, and the flow rates of acid, salts, and enzymes are precisely controlled to match physiological conditions. The system generates cyclical mixing (0.05 Hz) and mimics antral sieving, enabling data collection on emptying profiles, particle size reduction, and mass transfer. However, it does not accurately replicate peristaltic movements, is not transparent and fundus is always exposed to air (Liu *et al.,* 2019b; Verhoeckx *et al.,* 2015).

Human Gastric Simulator (HGS)

The Human Gastric Simulator (HGS) **(Figure 8)**, an *in vitro* model for food digestion diagnosis, has been devised to recreate the fluid mechanical conditions driving the disintegration and mixing of gastric contents, secretions, and emptying rates (Kong and Singh, 2010). The system comprises a latex flexible stomach reservoir, a roller-driven mechanical assembly for contractions, and systems for temperature control (37 ^{0}C), secretion,

and emptying. Peristaltic movements are generated by 12 rollers steered by a motor, while adjustable secretion flow rates and temperature allow realistic simulation of gastric conditions. Contents are emptied through a pylorus-like mechanism to mimic *in vivo* processes (Kong and Singh, 2010).

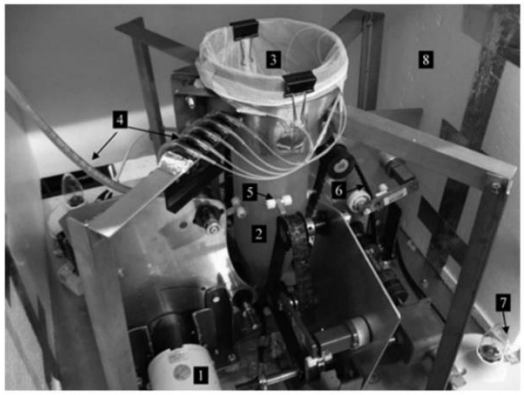

Figure 8. Human gastric simulator. (1) Motor (2) Gastric compartment (3) Mesh bag (4) Simulating secretion tubes (5) Tefl on roller set (6) Conveying belt (7) Insulated chamber. Adapted from Kong and Singh, 2010)

An improved version, the IHGS (Improved Human Gastric Simulator), enhances the simulation of the stomach's shape, contour, contractions, and other physical parameters, providing more accurate replication of human gastric dynamics (Dupont *et al.,* 2019).

Dynamic Gastric Simulation Model (DGSM)

The Dynamic Gastric Simulation Model (DGSM), developed by Chen *et al.* (2011) replicates gastric digestion by simulating compressive forces, secretions, and gastric emptying. An insulated acrylic jar with a PVC probe connected to a texture analyser makes up the model. The probe's up-and-down motions simulate gastric contractions, compressing the meal and producing particles smaller than 2 mm. Three cycles per minute are involved in this process. Mini pumps with variable flow regulate gastric secretions and emptying, guaranteeing an accurate representation of digestive processes (Tran Do *et al.,* 2016).

Gastric Digestion Simulator (GDS)

The Food Research Institute, NARO, created the human GDS to mimic the digestive functions of an antrum. A roller system for imitating antral contraction waves, a temperature control system, and a gastric compartment with trapezoidal geometry that resembles the human antrum are all elements of the device. Rollers are moved over the deformable sidewalls at regulated speeds and frequencies to produce progressive contractions. Through a glass window, food degradation may be visibly observed, and digestive processes can take up to 180 minutes. Systems for gastric secretion and emptying are included in a continuous version (c-GDS), which improves its dynamic capabilities (Kozu *et al.,* 2014).

Artificial gastric digestive system (AGDS)

AGDS uses 3D digital technology to replicate the structure and form of the human stomach. The technology used a pH-stat workstation to control pH and symmetrical and opposing rollers to simulate stomach peristalsis. Parameters such as force, pepsin and gastric juice secretion, gastric emptying, and pH changes were tracked and validated. The digestion of α-lactalbumin was compared across the AGDS, static, and semi-dynamic models, revealing differences in protein hydrolysis, peptide morphology, and amino acid accumulation. The AGDS, validated through mechanical and digestion experiments, demonstrated its potential as a dynamic gastric digestion model, offering accurate and reliable protein digestion profiles for food development applications (Liu *et al.,* 2019).

***In vitro* Dynamic System (DIDGI®)**

The DIDGI® system **(Figure 9)**, developed at the French National Institute for Agricultural Research (INRA, Rennes, France), simulates the stomach and small intestine using two glass-jacketed vessels. These vessels are maintained at physiological temperature using water pumped from a temperature-controlled bath. A Teflon membrane with 2 mm holes is positioned between the gastric and intestinal compartments to mimic the pyloric sieving effect. The system allows precise control of temperature, pH, meal flow rate, digestive secretions, and emptying rates for each compartment through computer simulations based on *in vivo* data. By contrasting the *in vitro* proteolysis kinetics with the *in vivo* data gathered on piglets, the new system was verified. The findings demonstrated the physiological significance of the recently created system and demonstrated a strong connection between *in vitro* and *in vivo* data (de La Pomélie *et al.,* 2019; Ménard *et al.,* 2014).

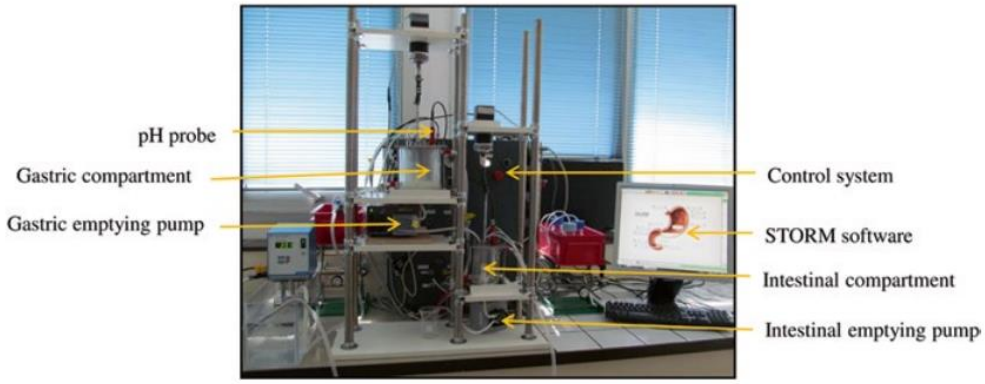

Figure 9. DIDGI system (Adapted from Verhoeckx *et al.,* 2015)

1.3.2. Fermentation models

Artificial Colon (ARCOL)

The artificial colon (ARCOL) is a fermenter designed to replicate the human colonic environment, simulating key factors such as pH, body temperature, ileal effluent supply, retention time, anaerobic conditions, and the absorption of water and fermentation metabolites. Healthy human faeces are used as inoculum, prepared under anaerobic conditions with N_2 gas. The system operates at 37°C with a pH of 6.3 and a mean retention time of 36 h. Nutrient mixtures mimicking ileal effluents are introduced to sustain fermentation. A dialysis system with hollow fiber membranes simulates *in vivo* electrolyte and metabolite concentrations, maintaining a realistic fermentation process (Cordonnier *et al.,* 2015).

Simulator of the Human Intestinal Microbial Ecosystem (SHIME®)

The SHIME® system, developed at Ghent University-Prodigest (Belgium), replicates the microbial ecosystem of the GI tract (Molly *et al.,* 1993). The stomach, small intestine, and the three primary sections of the large intestine (the descending, transverse, and ascending colons) are represented by the five reactors that make up this structure. With peristaltic pumps regulating content transfer and the addition of digestive fluid, the first two reactors use a fill-and-draw mechanism to mimic stomach acidity, pepsin digestion, and small intestinal digestion. Based on *in vivo* data, the final three reactors maintain controlled transit times and pH levels while simulating colonic areas by constant stirring using magnetic stirrers.

After digestion in the gastric and intestinal compartments, the slurry is transferred to the ascending colon vessel, where colonic digestion begins. The contents of the three colon compartments are continuously stirred, with strict regulation of volume and pH. Retention times in the upper digestive tract can be adjusted by modifying the flow rates from the gastric and intestinal compartments. In contrast, retention times in the colon compartments are primarily controlled by altering the compartment volume. The system operates at 37°C under anaerobic conditions, secured by flushing with N_2 gas daily, and uses fecal microbiota to mimic the metabolic processes of the gut. Depending on the specific human target group being studied, the retention time can range from 24 to 72 h. The conventional SHIME® setup lacks dialysis for nutrient absorption, peristalsis for natural motility, and host cells for simulating host-microbe interactions, though these limitations can be addressed with dialysis model and the Host Microbiota Interaction module (Ceuppens *et al.,* 2012; Possemiers *et al.,* 2013; Marzorati *et al.,* 2014). Advancements of SHIME® include:

- **M-SHIME® (Mucus-SHIME):** Integrates a mucosal compartment in the colonic regions to assess the selective adhesion of microorganisms to the mucus layer, a critical barrier against pathogens (Van den Abbeele *et al.,* 2013).
- **TWINSHIME®:** Runs two identical SHIME® systems in parallel for direct comparison of different samples under identical conditions (García-Villalba *et al.,* 2017).
- **Baby-SPIME:** To study gut microbiota of weaning piglets (Dufourny *et al.,* 2019)

The SHIME® model can simulate disease conditions, such as inflammatory bowel disease, through specific protocols (Dupont *et al.,* 2019). Its main strength lies in the inclusion of human microbiota for studying host-microbiota interactions. However, limitations include the absence of dialysis modules for nutrient absorption and reliance on magnetic stirrers rather than peristaltic mixing, which may reduce the physiological accuracy of digestion processes (Liu *et al.,* 2019).

TNO GI model (TIM)

The *in vitro* GI model (TIM) **(Figure 10)**, developed at the TNO Nutrition and Food Research Centre in the 1990s, is a computer-controlled, multi-compartmental dynamic system that simulates the GI environment. It includes glass units representing the stomach, duodenum, jejunum, and ileum, with flexible membranes to simulate peristalsis and adjustable temperatures for body-like conditions. All secretion flows can be programmed over time, and digestion products are removed through two systems: water-soluble products are extracted *via* dialysis membranes with an approximate 10 kDa molecular weight cutoff, connected to the jejunal and ileal compartments. Simulation protocols have been tailored for young, adult, and elderly humans, as well as for dogs, pigs, and calves, following the ingestion of various types of meals.

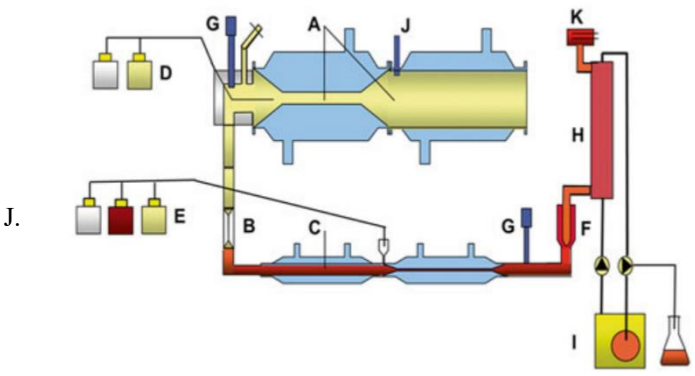

J.

Figure 10. TinyTIM, equipped with a dialysis membrane. A. gastric compartment; B. pyloric sphincter; C. duodenal compartment; D. gastric secretion; E. duodenal secretion; F. pre-filter; G. pH electrodes; H. dialysis membrane; I. dialysis system; pressure sensor; K. level sensor (Adapted from Verhoeckx *et al.,* 2015**)**

Several TIM models exist for different applications:

- **TIM-1** simulates the upper GI tract with 4 compartments (Liu *et al.,* 2019).
- **TIM-2** focuses on the colon to study fermentation (Liu *et al.,* 2019).
- **Tiny TIM** high-capacity version of TIM-1 with fewer compartments (Liu *et al.,* 2019).
- **TIM-agc** features an advanced gastric model (Bellmann *et al.,* 2016).

TIM systems are widely used in food and pharmacological research to study the bio-accessibility of macro nutrients, minerals, fat- and water-soluble vitamins, and bioactive compounds and drug release and absorption under various conditions, including age, health status, and disease. Although TIM-1 and TIM-2 complement each other as upper and lower GI tract models, they operate independently.

Simulator of the GI Tract (Simgi®)

The Simgi® system **(Figure 11)**, developed at the Institute of Food Science Research (Madrid, Spain), is a dynamic model designed to replicate GI digestion and colonic fermentation. It consists of five compartments simulating the stomach, small intestine, and the ascending, transverse, and descending colon. The stomach section includes a flexible silicone container surrounded by rigid plastic vessels, with peristaltic movements simulated by water at 37°C pumped through a jacket between the modules (Barroso *et al.,* 2015).

Digestive secretions, temperature, pressure, and emptying rates are computer-controlled, with gastric emptying following an exponential equation. The remaining compartments operate under anaerobic conditions, with continuous stirring and controlled pH to mimic colonic environments. Sampling points in each compartment allow for biochemical and microbiological analyses. The system effectively combines peristaltic contractions and chyme transit behaviours for realistic simulations of gastric and intestinal processes (Miralles *et al.,* 2018).

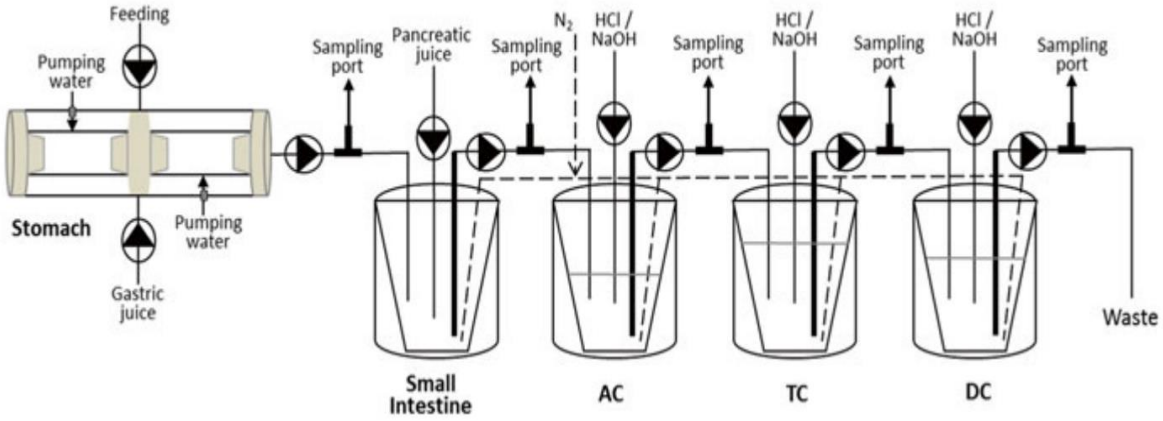

Figure 11. Schematic representation of SIMulator Gastro-Intestinal SIMGI (Adapted from Barroso *et al.,* 2015).

1.3.3. Complex Epithelial Cell Culture models (Insert/Transwell based)

In vitro digestion and fermentation models provide valuable insights into the breakdown and microbial transformation of dietary components. However, to further assess their physiological relevance, *in vitro* cell culture models are essential for evaluating cellular responses, including barrier integrity, immune modulation,

and nutrient absorption. This section explores the application of cell culture models in studying gut health, complementing the insights gained from digestion and fermentation systems.

Coculture

Caco-2/HT-29 and Caco-2/LS174T

The intestinal epithelium comprises diverse cell types, but absorptive enterocytes and mucus-secreting goblet cells, constitutes two major cell types for maintaining homeostasis. However, traditional monoculture models like Caco-2 cells, which differentiate into enterocytes with brush border enzymes, fail to capture the complexity of the epithelial layer, particularly the mucus barrier essential for physiological relevance (Hidalgo 1996; Atursson *et al.,* 2001). To overcome these limitations, co-cultivation of Caco-2 and HT-29-MTX cells has been developed, integrating enterocyte-like functionality with mucus production provided by HT-29-MTX cells. The co-culture protocol involves growing Caco-2 and HT-29MTX cells separately, mixing them in ratios of 90:10 to 75:25 (Caco-2/HT-29-MTX), and seeding them onto inserts. Co-cultures can then be used between days 21 and 25 for experiments such as permeability assessments and bacterial adhesion studies (Verhoeckx *et al.,* 2015). This model is particularly advantageous for studying nutrient and drug transport, as well as microbial interactions, as the mucus layer secreted by HT-29-MTX cells provides a biochemical and physical barrier, enhancing physiological relevance (Johansson *et al.* 2008; Shah *et al.,* 2006).

The Caco-2/LS174T co-culture model combines enterocyte-like Caco-2 cells with another mucus-secreting LS174T cell line to investigate cell-type-specific mucin expression mechanisms and mucin expression in colon cancer. However, the characterization of mucus secretion in this model presents challenges, as both Caco-2 and LS174T cell lines express MUC5AC mRNA, with Caco-2 showing the highest levels. Additionally, LS174T secretes MUC2, while Caco-2 does not (Cordonnier *et al.,* 2015; Van Klinken *et al.,* 1996).

Caco-2 and Dendritic Cells (DCs)

This model focuses on the interaction between epithelial cells and dendritic cells (DCs), which play a critical role in regulating innate and adaptive immune responses. Caco-2 cells are seeded on the apical of the filter inserts with 3 μm pores, while CD14+ monocyte-derived DCs on the basolateral side or they are both grown together in contact on basolateral. Monocytes are differentiated into DCs by stimulation with GM-CSF and IL-4, mimicking inflammatory DC phenotypes. The model enables the study of both contact-dependent or soluble factor-mediated interactions, elucidating mechanisms of antigen presentation and immune modulation (Segura *et al.,* 2013).

Caco-2 and Raji B Cells

This model was designed in 1997, to induce M cell-like phenotypes in epithelial cells, which are specialized for antigen sampling in the follicle-associated epithelium (FAE). Caco-2 cells are co-cultured with Raji B cells, leading to the formation of M-cell-like structures with reduced glycocalyx and microvilli, and enhanced phagocytic and transcytotic capabilities (Kernéis *et al.,* 1997). This system is used to study the translocation of antigens and bacteria across the epithelial barrier and their delivery to underlying immune cells, mimicking Peyer's patches in the gut-associated lymphoid tissue (Gullberg *et al.,* 2000). However, the limitation is that they it lacks mucus producing cells.

Caco-2 and Peripheral Blood Mononuclear Cells (PBMCs)

The Caco-2/PBMC co-culture model investigates the interaction between epithelial cells and circulating immune cells, focusing on cytokine signalling and immune activation. PBMCs are plated in the basolateral compartment of polarized Caco-2 monolayers, with or without prior activation using anti-CD3/CD28 or mitogenic lectins. This model is particularly useful for studying soluble factor-mediated crosstalk and the impact of epithelial TLR signalling on immune cell behaviour (de Kivit *et al.,* 2011).

Caco-2 and U937/THP-1 Monocytes

Differentiated U937/ THP-1 monocytes are co-cultured with polarized Caco-2 monolayers to study cytokine production, immune signalling, and epithelial response to inflammatory stimuli. U937 is a human monocytic cell line widely used to study immune responses, differentiation, and inflammation, and when differentiated with PMA into macrophages, it secretes a wide range of cytokines and chemokines either constitutively or in response to specific stimuli. (Lehmann, 1998). THP-1 cells are activated with IL-4, GM-CSF, TNFα, and ionomycin, simulating an inflammatory environment. This setup is particularly valuable for investigating gene expression changes and immune signalling pathways (Ishimoto *et al.*, 2011).

Caco-2 and Soluble Factors

This configuration separates Caco-2 cells and immune cells using filter inserts to prevent direct contact, allowing communication solely through soluble factors. Epithelial cells are seeded on 0.4 µm filters, while immune cells (e.g., U937) are cultured in the basolateral compartment. This model helps isolate and study the effects of secreted cytokines, chemokines, and other signalling molecules in the epithelial-immune cell crosstalk.

Triple cell culture

Caco-2/HT-29-MTX/Raji

Intestinal epithelial cell culture models, such as Caco-2 cells, are widely used to evaluate drug absorption and nanoparticle transcytosis across the intestinal mucosa. However, the presence of mucus and the role of specialized M cells significantly influence nanoparticle mobility and uptake. Therefore, this study developed a triple co-culture permeability model incorporating Caco-2 cells, mucus-secreting goblet cells, and M cells. Caco-2 and goblet cells were co-cultured on Transwell® inserts, and Raji B cells were introduced to the basolateral chamber **(Figure 12)** to induce M cell differentiation. Since there are no dedicated M cell lines and primary M cells are difficult to isolate, differentiation of enterocytes into M-like cells is required. This can be achieved using epithelial cell lines, such as the C2BBE1 clone of Caco-2 cells, seeded on the upper surface of Transwell® inserts. This model provides a more physiologically relevant platform for studying nanoparticle interactions with the intestinal mucosa (Schimpel *et al.,* 2014; Kesisoglou *et al.,* 2010; Corr *et al.,* 2006).

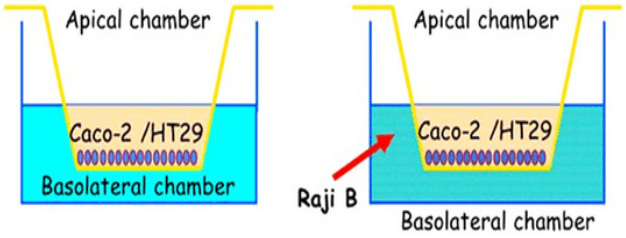

Figure 12. Triple cell culture of Caco-2/HT-29/Raji B cells using an insert.

Caco-2/HT-29-MTX/THP-1 or Caco-2/HT-29-MTX/RAW 264

The Caco-2/HT-29-MTX/THP-1 or Caco-2/HT-29-MTX/RAW 264.7 tri-culture models involve growing Caco-2 and HT-29-MTX cells on inserts with semipermeable membranes, with macrophage cell lines (THP-1 or RAW 264.7) in the basolateral compartment, where inflammatory stimuli are introduced. Both macrophage types use the same culture medium (RPMI 1640), but they differ in growth behaviour: THP-1 cells grow in suspension, while RAW 264.7 cells are adherent. These models have been shown to mimic the intestinal barrier's response during gut inflammation, as evidenced by a decrease in TEER and cytokines alterations (Taciak *et al.,* 2018; Berghaus *et al.,* 2010; Haddad *et al.,* 2023).

Caco-2/ HT-29-MTX/ HMVEC-d

On the apical side, Caco-2 and HT-29-MTX cells are co-seeded at a 3:1 ratio, cultured for 21 days, allowing for the differentiation of Caco-2 cells (Hubatsch *et al.,* 2007). Human Microvascular Endothelial Cells (HMVEC-d) are seeded on the basolateral side of the inverted Transwells on day 0 at 2×10^4 cells per insert, ensuring attachment by incubating the inverted plates at 37°C and 5% CO_2 for two h. HMVEC-d cells, derived from human dermal microvascular endothelial cells, are isolated from small vessels within the skin. These cells are widely used as a model for endothelial cell function and have been employed in studies of vascular biology and tissue-engineered models (Maschmeyer *et al.,* 2015; Schimek *et al.,* 2013). In triple cell culture systems, HMVEC-d cells contribute to mimicking the endothelial layer, enhancing the physiological relevance of *in vitro* intestinal models. After inversion back to the standard orientation, HMVEC-d cells are maintained in HMVEC-d medium. This model offers a physiologically relevant system for studying the interplay between epithelial and endothelial layers in the intestinal barrier (Grouls *et al.,* 2022).

3D-Flipwell Co-Culture Model for Gut Mucosal Microenvironment

A novel 3D-Flipwell system **(Figure 13),** replicating the stratified structure of microbiota, semi-permeable mucus, epithelial cells, and an underlying layer of immune cells, providing a robust *in vitro* model for investigating complex crosstalk.

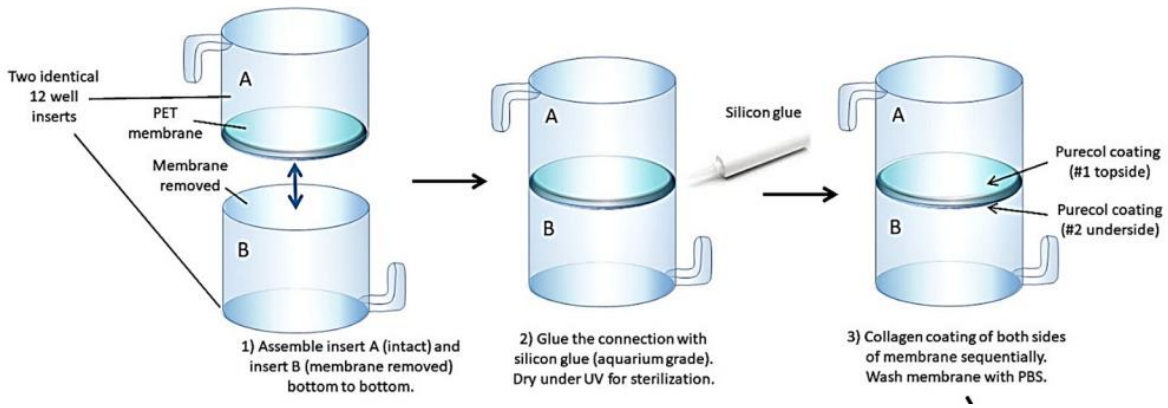

Figure 13. Schematic of the 3D Flipwell assembly (Adapted from Beamer *et al.,* 2023)

The 3D-Flipwell is constructed by joining two 0.4 µm polycarbonate membrane inserts bottom-to-bottom using silicone sealant. The system is assembled under sterile conditions and rigorously tested for sterility and leakage. The membrane is coated with a mix of PureCol and Poly-d-Lysine to promote cell adhesion on both sides. The upper membrane is seeded with colon epithelial cells (Caco-2 and HT-29-MTX in a 9:1 ratio) and

cultured for 7–10 days to allow polarization and mucus formation. Subsequently, the Flipwell is inverted, and THP-1 cells are seeded on the underside insert and differentiated into macrophages using PMA (100 ng/µL). After macrophage differentiation, the Flipwell is returned to its original orientation, with epithelial cells on top and macrophages at the bottom.

The 3D-Flipwell allows simultaneous analysis of bacterial co-culture, drug treatments, and the synchronous effects of stimuli on gut bacteria, mucus, epithelial cells, and immune cells. Its flexibility makes it suitable for advanced studies using confocal and electron microscopy to investigate cellular and molecular mechanisms underlying gut health and disease (Beamer *et al.,* 2023)

Quadricellular model (Caco-2/HT-29-MTX/NCI-H716/Raji-B)

The Caco-2/HT-29-MTX/NCI-H716/Raji-B quadricellular model represents a complex *in vitro* system designed to study the intestinal barrier, incorporating multiple cell types that contribute to its protection. NCI-H716 (human colourectal adenocarcinoma origin), cells are incubated for 48 h on Matrigel-coated Transwell inserts to induce differentiation. Next, Caco-2 and HT-29-MTX cells are seeded on the apical side at an 80:10:10 ratio (Caco-2/HT-29-MTX/differentiated NCI-H716). After 14 days, Raji B cells are introduced into the basolateral compartment to differentiate Caco-2 cells into M cells. The system can be maintained for 7 days before testing. However, this advanced model, like other static *in vitro* models, it does not account for microbiota interactions, which remain essential for a comprehensive understanding of gut physiology (Gautier *et al.,* 2022).

While these cell culture models provide valuable insights into intestinal physiology, barrier function, and immune responses, they also present notable limitations. These models are based on human cancer-derived cell lines, which may not fully recapitulate the complex architecture, differentiation patterns, and immune environment of the porcine intestinal epithelium. Moreover, the lack of dynamic factors such as peristalsis, vascularization, and native mucus composition can restrict their physiological relevance. To overcome these challenges, other models using primary cell culture**,** intestinal organoids derived from piglet tissues, and organ-on-chip platforms offer promising alternatives. These advanced models better mimic the three-dimensional structure, cellular diversity, and mechanical forces of the *in vivo* intestinal environment, providing more predictive and translational insights.

Organoids

Porcine intestinal organoids (PIOs) are three-dimensional (3D) polarized structures capable of self-organization and self-renewal, closely mimicking the architecture and function of native intestinal tissue. Comparative transcriptome analyses have shown that PIOs are more physiologically similar to *in vivo* epithelial tissues than immortalized cell lines like IPEC-J2 (Hee *et al.,* 2020). Developed by embedding intestinal crypts in a laminin-rich 3D matrix such as Matrigel and supplemented with key growth factors (Wnt3a, R-spondin1, Noggin) (Feng *et al.,* 2011), PIOs form villus- and crypt-like domains and can be cryopreserved and resuscitated for long-term studies (Derricot *et al.,* 2019). PIOs are increasingly used to study pathogen–host interactions, nutrition, and drug discovery, owing to the anatomical and genetic similarities between pigs and humans. However, limitations such as difficulties in long-term passaging, loss of 3D structure in monolayer cultures, absence of immune and vascular components, and reliance on Matrigel remain challenges. The future development of porcine stem cell-derived organoids and synthetic matrices offers potential for improving model reproducibility and expanding their applications in translational research (Ma *et al.,* 2022).

Organ-on-a-chip

Organ-on-a-chip technology offers a new approach to better replicate intestinal physiology *in vitro*. In a recent study, porcine intestinal organoids were integrated into a microphysiological system combining dynamic flow, peristaltic-like stretch, and co-culture with human intestinal microvascular endothelial cells. The resulting jejunal chip formed villi-like 3D structures, maintained tight junctions (F-actin, ZO-1, E-cadherin), and differentiated into major intestinal epithelial lineages including enterocytes, goblet cells, and enteroendocrine cells. Functional characterization revealed active drug transporters (P-gp, PEPT1) and CYP3A metabolic activity, confirming the chip's suitability for absorption, metabolism, and barrier function studies. Importantly, the model maintained a tight epithelial barrier that could be reversibly modulated by permeability enhancers like sodium caprate (C10). Compared to traditional static organoid cultures, this organ-on-a-chip system provides a dynamic and more physiologically relevant platform for studying porcine intestinal biology and for applications in drug development and permeability testing (Bacon *et al.*, 2024).

There is a growing need for physiologically relevant *in vitro* models that can accurately mimic the gastrointestinal environment of weaning piglets. This is crucial not only to better understand the mechanisms of action of dietary bioactives but also to reduce reliance on *in vivo* experimentation, aligning with ethical and economic considerations. To address this need, several *in vitro* models need to be adapted and combined to make it physiologically relevant. Models such as INFOGEST, dialysis-based absorption models, and batch fermentation using piglet fecal inoculum could be integrated. These models have already been successfully validated individually and applied in pig-related studies, supporting their suitability for simulating the digestive and microbial phases in piglets. Nevertheless, a key gap remains in the development of truly porcine-specific complex cell culture systems, which could better reflect piglet-specific immune signaling and barrier functions. Due to the lack of well-established porcine mucus-producing intestinal epithelial cell lines, a human coculture model (Caco-2/HT-29-MTX) integration with immune cells (U937) could represent the intestinal epithelium, mucus layer, and immune interactions. While this model is human-derived, it was selected based on the high physiological similarity between piglet and human gastrointestinal physiology during the early life stage. The integration of emerging technologies such as porcine intestinal organoids, primary epithelial cell cultures, or engineered co-culture systems would also greatly enhance the translational value of *in vitro* models in the future.

In summary, this review of literature highlights the complex interplay between dietary, microbial, and immunological factors affecting gastrointestinal health in weaning piglets. The gastrointestinal tract during this critical period is particularly vulnerable to dysfunction due to abrupt dietary transitions, immature immune responses, and shifts in microbial composition—factors that collectively compromise barrier integrity and increase disease risk. With the regulatory phase-out of in-feed antibiotics and pharmacological levels of zinc oxide in the European Union, there is an urgent need for alternative, sustainable strategies to maintain intestinal health. Prebiotic compounds such as inulin and chicory-derived bioactives have shown promise in supporting gut function through microbiota modulation, improved barrier function, and anti-inflammatory activity. Nevertheless, challenges such as seasonal variability in chicory cultivation, environmental sensitivities, and evolving regulatory frameworks must be addressed. Concurrently, the development of physiologically relevant and standardized *in vitro* models offers a promising avenue to reduce animal use in research, though current models still fall short of fully mimicking the complexity of the *in vivo* gut environment. Thus, an integrated approach combining nutritional strategies, regulatory awareness, and innovative methodological frameworks is essential to advance effective and ethically responsible solutions for improving gut health in piglet production systems.

2

Objectives and Experimental outline

2.1. Objectives

Based on the existing knowledge and the gaps identified, this thesis aimed to investigate two core research questions: (1) whether crude chicory flour, containing a broader range of bioactive compounds beyond inulin, provides added benefits over pure inulin in supporting gut health, and (2) whether a physiologically relevant *in vitro* approach can effectively mimic *in vivo* conditions and reduce the need for animal experiments. We hypothesized that crude chicory would improve gut health outcomes more effectively than inulin alone, particularly in terms of intestinal permeability, immune modulation, and microbial composition. Additionally, we expected that the integrated *in vitro* models would provide comparable insights to *in vivo* studies, offering a reliable and ethical alternative for evaluating the effects of dietary bioactives on intestinal health.

The gastrointestinal (GI) tract is a complex organ system that serves as the main site for nutrient digestion and absorption while also acting as a multi-layered barrier to protect the host from harmful substances. Weaning can disrupt the porcine gastrointestinal (GI) tract, leading to leaky gut, imbalance of microbiota and chronic inflammation. Inulin is well known for its positive impact on porcine gut health by promoting the growth of beneficial bacteria that potentially reduce inflammation. While crude *Cichorium intybus*-extracted inulin improves gut health, its extraction is costly and certain bioactives such as polyphenols, sesquiterpene lactones, essential oils, are removed. Therefore, the first objective **(Chapter 3)** of this thesis was:

I. To compare the effect of inulin and crude chicory flour on the intestinal permeability, inflammation, and microbiota of weaning piglet.

This objective investigates the effects of inulin and crude chicory flour on zootechnical performances, intestinal permeability, inflammation, and microbiota in weaning piglets, focusing on the potential role of bioactive components in chicory beyond inulin. The study also aimed to optimize parameters such as inulin dosage and employing an innovative three-sugar test to evaluate gut permeability, ensuring precise assessment of intestinal barrier function. Treatments were equated for inulin content to enable a direct comparison of their effects, offering insights into chicory's broader contributions to gut health.

Unlike rodent models where high-fat diets are used to induce gut dysfunction, weaning piglets already experience substantial intestinal stress due to abrupt dietary changes, immature immunity, and microbiota shifts. Introducing a high-fat diet in this context was unnecessary and could have added confounding effects. Additionally, high-fat inclusion does not align with nutritional regulations for piglet diets. This study aimed to evaluate the direct effects of inulin and chicory under physiologically relevant and nutritionally appropriate conditions.

Additionally, considering the ethical and economic concerns regarding the use of experimental animals post-weaning to test these bioactives, there is a growing demand for alternative cost-effective *in vitro* methods. There are models that can mimic *in vivo* environments, enabling the study of gut-related diseases characterized by barrier dysfunction, inflammation, or infection. A model is a simplification of reality, providing valuable insights but with inherent limitations. Enhancing models continually is crucial to better capture the complexities of real-world systems and improve their predictive accuracy. Therefore, the second objective **(Chapter 4)** of the thesis was:

II. To develop and combine new alternative *in vitro* methods (e.g., digestion-absorption-fermentation with cell culture) that can replace the use of experimental animals when testing bioactive molecules for intestinal animal health or against diseases.

In vitro studies investigating the effects of bioactives on the gastrointestinal tract of weaning piglets often omit standardized digestion and absorption steps prior to fermentation, resulting in inconsistencies across methodologies (Boudry *et al.,* 2012; Logtenberg *et al.,* 2020; Pham *et al.,* 2018; Tran *et al.,* 2016). Therefore, to study this objective we used a combined approach of the *in vitro* digestion (INFOGEST), absorption (dialysis) and fermentation (batch fermentation) protocols with a triple cell culture model. The INFOGEST protocol was selected because it has been validated for its physiological relevance in pigs. Its standardized nature makes it suitable for reproducible and comparable *in vitro* digestion studies (Egger *et al.,* 2017).

Key optimizations were planned to be implemented to ensure physiological relevance and comparability with *in vivo* conditions, including the use of feces from 21-day-old piglets to simulate the post-weaning gastrointestinal environment and the inclusion of mucins during fermentation to replicate the intestinal mucus layer. First goal within this framework was to show how digestion and dialysis can affect the overall results when compared to non-digested and non-dialyzed samples. Secondly, the objective was to use a complex cell culture model to mimic the intestinal epithelium, mucus, and immune response, enabling a more precise assessment of gut health interventions. These objectives aim to serve dual purpose of addressing weaning challenges by investigating bioactive compounds' effects on gut health and developing innovative *in vitro* approaches to advance intestinal research.

2.2. Experimental outline

The two *in vivo* experiments concerning to first objective were performed in ULiège, Gembloux Agro-Bio Tech, Belgium. The *in vitro* digestion, absorption and fermentation was conducted in Gembloux while testing of the fermentation supernatant on the triple cell culture model was done in ULille in France. The intestinal barrier comprises physical (intestinal epithelium), biochemical (antimicrobial peptides, mucus), immunological (gut-associated lymphoid tissue with B cells, T cells, dendritic cells, and neutrophils) and microbial barrier to play critical roles in maintaining homeostasis. The focus was on three different levels related to gut homeostasis:

I. Gut permeability,

II. The fermentation processes of the gut microbiota,

III. The immune response of the host.

Figure 14 outlines a comprehensive approach that uses *in vivo* and *in vitro* methods to study intestinal health. *In vivo* permeability determination was conducted to assess intestinal barrier integrity, while intestinal content samples were collected for microbiota and metabolite analysis, and ileum and colon tissues were examined for detailed intestinal assessments. The *in vitro* component included a static fermentation model to simulate microbial activity and a tri-cell culture system (Caco-2, HT-29, and macrophages) to mimic the intestinal epithelium, goblet cells, and immune components, respectively.

The integration of these methods allowed the determination of metabolites and microbiota, along with immune response analysis through gene expression profiling (using high throughput/Fluidigm) and cytokine release (ELISA).

The purpose was also making three different comparisons between *in vivo* and *in vitro* model these three levels **(Figure 14)** using integrative analysis (RGCCA) to compare it in the following manner **(Chapter 5):**

I. *In vivo* gut permeability compared to *in vitro* cell-based permeability determinations.

II. *In vivo* data of digestion-fermentation (metabolites and microbiota) compared to an *in vitro* static fermentation model.

III. *In vivo* data of the immune response compared to *in vitro* cell culture models.

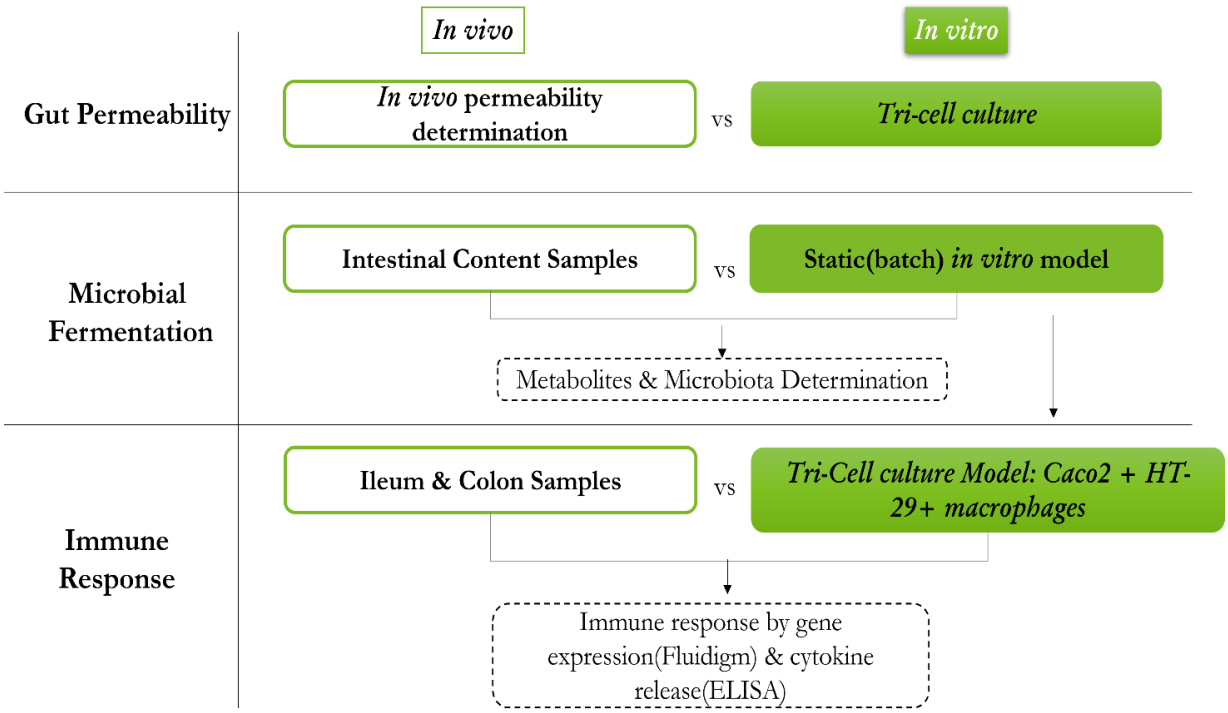

Figure 14. Experimental outline for the Ph.D. (Non-shaded boxes-Accomplished in ULiège and Shaded -in Ulille)

3

A comparative study of the effects of crude chicory and inulin on gut health in weaning piglets

(Article I)

A comparative study of the effects of crude chicory and inulin on gut health in weaning piglets

Tushar Kulkarni[a,b], Pawel Siegien[a], Luke Comer[c], Jimmy Vandel[e], Gabrielle Chataigne[b], Aurore Richel[a], José Wavreille[d], Benoit Cudennec[b], Anca Lucau[b,f], Nadia Everaert[c], Rozenn Ravallec[b,*], Martine Schroyen[a,b,*]

a. Precision Livestock and Nutrition Laboratory, TERRA Teaching and Research Centre, Gembloux Agro-Bio Tech, University of Liège, 5030 Gembloux, Belgium
b. UMR-T 1158, BioEcoAgro, University of Lille, University of Liege, 59650 Lille, France
c. Nutrition and Animal Microbiota EcoSystems lab, Division of A2H, Department of Biosystems, KU Leuven, 3001 Leuven, Belgium
d. Walloon Agricultural Research Centre, 5030 Gembloux, Belgium
e. US 41 - UAR 2014 – PLBS – Bilille platform, Univ. Lille, CNRS, Inserm, CHU Lille, Institut Pasteur de Lille, 59000 Lille, France
f. Joint Laboratory CHIC41H University of Lille-Florimond-Desprez, Cité scientifique, 59655 Villeneuve d'Ascq, France

*Corresponding authors at : Université de Liège - Gembloux Agro-Bio Tech, Département AgroBioChem - Animal Sciences, Passage des Déportés, 2, 5030 Gembloux, Belgium ; University of Lille - IUT A, Polytech Building, Lille, Scientific City, 59655 Villeneuve d'Ascq, France
Email adresses : martine.schroyen@uliege.be (M. Schroyen) and rozenn.ravallec@univ-lille.fr (R. Ravallec).

This chapter is adapted from the article published in Journal of Functional Foods:

Tushar Kulkarni, Pawel Siegien, Luke Comer, Jimmy Vandel, Gabrielle Chataigne, Aurore Richel, José Wavreille, Benoit Cudennec, Anca Lucau, Nadia Everaert, Rozenn Ravallec, Martine Schroyen. 2024. A comparative study of the effects of crude chicory and inulin on gut health in weaning piglets. Journal of Functional Foods, Volume 123. doi.org/10.1016/j.jff.2024.106578

3.1. Abstract

Dysfunction of the host-microbial balance and an impaired intestinal barrier can trigger inflammation and increase the antigen penetration. Inulin, commonly extracted from chicory root, is a prebiotic beneficial to gut health. The objective of this study was to compare the effect of chicory flour to inulin on gut health, few weeks after weaning. Two dose-dependent experiments (E1 and E2) were performed sequentially, each consisting of 80 castrated male piglets, weaned at day 21 and subsequently divided in 3 groups with *ad libitum* feed: control (Ctrl), inulin (INU) and crude chicory flour (CHI). For INU and CHI groups, a daily supplementation with the equated 'inulin content' increasing weekly was done by oral force-feeding, while the Ctrl groups received an isotonic sucrose solution. For E1, these doses were 1.5g/day, 2g/day, and 2.5g/day in W1, W2 and W3, respectively. For E2, these doses were 3g/day, 4g/day, and 5g/day in W1, W2 and W3, respectively. For each experiment at W0, W1 and W3, eight piglets per group were euthanized to assess gut structural and functional parameters. In E1, the CHI had lower average daily calorie intake (kcal/day) only at W3, while in E2 it was consistently lower than Ctrl and INU. In W3 of E2, CHI showed improved villi-to-crypt ratio and lower diarrhoea occurrence than INU and Ctrl. Both supplemented groups in E2 showed higher butyrate production and lower D-xylose permeability (W3), compared to Ctrl. Interestingly, in E2, CHI had a more dominant effect on increasing the abundance of health promoting genera like *Catenisphaera*, *Butyricoccus*, etc. and decreasing harmful genera like *Erysipelotrichaceae_UCG-002* and *Turicibacter*. In E2, on W3 several inflammatory target genes (*CXCL10, IL18, TNFα*) and inflammation signalling genes (*MyD88, NFκB1*) were downregulated in ileum of INU and CHI. In colon, both chicory and inulin, proved to be beneficial, as the inflammation signalling and inflammatory targets genes *NFκB1, DEFβ4A, TLR2* and *IFNα* were significantly downregulated. Therefore, crude chicory flour might also be a promising cost-effective alternative supplement to improve gut health in weaned piglets.

Keywords: Chicory, inulin, inflammation, weaning, gut microbiota, morphology.

Highlights

- Both, chicory and inulin enhanced butyrate production and gut barrier function.
- Integrative analysis using RGCCA identified deeper correlations between variables.
- Chicory supplementation led to improved gut morphology and a reduction in diarrhoea occurrence.
- Like inulin, chicory can reduce harmful and promote beneficial microbiota effectively.
- Chicory, rich in other bioactives, offer a more cost-effective alternative to inulin in improving gut health.

3.2. Introduction

The weaning period, a critical transition phase, presents significant challenges to gut health in both humans and animals (Campbell *et al.,* 2013; Pluske *et al.,* 2018b; Pohl *et al.,* 2015). Detrimental changes occur during this phase, encompassing disruptions in gut morphology, physiology, immunology, and function, such as changes in intestinal barrier integrity and gut microbiota composition, mucosal inflammation, villus atrophy, and crypt hyperplasia (Awad *et al.,* 2013; Bailey *et al.,* 2005; G. Boudry *et al.,* 2004; Lallès *et al.,* 2007; Moeser *et al.,* 2017a). Zinc oxide, previously used as a potential solution for weaning-related issues, was banned in Europe due to concerns over environmental impact and the development of antimicrobial resistance (European Commission, 2017; Pejsak *et al.,* 2023). Considering these restrictions, prebiotics, such as inulin, emerge as a promising alternative to replace banned feed additives and promote gut health.

Inulin, a fructan-based prebiotic composed of fructose units linked *via* β-(2-1)-d-fructosyl fructose linkages terminated with a glucose molecule linked through an α-(1-2) bond, has demonstrated various beneficial effects on gut health. It has been shown to reduce pro-inflammatory processes, enhance intestinal integrity, maintain gut morphology, and promote the composition of beneficial intestinal microbiota in different species including rodents, humans, and pigs (Apolinário *et al.,* 2014; Cani *et al.,* 2009; Chen *et al.,* 2017a; Liu *et al.,* 2016; Mensink *et al.,* 2015). Crude chicory roots, which are recognised for their substantial inulin content, serve as the primary source for commercial extraction of inulin. Inulin consists of a blend of linear oligomers and polymers with chain lengths ranging from 2 to 60 units. Oligofructose, with a Degree of Polymerization (DP) < 10, makes up for approximately 10% of total inulin, while 90% are long length inulin fractions (DP=11 to 60), with an average DP of around 25 (Niness, 1999b). Studies have shown that both chain length and dietary concentration of inulin play a crucial role in its prebiotic effect (Herosimczyk *et al.,* 2020). Inulin production from chicory involves two stages: extraction and initial purification of raw syrup, followed by refinement for commercialization (Shoaib *et al.,* 2016; Redondo-Cuenca *et al.,* 2021). The classical purification process involves multiple steps at high temperatures (80–90°C), causing inulin hydrolysis and degrading other bioactives (Franck and Leenheer, 2005). Although advanced extraction methods (Lingyun *et al.,* 2007; Loginova *et al.,* 2010) and membrane-based filtration technologies (Susan Sungsoo Cho, 2009) offer potential for obtaining high-quality long-chain inulin, increasing final costs by three times with an impact on inulin recovery and quality. Additionally, its production involves lower energy, water, and chemical inputs, making it more environmentally friendly. Additionally, whole-root utilization reduces waste and supports circular economy principles, enhancing its value as a functional feed additive. (Khuenpet *et al.,* 2017; Rubel *et al.,* 2015; Ruiz-Aceituno *et al.,* 2016).

In addition to inulin and oligofructose, crude chicory boasts a diverse range of bioactive compounds, including phenolic compounds, sesquiterpene lactones (such as lactucin, lactucopicrin, and 8-deoxy lactucin), guaianolid glycosides, caffeic acid derivatives (like chicoric acid, chlorogenic acid, isochlorogenic acid, and dicaffeoyl tartaric acid), hydroxycoumarins, flavonoids, alkaloids, steroids, terpenoids, volatile compounds, vitamins, β-carotene, zeaxanthin, etc. These bioactives have been associated with various beneficial effects, including reducing inflammation, modulating lipid metabolism, inhibiting the growth of certain pathogens, enhancing growth performance, antioxidant activity or anticancer properties (Ferioli and D'Antuono, 2012; Karioti *et al.,* 2008; Kocsis *et al.,* 2003; Pouille *et al.,* 2022b; San Andres *et al.,* 2019; Schumacher *et al.,* 2011).

It is now recognised that there exists a complex signalling interplay among the epithelium, mucosal immune system, and gut microbial ecosystem, which plays a critical role in preserving intestinal epithelial cell homeostasis, consequently influencing health and performance (Fouhse *et al.,* 2016). Thus, studying these three parameters concurrently serves a dual purpose, allowing for a comprehensive evaluation of the effects of crude chicory supplementation by shedding light on the intricate interactions within the gastrointestinal tract. Considering the potential benefits of crude chicory's bioactive components, the aim of this study was to compare the effects of inulin (positive control) and crude chicory flour on intestinal health by equating the inulin content to explore the potential contributions of other bioactive components of crude chicory on gut health during the weaning period.

3.3. Material and Methods

3.3.1. Experimental setup, Animals and Diets

Two independent *in vivo* experiments (E1 and E2) were conducted using 80 weaned male piglets (Pietrain × Landrace) per experiment, all weaned at 21 days of age with average body weights of 5.48 ± 0.5 kg (E1) and 5.36 ± 0.2 kg (E2). Upon arrival from the Walloon Agricultural Centre (Gembloux, Belgium), piglets were randomly allocated into 24 pens (3 piglets/pen), with pens assigned to one of three treatment groups: control (Ctrl), inulin (INU), and chicory (CHI). Each piglet was individually ear-tagged for identification. Supplementation in the INU and CHI groups was administered via oral force-feeding, with inulin content increasing weekly in E1 (W1: 1.5 g/day, W2: 2 g/day, W3: 2.5 g/day) and doubled in E2, divided into morning and evening doses to reduce bolus load. The force-feeding approach was chosen to ensure accurate and standardized dosing, especially in early post-weaning when voluntary feed intake is variable.

All piglets were housed under identical conditions with ambient temperatures maintained between 22–24 °C, using meshed-floored pens equipped with nipple drinkers and dry feeders to allow ad libitum access to water and basal feed. Feed intake was recorded daily per pen by weighing the remaining feed from the previous day. Piglets were weighed weekly using a cage-fitted precision balance to ensure accuracy. One piglet per pen was randomly selected and euthanized at W0, W1, and W3 for tissue and content collection. Euthanasia was performed using nitrogen-induced anoxia followed by exsanguination via jugular incision. Standardized sampling protocols were followed for all gastrointestinal compartments (duodenum, jejunum, ileum, cecum, colon), with portions snap frozen for molecular analysis or fixed in formaldehyde for histological examination. The small intestine was

divided based on length: the first 25% was designated as the duodenum, the middle 50% as the jejunum, and the final 25% as the ileum and proximal colon was used to sample the tissue and conent. All procedures complied with EU Directive 2010/63/EU and were approved by the Ethical Committee of the University of Liège (license 21-2385).

The inulin content for both groups was equated to ensure equivalence for the inulin related effect. The dosage was decided based on previous studies (C. H. *et al.,* 2005; Estrada *et al.,* 2001; Li *et al.,* 2018). Inulin (Orafti®SIPX) was sourced from Beneo, Belgium, while crude chicory flour (*Cichorium intybus*) came from Leroux-Waast Mill, France with a DP range of 2-60 for both **(Table 8)**. The Ctrl group received an isotonic sucrose solution to better mimic the osmolarity and energy content of test solutions, while also improving palatability, as water was freely available to piglets throughout the study Throughout the experiments, the piglets had *ad libitum* access to water and Baby-mix© feed from Quartes **(refer Table 5)**.

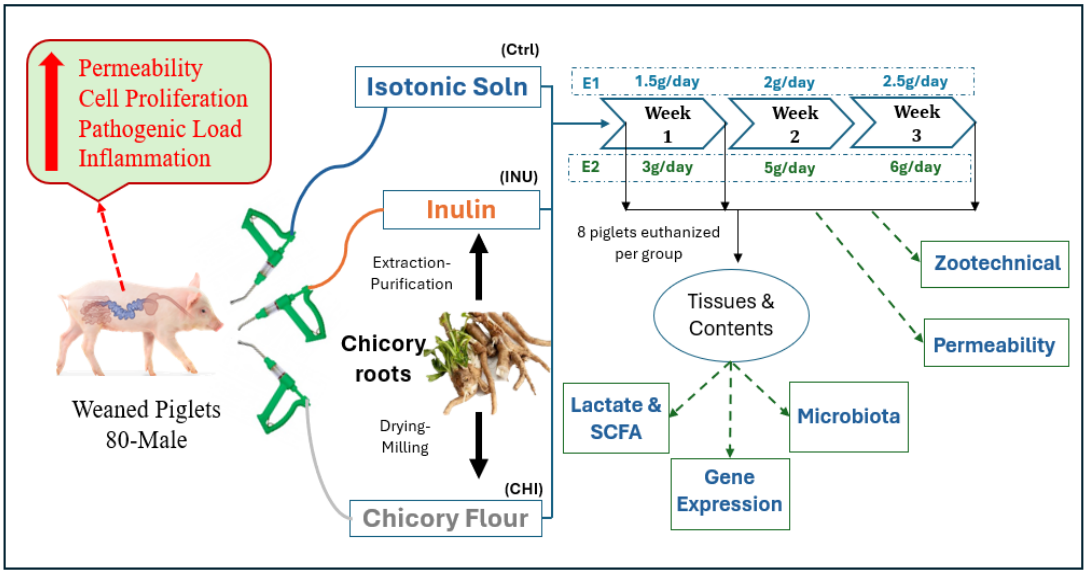

Figure 15. Experimental setup for E1 and E2

The temperature inside the room was kept at a constant 25°C, and the lighting schedule followed a pattern of 12 h of light followed by 12 h of darkness. At W0, W1 and W3, eight piglets per treatment were euthanized using Anoxia® Pallet Box v.1.1, employing inert nitrogen gas encapsulated in foam to rapidly reduce the atmospheric oxygen from 20.9% to 2% or less.

The W0 group consisted of untreated and just weaned piglets (Day 1- post-weaning). The gastrointestinal tract was then removed, and tissues and contents from the jejunum, ileum, caecum, colon, and rectum were collected from each piglet. The collected samples were immediately snap-frozen in liquid nitrogen and stored at -80°C for further analysis. Additionally, 5cm long segments from duodenum, jejunum and ileum were collected in formaldehyde for histomorphological measurements.

Table 5. Ingredient composition of the basal diet weaned pigs

Ingredients	%
Barley	30.6
Soy Feed	21.7
Maize	20
Wheat	16.3
Rice Bran	3
Dired Beet Pulp	2
Spelled Bran	2
Lysine	1.25
Methoinine	0.44
Palm Oil	1.3
Monocalcium Phosphate	0.4
Sodium Chloride	0.4
Calcium Carbonate	0.1
Other Additives	0.3
Vitamin A 15000 IU, Vitamin D3 2000 IU, Vitamin E (totally racemic α--tocopheryl acetate) 60 mg, Iron (Ferrous sulphate, monohydrate) 150 mg, Iodine (Calcium iodate, anhydrous) 3.00mg, Copper (Cupric sulfate pentahydrate) 140 mg, Manganese (Manganous oxide) 60 mg , Zinc (Zinc sulphate, monohydrate) 100 mg, Selenium (Sodium selenite) 0.40 mg	

3.3.2. Chemical Analyses

The nutrient composition of the experimental diets was assessed in accordance with the protocols outlined by the Association of Official Analytical Chemists (Horwitz, 2010). To determine the Neutral Detergent Fibre (NDF) and Acid Detergent Fibre (ADF) components, the Foss Fibrecap system was employed, following the methodology described by (Van Soest *et al.,* 1991).

For the analysis of monosaccharide composition (including rhamnose, arabinose, xylose, mannose, glucose, and galactose), samples underwent initial hydrolysis using H_2SO_4 (1M) for 3 h at 100°C. The resulting sugars were then derivatized and analysed using an HP Agilent 6890 series gas chromatograph (Agilent Technologies, Santa Clara, CA), equipped with a high-performance capillary column, HP1-methylsiloxane (Scientific Glass Engineering, Melbourne, Australia), and utilizing 2-deoxyglucose (Sigma-Aldrich Co., St Louis, MO) as an internal standard (Aguedo *et al.,* 2014; Englyst and Cummings, 1984).

Molecular weight distributions were analysed via size-exclusion high-performance liquid chromatography (HPSEC) using a Waters 2690 Alliance chromatograph and a refractometer Waters 2410, with a TSKGEL G3000 PWXL column (7 µm 7.8*300 mm) (Tosoh, Tokyo, Japan). The eluent, consisting of $NaNO_3$ / NaN_3 at ambient temperature, was delivered at a flow rate of 0.7 mL/min (Aguedo *et al.,* 2014). Peak molecular masses were determined using dextran standards from Sigma-Aldrich (Bornem, Belgium), which were utilized to construct

a calibration curve. Additionally, the polydispersity index (PDI) was calculated by dividing the weight-average molecular weight (M_w) by the number-average molecular weight (M_n) (Aguedo *et al.,* 2014).

3.3.3. Zootechnical Performance Metrices

During the experimental period, daily feed intake and weekly body weight gain were assessed for each treatment group, with a total of 8 pens per treatment and the occurrences were tallied on a weekly basis. The diarrhoea status of the piglets was visually evaluated by a single observer daily. Fecal scoring was performed using a scale ranging from 0 to 3, where 0 represented normal faeces, 1 indicated soft faeces, 2 denoted mild diarrhoea, and 3 indicated severe diarrhoea.

Figure 16. Fecal Scoring Scale adapted from (Pérez-Calvo *et al.,* 2019)

3.3.4. Histomorphological analysis

Duodenum, jejunum, and ileum tissues were cleaned using Phosphate Buffer Saline (PBS), cut into 5cm-long segments, and placed in formaldehyde on the day of dissection. Subsequently after 24 h, they were transferred to a 70% ethanol solution for long-term storage. To prepare the tissue samples for analysis, they were embedded in paraffin and sliced using a microtome with sharp blades (5µm thickness). Hematoxylin-eosin colouration was applied to the tissue sections. Several parameters were observed, including villi height, villi width, crypt depth, and the size of the muscularis layer, including the *lamina propria*. Measurements (approx. 50 values per animal per tissue) were conducted using the Toupview® application and a Toupcam® camera (UA510CA) mounted on an Olympus BX51 microscope at a magnification of 10x.

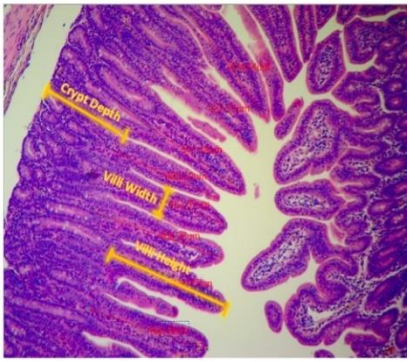

Figure 17. Histomorphological measurements for villi and crypts of duodenum, jejunum, and ileum

3.3.5. *In vivo* permeability (Lactulose, Mannitol and D-xylose)

In vivo intestinal permeability testing was conducted on the last day of W1 and W3 by orally force-feeding a cocktail of marker probes to overnight fasted piglets. The cocktail comprised D-xylose (100 mg/kg BW; VWR International, Belgium), mannitol (100 mg/kg BW; Sigma Aldrich, Belgium), and lactulose (500 mg/kg BW; Sigma Aldrich, Belgium). Blood samples were collected from the external jugular vein, one-hour post-administration, in gel and clot activator vacuum tubes (VWR International, Belgium) and subsequently centrifuged at 2000 g for 10 minutes at 4°C. The resulting serum samples were stored at −80°C until analysis.

For lactulose and mannitol estimation, serum samples were filtered through a 0.25 µm membrane and analysed utilizing High Performance Anion Exchange Chromatography with a Dionex CarboPac™ MA1 (Thermo Scientific, USA) column and a Pulsed Amperometric Detector (Dionex Pvt. Ltd.). The eluent comprised 612mM NaOH with a flow rate of 0.4 mL/min. Chromatograms were interpreted using Chromeleon Client software version 7.3. Regarding D-xylose analysis, standard solutions were prepared by dissolving D-xylose in saturated benzoic acid to achieve concentrations ranging from 0 to 800 mg/L. A phloroglucinol colour reagent solution, sourced from Sigma-Aldrich Co. (St Louis, MO, USA), was prepared using 0.5 g of phloroglucinol, 100 mL of glacial acetic acid, and 10 mL of concentrated hydrochloric acid. Standard and serum samples (50 µL) were mixed with 5 mL of the phloroglucinol colour reagent solution, heated at 100°C for 4 minutes, and then cooled in a water bath at room temperature. Absorbance was measured at 570 nm utilizing a spectrophotometer (VICTOR plate reader, PerkinElmer, Waltham, MA, USA). The blank utilized a 0 mg/L D-xylose standard solution, and D-xylose-free serum was employed for determining net absorptive concentrations (Uerlings, Arévalo Sureda, *et al.,* 2021).

3.3.6. Short Chain Fatty Acids (SCFA) composition

Samples of colon and cecum contents underwent analysis using an isocratic High-Performance Liquid Chromatography (HPLC) system featuring a Waters E2695 Alliance HPLC machine. The HPLC consisted of an Aminex HPX-87H ion exclusion column from BioRad (Hercules, CA, USA) and a UV detector set at 210 nm. The eluent flow rate was maintained at 0.6 ml/min of H_2SO_4 (mM) at 60 °C. Prior to analysis, the contents were centrifuged at 13,000 rpm for 15 minutes, and 1.6 mL of the supernatant was collected and acidified with H_2SO_4 (1M) to achieve a pH range of 2 to 3. Subsequently, the samples underwent double filtration using Chromafil AO-45/25 and Chromafil AO-20/25 filters. Peak integration was executed utilizing the Empower 3 software from Waters Corporation (Milford, MA, USA), with manual verification for accuracy. Quantification was conducted using an external standard calibration method. The expression of intermediate metabolites and the sum of SCFA was reported in mg/g of fresh content, while the quantities of acetate, propionate, butyrate, and branched-chain fatty acids (BCFAs) were expressed as a percentage ratio of the sum of SCFA (Leblois *et al.,* 2017).

3.3.7. Microbiota analysis

DNA was extracted from the colonic contents using the QIAamp PowerFaecal Pro DNA kit, Qiagen (Hilden, Germany) as per manufacturer's instruction. The DNA concentration and quality were determined using Nanodrop from Thermo Fisher Scientific (Waltham, MA, USA). For 16S rRNA gene sequencing, the V3-V4 region was amplified using Illumina MiSeq at GIGA (Genomics platform, ULiege, Belgium). The Amplicon Sequence Variant (ASV) determination was carried out with the Quantitative Insights into Microbial Ecology II 1.9.0 QIIME (Bolyen *et al.,* 2019) software using the DADA2 plugin, as it models and rectifies errors inherent in amplicon sequencing conducted with Illumina technology (Callahan *et al.,* 2016). Taxonomic classification utilized the SILVA database (version 138). Subsequent data visualization and statistical analyses were conducted in R Studio. A single ASV of the genus *Pseudomonas* was excluded from the analysis as it was identified as a contaminant in the negative control. Microbial α- diversity (Chao1, Shannon indexes, and Simpson index) and β- diversity (PERMANONVA) , were computed using the phyloseq package in R studio (Version 4.3.2). Microbiota results were analysed per time point using a Kruskal-Wallis test, with the treatment as a fixed factor. The Bonferroni Correction was applied to calculate the adjusted p-values and control the family-wise error rate (FWER) for microbiota and gene expression data sets.

3.3.8. Gene expression

Total RNA was extracted from ileum and colonic tissues using the ReliaPrep RNA Tissue Miniprep System Kit (Promega Corporation, Madison, WI). RNA concentration of 60 ng, determined by Nanodrop (Thermo Fisher Scientific, Waltham, MA), was converted into cDNA using the Reverse Transcription Master Mix (Fluidigm Corporation, South San Francisco, CA). High-throughput quantitative PCR (qPCR) was conducted, utilizing intron-spanning primer pairs **(Table 6)** designed via Primer-BLAST (NCBI), as outlined by (Uerlings, Arévalo Sureda, *et al.,* 2021). These primer pairs were validated through agarose gel electrophoresis and melting curves. The qPCR assays were performed in 48×48 dynamic array-integrated fluidic circuits (Standard BioTools Inc., South San Francisco, CA, USA) with the following protocol: 60s at 95°C, followed by 30 cycles (5s at 96°C and 20s at 60°C). Quantification cycles (Cq) were obtained using the Fluidigm real-time PCR analysis software 3.0.2 (Standard BioTools Inc., South San Francisco, CA, USA).

Housekeeping genes were assessed, and the three most stable genes between treatments were determined using NormFinder (Andersen *et al.,* 2004). Three reference genes were selected separately for colon and ileum tissues, as well as for different experimental conditions (E1 and E2). Relative gene expression levels were calculated utilizing the Pfaffl method (Pfaffl, 2001), and the geometric mean of the relative expression of the three most stable housekeeping genes was employed to normalize all samples.

Table 6. Primer sequences to investigate gene expression of ileum and colonic tissues.

Genes		Sequence		Accession no
		F (5'-3')	R (5'-3')	
Housekeeping genes	ACTB	*CTACGTCGCCCTGGACTTC*	*GCAGCTCGTAGCTCTTCTCC*	XM_003124280.5
	GAPDH	*GATGGTGAAGGTCGGAGTGAA*	*GTGGAGGTCAATGAAGGGGT*	XM_021091114.1
	HPRT1	*AATTCTTTGCTGACCTGCTGGA*	*TCCACCAATTACTTTTATATCGCCC*	XM_021079503.1
	PPIA	*GGGACCTGGAAACCAAGAAGTG*	*ACTTTGTCTGCAAACAGCTCCAATC*	XM_013985800.2
	RPL13a	*ATTGTGGCCAAGCAGGTACT*	*AATTGCCAGAAATGTTGATGC*	XM_013998640.2
	RPL32	*GCTTGAAGTGCTGCTAATGTG*	*GGATTGGTGACCCTGATGGC*	XM_021068582.1
	RPL4	*GAGAAACCGTCGCCGAATCC*	*CCCACCAGGAGCAAGTTTCAA*	XM_005659862.3
	TBP	*CGGACCACCGCACTGATATT*	*TTCTTCACTCTTGGCTCCCG*	XM_021085483.1
	YWHAZ	*TTGTAGGAGCCCGTAGGTCA*	*AGCACCTTCCGTCTTTTGCT*	NM_001315726.1
Apoptosis related genes	CASP3	*AAGCAAATCAATGGACTCTGGAA*	*TTGCAGCATCCACATCTGTACC*	NM_214131.1
	BAX	*CCCAGAGGCGGGGTTTCAT*	*CAATGCGCTTGAGACACTCG*	XM_013998624.2
	CASP1	*GTTATTCGGAAAGGGCCCCA*	*CACCGCCTGGGATTCTTGTA*	NM_214162.1
	JUN	*CTTTCCTCCTTCACGGTCCC*	*CACTTCACGTGGGGTGAGTT*	NM_213880.1
Barrier Integrity genes	CDH1	*AGCCCTGCAATCCTGGCTTT*	*AGAAACATAGACCGTCCTTGGC*	NM_001163060.1
	Claudin-1	*GGTGACAACATTGTGACGGC*	*TACCATCAAGGCACGGGTTG*	NM_001244539.1
	Claudin-3	*TATCACAGCGCGGATCACC*	*CTCTGCACCACGCAGTTCAT*	NM_001160075.1
	Claudin-4	*CTTCATCGGCAGCAACATCG*	*CGAGTCGTACACCTTGCACT*	XM_013995522.2
	MARVELD2	*CTCAGCCCCGCCATTACCTG*	*TAGAGGTGATGTGCTGTTGCC*	NM_001243948.1
	MUC1	*GGATTTCTGAATTGTTTTTGCAG*	*ACTGTCTTGGAAGGCCAGAA*	XM_021089728.1
	Occludin	*AACGTATTTATGACGAGCAGCCC*	*CACTTTCCCGTTGGACGAGTA*	NM_001163647.2
	ZO-1	*AAGGTCTGCCGAGACAACAG*	*TCACAGTGTGGTAAGCGCAG*	XM_021098827.1
Inflammation signalling pathway genes	AKT1	*CTAAGCCCAAACACCGCGT*	*TCAGGATCTTCATGGCGTAGT*	XM_021081499.1
	MAPK14	*TACCCGAGCGTTACCAGAAC*	*TTCACTGCAACACGTAACCCA*	XM_001929490.6
	MyD88	*GCATCACCATTCGAGATGACC*	*TCCTGCACAAACTGGGTATCG*	NM_001099923.1
	NFκB1	*AAGAAGTCCTACCCTCAGGTCA*	*CAGTGACAGTGCAGATCCCA*	NM_001048232.1
	NFκBIα	*GAGGATGAGCTGCCCTATGAC*	*CCATGGTCTTTTAGACACTTTCC*	NM_001005150.1
	NOD1	*GTCGTCAACACCGATCCAGT*	*CCTCCTTCTGGGCATAGCAC*	NM_001114277.1
	PPARγ	*ACAGCGACCTGGCGATATTTA*	*GAGGACTCTGGGTGGTTCAA*	XM_005669784.3
	TLR2	*GTTTTACGGAAATTGTGAAACTG*	*TCCACATTACCGAGGGATTT*	XM_005653576.3
	TLR4	*ATGATTCCTCGCATCCGCCT*	*AATTCAGCTCCATGCATTGGTAA*	NM_001113039.2
Inflammatory Target genes	CXCL10	*CCCACATGTTGAGATCATTGC*	*GCTTCTCTCTGTGTTCGAGGA*	NM_001008691.1
	DEFβ4a	*CAGGATTGAAGGGACCTGTT*	*CTTCACTTGGCCTGTGTGTC*	AY506573.1
	IFNβ	*TTCGAGGTCCCTGAGGAGATT*	*GCTGGAGCATCTCGTGGATAA*	NM_001003923.1
	IL1β	*CCAAAGAGGGACATGGAGAA*	*GGGCTTTTGTTCTGCTTGAG*	XM_021085847.1
	IL18	*CTGAAAACGATGAAGACCTGGA*	*CCTCAAACACGGCTTGATGTC*	XM_005667326.2
	IL6	*TGGGTTCAATCAGGAGACCT*	*CAGCCTCGACATTTCCCTTA*	NM_001252429.1
	IL8	*GACTTCCAAACTGGCTGTTGC*	*ATTTGGGGTGGAAAGGTGTG*	JF906514.1
	ILRN1	*TGCCTGTCCTGTGTCAAGTC*	*GTCCTGCTCGCTGTTCTTTC*	NM_214262.1
	MCP1	*CTCACTGCAGCCACCTTCT*	*CACTTGCTGCTGGTGACTCT*	NM_214214.1
	TNFα	*TCTGCCTACTGCACTTCGAG*	*GTTGATGCTCAAGGGGCCA*	NM_214022.1

Genes Abbreviations: ACTB - actin β-; GAPDH - glyceraldehyde-3-phosphate dehydrogenase; HPRT1 - hypoxanthine phosphoribosyl transferase 1; PPIA - peptidylprolyl isomerase A; RPL13a - ribosomal protein L13a; RPL32 - ribosomal protein L32; RPL4 - ribosomal protein L4; TBP - TATA box binding protein; YWHAZ - tyrosine 3-monooxygenase/tryptophan 5-monooxygenase activation protein zeta; CASP3 - caspase 3; BAX - BCL2-associated X protein; CASP1 - caspase 1; JUN - Jun proto-oncogene; CDH1 - E-cadherin; Claudin-1 - claudin-1; Claudin-3 - claudin-3; Claudin-4 - claudin-4; MARVELD2 - tricellular; MUC1 - mucin 1; Occludin - occludin; ZO-1 - zonula occludens-1; AKT1 - serine/threonine-protein kinase 1; MAPK14 - mitogen-activated protein kinase 14; MyD88 - myeloid differentiation primary response 88; NFκB1 - nuclear factor-kappa B; NFκBIα - nuclear factor-kappa B inhibitor α-; NOD1 - nucleotide-binding oligomerisation domain-containing protein 1; PPARγ - peroxisome proliferator-activated receptor gamma; TLR2 - toll-like receptor 2; TLR4 - toll-like receptor 4; CXCL10 - C-X-C motif chemokine 10; DEFβ4a - defensin β- 4a; IFNβ - interferon β-; IL1β - interleukin 1 β-; IL18 - interleukin 18; IL6 - interleukin 6; IL8 - interleukin 8; ILRN1 - interleukin-1 receptor antagonist; MCP1 - monocyte chemoattractant protein 1; TNFα - tumour necrosis factor α-.

3.3.9. Statistical Analyses

In the present study, all the variables were analysed using the general linear model (GLM) implemented in SAS Enterprise Guide 7.4 (SAS Institute Inc, Cary, NC) followed by Tukey's multiple range test was employed to discern significant differences among treatment means, with significance levels established at $p< 0.05$ (significant), $p < 0.01$ (highly significant), and $p<0.001$ (very highly significant). For microbiota analyses at each time point, the Kruskal-Wallis test followed by Dunn's test was performed. Amplicon Sequence Variant (ASV.) determination, taxonomic classification using the SILVA database (version 138), data visualization, and subsequent statistical analyses were conducted using R Studio. The p values were adjusted using Bonferroni correction to control the family-wise error rate (FWER).

Integration analysis was performed across multiple datasets to uncover potential relationships using supervised Regularized Generalized Canonical Correlation Analysis (RGCCA) (Tenenhaus and Tenenhaus, 2011) following treatment groups. Datasets variables have been grouped in 4 blocks following data types: "Clinical" (ADG, ADCI, Length, Diarrhoea Incidences), "Gut" (Histomorphology, Permeability, SCFA), "Gene Expression", and "Microbiota". RGCCA *tau* value was fixed at is optimal value with a *factorial scheme*. P-values of Pearson correlation coefficients (r) were adjusted for multiple testing using Bonferroni method . All analyses were performed using R version 4.3.1 and the following packages: RGCCA (v3.0.3), factoextra (v1.0.7), FactoMineR (v2.9), ggplot2 (v3.5.0), and corrplot (0.92).

3.4. Results

3.4.1. Growth performances and diarrhoea incidences

As shown in **Figure 18B**, in E1, the group fed with crude CHI exhibited significantly lower ADFI (Average Daily Feed Intake, g/day) only during W3, while in E2, it was lower for all three weeks when compared to the INU and Ctrl groups. Interestingly, this did not cause any significant difference in ADG (Average Daily Gain) (g/day) on W2 and W3 of both E1 and E2 **(Figure 18A)**. During W1 of E2, there was significant weight loss in the CHI group piglets compared to the INU group ($p < 0.05$). In E1, INU and CHI treatments had no effect on the occurrences of diarrhoea **(Figure 18C)**. However, in E2, the occurrence of severe diarrhoea (S3) was significantly lower for CHI than IN and Ctrl in W3 **(Figure 18D)**. In E2, during W2, the mild diarrhoea scores (S2) were lower for both the CHI and INU groups compared to Ctrl ($p < 0.001$).

Table 7. Nutrient Composition of Feed

Nutrients % Dry Matter (DM)	Feed
(DM) (g/Kg)	886
Protein	18
Fat	4.5
Ash	max 4.5
Sugars	4.7
NDF	17.7
ADF	5.69
Fructan	-
Calcium	0.7
Phosphorus	0.5
Sodium	0.2

Abbreviations: Acid Detergent Fibre (ADF); Dry Matter (DM); Neutral Detergent Fibre (NDF). NDF= hemicelluloses + cellulose + lignin. ADF= cellulose + lignin.

3.4.2. Duodenum, jejunum and ileum histomorphology

In W1, CHI and INU supplementation had no significant effect on villus height, width, or V:C ratio compared to the Ctrl group, neither in E1 nor in E2. However, after W3 of supplementation in E1, the INU group exhibited significantly higher villi height ($p < 0.01$), width ($p < 0.05$) in the ileum and a higher V:C ratio ($p<0.001$) than both CHI and Ctrl in both jejunum and ileum. Interestingly, CHI supplementation led to a significant reduction in crypt depth in the duodenum (W3, $p<0.001$) and jejunum (W1, $p < 0.01$) **(Table 9)**.

Table 8. Nutrient, monosaccharide composition and HPSEC profile of Inulin and Chicory Flour.

Nutrients % (DM)	Inulin	Chicory Flour
(DM) (g/kg)	940	930
Protein	3.85	4.4
Fat	1.3	1.2
Ash	max 9	max 9
Sugars	8.6	4.3
NDF	0.56	4.47
ADF	0.73	3.63
Fructan	76.2	57.1
Calcium	-	-
Phosphorus	-	0.169
Sodium	-	0.83
Monosaccharides (% of DM)		
Rhamnose	0.09	0.38
Arabinose	0.05	2.12
Xylose	0.08	0.46
Mannose	9.52	3.87
Glucose	15.82	10.51
Galactose	0.29	2.25
Fructose	8.57	10.9
Molecular weight Distribution		
M_w	1800	2000
M_n	1400	1500
PDI	1.28	1.33
DP_w	9.99	10.9
DP_n	7.41	8.2

M_w: Weight-Average Molecular Weight; M_n: Number-Average Molecular Weight; PDI: Poly Dispersity Index.
DP_w : Weight-Average Degree of Polymerization; DP_n : Number -Average Degree of Polymerization

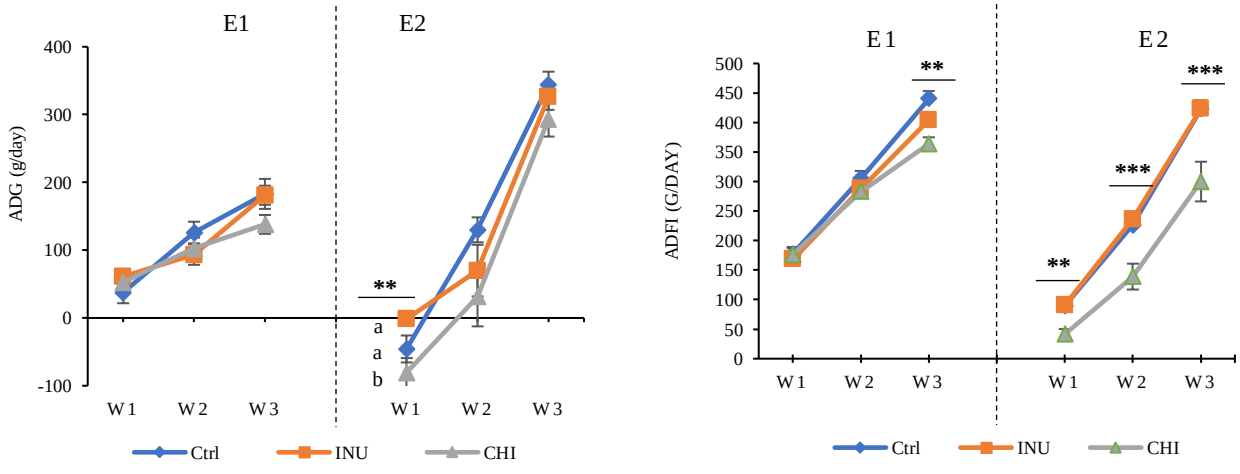

(A) **(B)**

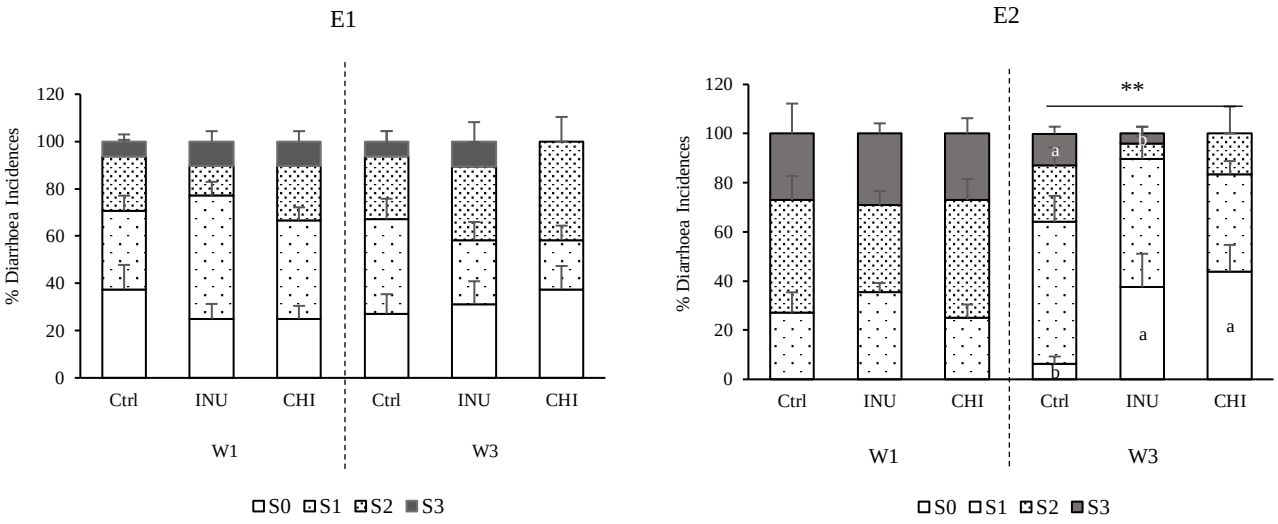

(C) **(D)**

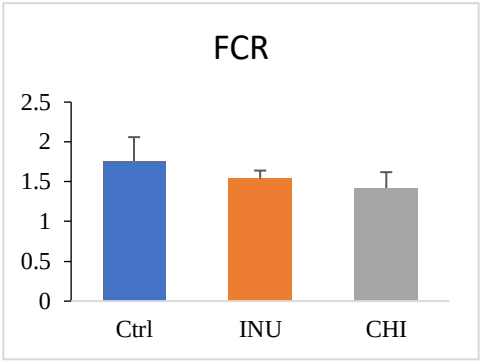

(E)

Figure 18. Effect of INU and CHI supplementation on weaning piglet at W1 and W3 in E1 and E2 on (A) Average Daily Gain (ADG) (g/day) (B) Average Daily Feed Intake (ADFI) (C) E1 (D) E2 % Diarrhoea Incidences (E) FCR (after 3 weeks in E2).

Values are means (n=8 piglets) ± SEM. Statistical analysis ANOVA+ Tukey's test, * $p < 0.05$, ** $p < 0.01$, *** $p < 0.001$. Abbreviations: S0: Normal faeces; S1: Soft faeces, S2: Mild diarrhoeas; S3: Severe diarrhoea. (FCR: Feed Conversion Ratio; CHI: Crude Chicory; INU: Inulin; Ctrl: Control)

Doubling the dose in E2 did not result in any significant effect on the histomorphological parameters of the duodenum. However, it did yield some interesting effect on the jejunum and ileum **(Table 10)**. In E2 (W3), chicory supplementation showed significantly higher villus height ($p < 0.01$) and V:C ratio ($p < 0.01$) than the Ctrl group piglets. Furthermore, CHI had even higher villus height than INU in the ileum in E2 (W3). Throughout both experiments, chicory and inulin supplementation did not influence the thickness of the duodenal, jejunum, or ileum's *muscularis mucosae* and *tela submucosa* or *tunica muscularis* layers **(Table 10)**.

Table 9. Effect of CHI and INU supplementation on histomorphological parameters of Duodenum, Jejunum and Ileum in E1 on W0, W1 and W3 post-weaning

Intestine Part	Week	Treat-ment	Villus Height (µm)	Villus Width (µm)	Crypt Depth (µm)	V:C ratio	Muscularis mucosae + Tela submucosae (µm)	*Tunica muscularis (µm)*
Duodenum	W0	Ctrl	287 ± 6	110 ± 3	262 ± 4	1.24± 0.03	47 ± 3	231 ± 3
	W1	Ctrl	279 ± 18	115 ± 4	277 ± 11	1.12 ± 0.14	45 ± 3	260 ± 8
		INU	265 ± 12	108 ± 7	259 ± 8	1.09 ± 0.07	47 ± 1	251 ± 15
		CHI	291 ± 14	116 ± 2	261 ± 8	1.13 ± 0.07	44 ± 2	249 ± 9
		p value	0.465	0.522	0.221	0.721	0.651	0.216
	W3	Ctrl	388 ± 11	120 ± 9	301 ± 7^{a}	1.29 ± 0.02	48 ± 1	250 ± 11
		INU	397 ± 10	119 ± 8	308 ± 8^{a}	1.38 ± 0.02	49 ± 3	266 ± 9
		CHI	375 ± 7	113 ± 4	263 ± 4^{b}	1.23 ± 0.03	47 ± 3	258 ± 13
		p value	0.572	0.2451	0.0005	0.433	0.5134	0.211
Jejunum	W0	Ctrl	388 ± 13	119 ± 5	206 ± 4	1.91 ± 0.06	48 ± 2	233 ± 2
	W1	Ctrl	385 ± 12	109 ± 6	233 ± 11^{b}	1.4 ± 0.02	43 ± 2	248 ± 8
		INU	399 ± 18	114 ± 5	268 ± 9^{a}	1.61 ± 0.032	44 ± 1	244 ± 10
		CHI	367 ± 15	125 ± 8	219 ± 12^{b}	1.67 ± 0.04	46 ± 3	241 ± 6
		p value	0.531	0.614	0.001	0.286	0.477	0.532
	W3	Ctrl	392 ± 5^{b}	120 ± 5	275 ± 15	1.39 ± 0.09^{b}	43 ± 3	271 ± 7
		INU	430 ± 7^{a}	123 ± 4	239 ± 11	1.80± 0.031^{a}	44 ± 3	259 ± 15
		CHI	386 ± 7^{b}	119 ± 5	246 ± 12	1.62 ± 0.09^{b}	47 ± 4	266 ± 8
		p value	0.001	0.552	0.115	0.0008	0.684	0.319
Ileum	W0	Ctrl	300 ± 12	110 ± 3	202 ± 7	1.44 ± 0.09	52.93 ± 2	255 ± 9
	W1	Ctrl	277 ± 12	117 ± 3	220 ± 13	1.27 ± 0.03	51 ± 2	274 ± 14
		INU	284 ± 9	118± 4	227 ± 10	1.26 ± 0.05	49 ± 2	293 ± 11
		CHI	294 ± 11	113 ± 3	216 ± 15	1.36 ± 0.05	48 ± 3	279 ± 15
		p value	0.521	0.674	0.341	0.172	0.66	0.473
	W3	Ctrl	301 ± 9^{b}	128 ± 2^{b}	221 ± 6	1.37 ± 0.04^{b}	46 ± 4	264 ± 17
		INU	385 ± 11^{a}	142 ± 3^{a}	227 ± 5	1.71 ± 0.04^{a}	44 ± 3	294 ± 9
		CHI	311 ± 11^{b}	127 ± 2^{b}	230 ± 3	1.35 ± 0.03^{b}	48 ± 2	282 ± 13
		p value	0.0008	0.002	0.248	0.0007	0.542	0.311

Values are means ± SEM, n = 8 per treatment group. Means in a column with timepoint without a common superscript letter differ ($p < 0.05$) as analysed by one-way ANOVA and the Tukey test. Abbreviations: V:C= Villi height: Crypt depth; CHI: Crude Chicory; INU: Inulin; Ctrl: Control)

Table 10. Effect of CHI and INU supplementation on histomorphological parameters of Duodenum, Jejunum, and Ileum in E2 at W0, W1 and W3 post-weaning.

Intestinal Part	Week	Treat-ments	Villus Height (µm) (V)	Villus Width (µm)	Crypt Depth (µm) (C)	V:C	Muscularis Mucosae + Tela submucosa (µm)	Tunica Muscularis (µm)
Duodenum	W0	Ctrl	257 ± 5	106 ± 3	215 ± 15	1.26 ± 0.08	55 ± 4	214 ± 6
	W1	Ctrl	238 ± 13	102 ± 4	205 ± 9	1.19 ± 0.101	47.7 ± 1.61	231 ± 19
		INU	261 ± 9	111 ± 5	237 ± 12	1.19 ± 0.09	47 ± 1.7	235 ± 16
		CHI	245 ± 16	97.3 ± 4	212 ± 8	1.14 ± 0.06	48.3 ± 2.14	207 ± 10
		p value	0.523	0.413	0.371	0.633	0.488	0.219
	W3	Ctrl	327 ± 15.7	116 ± 6	229 ± 15	1.46 ± 0.07	44 ± 2.78	226 ± 11
		INU	338 ± 24.4	112 ± 6	233 ± 14	1.46 ± 0.08	42 ± 2.93	243 ± 20
		CHI	370 ± 12.9	118 ± 6	236 ± 11	1.6 ± 0.13	41 ± 2.36	205 ± 10
		p value	0.55	0.3535	0.441	0.315	0.467	0.214
Jejunum	W0	Ctrl	264 ± 12.5	102 ± 5	222.94 ± 16	1.24 ± 0.11	80.9 ± 45.5	270 ± 14
	W1	Ctrl	331 ± 9.14	133 ± 15.9	237 ± 18^{b}	1.35 ± 0.09	45.2 ± 1.49	259 ± 17.1
		INU	306 ± 15.2	118 ± 5.45	238 ± 6.76^{b}	1.31 ± 0.08	50.1 ± 2.8	250 ± 9.23
		CHI	340 ± 12.7	117 ± 4.34	298 ± 7.53^{a}	1.17 ± 0.04	46.3 ± 1.32	233 ± 6.32
		p value	0.421	0.601	0.01	0.217	0.487	0.515
	W3	Ctrl	339 ± 5.25^{b}	139 ± 6.68	255 ± 18.5	1.27 ± 0.03^{b}	51 ± 3.19	247 ± 6.72
		INU	369 ± 26.2^{ab}	127 ± 8.4	260 ± 5.98	1.35 ± 0.2^{ab}	52.5 ± 2.96	253 ± 8.03
		CHI	420 ± 20.3^{a}	139 ± 4.11	236 ± 8.69	1.79 ± 0.13^{a}	58.5 ± 1.64	266 ± 20.6
		p value	0.033	0.353	0.633	0.03	0.421	0.221
Ileum	W0	Ctrl	262 ± 6	122 ± 5	166 ± 3.53	1.59 ± 0.06	28 ± 2	243 ± 4
	W1	Ctrl	247 ± 11.8	94 ± 4.72	215 ± 8.2	1.17 ± 0.07	58 ± 3.2	232 ± 10.7
		INU	245 ± 11.4	108 ± 6.94	224 ± 7.34	1.11 ± 0.07	53.9 ± 3.89	256 ± 7.1
		CHI	239 ± 7.91	110 ± 5.46	200 ± 10.2	1.22 ± 0.07	49.3 ± 2.13	246 ± 7.19
		p value	0.438	0.122	0.3625	0.396	0.438	0.072
	W3	Ctrl	338 ± 14.2^{b}	133 ± 2.54^{b}	206 ± 8.33	1.41 ± 0.17^{b}	44.6 ± 1.41	274 ± 10.9
		INU	323 ± 21.7^{b}	155 ± 9.26^{a}	243 ± 19.9	1.67 ± 0.1^{ab}	43.8 ± 1.77	288 ± 16.7
		CHI	440 ± 28^{a}	155 ± 2.57^{a}	214 ± 8.9	2.1 ± 0.15^{a}	44.4 ± 2.07	285 ± 7.65
		p value	0.002	0.015	0.427	0.008	0.746	0.341

Values are means ± SEM, n = 8 per treatment group. Means in a column with timepoint without a common superscript letter differ ($p < 0.05$) as analysed by one-way ANOVA and the Tukey test. Abbreviations: V:C= Villi height: Crypt depth; CHI: Crude Chicory; INU: Inulin; Ctrl: Control)

3.4.3. Intestinal permeability of lactulose, mannitol, and D-Xylose

The serum concentrations of lactulose and mannitol in the blood exhibited no statistically significant differences across the Ctrl, INU, and CHI groups, in both experimental phases E1 and E2. However, in E2, on W3, although not statistically significant (p=0.057), the CHI group had the lowest L:M (Lactulose: Mannitol) ratio and a 50% reduction in plasma lactulose concentration relative to both the Ctrl and INU groups **(Figure 19A)**. However, at W3, INU and CHI group had decreased levels of D-xylose ($p < 0.05$) compared to the Ctrl group in E1 ($p < 0.05$) and E2 ($p < 0.01$) **(Figure 19B)**.

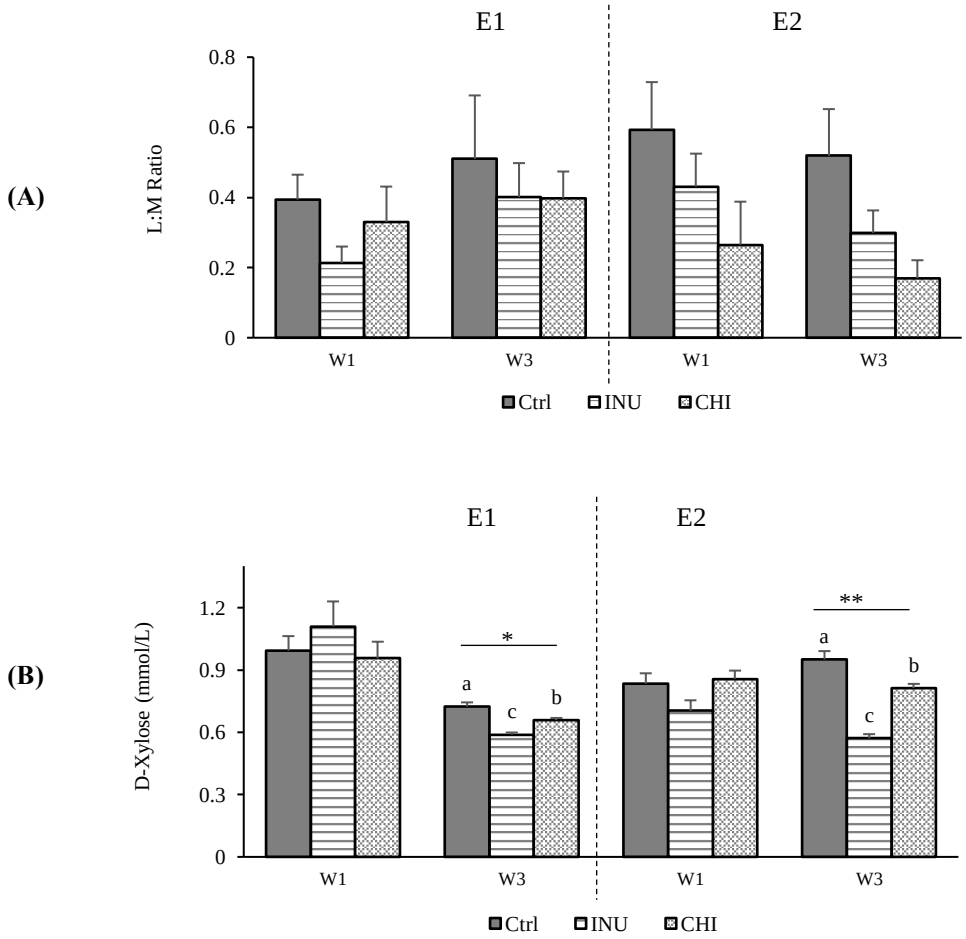

Figure 19. Effect of INU and CHI supplementation on weaning piglet at W1 and W3 in E1 and E2 on permeability of (A) Lactulose: Mannitol (L:M) Ratio and (B) D-Xylose concentration, measured in serum samples.
Values are means (n=8 piglets) ± SEM. Statistical analysis ANOVA: Tukey's test, Bars with different letters are significantly different (* $p < 0.05$, ** $p < 0.01$, *** $p < 0.001$) (CHI: Crude Chicory; INU: Inulin; Ctrl: Control).

3.4.4. Cecal and colonic microbial metabolites

The analysis of cecal and colonic contents at W1 and W3 indicated that CHI and INU treatments in E1 **(Figure 21)** did not elicit significant alterations in SCFA profiles. In E2 **(Figure 20)** at W3, both the INU and CHI groups exhibited higher lactate levels ($p < 0.01$) and lower propionate levels ($p < 0.001$) in cecal content compared to Ctrl group. Conversely, during W1 of E2, significantly elevated lactate ($p < 0.001$) and butyrate ($p < 0.001$) levels were detected in the colonic content of the INU and CHI groups compared to the Ctrl group. Moreover, solely the INU group demonstrated a significantly heightened concentration of total SCFA ($p < 0.001$) in W1. Subsequently, by W3, both the INU and CHI groups demonstrated significantly low acetate levels ($p < 0.001$) and exhibited the highest levels of butyrate ($p < 0.001$) in comparison to the Ctrl group.

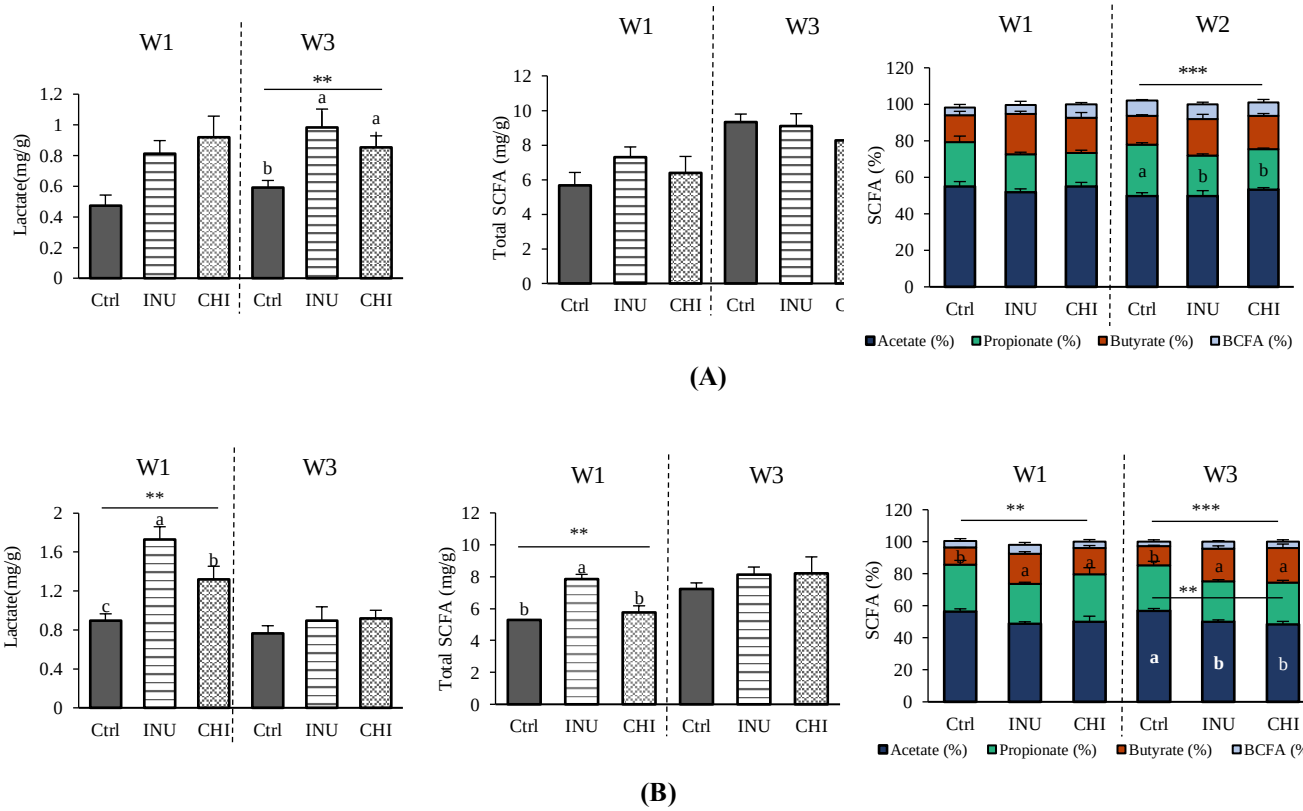

Figure 20. Effect of INU and CHI supplementation in E2 on Lactate, Total Short Chain Fatty Acids (SCFA) and % composition of Acetate, Propionate, Butyrate and Branch Chain Fatty Acids in (A) Cecal and (B) Colonic content.
Values are means (n=8 piglets) ± SEM. Statistics: ANOVA: Tukey's test. Bars with different letters are significantly different (* $p < 0.05$, ** $p < 0.01$, *** $p < 0.001$) (CHI: Crude Chicory; INU: Inulin; Ctrl: Control).

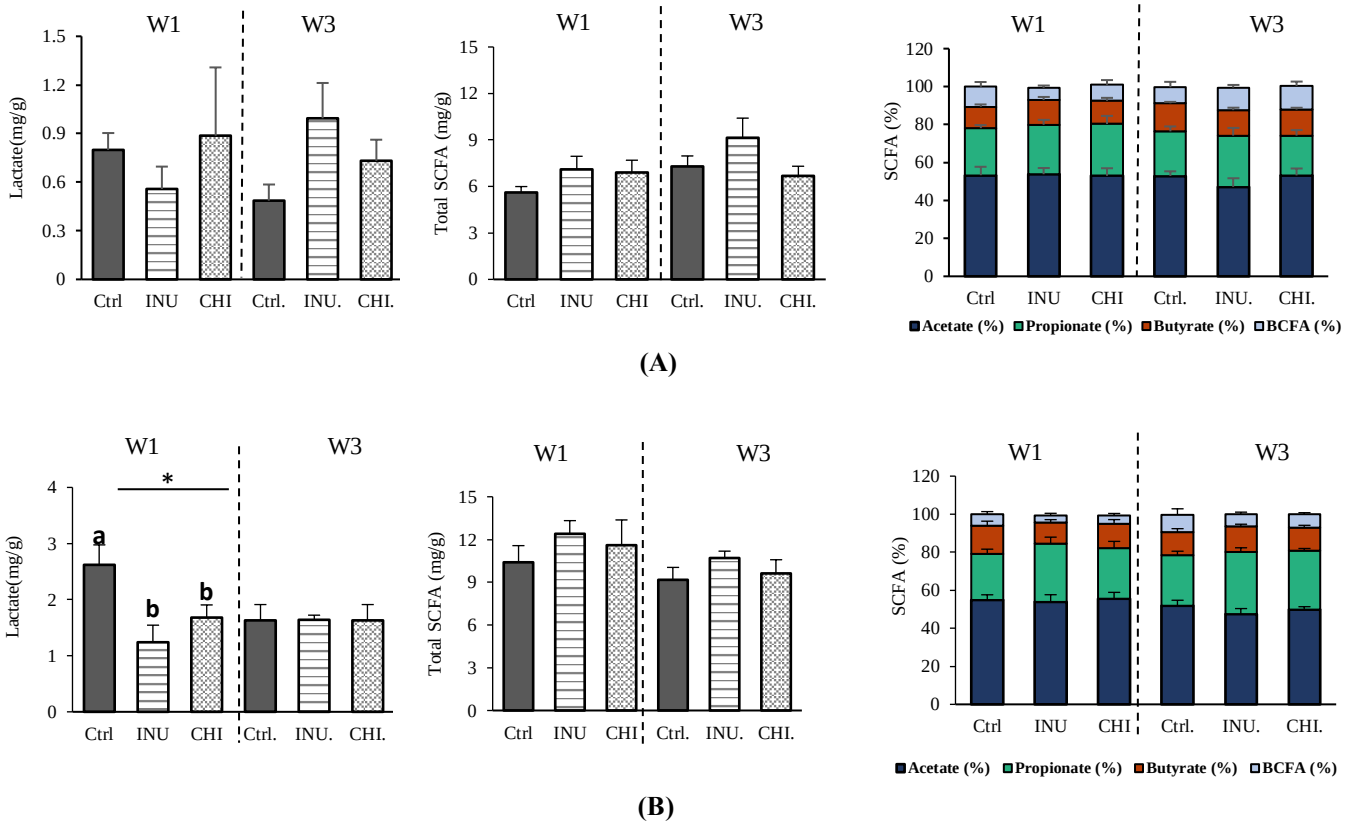

Figure 21. Effect of INU and CHI supplementation in E1 on Lactate, Total SCFA and % composition of Acetate, Propionate, Butyrate and BCFA in (A) Cecal and (B) Colonic content.
Values are means (n=8 piglets) ± SEM. Statistical analysis ANOVA: Tukey's test, * $p < 0.05$, ** $p < 0.01$, *** $p < 0.001$ (CHI: Crude Chicory; INU: Inulin; Ctrl: Control).

3.4.5. Microbiota diversity and abundance

The taxonomic diversity was evaluated and compared utilizing various indices, including Chao1, Shannon, and Simpson. A- diversity analysis revealed no significant differences between treatments across both the experiments, E1 and E2 **(Figure 23 and 22)**, indicating a stable diversity across both groups. To further elucidate the dissimilarities between samples, Principal Coordinates Analysis (PCoA) was conducted employing the Bray-Curtis dissimilarity index. Regarding β- diversity at the ASV level, the impact of inulin and crude chicory was explored. Notably, statistically significant differences were observed at W3 of E1 (PERMANOVA, adj.$p < 0.05$) and W1 of E2 (PERMANOVA, adj.$p < 0.01$), suggesting distinct community compositions influenced by these treatments at specific timepoints. Among the 24 phyla identified through sequencing, Firmicutes and Bacteroidota emerged as the predominant phyla W1 and W3 timepoints in both E2 and E1

Specifically, in W1 of E1, Bacteroidota exhibited significantly higher abundance in the INU and CHI group compared to the Ctrl group (adj.$p < 0.01$), but this difference was not evident at W3. Similarly, in E2, the relative abundance of Firmicutes was notably elevated in the INU and CHI group compared to the Ctrl group at W1 (adj.$p < 0.05$), yet no significant disparities were observed at W3. Other notable phyla present at levels exceeding 1% included Proteobacteria, Spirochaetota, and Actinobacteriota.

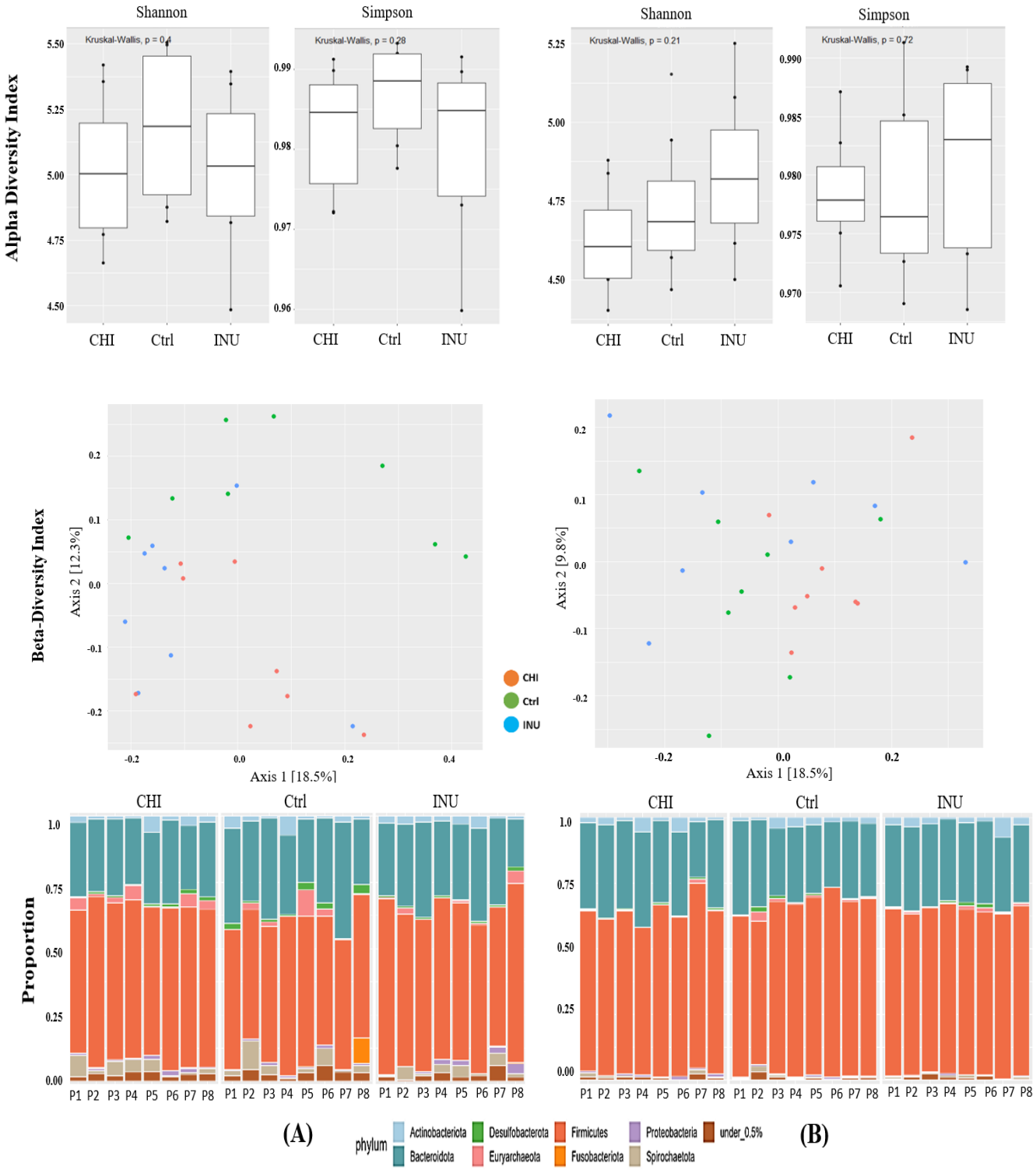

Figure 22. Effect of INU and CHI in E2 on Shannon and Simpson Index in A- (α) diversity and PCoA plot analysis (Bray-Curtis) for B- (β) diversity and abundance at phylum level composition of microbiota at (A) W1 (B) W3. The β-diversity PERMANOVA p values were 0.002 (A) and 0.535 (B).

Values are means ± SEM, n = 8 per treatment except for phylum abundance as values are shown for each piglet per treatment group. (CHI: Crude Chicory; INU: Inulin; Ctrl: Control).

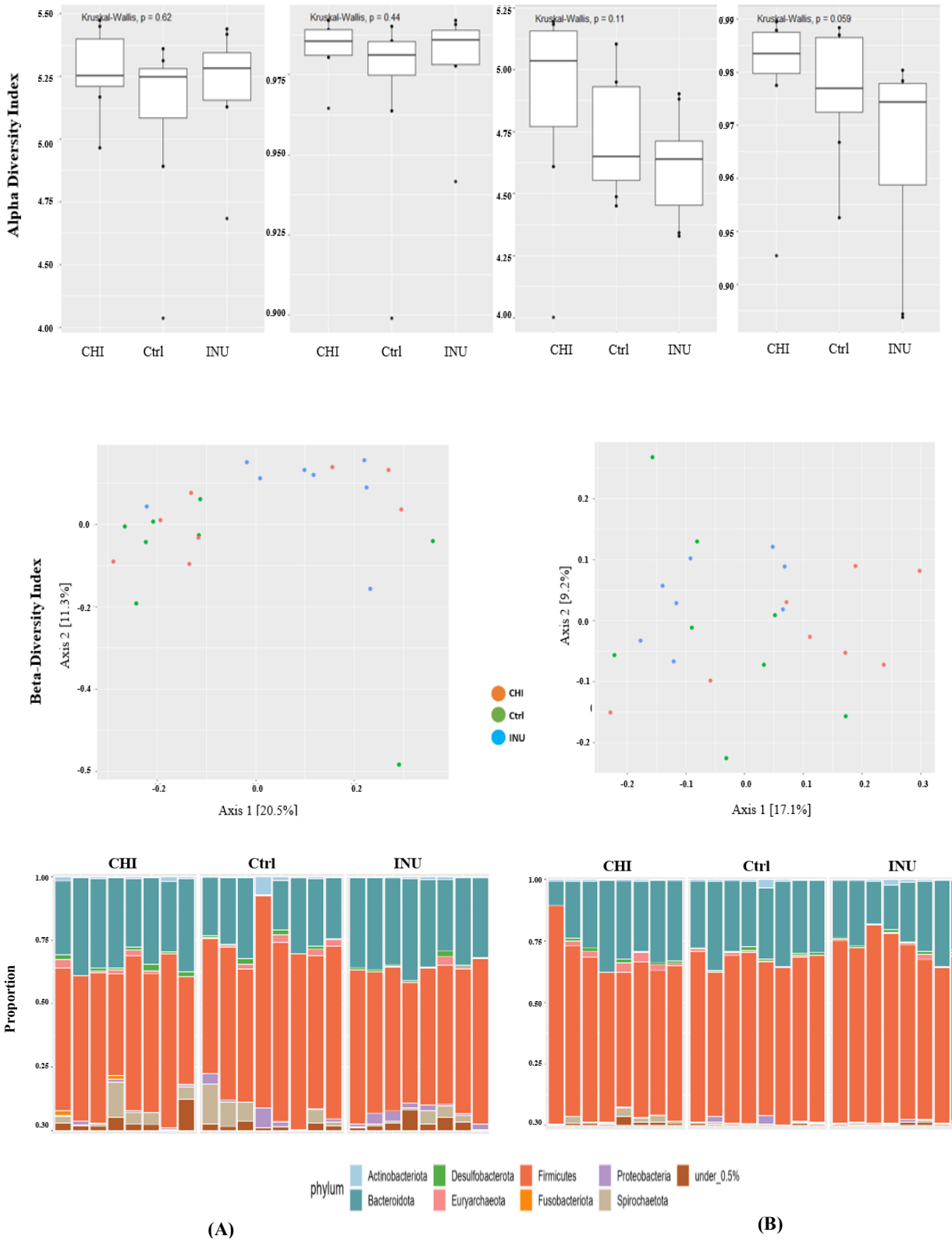

Figure 23. Effect of INU and CHI in E1 on Shannon and Simpson Index in A- (α) diversity and PCoA plot analysis (Bray-Curtis) for B- (β) diversity and abundance at phylum level composition of microbiota at (A)W1 (B) W3. The β-diversity PERMANOVA p values were 0.117 (A) and 0.04 (B).

Values are means ± SEM, n = 8 per treatment except for phylum abundance as values are shown for each piglet per treatment group. (CHI: Crude Chicory; INU: Inulin; Ctrl: Control)

The alterations observed in the colonic microbiota at the genus level, predominantly consisted, *Prevotella*, *Lactobacillus*, *Lachnospiraceae*, and *Megasphaera* emerged as the most abundant genera across both experiments. In E1 **(Table 11)** at W1, a notable increase in the relative abundance of *Prevotella* was discerned in the INU and CHI group (adj. $p < 0.05$). Furthermore, ASVs affiliated with *Succinivibrio* exhibited significantly higher abundance in the INU group compared to CHI and Ctrl (adj.$p < 0.05$). However, at W3, the relative abundance of *Megasphaera* (adj.$p < 0.05$) and *Dialister* (adj.$p < 0.05$) was significantly elevated in the INU group compared to both CHI and Ctrl groups.

At W1 of the E2 **(Table 12)**, there was a dramatic increase in the abundance of *Catenibacterium*, with a sevenfold higher population observed in the crude CHI-fed (CHI) group (7.86 ± 1.63) and a fourfold increase in the INU-fed (INU) group (4.53 ± 2.1) compared to the control (Ctrl) group (0.67 ± 0.18), as evidenced by statistical significance (adj. $p < 0.01$). Additionally, the abundance of *Megasphaera* was notably elevated in the INU and CHI groups compared to the Ctrl group, although this difference was not statistically significant (adj.p=0.051). Upon expanding the analysis to include genera with less than 1% relative abundance (data not shown), seven genera exhibited significant differences among the treatment groups. Piglets fed crude chicory exhibited a substantially higher abundance of *Catemisphaera* ($p < 0.01$), a member of the *Ruminococcaceae* family, compared to those fed with INU. Interestingly, Ctrl group showed even lower levels of *Catemisphaera*. Furthermore, the *Collinsella* genus was significantly more abundant ($p < 0.05$) in the CHI group compared to the Ctrl and INU groups. As shown in the **Table 4** the microbiota composition of W3 of E2, there were 4 genera with significant differences (relative abundance higher than 1%). The abundance of *Unclassified Lachnospiraceae* was found to be significantly high (adj.$p < 0.01$) for the Ctrl compared to the INU and CHI group colonic content. Interestingly the *Streptococcus* abundance was significantly altered (adj.$p < 0.05$) by the addition of CHI (0.41 ± 0.11) and then INU (1.67 ± 0.55) when compared to Ctrl (4.03 ± 1.8).

The inclusion of the crude CHI and INU increased (p=0.05) the population of *Ruminococcus* genus than Ctrl. On the contrary, CHI inclusion caused significant reduction (p=0.01) in the abundance of *Erysipelotrichaceae_UCG-002* than Ctrl and INU. When broadening the analysis in W3-E2 to encompass genera with relative abundances below 1% (Data not shown) it was found that, *Butyricicoccus* showed significant reduction in relative abundance across the INU fed, and CHI-fed groups (adj.$p < 0.05$) as compared to Ctrl. *Colidextribacter*, on the other hand exhibited significant increase (adj.$p < 0.05$) in relative abundance among the INU and CHI groups contrast with the Ctrl group.

Table 11. Relative abundance (≥1%) at genera level in E1 at W1 and W3 after supplementation of INU and CHI.

	Genus	Control	Inulin	Crude Chicory	p value
Week 1 (W1)	*Prevotella*	4.71 ± 1.74[b]	13.11 ± 2.30[a]	9.92 ± 3.49[a]	0.046
	Unclassified Lachnospiraceae	13.48 ± 1.91	12.79 ± 1.01	13.13 ± 1.01	0.505
	Lactobacillus	17.24 ± 5.81	7.31 ± 1.93	8.24 ± 2.48	0.251
	Unclassified Prevotellaceae	5.6 ± 1	5.67 ± 0.72	5.34 ± 1.38	0.833
	Megasphaera	3.69 ± 1.91	4.12 ± 1.30	2.4 ± 1.15	0.183
	Rikenellaceae_RC9_gut_group	2.67 ± 1.09	3.77 ± 1.02	2.84 ± 0.75	0.590
	Blautia	1.83 ± 0.56	3.32 ± 0.50	2.22 ± 0.48	0.172
	Muribaculaceae	3.65 ± 1.22	2.94 ± 0.38	3.69 ± 1.16	0.939
	Streptococcus	1.5 ± 0.8	2.76 ± 2.57	0.75 ± 0.35	0.322
	Alloprevotella	1.53 ± 0.47	2.63 ± 0.64	2.29 ± 0.79	0.349
	Unclassified Bacteroidales	1.47 ± 0.28	2.46 ± 0.59	3.76 ± 0.91	0.208
	Anaerovibrio	0.91 ± 0.37	2.32 ± 0.69	0.73 ± 0.16	0.097
	Phascolarctobacterium	1.56 ± 0.26	1.78 ± 0.15	1.49 ± 0.2	0.415
	Treponema	4.72 ± 1.97	1.73 ± 0.69	3.45 ± 1.46	0.792
	Faecalibacterium	1.17 ± 0.86	1.58 ± 0.54	0.91 ± 0.29	0.172
	Catenibacterium	1.39 ± 0.9	1.47 ± 0.66	0.74 ± 0.24	0.907
	Succinivibrio	0.69 ± 0.14[b]	1.42 ± 0.44[a]	0.41 ± 0.14[b]	0.036
	Christensenellaceae_R-7_group	2.22 ± 0.69	1.40 ± 0.71	2.56 ± 0.61	0.343
	Clostridium_sensu_stricto_1	1.46 ± 0.22	1.08 ± 0.47	1.14 ± 0.35	0.221
	Unclassified Oscillospiraceae	1.57 ± 0.52	1.04 ± 0.15	1.4 ± 0.26	0.618
	Prevotellaceae_UCG-003	0.43 ± 0.08[b]	1.01 ± 0.18[a]	0.48 ± 0.15[b]	0.018
	Campylobacter	0.07 ± 0.04	0.95 ± 0.69	0.64 ± 0.41	0.155
	UCG-005	1.19 ± 0.3	0.94 ± 0.38	1.06 ± 0.2	0.507
	[Eubacterium]_coprostanoligenes_group	1.38 ± 0.46	0.94 ± 0.14	1.32 ± 0.28	0.733
	Prevotellaceae_NK3B31_group	0.24 ± 0.13	0.86 ± 0.36	0.41 ± 0.23	0.306
	Subdoligranulum	0.59 ± 0.19	0.82 ± 0.22	1.13 ± 0.38	0.586
	Methanobrevibacter	1.35 ± 0.45	0.64 ± 0.41	1.13 ± 0.42	0.507
	NK4A214_group	1.02 ± 0.27	0.58 ± 0.22	1.04 ± 0.19	0.275
	Chlamydia	0.07 ± 0.05	0.53 ± 0.28	1.18 ± 0.86	0.312
	Catenisphaera	0.92 ± 0.84	0.44 ± 0.13	1.02 ± 0.75	0.095
	Escherichia-Shigella	1.11 ± 0.94	0.23 ± 0.19	0.13 ± 0.08	0.651
Week 3 (W3)	*Lactobacillus*	13.8 ± 2.44	16.6 ± 2.35	10.54 ± 3.28	0.172
	Prevotella	17.08 ± 1.81	14.24 ± 1.5	11.11 ± 2.77	0.061
	Unclassified Lachnospiraceae	13.4 ± 1.07	12.19 ± 0.99	11.3 ± 1.22	0.590
	Megasphaera	4.48 ± 0.4[ab]	5.79 ± 0.68[a]	3.93 ± 1.21[b]	0.020
	Blautia	4.46 ± 0.56	4.78 ± 0.44	3.9 ± 0.8	0.633
	Streptococcus	2.22 ± 0.88	4.42 ± 3.38	2.58 ± 1.01	0.500
	Dialister	1.54 ± 0.5[b]	2.58 ± 0.21[a]	1.27 ± 0.26[b]	0.030
	Muribaculaceae	2.61 ± 0.43	2.27 ± 0.42	4.43 ± 1.19	0.394
	Rikenellaceae_RC9_gut_group	2.24 ± 0.39	2.26 ± 0.31	3.62 ± 0.56	0.130
	Subdoligranulum	2.04 ± 0.45	2.2 ± 0.56	1.28 ± 0.19	0.281
	Unclassified Prevotellaceae	2.51 ± 0.43	2.07 ± 0.53	2.66 ± 0.59	0.431
	Unclassified Bacteroidales	2.25 ± 0.28	2.02 ± 0.49	3.2 ± 0.61	0.180
	Catenibacterium	1.09 ± 0.26	1.61 ± 0.38	1.63 ± 0.43	0.539
	Faecalibacterium	1.62 ± 0.14	1.51 ± 0.29	1.14 ± 0.19	0.181
	Unclassified Butyricicoccaceae	1.43 ± 0.22	1.5 ± 0.22	2.11 ± 0.46	0.471
	Christensenellaceae_R-7_group	1.1 ± 0.23	1.46 ± 0.51	1.81 ± 0.52	0.589
	Alloprevotella	1.69 ± 0.58	0.92 ± 0.4	1.12 ± 0.42	0.332
	Ruminococcus	1.04 ± 0.16	0.88 ± 0.18	1.13 ± 0.16	0.357
	Lachnospiraceae_NK3A20_group	0.62 ± 0.16	0.85 ± 0.06	0.7 ± 0.09	0.399
	Clostridia_UCG-014	1.19 ± 0.24	0.84 ± 0.12	1.01 ± 0.16	0.464
	[Eubacterium]_coprostanoligenes_group	0.79 ± 0.1	0.82 ± 0.09	1.18 ± 0.25	0.437
	Unclassified Peptostreptococcaceae	0.73 ± 0.25	0.77 ± 0.27	1.39 ± 0.33	0.086
	Clostridium_sensu_stricto_1	1.53 ± 0.48	0.7 ± 0.21	3.67 ± 1.1	0.071
	Unclassified Oscillospiraceae	0.7 ± 0.09	0.69 ± 0.08	1.04 ± 0.23	0.281
	Treponema	0.34 ± 0.07	0.42 ± 0.12	1.45 ± 0.44	0.157
	Methanobrevibacter	0.21 ± 0.05	0.28 ± 0.12	1.04 ± 0.35	0.270
	Prevotellaceae_UCG-003	0.53 ± 0.17	0.23 ± 0.06	1.01 ± 0.24	0.084

Values are means ± SEM, n = 8 per treatment group. Means in a column with timepoint without a common superscript letter differ ($p < 0.05$, Bonferroni correction). The composition expressed in % is only for genera with a relative abundance ≥1% for either of the group.

Table 12. Relative abundance (≥1%) at genera level in E2 at W1 and W3 after supplementation of INU and CHI.

	Genus	Control	Inulin	Crude Chicory	p values
Week 1 (W1)	*Unclassified Lachnospiraceae*	13.05 ± 1.97	13.76 ± 1.21	10.91 ± 1.06	0.393
	Prevotella	6.21 ± 2.13	12.02 ± 2.06	9.27 ± 1.82	0.096
	Lactobacillus	4.39 ± 1.74	7.06 ± 2.23	1.75 ± 0.66	0.096
	Catenibacterium	0.67 ± 0.18^{c}	4.53 ± 2.1^{ab}	7.86 ± 1.63^{a}	0.001
	Unclassified Prevotellaceae	7.89 ± 1.74	4.32 ± 0.66	4.6 ± 0.52	0.162
	Megasphaera	1.13 ± 0.56	4.23 ± 0.9	2.81 ± 0.9	0.051
	Unclassified Bacteroidales	2.91 ± 0.69	3.41 ± 0.55	2.94 ± 0.63	0.652
	Muribaculaceae	2.83 ± 0.52	3.31 ± 0.66	2.24 ± 0.48	0.431
	Treponema	3.02 ± 1.2	2.42 ± 0.68	2.92 ± 0.91	0.970
	Christensenellaceae_R-7_group	2.99 ± 0.88	2.01 ± 0.31	4.54 ± 1.39	0.249
	Blautia	1.44 ± 0.27	1.95 ± 0.3	1.52 ± 0.29	0.343
	Alloprevotella	3.53 ± 0.83	1.87 ± 0.78	1.44 ± 0.26	0.114
	Rikenellaceae_RC9_gut_group	2.58 ± 0.53	1.86 ± 0.2	2.9 ± 0.65	0.393
	Unclassified Oscillospiraceae	2.71 ± 0.91	1.55 ± 0.24	1.78 ± 0.29	0.898
	Faecalibacterium	0.68 ± 0.27	1.5 ± 0.35	2.16 ± 1.02	0.338
	Bifidobacterium	1.77 ± 0.82	1.48 ± 0.45	1.12 ± 0.66	0.353
	Phascolarctobacterium	1.27 ± 0.12	1.4 ± 0.2	1.63 ± 0.23	0.332
	Ruminococcus	2.09 ± 0.29	1.37 ± 0.21	1.32 ± 0.2	0.129
	Subdoligranulum	1.36 ± 0.47	1.22 ± 0.25	1.11 ± 0.27	0.911
	[Eubacterium]_coprostanoligenes	1.73 ± 0.29	1.19 ± 0.11	1.57 ± 0.28	0.367
	Methanobrevibacter	2.11 ± 1.15	1.18 ± 0.59	2.73 ± 0.74	0.229
	UCG-005	1.26 ± 0.39	1.14 ± 0.14	0.88 ± 0.08	0.385
	Mitsuokella	0.27 ± 0.17	0.97 ± 0.5	1.68 ± 0.87	0.077
	Catenisphaera	0.21 ± 0.09^{c}	0.95 ± 0.26^{b}	1.7 ± 0.35^{a}	0.001
	Clostridium_sensu_stricto_1	1.83 ± 0.63	0.94 ± 0.56	0.59 ± 0.17	0.264
	Holdemanella	0.51 ± 0.1	0.91 ± 0.16	1.19 ± 0.31	0.100
	Unclassified Peptostreptococcaceae	1.89 ± 0.67^{a}	0.78 ± 0.38^{b}	0.46 ± 0.15^{c}	0.043
	Anaerovibrio	1 ± 0.29	0.57 ± 0.11	0.42 ± 0.16	0.238
	NK4A214_group	1.04 ± 0.19	0.75 ± 0.08	0.94 ± 0.11	0.447
Week 3 (W3)	*Prevotella*	20.16 ± 1.53	18.54 ± 2.8	19.13 ± 1.53	0.859
	Unclassified Lachnospiraceae	15.33 ± 0.22^{a}	13.69 ± 0.68^{b}	12.71 ± 0.7^{b}	0.004
	Lactobacillus	11.84 ± 1.2	10.08 ± 2.25	15.08 ± 2.37	0.178
	Megasphaera	4.46 ± 0.28	4.21 ± 0.21	4.87 ± 0.81	0.605
	Unclassified Prevotellaceae	2.98 ± 0.7	4.08 ± 0.59	4.07 ± 0.64	0.134
	Blautia	3.13 ± 0.32	3.5 ± 0.56	3.17 ± 0.3	0.462
	Catenibacterium	1.55 ± 0.29	2.96 ± 0.95	2.18 ± 0.58	0.573
	Muribaculaceae	1.32 ± 0.17	2.33 ± 0.68	2.18 ± 0.56	0.581
	Mitsuokella	1.45 ± 0.28	1.96 ± 0.52	0.86 ± 0.33	0.174
	Streptococcus	4.03 ± 1.8^{a}	1.67 ± 0.55^{b}	0.41 ± 0.11^{c}	0.037
	Dialister	1.96 ± 0.27	1.63 ± 0.29	1.46 ± 0.25	0.310
	uncultured	1.49 ± 0.19	1.57 ± 0.13	1.18 ± 0.14	0.174
	Ruminococcus	0.94 ± 0.08^{b}	1.55 ± 0.29^{a}	1.42 ± 0.25^{a}	0.050
	Unclassified Bacteroidales	1.19 ± 0.24	1.5 ± 0.43	1.56 ± 0.35	0.785
	Faecalibacterium	1.28 ± 0.21	1.41 ± 0.31	1.26 ± 0.24	0.949
	Rikenellaceae_RC9_gut_group	1.04 ± 0.1	1.34 ± 0.3	1.36 ± 0.29	0.761
	Bifidobacterium	1.11 ± 0.37	1.33 ± 0.51	1.45 ± 0.76	0.860
	Alloprevotella	1.09 ± 0.12	1.19 ± 0.34	0.97 ± 0.22	0.739
	Erysipelotrichaceae_UCG-002	1.48 ± 0.91^{a}	1.14 ± 0.77^{a}	0.04 ± 0.02^{b}	0.010
	Unclassified Atopobiaceae	0.72 ± 0.2	1.13 ± 0.41	0.41 ± 0.09	0.247
	Subdoligranulum	1.7 ± 0.35	1.12 ± 0.19	1.45 ± 0.28	0.442
	Christensenellaceae_R-7_group	0.54 ± 0.12	1.11 ± 0.4	1.08 ± 0.59	0.838
	Clostridia_UCG-014	1.15 ± 0.15	0.97 ± 0.16	1.01 ± 0.17	0.613

Values are means ± SEM, n = 8 per treatment group. Means in a column with timepoint without a common superscript letter differ, (Kruskal–Wallis, followed by Dunn's test adj. ($p < 0.05$). The composition expressed in % is only for genera with a relative abundance ≥1% for either of the group.

3.4.6. Relative gene expression in Ileum and colonic tissues

The results pertaining to Barrier Integrity Genes showed a mixed pattern of results in both, E1 (data not shown) and E2 **(Figure 24)**. On one hand, in the colon, an upregulation of *ZO-1* was observed at W1 of E1 in the CHI-fed piglets (adj.p < 0.05) but on the other hand it was found to be downregulated (adj.p < 0.05) in W3 of E2 in CHI group. In the ileum at W1 in E1, INU and crude CHI-supplemented piglets showed an upregulation of *MUC1* (adj.p < 0.05) and Occludin (p=0.018). While in E2, *MUC1* (p=0.04) was upregulated in the colon at W3 in CHI group. Additionally, the apoptosis related gene *CASP3* was downregulated in INU fed piglets in both E1 (adj.p < 0.01) and E2 (adj. p < 0.05) at W3 in the ileum.

The analysis of gene expression in colon tissue following CHI and INU supplementation demonstrated limited overall impact on inflammatory target and signalling pathway target genes. This indicates that crude CHI or INU at this dosage had a minor effect in reducing inflammation. However, in E2, when the dosage was doubled, an effect was seen on some genes in the ileum as well as the in colon. In the ileum, at W3, three pro-inflammatory genes (*CXCL10, IL18, TNFα*) and inflammation signalling genes (*NFκB1* (adj.p < 0.05) were downregulated in INU and CHI groups. In the case of colonic tissue, a significant (adj.p < 0.05) downregulation of inflammation signalling pathway genes like *TANK* and *TLR2* as well as inflammatory target genes like *CXCL10* and *INFγ* genes were observed at W1. Similarly, at W3, both CHI and INU proved to be beneficial at this higher dosage level in colon tissue, as inflammation signalling (*NFκB1* (adj.p < 0.01), *TLR2* (adj.p < 0.05) and inflammatory target genes (*DEFβ4A* (adj.p < 0.05), and *TNFα* (adj.p < 0.05)) were significantly downregulated compared to the Ctrl group.

3.4.7. Integrative Analysis

As seen in **Figure 25** of PCA and correlation plots in E2, at both W1, and W3, there was a significant (adj.p < 0.05) positive correlation of ADG (r=0.887, 0.729) and Average Daily Calorie Intake (ADCI) (r=0.0.837, 0.662) to dimension 1. The supervised RGCCA plots for the Gut block **(Figure 26A)** show that, at W3, component 1 separates the Ctrl samples from CHI and INU samples. The INU and CHI samples were separated by component 2. Pearson correlation analysis demonstrated significant positive correlation (r=0.671, adj.p <0.05) between ileum villus width and component 1 while a strong significant negative correlation between ileum V:C ratio and component 2 (r=-0.83, adj.p < 0.05) as represented in variables plots. Similar observations were made in case of jejunum and duodenum crypt depth in W1. RGCCA also shows a positive correlation between cecum butyrate (r=0.411, p>0.05) and colon butyrate (r=0.817, adj.p <0.05) in W3 (as well in W1). Along the component 1, Ctrl samples are distinct from INU and CHI and D-Xylose (r=-0.565, p < 0.05) as well as L:M ratio (r=-0.558, p < 0.05) were negatively correlated to this component.

In the similar supervised RGCCA (W1) for the Microbiota block, variable plot shows a significant negative correlation between component 1 and some microbes like *Megasphaera* (r=-0.755, adj.p < 0.05) and *Prevotella* (r=-0.737, adj.p < 0.05) thus separating the clusters of Ctrl from CHI and INU. CHI and INU samples were separated on the component 2 as expected across the different blocks. While in W3 **(Figure 26C)**, *Ruminococcus* (r=0.794) tend to have significant positive correlation while *Butyricoccus* (r=-0.589), *Lachanospiraceae* (r=-0.628), *Slackia* (r=-0.557), *Prevotella* (r=-0.509) and *Streptococcus* (r=-0.473) significant negative correlation with component 1 (p < 0.05). A significant positive correlation by supervised RGCCA (r=0.817) of butyrate with component 1 was found **(Figure 7A)**. Also, negative correlation with component 1 of several colonic (*NFκB1* (r=-0.837), *CASP1* (r=-

0.744), *MAPK14* (r=-0.696) as well as Ileum (*IL18* (r=-0.835), *CASP3* (r=-0.79), *CXCL10* (r=-0.782), *TANK* (r=-0.758), *MyD88* (r=-0.696) genes **(Figure 26B).**

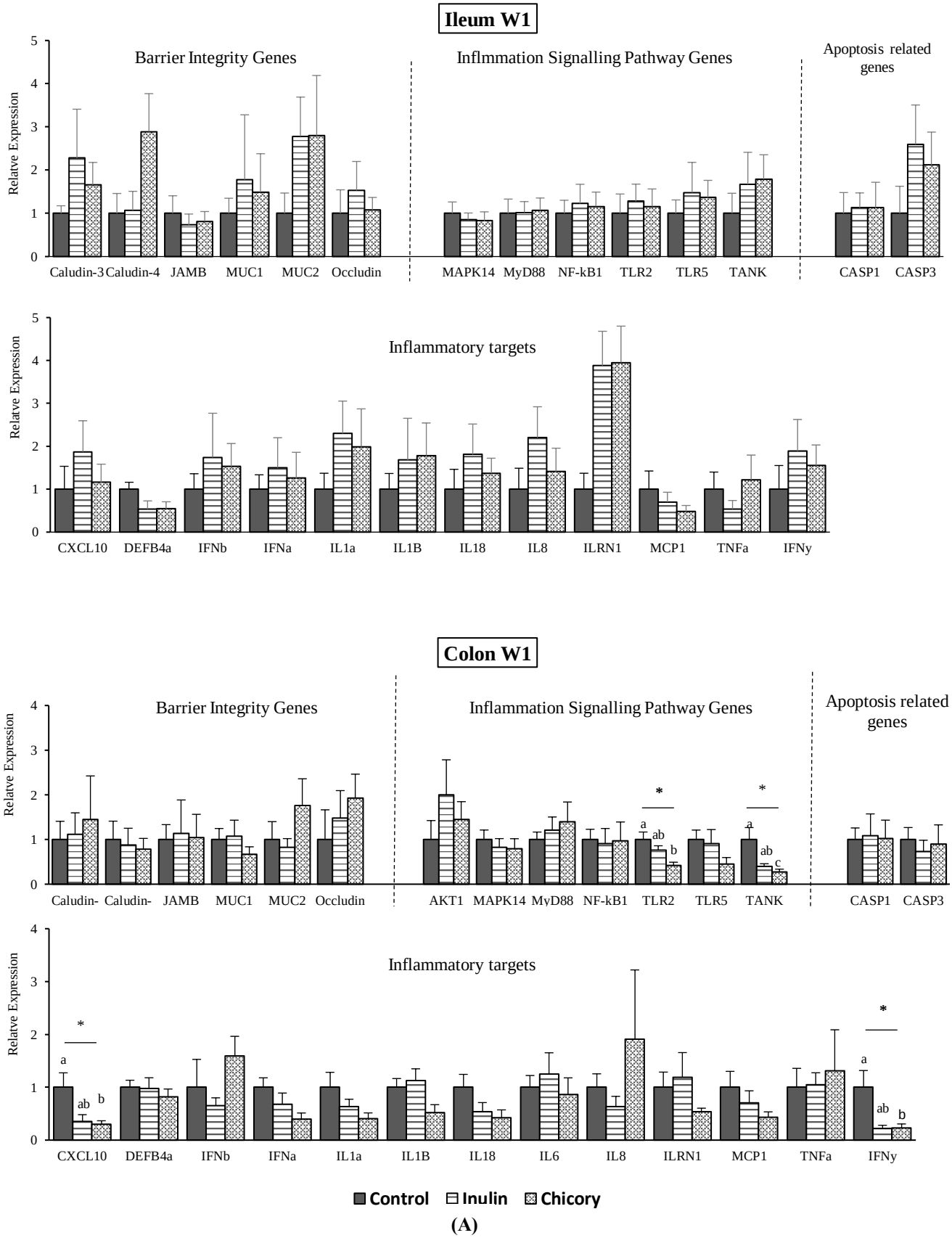

(A)

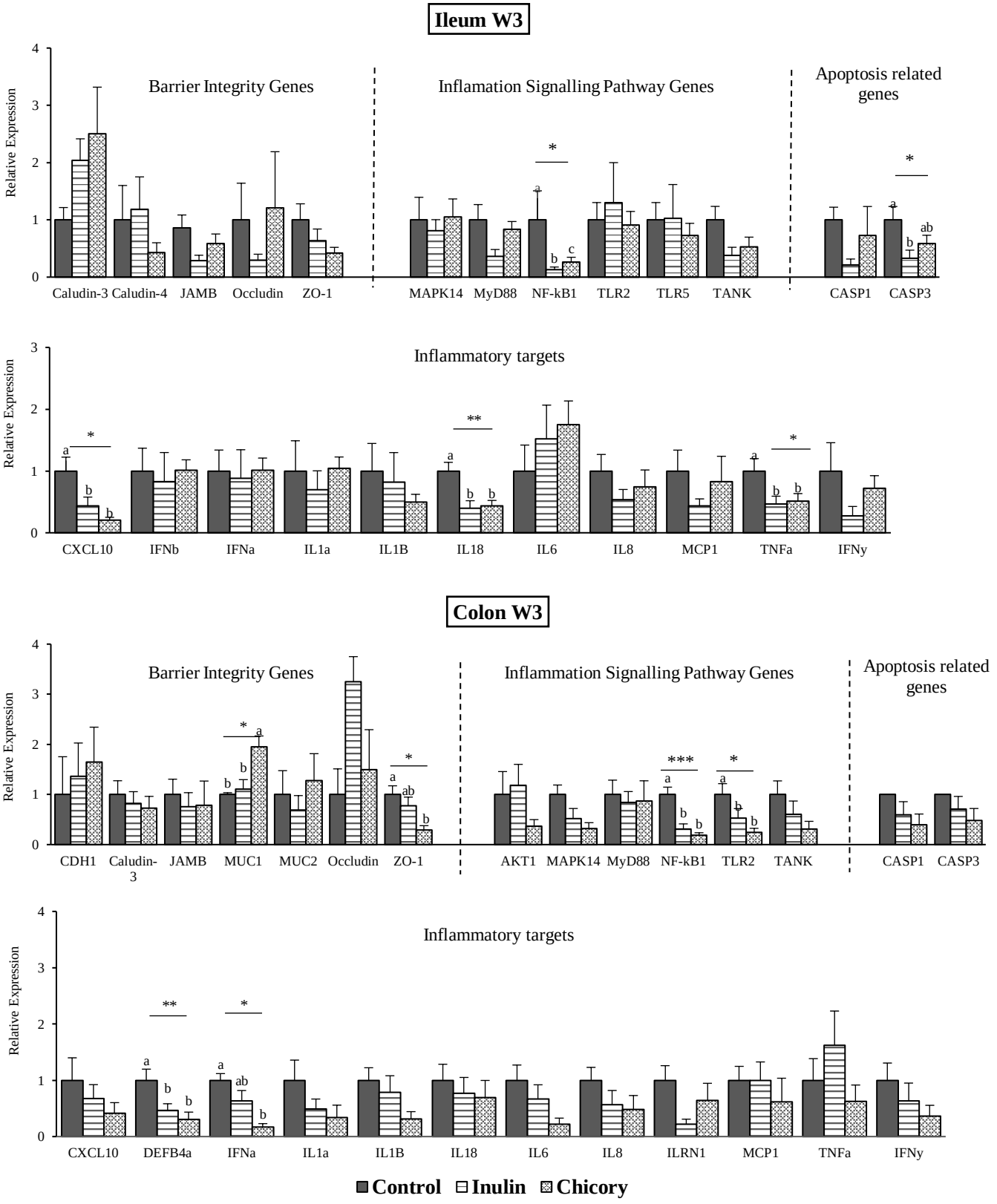

(B)

Figure 24. Effect of INU and CHI in E2 on expression of barrier integrity, inflammation signalling pathway and apoptosis related genes in Ileum and Colon at (A) W1 and (B) W3.

Values are means (n=8 piglets) ± SEM. Statistical analysis was performed using one way ANOVA and Tukey's test. Bars with different letters are significantly different (*p < 0.05, **p < 0.01, ***p < 0.001)

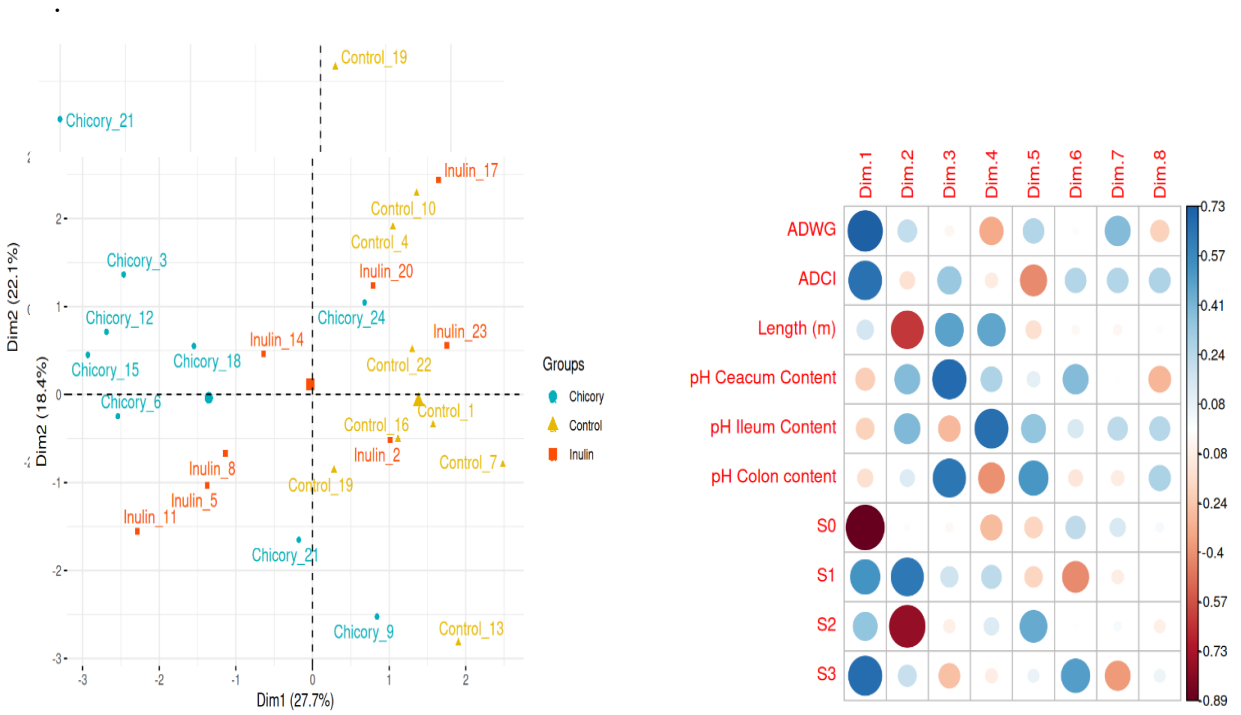

(A) **(B)**

Figure 25. Principal Component Analysis (PCA) plots (Dim 1 and Dim 2) and correlation plots for (A) W1 and (B) W3 of E2 considering only the variables of the 'Clinic' block. Samples in the PCA plot are coloured by group.
Colour and size of circles in the correlation plot represent Pearson correlation level (from negative correlations in red to positive correlations in blue and larger circle for higher absolute correlation value) of each 'Clinic' variable with each of the first 8 components of the PCA (range –0.89 to 0.91). (CHI: Crude Chicory; INU: Inulin; Ctrl: Control)

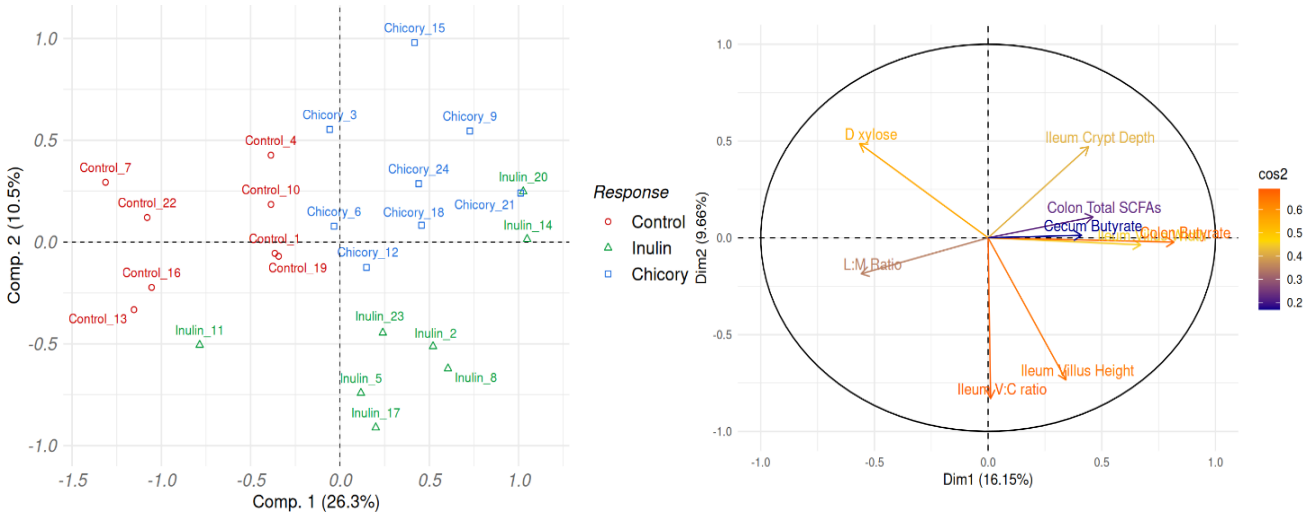

(A)

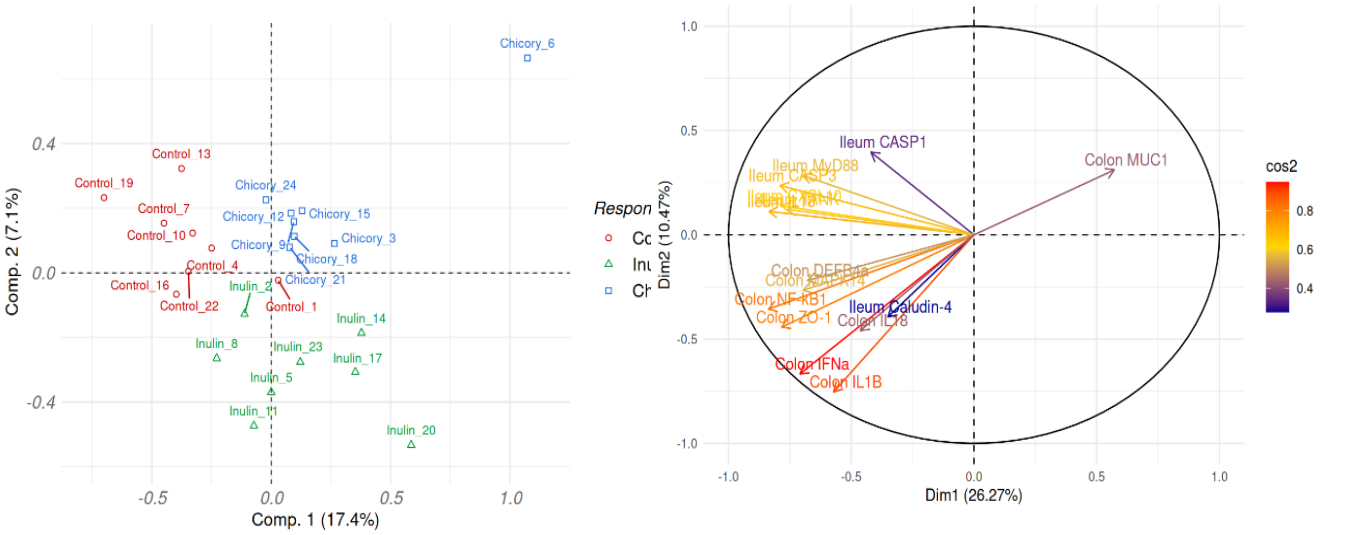

(B)

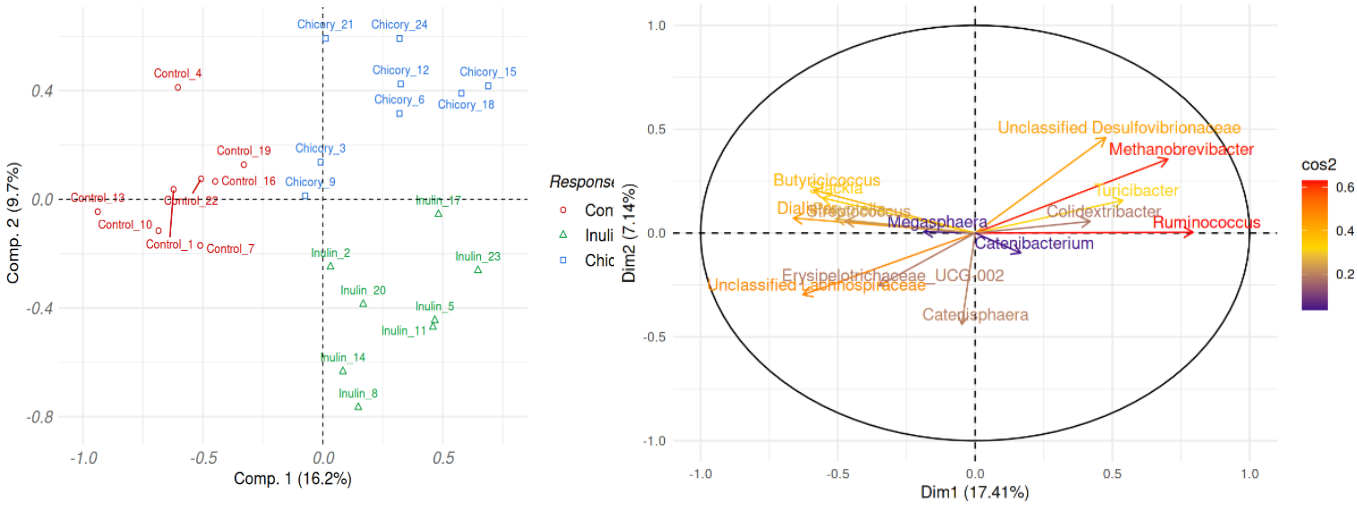

(C)

Figure 26. Individuals (left) and variables (right) plots from supervised RGCCA displayed for components 1 and 2 considering the variables from (A) Gut, (B) Gene Expression and (C) Microbiota blocks at W3 in E2.

Samples in the individual's plots are coloured by group similarly as PCA. Arrows colour and length in the variable plot are based on square cosine (cos2) indicating the quality of the representation of the variables by the two first components of RGCCA for a given block (higher cos2 value, represented by long red arrow, means a better representation of the variable by the two first components). Direction of arrows indicates which components represent the corresponding variables, horizontal for component 1, vertical for component 2 and diagonal for both components. (CHI: Crude Chicory; INU: Inulin; Ctrl: Control)

3.5. Discussion

The gastrointestinal tract's intricate layers, encompassing the physical, biochemical, and immunological realms, serve as barriers against the infiltration of harmful microorganisms, toxins, and antigens (Barreau and Hugot, 2014; Mu *et al.,* 2017b). To address the variability in inulin dosages documented in prior research on weaned piglets, we conducted two distinct animal experiments, with force-feeding, which unlike most previous studies, sought to monitor the exact amount of supplementation (Apper *et al.,* 2016; Ayuso *et al.,* 2020; C. H. *et al.,* 2005; Sabater-Molina *et al.,* 2011; Trevisi *et al.,* 2008; Wu *et al.,* 2020).

Crude chicory roots (*Cichorium intybus L.*) have a diverse nutritional profile, offering a plethora of bioactive compounds besides inulin. The chemical analysis of crude chicory flour **(see Table 8)** reveals high levels of Neutral Detergent Fiber (NDF), and Acid Detergent Fiber (ADF) compared to pure inulin. This composition (high cellulose and hemicellulose content) likely contributes to slower digestion rates and reduced palatability compared to pure inulin (Weimer, 1996), which may explain the lower Average Daily Feed Intake (ADFI) (kcal/day) in the CHI group during W3 of E1 and throughout E2. Furthermore, the reduced ADFI might be influenced by intestinal hormones such as cholecystokinin (CCK) and glucagon-like peptide-1 (GLP-1), pivotal in the gut-brain axis, regulating appetite and food intake (Caron *et al.,* 2017; Morton *et al.,* 2006; Wren and Bloom, 2007). Notably, (Fouré *et al.,* 2018) demonstrated increased secretion of CCK and GLP-1 following crude chicory supplementation, and this was elevated even more with sesquiterpene lactones. Additionally, the presence of SCFA in the colonic lumen might augment GLP-1 levels and diminish ghrelin levels (Susan Sungsoo Cho, 2009; Tarini and Wolever, 2010). Notably, lack of impact on weight gain or average calorie intake, consistent with various studies (Barszcz *et al.,* 2016, 2018, 2020; Li *et al.,* 2018; Liu *et al.,* 2012; Uerlings, *et al.,* 2021; Wang *et al.,* 2020). Moreover, a review by (Hughes *et al.,* 2021) highlights multiple human studies reporting no effect of inulin-type fructans consumption on body weight or BMI (Byrne *et al.,* 2019; Pol *et al.,* 2018; Reimer *et al.,* 2017; Weitkunat *et al.,* 2017).

Stress-induced diarrhoea poses a significant threat to the gut health of weaned piglets, rendering them more susceptible to intestinal inflammation and post-weaning diarrhoea due to the rapid proliferation of pathogenic bacteria and a decline in microbial diversity (Lange *et al.,* 2010; Pluske, 2016; Qiu *et al.,* 2021; Winter *et al.,* 2013b). Lower incidences of mild diarrhoea in INU and CHI in E2, exhibited prebiotic effects. The lack of normal faeces in E2 during Week 1 could be attributed to increased stress and gastrointestinal disturbance caused by the higher frequency of handling and double dosing, both of which are known to negatively impact gut motility, barrier function, and microbial balance. It is well-established that oligosaccharides possess anti-inflammatory properties and anti-adhesive activity, inhibiting pathogen binding (Quintero *et al.,* 2011; Zenhom *et al.,* 2011). Remarkably, at W3 in E2, supplementation of chicory flour led to fewer instances of severe diarrhoea (S3), surpassing the effect of inulin. Several microbial and metabolite modulations can be connected to this effect, which will be discussed later.

Weaning triggers changes in the gastrointestinal tract, such as small intestinal villi atrophy and crypt hyperplasia, leading to the loss of mature enterocytes leading to a reduced nutrient absorption (Lalles *et al.,* 2004; Moeser *et al.,* 2017a; Zheng *et al.,* 2021). After W3 of supplementation in E1, noteworthy improvements were observed on parameters like histomorphology, D-xylose permeability, and beneficial microbiota composition but only in the INU, despite comparable 'inulin content' between INU and CHI. However, doubling the dose in E2 led to some enhancements in the jejunum and ileum of CHI-fed piglets as CHI exhibited greater average villus height than INU in the ileum. This finding aligns with (Liu *et al.,* 2012; Uerlings, Arévalo Sureda, *et al.,* 2021), who also reported increased villus height in piglets fed with a crude chicory root diet compared to

controls. Similarly, Wan *et al.,* 2020 demonstrated increased villus height and V:C ratio in both jejunum and ileum after 3 weeks of supplementation with 2.5 g/kg and 5.0 g/kg of inulin. They associated these improvements in intestinal morphology with elevated serum IGF-1 concentration, considering its critical role in organ development and growth (Walton *et al.,* 1995). This histomorphological improvements could also potentially be associated with the higher butyrate levels observed in both the INU and CHI groups in our study (E2). Bawish *et al.,* 2023 similarly observed a significant rise in IGF-1 levels after supplementing with sodium butyrate for 3 to 5 weeks. The supervised RGCCA **(Figure 26A)** confirmed a significant positive correlation of ileum villus width (r=0.761) with colon butyrate (r=0.817) produced at W3 thus indicating an increasing absorptive surface area during the recovery period of weaning stress. Throughout both experiments, there was a lack of impact on the thickness of the *muscularis mucosae*, *tela submucosa*, or *tunica muscularis* layers, which was also reported by (Liu *et al.,* 2012) following crude chicory supplementation. However, in contrast, (Uerlings *et al.,* 2021) observed that pigs treated with inulin displayed variations in the thickness of the duodenal *muscularis mucosae* and *tela submucosa* layers on days 10–11 and 31–32.

Inadequate early nutritional intervention can exacerbate morphological disruptions triggered by weaning stress, impairing the absorptive capacity and performance of weaned pigs (Brown *et al.,* 2006; Lalles *et al.,* 2004). Recognizing the potential of prebiotics like inulin to preserve intestinal mucosal barrier function (Uerlings *et al.,* 2020; Wan *et al.,* 2020), our study sought to determine if crude CHI could offer comparable or superior effects. Unlike in humans, assessing sugars in urine in pigs presents complexities due to the necessity of urine collection methods such as metabolism cages, urinary bladder urethral catheterization, cystocentesis, or attached bags. These procedures can induce stress in piglets, potentially compromising intestinal integrity and function. Given that a single blood measurement may be influenced by pre-mucosal and post-mucosal factors, we opted to employ a '3 sugar cocktail' (Hu *et al.,* 2023; Ortega and Szabó, 2021) to study the barrier integrity. While weaning compromises paracellular barrier function (Kim *et al.,* 2019b), CHI showed a trend, although statistically insignificant, towards reducing the L:M ratio (adj.p =0.057), suggesting reduced permeability. Interestingly, D-Xylose exhibited a reduced permeability in the INU group compared to CHI, aligning with those of Uerlings *et al.* (2021). The supervised RGCCA **(Figure 26A)** shows that butyrate may contribute to maintaining gut barrier function and reducing intestinal permeability as D-xylose (r=-0.565) and L:M (r=-0.558) were negatively correlated with colon butyrate (r=0.871) and villus width (r=0.671) in W3.

The decreased permeability in INU and CHI groups may underlie the lower diarrhoea incidence in these groups because a good mucosal barrier prevents harmful substance translocation and maintains fluid balance (Arrieta, 2006b; Groschwitz and Hogan, 2009; Wijtten *et al.,* 2011). While our study did not find consistent differences in tight junction gene expression, the downregulation of leucocyte elastase inhibitor (SERPINB1) observed in crude CHI-fed pigs suggests a potential mechanism for intestinal barrier modulation (Herosimczyk *et al.,* 2018; Uchiyama *et al.,* 2012). To obtain a clearer understanding of the effect of chicory on barrier junction network it would be recommended to determine changes at the protein level.

Despite the absence of a significant impact on the total SCFA production in E2, both chicory and inulin supplementation led to changes in SCFA composition. Specifically, acetate levels were generally reduced (with a significant decrease observed only in W1), while butyrate levels were notably elevated in both W1 and W3 for both the INU and CHI groups. Although literature reports disparities in SCFA levels post-INU supplementation (Eberhard *et al.,* 2007; Halas *et al.,* 2009), our findings of E2 are consistent with previous studies by Liu *et al.,* 2012; Loh *et al.,* 2006; Mair *et al.,* 2010; Mikkelsen and Jensen, 2004. The reduced acetic acid concentration in colonic content may result from butyrate-producing bacteria utilizing acetate, with some

acting as net consumers (Barcenilla *et al.,* 2000), highlighting acetic acid's role in cross-feeding interactions among colonic bacteria (De Vuyst *et al.,* 2014; De Vuyst and Leroy, 2011; Moens *et al.,* 2017). In the case of inulin-type fructans, two primary cross-feeding mechanisms have been identified: one involving the release of short-chain oligosaccharides and monosaccharides by *Bifidobacterium* spp. during prebiotic degradation, and another involving the utilization of fermentation end-products—such as acetate and lactate—produced by *Bifidobacterium* during fructan metabolism (Belenguer *et al.,* 2006; Falony *et al.,* 2006; Rossi *et al.,* 2005). This effect of CHI and INU could also be supported by supervised RGCCA as it shows a significant negative correlation of butyrate (r=0.817) with acetate (r=-0.796) in colon at W3. In contrast, Nakayama *et al.,* 2020 reported a significant increase in acetate and butyrate production in the inulin-supplemented group *in vitro*, albeit with a higher Average Degree of Polymerization (DP_w=21.7) compared to our study (DP_w=13-14). Studies suggest that INU-type fructans with a broader range of DP, such as oligofructose-enriched inulin, exhibit greater butyrate production than other types (Hernot *et al.,* 2009). Thus, comparing very crude chicory or very pure inulin might have not provided a balanced representation of long-length fractions of INU and oligofructose content.

The increase in butyrate production, consistent with few other findings from previous inulin supplementation studies (Bastard *et al.,* 2020; Uerlings *et al.,* 2019; Wang *et al.,* 2020), underscores its beneficial impact on gut health. Butyrate is known for its ability to improve intestinal barrier function and possesses anti-inflammatory, anti-cancer, and antioxidant properties (Corrêa-Oliveira *et al.,* 2016; Cui *et al.,* 2019; Hamer *et al.,* 2008; Hodgkinson *et al.,* 2023; Bastard *et al.,* 2020; Millard *et al.,* 2002; Rivière *et al.,* 2016) Additionally, the reduction in mild and severe diarrhoea incidences during W1 and W3 respectively, of E2 following crude chicory and inulin supplementation may also be linked to increased butyrate production in the colon. Xiong *et al.,* (2019) demonstrated that dietary supplementation of 0.1% sodium butyrate reduced diarrhoea and improved gut integrity in weaned pigs. Our study revealed an increase in the abundance of several genera known for butyrate production, suggesting their contribution to butyrate synthesis. Therefore, the observed outcomes at the end of W3 in the CHI and INU groups, such as improved permeability, reduced expression of pro-inflammatory genes, decreased diarrhoea, and enhanced histomorphology, may be attributed to increased butyrate production.

Microbial metabolites play a crucial role in immune function and inflammatory processes by impacting epithelial cells, dendritic cells, T cells, and intestinal permeability (Levy *et al.,* 2017). But SCFA levels provide only a snapshot due to rapid absorption (Cummings *et al.,* 1987). CHI and INU showed comparable butyrate production, suggesting an independent effect from other chicory bioactives. Thus, further exploration of the gut microbiota is crucial. Early-life microbial colonisation has a substantial impact on the development of the intestinal and immune systems, with long-term benefits for immunological function (Laforest-Lapointe and Arrieta, 2017). Inulin's effect on the microbiota has been extensively investigated (Cunningham *et al.,* 2021). It is however interesting to determine whether when supplementing with chicory positive effects are simply due to inulin or if other bioactives also contribute to microbiota changes. The increased abundance of Firmicutes and Bacteroidetes, the predominant bacterial phyla, following supplementation with inulin and chicory in both experiments, corresponds with findings by Juhász *et al.,* 2022. The higher total SCFA concentration observed in the CHI and INU groups in W1 of E2 may be attributed to many bacteria within these phyla, with hydrolytic enzymes capable of degrading non-starch carbohydrates (Dodd *et al.,* 2011; He *et al.,* 2021). Our study also revealed disparate microbial responses between experiments despite similar nutrient interventions but at different dosages, underscoring the challenges in replicating experiments related to microbiota composition. Inulin is known for its capacity to modulate *Lactobacillus* and *Bifidobacterium* that produce fatty acids such as

acetic acid, propionic acid, butyric acid, succinic acid, and pyruvate in humans and rodents (Kleessen *et al.,* 2007; Bastard *et al.,* 2020; Nilsson and Björck, 1988; W. Wang *et al.,* 2020), yet its impact in pigs is inconsistent (Loh *et al.,* 2006). In our study, although *Lactobacillus* was found to be highest in the CHI group in E2 at W3, there were no significant differences, which is in accordance with previous findings (Loh *et al.,* 2006; Mair *et al.,* 2010; Metzler-Zebeli *et al.,* 2009; Uerlings, Arévalo Sureda, *et al.,* 2021).

The 2-3 times higher abundance of *Prevotella* after W1 in E1 **(Table 11)**, along with *Megaspheara*, *Dialister*, and *Succinovibrio*, is associated with improved intestinal health and has been previously observed in pigs fed with inulin (Dou *et al.,* 2017; Nielsen *et al.,* 2016; Van den Abbeele *et al.,* 2018; Wu *et al.,* 2020). The prevalence of the harmful microbe, *Turicibacter,* linked to steroid and lipid metabolism, was significantly reduced in both the INU and CHI groups. This bacterium is negatively correlated with protein and energy digestibility in low-fiber fed growing-finishing pigs (Sciellour *et al.,* 2018).

Interestingly, in E2, likely attributable to the higher supplementation dose, a significant increase in beneficial microbiota and a reduction in harmful one a significant enhancement in most of the beneficial or reduction in harmful effect causing microbiota was observed in the CHI group compared to both the INU groups. Major abundant (>1%) genus affected by chicory or inulin were *Catenibacterium*, *Megasphaera*, *Catenispaera*, *Peptostreptococcaecea*, *Lachanospiraceae*, *Streptococcus*, *Ruminococcus*, *Erysipelotrichaceae*. Minor (<1%) abundance genera were also found to be altered like *unclassified Desulfovibrionaceae*, *Butyricoccus*, *Collinsela* and *Colidextribacter*. *Megasphaera* (r=-0.755) and *Prevotella* (r=-0.737) were negatively correlated with *Colidextribacter* (r=0.733) and *Cornybacterium* (r=0.695). *Catenibacterium* was the fourth most abundant genus, with significantly greater levels in both CHI and INU groups during W1 of E2. While inulin-type fructans have been shown to increase *Catenibacterium* levels (Neyrinck *et al.,* 2021; Rodriguez *et al.,* 2022; Sarmiento-Andrade *et al.,* 2022), it was surprising to find a seven-fold increase in CHI compared to the Ctrl, whereas the increase with INU was only 1.5-fold, indicating additional positive effects from other bioactives in CHI. According to Juśkiewicz *et al.,* 2011, crude chicory roots contain phenolic chemicals such as Monocaffeoyllquinic acids (MCQA), dicaffeoylquinic acids (DCQA), and chicoric acid. Silva *et al.,* 2022 experienced a comparable rise (13.4-fold) with polyphenol-enriched supplements, as did Peron *et al.,* 2022.

Although bacteria of the genus *Megasphaera* are nonfructan-degrader, increase in its abundance after W1 (E2) of supplementation was observed in the colon of piglets fed with chicory and inulin (adj.p=0.051) which aligns with other studies (Barszcz *et al.,* 2016; Halas *et al.,* 2009). *Megasphaera* can produce SCFA, vitamins and essential amino acids (Shetty *et al.,* 2013). Similarly, *Catenisphaera* showed significant enrichment in CHI (1.7% ± 0.35) compared to INU (0.95% ± 0.26), while the Ctrl group had very low abundance (0.21% ± 0.09). Furthermore, the supervised RGCCA **(Figure 26C)** shows the negative correlation of *Catenisphaera* (r=-0.713) with *Ruminicoccus*. Yang *et al.,* 2022 also observed increased *Catenisphaera* abundance in pigs fed a fiber-rich diet (inulin and cellulose). This genus has been associated with mitigating inflammation, *E. coli* infection, weaning diarrhoea, and various diseases in pigs across multiple studies (Hankel *et al.,* 2022; Hou *et al.,* 2020; Smith *et al.,* 2020; Su *et al.,* 2021).

The reduction in the relative abundance of *unclassified Peptostreptococcaecea* upon prebiotics supplementation has also been documented by Wu *et al.,* 2020 and Wu *et al.,* 2023. While some members of this family are considered opportunistic pathogens, others are commensal bacteria vital for gut health. Thus, drawing definitive conclusions regarding the role of *unclassified Peptostreptococcaceae* in crude CHI or INU is challenging. Regarding *Desulfovibrio*, Sarmiento-Andrade *et al.,* 2022 noted inulin concentration positively correlating with butyrate and negatively correlating with *Desulfovibrionaceae* abundance, consistent with our

findings of increased butyrate and a four-fold reduction in *Desulfovibrionaceae* genus abundance in the INU and CHI groups. RGCCA shows that *Desulfovibrionaceae* (r=0.816) was negatively correlated to *Prevotella* (r=-0.735). The genus *Collinsella*, although relatively low in abundance (<1%), exhibited a threefold increase in prevalence among piglets in the CHI group. This finding is consistent with the study by Carlson *et al.,* (2017), which reported heightened levels of *Collinsella* following both INU and WholeFiber supplementation. Notably, clinical investigations have highlighted the capacity of INU-type fructans to significantly foster the growth of *Collinsella*, correlating with elevated urinary hippurate levels (Dewulf *et al.,* 2013) which is associated with reduced inflammation Hippurate, a metabolite originating from the gut, demonstrates reduced concentrations in individuals afflicted with conditions such as obesity, diabetes, colourectal cancer, and inflammatory bowel diseases (Calvani *et al.,* 2010; Kassinen *et al.,* 2007; Salek *et al.,* 2007; Waldram *et al.,* 2009). The rise in *Ruminococcaceae* genera in CHI is beneficial due to their capacity to hydrolyse starch and other sugars, generating butyrate and other SCFA (Biddle *et al.,* 2013; J. Wong *et al.,* 2014).

Furthermore, we observed a significant reduction in the *Erysipelotrichaceae-UGC-002* genus in the CHI group compared to INU which aligns with Wu *et al.,* 2020 and Neyrinck *et al.,* 2021. Mizutani *et al.,* 2021 identified increased *Erysipelotrichaceae* prevalence alongside significant decreases in *Ruminococcaceae* and *Dialister* in patients with diarrhoea. However, our findings indicate that crude chicory treatment resulted in a substantial decrease in *Erysipelotrichaceae* abundance, coupled with increased *Ruminococcaceae* and *Dialister* than INU, suggesting additional bioactive effects of chicory. Furthermore, Kaakoush, 2015 showed a statistical decrease in one *Erysipelotrichaceae* species within the inulin group, correlating with reduced calprotectin levels and diminished gastrointestinal tract inflammation in patients with colourectal cancer or inflammatory bowel disease. Alterations in the gastrointestinal microbiota can influence immune cell markers, with an uptick in beneficial bacteria competing for binding sites, consequently diminishing the attachment of pathogenic bacteria (Pahumunto *et al.,* 2023).

As seen in the **Figure 26C,** crude chicory supplementation exhibited a more pronounced effect than INU on the *Streptococcus* genus, with a significant 8-10-fold reduction in abundance observed after chicory supplementation for W3 compared to the Ctrl group (Li *et al.,* 2021; Yang *et al.,* 2017). *Streptococcus* (r=-0.473) was found to be negatively correlated to *Ruminococcaceae* (r=0.794) (without Boneferroni correction) suggesting a competitive interaction between these genera, resulting in reduction of *Streptococcus. Streptococcus* strains encompass both commensal and pathogenic species implicated in inflammatory diseases, particularly in the gastrointestinal tract mucosa (Dinis *et al.,* 2014; Herrera *et al.,* 2009; Rooks *et al.,* 2014). Our findings suggest that the reduction in *Streptococcus* abundance in CHI may be associated with downregulation of pro-inflammatory genes (*CXCL10, IL18, TNFα*), as evidenced by lower expression levels in the CHI group compared to INU, potentially mediated through Toll-Like Receptor 2 (TLR2) modulation (Frolova *et al.,* 2008). This added effect of CHI supplementation could be attributed to bioactives like caffeic acid, known for its antimicrobial and anti-inflammatory effects in macrophages by inhibiting nitrite, tumour necrosis factor α- (TNFα) and prostaglandin E2 (PGE2) production by the NF-kB dependent pathway. (Sorgi *et al.,* 2021).

The RGCCA in **Figure 27D** underscores the close relationship between gut microbiota composition and inflammatory response as seen by gene expression (Li *et al.,* 2020). Weaning induces inflammatory responses in the gut, characterized by increased production of pro-inflammatory cytokines such as TNFα, IL6, and INFγ, as well as the upregulation of pathways like MAPK and Ras signalling (Bomba *et al.,* 2014b; Hu *et al.,* 2013b). The intestinal mucosa, harbouring the largest reservoir of macrophages in the body, plays an essential role in managing gut inflammation and maintaining immunological balance (Elshahed *et al.,* 2021). In E1, inulin and chicory supplementation yielded fewer changes in inflammatory and inflammation signalling pathway genes.

The lack of additional gene expression effects may be due to lower microbial load or the low doses of inulin and chicory. Herosimczyk *et al.,* 2020 noted an upregulation of intestinal proliferation genes only at 3% INU, while Mair *et al.,* 2010 found minimal impact with 0.4% supplementation.

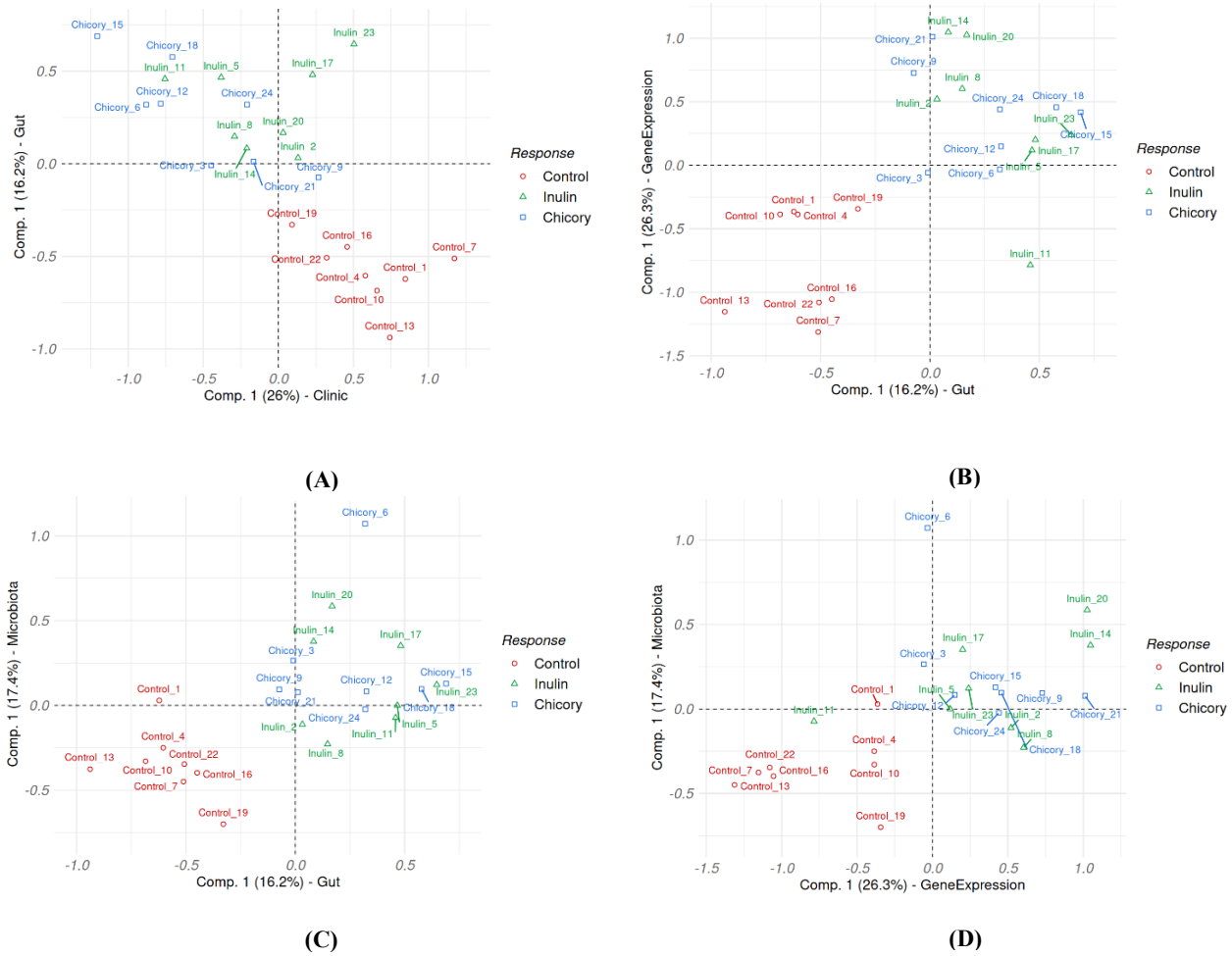

Figure 27. Biplot illustrating the correlation between the first components (Comp. 1) for block pairs in W3 of E2 from supervised RGCCA among (A) Gut-Clinical (B) Gene Expression-Gut (C) Microbiota-Gut (D) Microbiota-Gene Expression.

Samples are coloured by group. The first component of each block is shown in the individual plots of figure 26. RGCCA defines the components of each block by maximizing the association between the blocks, the more the resulting components are associated between the blocks, the more the projection of the samples on the biplot follows a linear trend.

In E2 (W1), the downregulation of the proinflammatory genes (*CXCL10* and *INFγ*) and inflammation signalling pathway genes (*TLR2* and *TANK*) in the colon of INU and CHI groups may be attributed to higher butyrate, which has been shown to significantly inhibit the production of proinflammatory cytokines like *INFγ* and *IL2* (Cavaglieri *et al.,* 2009). In W3, the RGCCA shows that many genes in the colon (*NFκB1, CASP1, MAPK14*) as well as in the ileum (*IL18, CASP3, CXCL10, TANK, MyD88*) were found to be altered in CHI or INU groups. Furthermore, distinct gene expression patterns and differences between these two groups of samples were observed. These observations may reflect underlying biological differences, responses, or effects associated with the inulin or chicory treatment or conditions compared to the Ctrl group. TNFα, a transmembrane protein pivotal in systemic inflammation, can induce apoptosis by activating caspases, thereby

enhancing apoptotic activity in the colon mucosa (EL Andaloussi *et al.,* 2013). Our findings align with studies by (Uerlings *et al.,* 2019), and Wang *et al.,* 2020, showing significant downregulation of both *TNFα* and *CASP3* in the ileum tissues of piglets of INU and CHI group at W3. This suggests a positive correlation between TNFα and CASP3 in ileal mucosa, potentially indicating a beneficial effect of crude chicory in suppressing mucosal inflammation. Additionally, chicoric acid, a bioactive found in chicory, has been shown to significantly decrease caspase3 and TNFα levels Alharthi, 2023. Increased butyrate production in W3 could activate the NLRP3 inflammasome via GPR43 and GPR109A or intrinsic inhibition of histone deacetylases (HDACs), thus reducing TNFα expression (MacDonald and Howe, 2009; Macia *et al.,* 2015; Zimmerman *et al.,* 2012). The higher permeability observed in the Ctrl group may be related to elevated TNFα levels, as TNFα can increase intestinal permeability by up-regulating myosin light chain kinase (MLCK) protein expression, leading to tight junction disintegration and intestinal barrier dysfunction (Al-Sadi *et al.,* 2016; Berkes, 2003; Kucharzik *et al.,* 2006). Therefore, the reduced expression of TNFα by CHI could decrease the influx of toxins and pathogens into the intestine.

Like our findings in the INU and crude CHI groups, Vogt *et al.,* 2015 also observed an inulin mediated effect involving the suppression of NFκB1 and the JNK pathway. Butyrate has been shown in other studies to inhibit NFκB1 activation and upregulate other cytoplasmic inhibitors of NFκB1, thereby reducing inflammation (Segain, 2000; Tedelind *et al.,* 2007). NFκB is a pivotal transcription regulation factor that triggers the release of inflammatory mediators, including IL-1, IL6, TNFα, COX-2, and iNOS, regulating cellular inflammatory responses. Chicoric acid has been demonstrated the ability to ameliorate lipopolysaccharide (LPS)-induced inflammation both *in vitro* and *in vivo* by downregulating *NFκB* and *TNFα* genes (Kassab *et al.,* 2022; Liu *et al.,* 2017; Zheng *et al.,* 2021). However, *Echinacea* extracts containing chicoric acid were reported to upregulate LPS-induced TNFα in rat alveolar macrophages (Goel *et al.,* 2002). Chicoric acid has been shown to downregulate several proinflammatory factors, including NO synthase, COX-2, prostaglandin E2, IL1β, IL12, and IL18 (Kour *et al.,* 2016; Matthias *et al.,* 2007). Other colonic genes downregulated by CHI and INU treatment included *DEFβ4a, IFNα, MAPK14*, and *TLR2*. MAPKs have been implicated in the regulation of pro-inflammatory cytokine release, including TNFα, IL1β, and IL6 (Jia *et al.,* 2020; Qian *et al.,* 2015a). Chicoric acid supplementation decreased the expression of nitric oxide synthase and MAPK14 at the molecular level (Alharthi, 2023). Pouille *et al.,* 2022 proved that fructose, chlorogenic acids and sesquiterpene lactones contained in chicory flour have an anti-inflammatory effect on TNFα, IL1β and IL8. In crude chicory-fed piglets, higher MUC1 expression reflects a strengthened cellular defence against pathogen adhesion at the epithelial surface, whereas MUC2, being more relevant to colon mucus barrier structure, remained unchanged, indicating that chicory preferentially enhances surface protection rather than mucus bulk production. Chicory's phenolic compounds could be behind this action as phenolics are recently being shown to upregulate the expression of MUC1 (Ma *et al.,* 2025).

Establishing correlations using RGCCA also allowed correlating multi-blocks data and thus shows relationships between heterogenous variables **(Figure 27)**. The results presented above indicate that crude CHI significantly contributed to reducing inflammation, equally or sometimes even more effectively than INU alone. In a recent study by (Matvieieva *et al.,* 2023), the ethanolic extract of chicory roots was found to contain 33 diverse polyphenols, including high amounts of gallic and caffeic acids. Additionally, the hairy portion of the root exhibited the presence of rutin, apigenin, kaempferol, quercetin, and their derivatives, highlighting anti-inflammatory and antioxidant properties of these bioactives found in chicory. This suggests that the beneficial effects of chicory extend beyond just its inulin content to include other bioactives, as mentioned earlier.

3.6. Conclusion

This study provides the first comparative investigation in piglets evaluating the combined effects of inulin and bioactive compounds naturally present in crude chicory on gut health. By employing a controlled force-feeding approach to ensure accurate dosing, we demonstrated that chicory, beyond its inulin content, modulated gut microbiota composition and enhanced butyrate production—effects particularly evident in Experiment 2 (E2). Chicory supplementation notably reduced severe diarrhoea incidence after three weeks in E2, suggesting a time- and dose-dependent response. Histomorphological improvements, including increased villus height and villus-to-crypt ratios, were observed in both experiments, especially at higher inclusion levels (1.7–2%) of chicory and inulin. Furthermore, transcriptomic analysis revealed downregulation of key pro-inflammatory genes and pathways in the colon and ileum at W3, indicating anti-inflammatory properties of both fibers, with chicory exhibiting a stronger effect. While inulin is well established as a prebiotic, our data support the added value of crude chicory as a cost-effective dietary intervention, potentially offering broader benefits through its additional phytochemicals, including chicoric acid and polyphenols. Further studies are necessary to elucidate the mechanistic contributions of these bioactives and to refine dietary strategies for enhanced gut health in both animal and human models.

Acknowledgments

This research was funded by the Hauts-de-France region (half PhD funding), as well as within the BiHauts Eco de France CPER/FEDER 2021-2027 program, which is financed by the European Union, the French State, and the Hauts-de-France Region. The authors would also like to thank Sylvie Mabille, Pauline Lemal and Vincent Servais for technical support in the lab and during *in vivo* trials.

4

In vitro digestion, absorption and fermentation of inulin and crude chicory flour: Reflecting weaning piglet colonic physiology

Article II

In vitro digestion, absorption and fermentation of inulin and crude chicory flour: Reflecting weaning piglet colonic physiology

Tushar Kulkarni[a,b], Pawel Siegien[a], Jimmy Vandel[e], Luke Comer[c], Benoit Cudennec[b], Sandy Theysgeur[b], Camille Dugardin[b], Anca Lucau-Danila[b,d], Nadia Everaert[c], Martine Schroyen[a,b,*] Rozenn Ravallec[b,*],

a. Precision Livestock and Nutrition Laboratory, TERRA Teaching and Research Centre, Gembloux Agro-Bio Tech, University of Liège, 5030 Gembloux, Belgium
b. UMR-T 1158, BioEcoAgro, University of Lille, University of Liege, 59650 Lille, France
c. Nutrition and Animal Microbiota EcoSystems lab, Division of A2H, Department of Biosystems, KU Leuven, 3001 Leuven, Belgium
d. Joint Laboratory CHIC41H University of Lille-Florimond - Desprez, Cité scientifique, 59655 Villeneuve d'Ascq, France
e. US 41 - UAR 2014 – PLBS – Bililleplatform, Univ. Lille, CNRS, Inserm, CHU Lille, Institut Pasteur de Lille, 59000 Lille, France

*Corresponding authors at : Université de Liège - Gembloux Agro-Bio Tech, Département AgroBioChem - Animal Sciences, Passage des Déportés, 2, 5030 Gembloux, Belgium; University of Lille - IUT A, Polytech Building, Lille, Scientific City, 59655 Villeneuve d'Ascq, France
Email adresses : rozenn.ravallec@univ-lille.fr (R. Ravallec) and martine.schroyen@uliege.be (M. Schroyen)

This chapter is adapted from the article submitted to Journal of Agricultural and Food Chemistry.

4.1. Abstract

Weaning can disrupt the porcine gastrointestinal (GI) tract, leading to impaired gut microbiota and metabolite imbalance. Although inulin extracted from *Cichorium intybus* is known to support gut health, its extraction is costly (3x) and results in the loss of additional bioactives present in the whole plant. This study aimed to compare the effects of purified inulin (Inu) and crude chicory flour (Chi) using an *in vitro* model simulating digestion (using porcine enzymes), absorption via dialysis, and colonic fermentation with weaned piglet fecal inoculum. Additionally, we investigated how *in vitro* digestion and absorption influence fermentation kinetics, microbial community composition, and metabolite production.

Two separate *in vitro* experiments were designed to assess the fermentation characteristics of Inu and Chi in either their non-digested/non-dialyzed (ND, E1) form or following simulated digestion and dialysed (DD, E2). E1 included three treatments: Inulin without equated (Inu w/eq.), Chi equated (Inu eq.), and Chi equated (Chi eq.). E2 included ten groups: Inu (w/eq.), Inu eq., Chi eq., Feed (F), and F supplemented with 0.5%, 1%, or 2% of either inulin (F0.5I, F1I, F2I) or chicory (F0.5C, F1C, F2C). In both experiments, the inulin content was equated between Inu eq. & Chi eq. or F0.5I, F1I, F2I & F0.5C, F1C, F2C, respectively.

In both experiments, Inu eq. generated more gas than Chi eq., while among the feed-based treatments, only F2I produced significantly more gas than F, F0.5I, and F1I ($p < 0.001$). In Experiment 2, Inu eq. yielded higher total SCFA concentrations than Chi eq., which contrasted with E1. The F2C group showed significantly higher butyrate levels than F2I ($p < 0.001$), despite no significant difference between Chi eq. and Inu eq. alone. Chi eq. and F2C also exhibited greater microbial α-diversity (Shannon and Simpson indices) than Inu eq. and F2I, respectively ($p < 0.05$). Overall, alpha diversity was higher in DD samples (E2) than in ND samples (E1), indicating that simulated digestion and dialysis influenced microbial composition. Both Inu eq. and Chi eq. promoted the growth of beneficial genera, but Chi eq. more strongly enriched *Lactobacillus*, *Bifidobacterium*, *Butyricicoccus*, and *Ruminococcus* ($p < 0.001$) after 12 hours of fermentation. In conclusion inulin showed a higher gas production than crude chicory while cost-effective crude chicory and its feed-based counterpart (F2C) demonstrated fermentation profiles comparable to or more favourable than inulin or F2I, particularly in terms of butyrate production and microbial diversity.

Keywords: Chicory, Inulin, *in vitro*, digestion, fermentation, microbiota, inflammation.

4.2. Introduction

The gastrointestinal (GI) tract functions as a complex defence system, consisting of the intestinal epithelium, antimicrobial peptides, mucus, immune cells, and commensal bacteria (Zihni *et al.,* 2016). The balance between epithelial cells, immune cells within the lamina propria, and the microbiota is vital for maintaining mucosal integrity. Disruption of this balance is linked to various diseases in humans and animals. Such dysregulation can lead to the translocation of antigens, initiating immune responses and weakening the epithelial barrier, which perpetuates chronic inflammation. During this process, leukocytes release inflammatory mediators—cytokines like IL-1, IL6, IL8, TNFα, and IFNγ—that disrupt mucosal homeostasis and increase epithelial permeability (Luissint *et al.,* 2016).

Previous research has shown that inulin-type fructans (mostly extracted from chicory) can significantly improve gut epithelial barrier function (Akbari *et al.,* 2017; Kulkarni *et al.,* 2024). The fermentation of prebiotic by gut microbiota leads to the production of SCFA, which are known to enhance epithelial barrier integrity in both *in vitro* and *in vivo* models. Among the SCFA, butyrate stands out due to its crucial role in gut health—it provides a primary energy source for colonocytes, reducing intestinal inflammation, and strengthening the intestinal barrier (Vinolo *et al.,* 2011). The saccharolytic fermentation of dietary fibers, producing SCFA such as butyrate, is therefore vital for maintaining a healthy gut environment and robust intestinal barrier function (Peng *et al.,* 2009; Uerlings *et al.,* 2019). Recent studies have revealed that chicory, beyond its inulin content, is rich in various bioactive compounds, such as sesquiterpene lactones (STLs), guaianolid glycosides, caffeic acid derivatives, hydroxycoumarins, flavonoids, alkaloids, steroids, terpenoids, etc. These bioactive compounds have been linked to numerous health benefits, including anti-inflammatory effects, modulation of lipid metabolism, inhibition of pathogen growth, enhancement of growth performance, antioxidant properties, and potential cancer prevention (Chadwick *et al.,* 2013; Ferioli and D'Antuono, 2012; Karioti *et al.,* 2008; Kocsis *et al.,* 2003; Pouille *et al.,* 2022a; San Andres *et al.,* 2019; Schumacher *et al.,* 2011).

To test the effects of such bioactive molecules, the use of laboratory animals is facing growing scrutiny due to ethical, economic, and scientific concerns, underscoring the need for alternative *in vitro* methods that can accurately replicate *in vivo* environments like the GI tract. Over the years, various *in vitro* models have been employed to investigate the effects of bioactive fibers during digestion, absorption, and fermentation. However, the use of *in vitro* digestion and absorption steps prior to fermentation is not consistently applied in studies evaluating the effects of dietary fibers and bioactives on the GI tract of weaning piglets (Boudry *et al.,* 2012; Logtenberg *et al.,* 2020; Pham *et al.,* 2018; Tran *et al.,* 2016).

Therefore, in this study, we employed a combined *in vitro* approach incorporating static digestion (INFOGEST), absorption (dialysis), and batch fermentation using fecal inoculum from weaning piglets. This methodology was designed to better mimic physiological conditions and to provide deeper insight into host–microbiota interactions while reducing reliance on animal testing (Isenring *et al.,* 2023). The objective of this chapter was to evaluate the effects of Chi and Inu on microbial fermentation by assessing gas kinetics, SCFA and BCFA production, and microbiota composition. Additionally, we aimed to understand how *in vitro* digestion and absorption influence these parameters in both raw substrates and feed-integrated forms.

4.3. Material and Methods

4.3.1. Chemical Analysis and Experimental Setup

Inu was procured from Beneo, Belgium, and Chi from Leroux-Waast Mill, France, both with a degree of polymerization (DP) ranging from 2 to 60 **(Table 1)**. Baby-mix© feed was obtained from Quartes. The nutrient composition was analysed according to the protocols established by the Association of Official Analytical Chemists (Horwitz, 2010). Neutral Detergent Fibre (NDF) and Acid Detergent Fibre (ADF) were measured using the Foss Fibrecap system, following the methodology of Van Soest *et al.* (1991).

For the determination of monosaccharide composition, including rhamnose, arabinose, xylose, mannose, glucose, and galactose, samples were hydrolysed with 1M H_2SO_4 for 3 h at 100 °C. The hydrolysed sugars were derivatized and analysed using an HP Agilent 6890 gas chromatograph (Agilent Technologies, Santa Clara, CA) fitted with an HP1-methylsiloxane capillary column (Scientific Glass Engineering, Melbourne, Australia), using 2-deoxyglucose (Sigma-Aldrich Co., St Louis, MO) as the internal standard (Aguedo *et al.,* 2014; Englyst and Cummings, 1984).

Molecular weight distributions were assessed via size-exclusion high-performance liquid chromatography (HPSEC) on a Waters 2690 Alliance chromatograph with a Waters 2410 refractometer and a TSKGEL G3000 PWXL column (7 µm, 7.8 × 300 mm) (Tosoh, Tokyo, Japan). The eluent, $NaNO_3/NaN_3$, was maintained at ambient temperature with a flow rate of 0.7 mL/min (Aguedo *et al.,* 2014). Dextran standards from Sigma-Aldrich (Bornem, Belgium) were used to construct a calibration curve for peak molecular mass determination, and the polydispersity index (PDI) was calculated by dividing the weight-average molecular weight (M_w) by the number-average molecular weight (M_n) (Aguedo *et al.*, 2014).

Two experiments were conducted to investigate the effects of direct fermentation of raw (Non-Digested/Non-Dialyzed, ND) samples (Experiment 1, E1) compared to *in vitro* digested and dialyzed (DD) samples prior to fermentation (Experiment 2, E2). The 'inulin content' was equated (eq.) based on the manufacturer's specifications between both the Inu eq. and Chi eq. across both experiments to ensure equivalence in inulin-related effects. E1 included three groups: Inu w/eq. (without equivalent inulin), Inu eq., Chi eq. E2 consisted of ten groups: Inu (w/eq.), Inu eq., Chi eq., Feed (F), F+0.5% Inu (F0.5I), F+0.5% Chi (F0.5C), F+1% Inu (F1I), F+1% Chi (F1C), F+2% Inu (F2I), and F+2% Chi (F2C). Feces were collected from multiple weaned piglets and pooled to generate a uniform inoculum. This pooled sample was used across all treatments. A single batch of each fiber substrate was subjected to three technical replicates of *in vitro* digestion and dialysis, from which one representative digest was selected for subsequent fermentation. The selected digest was then used to initiate four technical replicates of *in vitro* batch fermentation. From one of these fermentation replicates, 12 technical replicates were prepared for downstream application in the triple cell culture model.

4.3.2. *In vitro* Digestion Process (INFOGEST 2.0)

The static *in vitro* gastrointestinal digestion of samples from E2 was performed using the method described by Egger *et al.* (2017); and Brodkorb *et al.* (2019). For the oral phase, 2 g of powdered sample was solubilized in 8mL of water and then mixed with 8 mL of Simulated Salivary Fluid containing 0.3M $CaCl_2$ and amylase (75 U/mL, Merck, Darmstadt, A3176,). The samples were incubated for 2 minutes at 37 °C in a thermostatic shaking bath (160 rpm, pH 7). During the gastric phase, 12 mL of Simulated Gastric Fluid containing pepsin (6,500 U/mL, Sigma, P6887) were added and the samples were incubated for 2 h at 37 °C in a thermostatic shaking

bath (130 rpm) at pH 3. For the intestinal phase, gastric chyme was mixed with 20 mL of Stimulated Intestinal Fluid containing bile acids and pancreatin (45 U/mL Sigma, P1750). Pancreatin is a complex mixture of digestive enzymes—primarily trypsin, amylase, lipase, ribonuclease, and protease—secreted by the exocrine pancreas of pigs. The pH was adjusted to 7.0 and the samples were incubated for 2 h at 37 °C in a thermostatic shaking bath. To assess the effect of digestion, digesta was collected at the end of the experiment, heated at 95°C for 5 minutes to denature enzymes, centrifuged at 13,400g for 5 minutes, and stored at −20°C for further analysis.

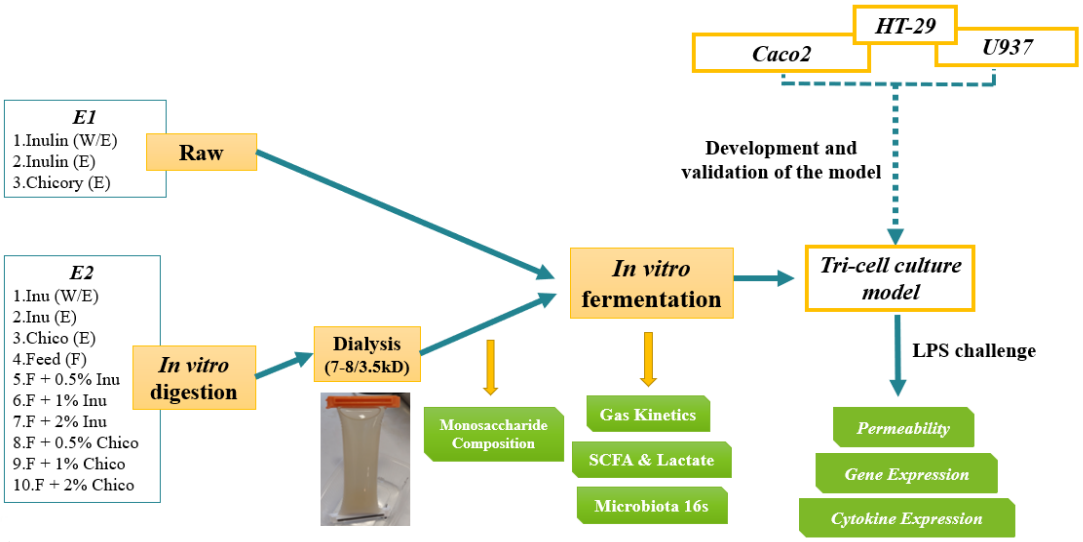

Figure 28. Experimental setup of E1 and E2

In Experiment 1 (E1), samples were directly subjected to *in vitro* fermentation, while in Experiment 2 (E2), they first underwent *in vitro* digestion and dialysis. Dialysis was performed using two membrane sizes to assess their suitability for mimicking absorption. The fermentation supernatants from both experiments were then stored at -80 ^{0}C to be used to treat LPS-challenged cells to study inflammation.

4.3.3. *In vitro* Absorption (Dialysis)

This dialysis step simulates intestinal absorption occurring in the small intestine. Following the intestinal phase of *in vitro* digestion, the digesta from E2 samples were subjected to dialysis using cellulose membranes (3.5 kDa; Spectrum Labs, Breda, The Netherlands) for 24 h, with continuous stirring and periodic water renewal at intervals of 3, 6, 9, 12, 18, and 24 h (Uerlings *et al.,* 2020). After dialysis, the hydrolysed residues were freeze-dried (Delta 1-24 LSC, Christ, Analis, Namur, Belgium).

4.3.4. Fecal Collection and Batch Fermentation

Fecal samples were collected from male piglets weaned at 21 days from the CRAw farm, Belgium, through rectal stimulation with a sterile swab. This procedure adhered to European regulations (EU Directive 2010/63/EU) and Belgian laws for scientific purposes and received approval from the University of Liège's ethical committee (License: 21-2385). The faeces were transferred into a sterile whirl pack and pooled under anaerobic conditions in an InVivo2 hypoxia workstation (Led Techno, Heusden-Zolder, Belgium) at 39 °C. They were then snap-frozen in liquid nitrogen and stored at -80°C. For fermentation, the fecal inoculum (2.5%

w/v) was prepared by mixing faeces with a buffer solution containing salts and minerals (pH 6.8) (Menke, 1988), without a reducing agent (Poelaert *et al.,* 2018). The mixture was homogenized using an Awel™ Microbiology Stomacher (Led Techno) for 30 seconds and filtered through a 200 µm metallic sieve. Each fermentation vial, containing 0.1 g of sample from ND or DD and three mucin carriers, was filled with 15 mL of the fecal inoculum, sealed, and incubated at 39 °C in a shaking water bath (50 rpm) for 48 h. Mucin microcosms (Tran *et al.,* 2016b) were included to promote mucus-associated microbial growth. Samples were collected at each timepoint and stored at -80 °C for metabolite and microbiota analysis. Fermentation broths from the 4 and 12 hr timepoint were sterile-filtered with 0.22-µm pore filters and were stored at -80 °C used in cell culture application.

4.3.5. Gas Production Kinetics

Gas volumes (n = 3 vials per treatment) were measured using a Tracker 200 manometer (Bailey and Mackey Ltd, Birmingham, UK) at intervals of 2, 5, 8, 12, 16, 20, 24, 48, and 72 h. The gas production was normalized using values from the blank and data were fitted to a monophasic model according to Groot *et al.* (1996),

$$G = \frac{\mathrm{A \times t^C}}{\mathrm{t^C + B^C}}$$

$$RMAX = \frac{\mathrm{A \times B^C \times C \times Tmax^{-c-1}}}{(1 + \mathrm{B^C \times Tmax^{-C}})^2}$$

$$TMAX = \mathrm{B} \times \left(\frac{\mathrm{C} - 1}{\mathrm{C} + 1}\right)^{\frac{1}{C}}$$

where A (mL/g DM) is the maximum gas volume, G (mL/g DM) represents gas accumulation at a specific time, B (h) is the time to half-maximal gas production (G = A/2), R_{max} is the maximum rate of gas production (mL/g DM h^{-1}), and T_{max} is the time to reach R_{max}.

4.3.6. SCFA and Lactate Quantification by HPLC

Fermented samples collected at various timepoints were analysed using an isocratic High-Performance Liquid Chromatography (HPLC) system, incorporating a Waters E2695 Alliance HPLC machine. The system was equipped with a Bio-Rad Aminex HPX-87H ion exclusion column (Hercules, CA, USA), micro-guard cation H^+ precolumn and a UV detector set at 210 nm. The eluent used was H_2SO_4 (mM) at a flow rate of 0.6 mL/min, maintained at 60 °C. Prior to analysis, the samples were centrifuged at 13,000 rpm for 15 minutes, and 1.6 mL of the supernatant was acidified with 1M H_2SO_4 to achieve a pH between 2 and 3. The supernatant was then filtered twice using Chromafil AO-45/25 and AO-20/25 filters. Peak integration was performed using Empower 3 software (Waters Corporation, Milford, MA, USA), with manual verification to ensure accuracy. Quantification was carried out via external standard calibration. The concentrations of intermediate metabolites and the total SCFA were expressed as mg/g of fresh content. Additionally, the proportions of acetate, propionate, butyrate, and branched-chain fatty acids (BCFAs) were presented as percentage ratios of the total SCFA (Leblois *et al.,* 2017).

4.3.7. Microbiota Composition Analysis

DNA was extracted from the fermented samples collected at the 4 and 12 hr timepoint of both the experiments using the QIAamp PowerFecal Pro DNA Kit (Qiagen, Hilden, Germany) following the manufacturer's protocol. DNA concentration and quality were assessed using a NanoDrop spectrophotometer (Thermo Fisher Scientific, Waltham, MA, USA). For 16S rRNA gene sequencing, the V3-V4 hypervariable regions were amplified and sequenced on an Illumina MiSeq platform at the GIGA Genomics Platform (ULiège, Belgium).

4.3.8. Statistical Analysis

In this study, one way ANOVA with |Dunnett or Tukey's multiple range test to determine significant differences among treatment means using SAS Enterprise Guide 7.4 (SAS Institute Inc, Cary, NC). The bars labelled by different letters indicating significant differences within each cytokine at specific timepoints. Significance thresholds were established as follows: *$p < 0.05$ (significant), **$p < 0.01$ (highly significant), and ***$p < 0.001$ (very highly significant) based on the ANOVA. For microbiota analyses at each timepoint, the Kruskal-Wallis test followed by Dunn's test was performed.

Amplicon sequence variant (ASV) determination was conducted using Quantitative Insights into Microbial Ecology II (QIIME 2, version 1.9.0) software (Bolyen *et al.,* 2019), utilizing the DADA2 plugin to correct for sequencing errors specific to Illumina technology (Callahan *et al.,* 2016). Taxonomic classification was performed using the SILVA database (version 138). Data visualization and statistical analyses were performed in R Studio (version 4.3.2). A single ASV from the genus *Pseudomonas* was identified as a contaminant in the negative control and was excluded from further analysis. Microbial α- diversity indices (Chao1, Shannon, and Simpson) and β- diversity (Bray-Curtis) were calculated using the phyloseq package in R. The Kruskal-Wallis test was used for statistical analysis of microbiota composition at each timepoint, with treatment as a fixed factor. To control for the family-wise error rate (FWER), the Bonferroni correction was applied to adjust p-values for the abundance datasets.

To uncover potential relationships among treatment groups, an integrative analysis was conducted across multiple datasets at the 12 h timepoint using supervised and unsupervised approaches with Regularized Generalized Canonical Correlation Analysis (RGCCA) (Tenenhaus and Tenenhaus, 2011). The datasets were categorized into four distinct blocks based on data types: 'Gas Kinetics' (A, B, T_{max}, R_{max}), Total and Individual Short-Chain Fatty Acids ('TCSFA') (acetate, propionate, butyrate, BCFAs), 'A- Diversity' Metrics (Shannon, Simpson, Chao1), and 'Genera Abundance'. The tau parameter in RGCCA was set to its optimal value based on a factorial scheme. In addition, Principal Component Analysis (PCA) was performed on cytokine and gene expression datasets to identify patterns. Pearson correlation coefficients (r) were calculated, and p-values were adjusted for multiple comparisons using the Bonferroni correction to ensure statistical rigor. All analyses were conducted using R version 4.4.2 with the following packages: RGCCA (v3.0.3), factoextra (v1.0.7), FactoMineR (v2.9), ggplot2 (v3.5.1), corrplot (v0.92), corr (v0.4.4), dplyr (v1.1.4), and stringr (v1.5.1).

4.4. Results

4.4.1. HSPEC profile of ND vs DD

The molecular weight distribution and polymerization profile of inulin and crude chicory fractions, dialyzed using 3.5 kDa and 6–8 kDa membranes, are presented in Tables 13. In the case of inulin, no significant differences were observed between the two membrane sizes for M_w, M_n, PDI, DP_w, or DP_n, suggesting minimal impact of membrane cut-off on the molecular profile. However, for chicory, dialysis with the 6–8 kDa membrane resulted in significantly higher M_w, M_n, DPw, and DP_n compared to both ND chicory and the 3.5 kDa fraction ($p < 0.01$).

Table 13: HSPEC profile of Non-Digested/Non-Dialyzed (ND) and Digested and Dialyzed (DD) Inulin and Chicory flour

		ND	**DD (3.5)**	**DD (6-8)**	p-value
Inulin	Mw	1762 ± 13.3	1963 ± 1.73	2050 ± 230	0.3553
	Mn	1350 ± 9.81	1500 ± 1.15	1550 ± 165	0.3676
	PDI	1.31 ± 0.0168	1.31 ± 0.00188	1.33 ± 0.134	0.9601
	DPw	9.79 ± 0.0738	10.9 ± 0.00962	11.4 ± 1.28	0.3553
	DPn	7.5 ± 0.0545	8.33 ± 0.00642	8.61 ± 0.917	0.3676
Crude Chicory Flour	Mw	2359 ± 39.8^{b}	2320 ± 15.9^{b}	2564 ± 29.4^{a}	0.002
	Mn	1765 ± 28.3^{b}	1740 ± 12.4^{b}	1893 ± 17.9^{a}	0.003
	PDI	1.34 ± 0.00115	1.34 ± 0.00044	1.35 ± 0.0284	0.67
	DPw	13.1 ± 0.221^{b}	12.9 ± 0.0883^{b}	14.2 ± 0.164^{a}	0.002
	DPn	9.81 ± 0.157^{b}	9.66 ± 0.069^{b}	10.5 ± 0.0994^{a}	0.004

Values are presented as mean ± SEM. Different superscript letters within the same row indicate significant differences among treatments based on one-way ANOVA followed by Tukey's post hoc test ($p < 0.05$). M_w: Weight-Average Molecular Weight; M_n: Number-Average Molecular Weight; PDI: Poly Dispersity Index. DP_w : Weight-Average Degree of Polymerization; DP_n : Number - Average Degree of Polymerization

4.4.2. Fermentation Gas Kinetics of Inu Vs Chi

As shown in **Table 14**, in both E1 and E2, Chi eq. had the lowest R_{max} (maximum rate of gas production) ($p < 0.001$, $p < 0.001$) and A value (total gas produced) ($p < 0.01$, $p < 0.001$) compared to Inu eq. In E1, Inu fermented faster with a lower B value (half asymptote) than Chi eq. ($p < 0.001$). After DD in E2, Chi eq.'s B value increased and was not significantly different from Inu eq. The T_{max} (time to reach R_{max}) was higher for Chi in E1 ($p < 0.001$) but shortest in E2 ($p < 0.001$). In E2, F2C slightly increased total gas production with increasing concentration, but this was not significant. Conversely, F2I significantly increased total gas production (A) ($p < 0.001$) compared to F, F0.5I and F1I, though other gas kinetics parameters remained unaffected. However, F2C showed no significant difference from F2I.

Table 14: Fermentations parameters (A, B, R_{max}, T_{max}) modelled according to Groot *et al* of Inulin and Chicory Flour in the presence of pre-weaned piglet faecal inoculum (n=4 fermentation vials)

E	Ingredients	A (ml/g DM)	B (h)	R_{max} (mL g-1 DM h-1)	T_{max} (h)
ND (E1)	**Inu w/eq.**	$224^{a} \pm 5.67$	$5.56^{b} \pm 0.11$	$41.4^{a} \pm 2.07$	$4.81^{a} \pm 0.03$
	Inu eq.	$225^{a} \pm 5.17$	$5.08^{b} \pm 0.02$	$39.17^{a} \pm 2.05$	$4.13^{b} \pm 0.09$
	Chi eq.	$200^{b} \pm 3.14$	$6.19^{a} \pm 0.08$	$25.96^{b} \pm 0.7$	$4.76^{a} \pm 0.04$
	P value	0.007	<0.001	0.003	<0.001
DD (E2)	**Inu w/eq.**	$371^{a} \pm 11.2$	6.56 ± 0.575	$40.4^{a} \pm 7.09$	$4.1^{a} \pm 0.0556$
	Inu eq.	$314^{a} \pm 15$	6.07 ± 0.263	$40.3^{a} \pm 2.44$	$4.44^{a} \pm 0.316$
	Chi eq.	$219^{b} \pm 14.6$	7.61 ± 0.643	$18.2^{b} \pm 2.22$	$2.41^{b} \pm 0.335$
	p value	<0.001	NS	<0.001	<0.001
	F	$172^{b} \pm 21.2$	6.27 ± 0.449	$16.8^{bc} \pm 2.03$	$2.08^{bc} \pm 0.385$
	F0.5I	$171^{b} \pm 8.46$	7.39 ± 0.519	$14.2^{c} \pm 0.501$	$2.91^{ac} \pm 0.286$
	F1I	$170^{b} \pm 8.72$	8.23 ± 0.684	$12.8^{c} \pm 1.35$	$3.46^{ab} \pm 0.261$
	F2I	$243^{a} \pm 6.61$	6.43 ± 0.3	$25.1^{a} \pm 2.24$	$3.62^{a} \pm 0.44$
	F0.5C	$208^{ab} \pm 12.2$	6.34 ± 0.432	$20.2^{ac} \pm 0.723$	$2.01^{bc} \pm 0.247$
	F1C	$215^{ab} \pm 15.1$	7.18 ± 0.535	$18.4^{ac} \pm 1.02$	$2.92^{ac} \pm 0.28$
	F2C	$228^{ab} \pm 18.2$	6.29 ± 0.138	$22.3^{ab} \pm 2.04$	$1.97^{c} \pm 0.162$
	P value	<0.001	0.2387	<0.001	<0.001

A-Total gas produced; B-time to half asymptote; R_{max}-maximum rate of gas; T_{max}- time at which R_{max} is reached. Gas production parameters were measured with a manometer over a 48-h period. Values are means ± SEM, n = 4 per treatment group. Means in a column without a common superscript letter differ ($p < 0.05$) as analysed by one-way ANOVA and the TUKEY test. Normalized using the values from blank. Inulin equated (Inu eq.), Chicory equated (Chi eq.), Feed (F), Feed+2% Chicory (F2C), Feed+2% Inulin (F2I).

4.4.3. Lactate and SCFA Production

The fermentation of different ingredients was monitored over 24 h, measuring lactate **(Table 15)**, SCFA, and BCFA profiles. Data were compared under two conditions: fermentation of ND in E1 **(Figure 29)** and DD in E2 **(Figure 30)**. Lactate production was generally lower in digested samples compared to undigested samples, especially at the 4 h timepoint, indicating the impact of DD on lactate production.

Table 15. Lactate production in E1 and E2. These are net values for different times and ingredients, as those were normalized for blank (mucin+ inoculum) fermentation products.

E1 (ND)		
Time (h)	**Ingredients**	**Lactate (mmol/g)**
4	Inu w/e	2.39 ± 0.21[a]
	Inu eq.	1.76 ± 0.07[b]
	Chi eq.	1.3 ± 0.029[c]
12	Inu w/e	0.08 ± 0.01
	Inu eq.	0.07 ± 0.02
	Chi eq.	0.111 ± 0.0044
24	Inu w/e	0.13 ± 0.05
	Inu eq.	0.12 ± 0.03
	Chi eq.	0.15 ± 0.04
p value ingredient		<0.001
p value time		<0.001
p value ingredient X time		<0.001

Mean values (n=4 vials of fermentation) ± SEM. The unlike a, b, c letters for the same column and at one timepoint shows the significance different ($p < 0.05$). Inulin equated (Inu eq.), Chicory equated (Chi eq.), Feed (F), Feed+2% Chicory (F2C), Feed+2% Inulin (F2I).

E2 (DD)		
Time (h)	Ingredients	Lactate (mmol/g)
4	Inu w/e	0.497 ± 0.0588[a]
	Inu eq.	0.512 ± 0.0455[a]
	Chi eq.	0.0258 ± 0.0258[b]
	F	0.102 ± 0.0496[ab]
	F0.5I	0.0674 ± 0.047[ab]
	F1I	0.0839 ± 0.0452[ab]
	F2I	0.214 ± 0.0593[ab]
	F0.5C	0.417 ± 0.248[ab]
	F1C	0.168 ± 0.0578[ab]
	F2C	0.212 ± 0.0722[ab]
12	Inu w/e	0.158 ± 0.0912[ab]
	Inu eq.	0.0959 ± 0.0959[ab]
	Chi eq.	0.0107 ± 0.0107[b]
	F	0.47 ± 0.158[a]
	F0.5I	0.308 ± 0.0231[ab]
	F1I	0.463 ± 0.0733[a]
	F2I	-
	F0.5C	0.218 ± 0.115[ab]
	F1C	0.209 ± 0.0677[ab]
	F2C	-
24	Inu w/e	0.352 ± 0.312
	Inu eq.	0.3 ± 0.289
	Chi eq.	0.328 ± 0.238
	F	0.5 ± 0.338
	F0.5I	0.386 ± 0.351
	F1I	0.575 ± 0.34
	F2I	0.142 ± 0.142
	F0.5C	0.443 ± 0.325
	F1C	0.482 ± 0.319
	F2C	0.264 ± 0.264
p ingredients		0.3148
p time		0.0725
p time*Ingredients		0.1395

Mean values (n=4 vials of fermentation) ± SEM. The unlike a, b, c letters for the same column and at one timepoint shows the significance different ($p < 0.05$). Inulin equated (Inu eq.), Chicory equated (Chi eq.), Feed (F), Feed+2% Chicory (F2C), Feed+2% Inulin (F2I).

At 4 h, in E1, lactate production was significantly higher ($p < 0.001$) in both Inu groups compared to Chi eq. By 24 hr, total SCFA production was significantly higher in the Chi eq. group compared to the Inu eq. in E1, but in E2, Chi eq. had lower SCFA levels that Inu eq. at 12 h but not at 24 h. No significant differences in SCFA production were observed among the feed-associated groups. Similarly, no significant differences in total SCFA production were found between DD and ND.

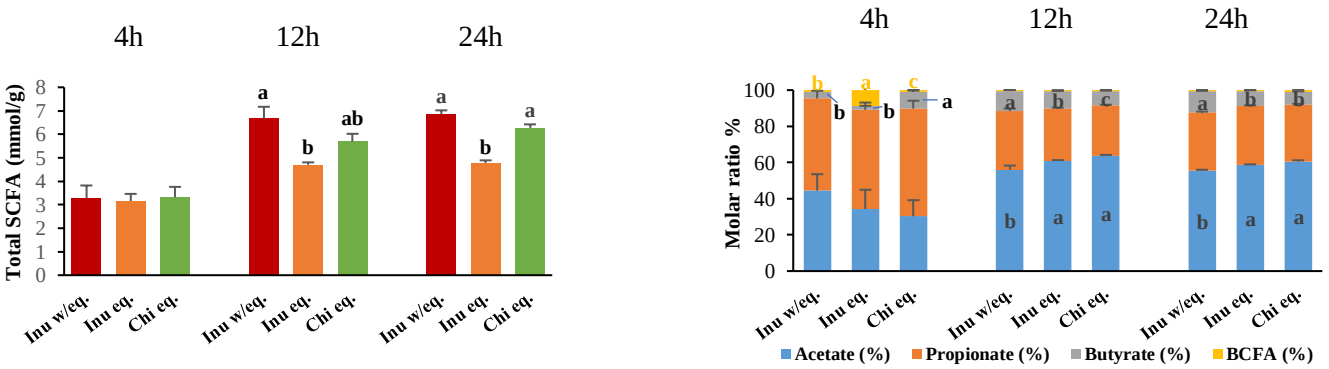

p values	Total SCFA (mmol/g)	Acetate (%)	Propionate (%)	Butyrate (%)	BCFA (%)
p Ingredients	<0.001	<0.001	<0.001	<0.001	0.0052
p Time	0.7078	0.2336	0.007	<0.001	<0.001
p Time*Ingredients	0.0957	<0.001	0.0386	<0.001	0.0045

Figure 29. Total SCFA and molar ratios (%) of the ND (E1) samples. These are net values for different timepoints (4, 12 and 24h) and ingredients, normalized for blank fermentation. Mean values (n = 4 fermentation vials) ± SEM.

The unlike a, b, c letters at one timepoint shows the significance different ($p < 0.05$). Statistics: ANOVA: Tukey's test.. Branch Chain Fatty Acids (BCFAs) = Isobutyrate + Isovalerate + Valerate; Total Short Chain Fatty Acids (SCFA) = Acetic + Propionic + Isobutyrate + Butyrate + Isovalerate + Valerate. Inulin equated (Inu eq.), Chicory equated (Chi eq.), Feed (F), Feed+2% Chicory (F2C), Feed+2% Inulin (F2I).

Interestingly, butyrate production peaked in Chi eq. at 4 h ($p < 0.001$) but was not different to Inu eq. after 24 h. BCFA production was higher in the Inu groups ($p < 0.005$) at 4 h but decreased at 12 h. On the other hand, in the E2, lactate production was lower for Chi eq. than Inu eq. ($p < 0.05$). Also, acetate levels were significantly higher ($p < 0.05$) in the Inu w/eq., Inu eq. and F2I groups compared to Chi eq. or some other feed-associated groups at 4 and 12 h. BCFA levels were significantly elevated ($p < 0.001$) in all other groups compared to Inu eq. and F2I. BCFA levels were generally elevated in DD compared to ND. The interaction between ingredients and the timepoints was significant ($p < 0.001$) for all the measured metabolites, except for Total SCFA in E1.

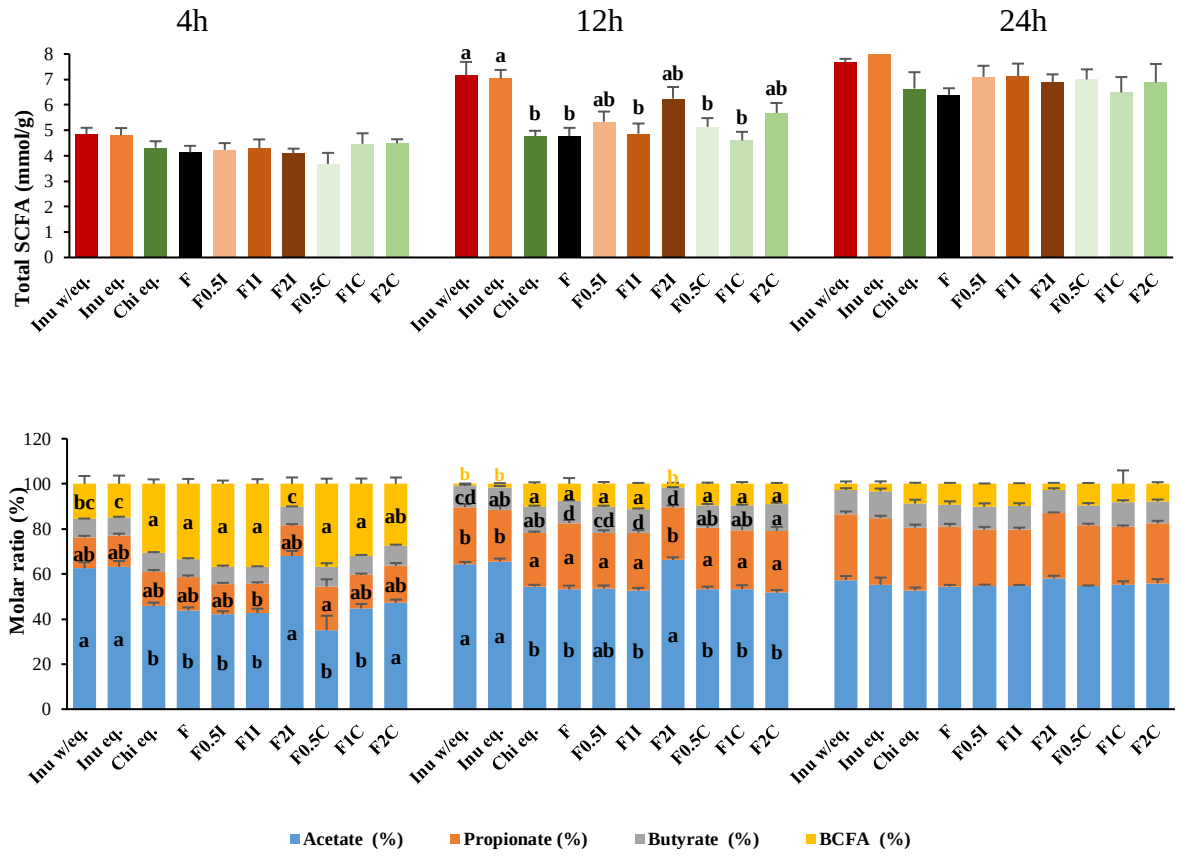

p values	Total SCFA (mmol/g)	Acetate (%)	Propionate (%)	Butyrate (%)	BCFA (%)
p Ingredients	<0.001	<0.001	0.0066	0.001	<0.001
p Time	<0.001	<0.001	<0.001	<0.001	<0.001
p Time*Ingredients	<0.001	<0.001	<0.001	<0.001	<0.001

Figure 30. Total SCFA and molar ratios (%) of the DD (E2) samples. These are net values for different timepoints (4, 12 and 24h) and ingredients, normalized for blank fermentation.

Mean values (n = 4 fermentation vials) ± SEM. The unlike a, b, c letters at one timepoint shows the significance different ($p < 0.05$). Statistics: ANOVA: Tukey's test. Branch Chain Fatty Acids (BCFAs) = Isobutyrate + Isovalerate + Valerate; Total Short Chain Fatty Acids (SCFA) = Acetic + Propionic + Isobutyrate + Butyrate + Isovalerate + Valerate. Inulin equated (Inu eq.), Chicory equated (Chi eq.), Feed (F), Feed+2% Chicory (F2C), Feed+2% Inulin (F2I).

4.4.4. α- diversity & β- diversity

Taxonomic diversity was assessed and compared using several indices, including Chao1, Shannon, and Simpson. A- diversity analysis revealed significant differences between treatments in both E1 and E2 **(Table 16)**. In E1, except for the Shannon index at 4 h, no significant differences were observed between Inu eq. and Chi eq. at both the 4 h and 12 h timepoints for any α- diversity indices. In E2, for the Shannon index, Chi eq., and F2C had significantly higher values (adj. $p < 0.05$), followed by F2I, with the lowest values observed for Inu eq. Regarding the Simpson index, Inu eq. had lower values than Chi eq. (adj. $p < 0.05$), while F2I was not significantly different from F2C. At the 12 h timepoint, Inu eq. and F2I showed the lowest values for the Chao1 (adj. $p < 0.01$), Shannon (adj. $p < 0.01$), and Simpson (adj.$p < 0.01$) indices compared to all other categories. From a ND vs DD point of view, DD samples had slightly higher α- diversity values than ND samples.

Table 16. Effect of Inu and Chi in E2 on Chao1, Shannon and Simpson Index in A- (α) diversity at ASV level.

E	Timepoint (h)	Categories	Chao1	Shannon	Simpson
E1	6	**Inu w/eq.**	216 ± 15.3	3.57^{b} ± 0.009	0.92^{b} ± 0.003
		Inu eq.	240 ± 8	3.69^{b} ± 0.033	0.93^{a} ± 0.004
		Chi eq.	240 ± 8.25	3.8^{a} ± 0.02	0.94^{a} ± 0.002
		p value	0.09	0.016	0.019
	12	**Inu w/ eq.**	262 ± 8.29	4.02 ± 0.01	0.954 ± 0.002
		InuE	289 ± 9.17	4.05 ± 0.029	0.95 ± 0.0022
		ChicoE	242 ± 13	4.1 ± 0.035	0.954 ± 0.001
		p value	0.472	0.127	0.221
E2	6	**Inu w/eq.**	289 ± 24	4.24^{c} ± 0.17	0.959^{c} ± 0.008
		Inu eq.	326 ± 11.5	4.31^{c} ± 0.04	0.963^{b} ± 0.002
		Chico eq.	321 ± 20.5	4.67^{a} ± 0.02	0.979^{a} ± 0.001
		F	346 ± 8.19	4.7^{a} ± 0.02	0.978^{a} ± 0.001
		F2I	319 ± 9.49	4.55^{b} ± 0.03	0.974^{ab} ± 0.002
		F2C	332 ± 21.2	4.68^{a} ± 0.05	0.978^{a} ± 0.001
		p value	0.251	0.0203	0.0166
	12	**Inu w/eq.**	277^{b} ± 13.9	4.25^{d} ± 0.044	0.966^{c} ± 0.002
		Inu eq.	283^{b} ± 21	4.27^{d} ± 0.05	0.964^{c} ± 0.002
		Chico eq.	380^{a} ± 11.2	4.94^{b} ± 0.01	0.985^{a} ± 0.0004
		F	358^{ab} ± 8.21	4.97^{ab} ± 0.01	0.986^{a} ± 0.001
		F2I	271^{b} ± 27.2	4.46^{c} ± 0.05	0.973^{b} ± 0.001
		F2C	402^{a} ± 9.53	5.03^{ab} ± 0.01	0.986^{a} ± 0.001
		p value	0.0076	0.0022	0.0047

Values are means ± SEM, n = 8 per treatment group. Means in a column without a common superscript letter differ, (Kruskal–Wallis, followed by Dunn's test adj. ($p < 0.05$) adjusted using Bonferoni correction. Inulin equated (Inu eq.), Chicory equated (Chi eq.), Feed (F), Feed+2% Chicory (F2C), Feed+2% Inulin (F2I).

The distinct clustering clearly shows the influence of Inu and Chi on microbial communities at 4 h and 12 h of fermentation **(Figure 31)**. Regarding β- diversity at the ASV level, Inu and Chi significantly differed (adj. $p < 0.001$). Inu w/eq., Inu eq. and F2I appeared in the same cluster while Chi eq., F0.5C, F1C, F2C, F0.5I and F1C formed a separate cluster.

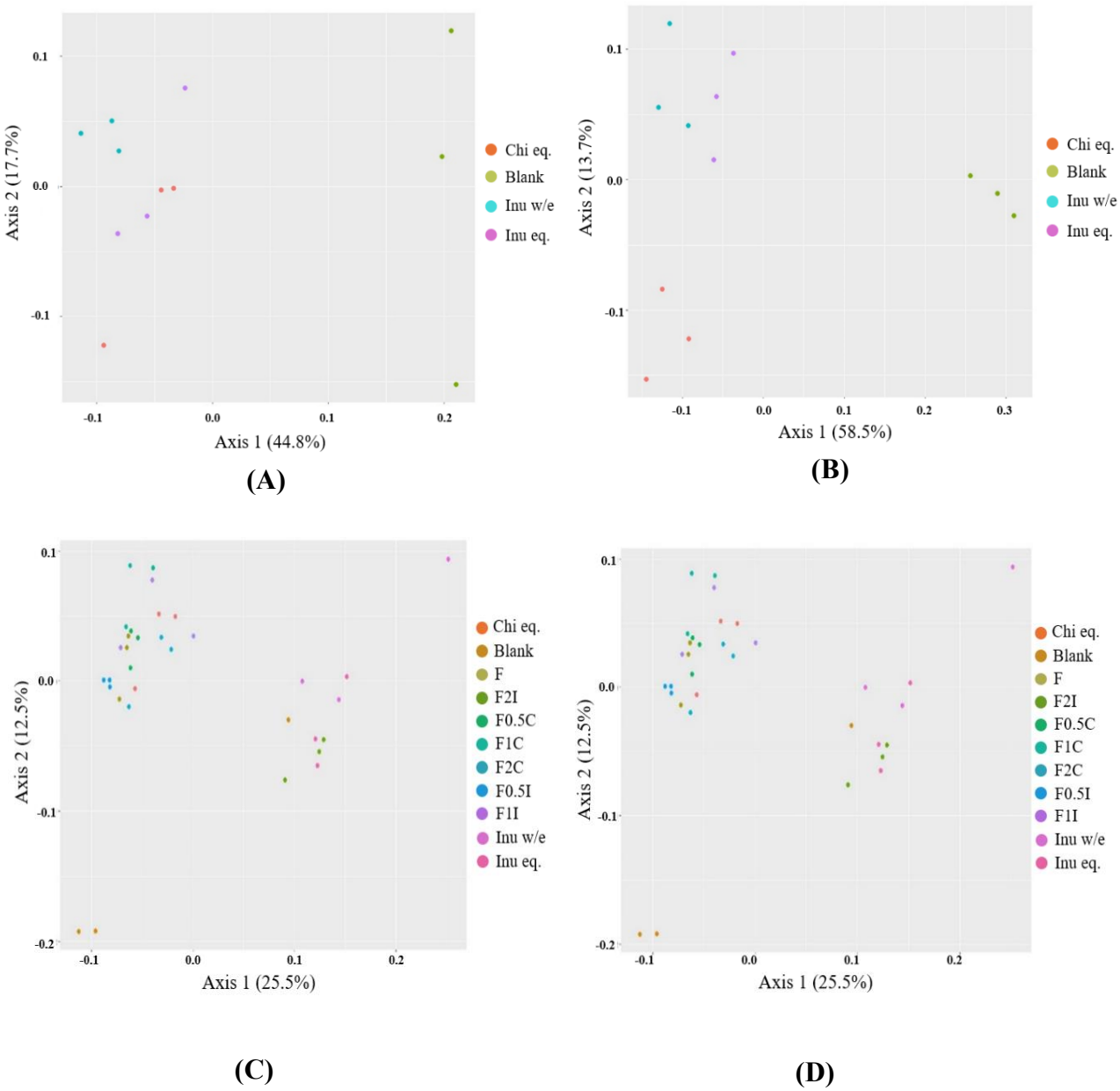

Figure 31. PCoA plot analysis (Bray-Curtis) for B- (β) diversity of microbiota of E1 at (A) 4 h (B) 12 h and E2 at (C) 4 h and (D) 12 h. The β-diversity PERMANOVA p - values were less than 0.001 for all the plots.

4.4.5. Effect on the abundance of the microbiota at 4 and 12 hr

Among the 24 phyla identified through sequencing, Firmicutes and Bacteroidota were the predominant phyla at both timepoints in both experiments, E1 **(Table 17)** and E2 **(Table 18)**. A decrease in the abundance of Firmicutes and a corresponding increase in Bacteroidota were observed after 12 h of fermentation compared to 4 h in both experiments (adj. $p < 0.05$). In E1, at 12 h, Desulfobacterota abundance was significantly higher in the Inu eq. group than in Chi eq. (adj. $p < 0.05$). In E2, Bacteroidota abundance was significantly higher in the F2I group compared to F2C (adj. $p < 0.05$) at both timepoints. Furthermore, in E2, Fusobacteriota (adj. $p < 0.01$) and Proteobacteria (adj. $p=0.005$) were significantly more abundant in the Chi eq., F, and F2C groups than in Inu eq. or F2I at both timepoints.

Both experiments also revealed significant differences in *Streptococcus* abundance between treatments at 4 and 12 h. In E1, Chi eq. exhibited a significantly lower *Streptococcus* abundance compared to Inu eq. (adj. $p < 0.01$) at 12 h. In contrast, in E2, Chi eq. and F2C showed the highest *Streptococcus* abundance compared to Inu eq. and F2I, respectively, at both timepoints (adj. $p < 0.01$). During E2, the relative abundance of *Lactobacillus* was higher in the Chi eq. group compared to Inu eq. (adj. $p < 0.01$). Similarly, F2C group exhibited consistently higher *Lactobacillus* levels compared to F2I (adj. $p < 0.01$). In E2, *Fecalibacterium* abundance was significantly lower in Chi eq. compared to Inu eq. at both timepoints (adj. $p < 0.01$). A similar pattern was observed when comparing F2I and F2C, with F2C showing consistently lower *Fecalibacterium* levels (adj. $p < 0.01$).

In E2, *Solobacterium* levels were significantly lower in Inu eq. and F2I compared to Chi eq. and F2C (adj. $p < 0.01$), respectively. At 4 h, *Blautia* levels were significantly higher in Inu eq. than in Chi eq. (adj. $p < 0.05$) in E2, whereas at 12 h, this trend was observed in both E1 (adj. $p < 0.05$) and E2 (adj. $p < 0.05$). No significant differences were found when comparing feed treatments within F2I and F2C. In E2, the abundance of *Holdemanella* was higher in Inu eq. and F2I compared to Chi eq. and F2C, respectively, at both timepoints (adj. $p < 0.01$), suggesting a greater influence of inulin on this genus after DD. A similar pattern was observed for *Lachnospiraceae* (unclassified), which had higher abundance in Inu eq., but the opposite trend was noted at the 12 h timepoint, where Chi eq. showed significantly higher levels than Inu eq. (adj.$p < 0.05$). Comparing feed treatments, F2C had higher *Lachnospiraceae* levels than F2I, although this was only significant at the 12 h timepoint (adj.$p <0.05$).

Subdoligranulum was more abundant in the Inu eq. group compared to Chi eq. in E2 at both timepoints, with F2I showing significantly higher levels than F2C only at 12 h (adj. $p < 0.05$). Additional genera from Firmicutes (e.g., *Mitsuokella, Acidaminococcus, Christensenellaceae_R-7_group, Phascolarctobacterium*), Bacteroidota (*Muribaculaceae*), Fusobacteriota (*Fusobacterium*), Proteobacteria (*Shigella*), and Actinobacteriota were significantly higher (adj. $p < 0.01$) in Chi eq. compared to Inu eq. at the 4 h timepoint in E2. However, differential effects were observed when these genera were combined with feed, with significant differences also seen at the 12 h timepoint for *Fusobacterium, Shigella,* and genera from *Actinobacteriota* (adj. $p < 0.01$).

Table 17: Microbiota composition of the fermentation broths of E1 after 4 and 12 h.

Phylum-Genera	Inu eq.	Chi eq.	adj. p value
	4h		
Firmicutes	**86.69 ± 3.91**	**83.89 ± 2.43**	**0.910**
Streptococcus	21.54 ± 1.27	19.2 ± 0.48	0.027
Catenibacterium	9.43 ± 2.03	10.07 ± 1.19	0.092
Unclassified Lachnospiraceae	10.1 ± 0.86	9.99 ± 0.64	0.578
Lactobacillus	6.88 ± 0.73	7.92 ± 0.32	0.563
Blautia	7.37 ± 0.3	6.39 ± 0.46	0.066
Faecalibacterium	3.01 ± 0.24	3.97 ± 0.36	0.532
Holdemanella	3.52 ± 0.27	3.72 ± 0.34	0.442
Enterococcus	8.92 ± 1.42	3.57 ± 0.32	0.033
Subdoligranulum	3.36 ± 0.27	4.86 ± 0.03	0.053
Solobacterium	1.61 ± 0.03	2.03 ± 0.12	0.082
Clostridium_sensu_stricto_1	1.25 ± 0.18	1.35 ± 0.05	0.053
Sharpea	1.03 ± 0.04	1.05 ± 0.01	0.369
Mogibacterium	0.44 ± 0.02	0.44 ± 0.03	0.092
Unclassified Peptostreptococcaceae	0.6 ± 0.1	0.71 ± 0.01	0.055
Christensenellaceae_R-7_group	0.41 ± 0.03	0.42 ± 0.02	0.050
Ruminococcaceae UCG-005	0.46 ± 0.06	0.38 ± 0.02	0.066
Proteobacteria	**8.22 ± 3.87**	**11.28 ± 2**	**0.922**
Escherichia-Shigella	8.21 ± 3.86	11.26 ± 1.99	0.922
Actinobacteriota	**2.34 ± 0.34**	**2.23 ± 0.04**	**0.099**
Collinsella	0.6 ± 0.14	0.47 ± 0.01	0.055
Unclassified Atopobiaceae	0.72 ± 0.13	0.64 ± 0.04	0.270
Bacteroidota	**2.22 ± 0.45**	**2.03 ± 0.46**	**0.424**
Muribaculaceae	1.53 ± 0.3	1.38 ± 0.24	0.789
	12h		
Firmicutes	**70.65 ± 2.09**	**66.34 ± 1.98**	**0.063**
Enterococcus	18.6 ± 0.64	17.43 ± 0.02	0.328
Unclassified Lachnospiraceae	8.92 ± 0.36	9.46 ± 0.09	0.123
Blautia	8.51 ± 0.54	6.98 ± 0.35	0.016
Holdemanella	7.32 ± 0.44	6.49 ± 0.37	0.066
Catenibacterium	4.43 ± 0.14	5.44 ± 0.45	0.033
Streptococcus	6.34 ± 0.43	4.08 ± 0.49	0.022
Faecalibacterium	2.53 ± 0.29	2.69 ± 0.35	0.578
Subdoligranulum	2.4 ± 0.44	2.14 ± 0.22	0.092
Lactobacillus	1.99 ± 0.33	2.04 ± 0.2	0.092
Sharpea	1.54 ± 0.05	1.75 ± 0.19	0.070
Phascolarctobacterium	0.62 ± 0.04	0.72 ± 0.01	0.055
Solobacterium	0.7 ± 0.03	0.68 ± 0.03	0.233
Clostridium_sensu_stricto_1	0.38 ± 0.05	0.31 ± 0.01	0.055
Bacteroidota	**21.91 ± 2.62**	**26.76 ± 1.98**	**0.270**
Prevotella	13.86 ± 2.6	18.38 ± 1.87	0.055
Muribaculaceae	2.59 ± 0.29	2.27 ± 0.23	0.069
Bacteroides	1.33 ± 0.08	1.86 ± 0.23	0.362
Unclassified Prevotellaceae	1.13 ± 0.03	1.56[a] ± 0.07	0.033
Unclassified Bacteroidales	0.97 ± 0.04	0.83 ± 0.04	0.432
Proteobacteria	**5.24 ± 0.52**	**4.8 ± 0.25**	**0.063**
Escherichia-Shigella	5.15 ± 0.53	4.73 ± 0.25	0.066
Desulfovibrio	0.8 ± 0.06	0.53 ± 0.05	0.027
Actinobacteriota	**0.82 ± 0.2**	**0.71 ± 0.08**	**0.183**
Fusobacteriota	**0.28 ± 0.11**	**0.66 ± 0.39**	**0.063**
Fusobacterium	0.28 ± 0.11	0.66 ± 0.39	0.053
Desulfobacterota	**0.83 ± 0.06**	**0.54 ± 0.03**	**0.031**

Values are means ± SEM, n = 8 per treatment group. Means in a row with timepoint without a common superscript letter differ, (Kruskal–Wallis, followed by Dunn's test adj. ($p < 0.05$). The composition expressed in % is only for genera with a relative abundance ≥1% for either of the group. Inulin equated (Inu eq.), Chicory equated (Chi eq.), Feed (F), Feed+2% Chicory (F2C), Feed+2% Inulin (F2I).

Table 18. Microbiota composition of the fermentation broths of E2 after 4 and 12 h.

Phylum	Inu eq.	Chi eq.	F	F2I	F2C	adj. p value
			4h			
Firmicutes	**81.46^{a} ± 0.46**	**74.79^{b} ± 0.58**	**74.75^{b} ± 0.64**	**77.42^{b} ± 0.3**	**77.48^{b} ± 0.47**	**0.005**
Unclassified Lachnospiraceae	17.22 ^{a} ± 0.23	15.03^{b} ± 0.27	14.86^{b} ± 0.28	16.74^{ab} ± 0.22	15.24^{b} ± 0.49	0.021
Blautia	16.46^{a} ± 0.48	12.03^{c} ± 0.48	12.01^{c} ± 0.32	13.51^{b} ± 0.1	12.61^{bc} ± 0.66	0.041
Lactobacillus	4.41^{b} ± 0.17	11.66^{a} ± 0.09	12.73^{a} ± 0.62	5.57^{b} ± 0.67	11.53^{a} ± 0.31	0.006
Subdoligranulum	8.01^{a} ± 0.11	6.83^{bc} ± 0.09	6.3^{c} ± 0.12	8.35^{a} ± 0.32	7.04^{b} ± 0.2	0.024
Streptococcus	1.67^{c} ± 0.06	3.45^{b} ± 0.07	3.48^{b} ± 0.12	1.19^{c} ± 0.09	5.04^{a} ± 0.34	0.002
Catenibacterium	3.94 ± 0.69	2.85 ± 0.07	2.57 ± 0.1	3.95 ± 0.17	2.56 ± 0.05	0.088
Solobacterium	1.4^{c} ± 0.11	2.38^{ab} ± 0.09	2.63^{a} ± 0.07	1.07^{c} ± 0.02	2.39^{ab} ± 0.13	0.004
Holdemanella	13.62^{a} ± 1.02	1.89^{cd} ± 0.13	1.11^{d} ± 0.09	9.2^{b} ± 0.87	2.13^{c} ± 0.12	0.002
Mitsuokella	0.92^{bc} ± 0.06	1.46^{a} ± 0.08	1.28^{ab} ± 0.1	0.75^{c} ± 0.02	1.57^{a} ± 0.13	0.007
Faecalibacterium	2.57^{b} ± 0.36	1.16^{c} ± 0.33	1.23^{c} ± 0.26	4.09^{a} ± 0.02	1.05^{c} ± 0.12	0.009
Acidaminococcus	0.65^{c} ± 0.05	1.15^{ab} ± 0.05	1.4^{a} ± 0.03	0.6^{c} ± 0.04	1.04^{b} ± 0.04	0.003
Phascolarctobacterium	0.66^{c} ± 0.01	1.04^{a} ± 0.06	1.05^{a} ± 0.05	0.78^{b} ± 0.02	1.03^{a} ± 0.06	0.008
Bacteroidota	**14.21^{c} ± 1.21**	**16.15^{bc} ± 0.34**	**15.29^{c} ± 0.52**	**19.78^{a} ± 0.32**	**15.39 ± 0.45^{c}**	**0.029**
Prevotella	6.69 ± 0.87	6.63 ± 0.02	5.94 ± 0.61	10.81 ± 0.14	6.2 ± 0.35	0.150
Muribaculaceae	3.21^{c} ± 0.12	5.22^{ab} ± 0.12	4.97^{b} ± 0.09	3.47^{c} ± 0.15	5.07^{ab} ± 0.37	0.005
Unclassified Prevotellaceae	1.4^{c} ± 0.07	1.82^{ab} ± 0.21	1.81^{b} ± 0.05	2.21^{a} ± 0.07	1.51^{bc} ± 0.05	0.034
Unclassified Bacteroidales	1 ± 0.06	1 ± 0.06	1.04 ± 0.01	1.11 ± 0.03	0.96 ± 0.01	0.051
Fusobacteriota	**1.83^{d} ± 0.71**	**4.62^{ab} ± 0.44**	**5.58^{a} ± 0.36**	**0.61^{d} ± 0.16**	**3.21^{bc} ± 0.69**	**0.001**
Fusobacterium	1.83^{cd} ± 0.71	4.62^{b} ± 0.44	5.58^{a} ± 0.36	0.61^{d} ± 0.16	3.21^{abc} ± 0.69	0.001
Proteobacteria	**1.22^{bc} ± 0.24**	**2.24^{a} ± 0.16**	**2.21^{a} ± 0.09**	**0.82^{c} ± 0.04**	**1.74^{ab} ± 0.26**	**0.005**
Escherichia-Shigella	0.89^{bc} ± 0.16	1.95^{a} ± 0.12	1.92^{a} ± 0.07	0.62^{c} ± 0.02	1.59^{ab} ± 0.24	0.008
Actinobacteriota	**1.01 ± 0.09**	**1.86 ± 0.14**	**1.79 ± 0.16**	**1.2 ± 0.06**	**1.8 ± 0.16**	**0.096**
			12h			
Firmicutes	**69.6 ± 0.65**	**66.99 ± 0.9**	**67.51 ± 0.93**	**66.33 ± 1.06**	**67.9 ± 1.29**	**0.198**
Unclassified Lachnospiraceae	13.77^{c} ± 0.19	20.05^{a} ± 1.06	19.7^{a} ± 0.49	15.54^{b} ± 0.45	19.88^{a} ± 0.25	0.021
Blautia	13.02^{a} ± 0.33	8.47^{b} ± 0.14	7.95^{c} ± 0.35	10.79^{ab} ± 0.7	8.05^{c} ± 0.27	0.041
Lactobacillus	3.64^{c} ± 0.31	7.54^{b} ± 0.23	9.37^{a} ± 0.52	3.22^{c} ± 0.48	7.57^{b} ± 0.68	0.006
Subdoligranulum	7.55^{a} ± 0.59	4.09^{b} ± 0.13	3.56^{c} ± 0.1	5.96^{a} ± 0.09	3.98^{bc} ± 0.11	0.024
Muribaculaceae	3.29^{d} ± 0.19	4.08^{ab} ± 0.25	3.89^{b} ± 0.07	2.92^{d} ± 0.08	4.4^{a} ± 0.05	0.005
Streptococcus	1.31^{c} ± 0.09	3.9^{ab} ± 0.07	3.03^{b} ± 0.2	0.89^{d} ± 0.09	4.81^{a} ± 0.68	0.002
Holdemanella	13.14^{a} ± 1.17	2.03^{b} ± 0.14	1.04^{c} ± 0.04	10.65^{a} ± 0.07	1.81^{b} ± 0.09	0.002
Solobacterium	0.98^{c} ± 0.05	1.93^{ab} ± 0.05	2.03^{a} ± 0.01	0.83^{c} ± 0.01	1.76^{b} ± 0.04	0.004
Catenibacterium	3.35 ± 0.51	1.76 ± 0.07	1.49 ± 0.02	3.56 ± 0.14	1.08 ± 0.12	0.076
Faecalibacterium	2.88^{a} ± 0.16	1.27^{c} ± 0.15	1.23^{c} ± 0.03	3.36^{a} ± 0.12	1.88^{bc} ± 0.28	0.009
Ruminococcus	0.42^{b} ± 0.08	1.01^{a} ± 0.18	1.31^{a} ± 0.07	1.23^{a} ± 0.08	1.26^{a} ± 0.05	0.005
Sharpea	1.31^{a} ± 0.16	0.58^{b} ± 0.05	0.5^{b} ± 0.05	1.11^{a} ± 0.05	0.6^{b} ± 0.05	0.029
Clostridium_sensu_stricto_1	0.23^{b} ± 0.04	0.54^{ab} ± 0.02	0.6^{a} ± 0.15	0.26^{b} ± 0.001	0.52^{ab} ± 0.01	0.008
Bacteroidota	**27.75 ^{ab} ± 0.77**	**23.87 ^{b} ± 0.6**	**23.91^{b} ± 0.36**	**30.94^{a} ± 0.66**	**24.35^{b} ± 0.35**	**0.022**

Prevotella	19 ± 0.56	12.61 ± 0.47	11.88 ± 0.24	21.98 ± 0.35	11.48 ± 0.22	0.150
Unclassified Prevotellaceae	1.49^{c} ± 0.08	3.44^{a} ± 0.15	3.66^{a} ± 0.17	2.38^{bc} ± 0.18	3.26^{a} ± 0.11	0.034
Unclassified Bacteroidales	1.47 ± 0.05	1.08 ± 0.03	1.25 ± 0.06	1.34 ± 0.1	1.32 ± 0.08	0.051
Alloprevotella	0.52^{ab} ± 0.02	0.56^{ab} ± 0.07	0.58^{ab} ± 0.1	0.38^{b} ± 0.08	0.78^{a} ± 0.07	0.016
Fusobacteriota	**0.32 ± 0.07^{b}**	**$4.69^{a} \pm 1.06$**	**$4.16^{a} \pm 0.42$**	**$0.73^{b} \pm 0.26$**	**$3.3^{a} \pm 0.79$**	**0.014**
Fusobacterium	0.32 ± 0.07^{b}	4.69^{a} ± 1.06	4.16^{a} ± 0.42	0.73^{b} ± 0.26	3.3^{a} ± 0.79	0.001
Proteobacteria	**$0.84^{b} \pm 0.03$**	**$2.4^{a} \pm 0.26$**	**$2.23^{a} \pm 0.25$**	**$0.86^{b} \pm 0.12$**	**$2.39^{a} \pm 0.28$**	**0.010**
Escherichia-Shigella	0.64^{c} ± 0.01	1.78^{ab} ± 0.21	1.75^{ab} ± 0.23	0.64^{c} ± 0.06	1.54^{b} ± 0.2	0.008
Desulfovibrio	0.33^{b} ± 0.06	0.58^{a} ± 0.02	0.65^{a} ± 0.03	0.28^{b} ± 0.01	0.59^{a} ± 0.04	0.010
Actinobacteriota	**$1.05^{ab} \pm 0.07$**	**$1.27^{a} \pm 0.18$**	**$1.27^{a} \pm 0.06$**	**$0.75^{c} \pm 0.05$**	**$1.15^{a} \pm 0.1$**	**0.016**
Desulfobacterota	**$0.34^{b} \pm 0.06$**	**$0.61^{a} \pm 0.02$**	**$0.69^{a} \pm 0.03$**	**$0.28^{b} \pm 0.01$**	**$0.6^{a} \pm 0.04$**	**0.002**

Values are means ± SEM, n = 8 per treatment group. Means in a column with timepoint without a common superscript letter differ, (Kruskal–Wallis, followed by Dunn's test adj. ($p < 0.05$) and Bonferroni correction. The composition expressed in % is only for genera with a relative abundance ≥1% for either of the group. Inulin equated (Inu eq.), Chicory equated (Chi eq.), Feed (F), Feed+2% Chicory (F2C), Feed+2% Inulin (F2I).

4.4.6. Integration Analysis

The RGCCA plots **(Figure 32A)** for Gas Kinetics block show that Component 1 (70.4%) separates Inu eq. from the other treatment groups. The variable projection indicates strong significant positive correlations (adj. $p < 0.01$) for A (r=0.887), C (r=0.938) and R_{max} (r=0.936) with Component 1, primarily driving the separation of Inu eq. from the rest. B has a weaker non-significant correlation with both dimensions, suggesting a limited role in defining treatment-specific effects.

The RGCCA plots **(Figure 32B)** show treatment-specific clustering along Component 1 (50.9%) and Component 2 (21.4%) for SCFA block. Component 1 separates the F2C and Chi eq. groups from F2I and Inu eq., while Component 2 clearly distinguishes F, F2C, and F2I. Variable projections reveal that acetate and total SCFA production are significantly negatively correlated with Component 1 (r = -0.968, r=-0.725; adj. $p < 0.001$) while BCFA are significantly positively correlated (r=0.949; adj. $p < 0.001$), contributing to the separation of F2C and F2I. While lactate strongly correlates with Component 2 (r = 0.75, adj. $p < 0.05$), driving differentiation along this component.

The RGCCA plot **(Figure 39)** based on genera abundance, shows that Component 1 (45%) separates Inu eq. and F2I as a close cluster from the remaining treatment groups. Chi eq. lies partially distinct but closer to F and F2C, which overlap along Component 1. Higher abundance genera like *Blautia* (r = 0.921), *Holdemanella* (r = 0.974), *Catenisphaera* (r = 0.971), and Prevotella (r = 0.947), were found to be significantly positively correlated with Component 1 (adj.$p < 0.001$). Negative correlations along Component 1 were observed for *Solobacterium* (r = -0.948), *Ruminococcus* (r = -0.945), and *Lactobacillus* (r = -0.925).

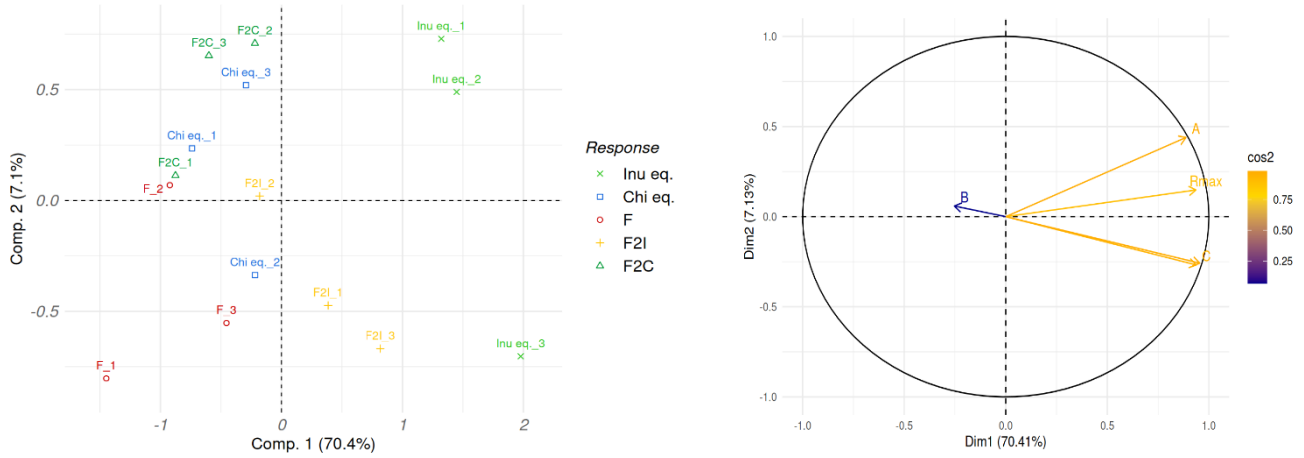

(A)

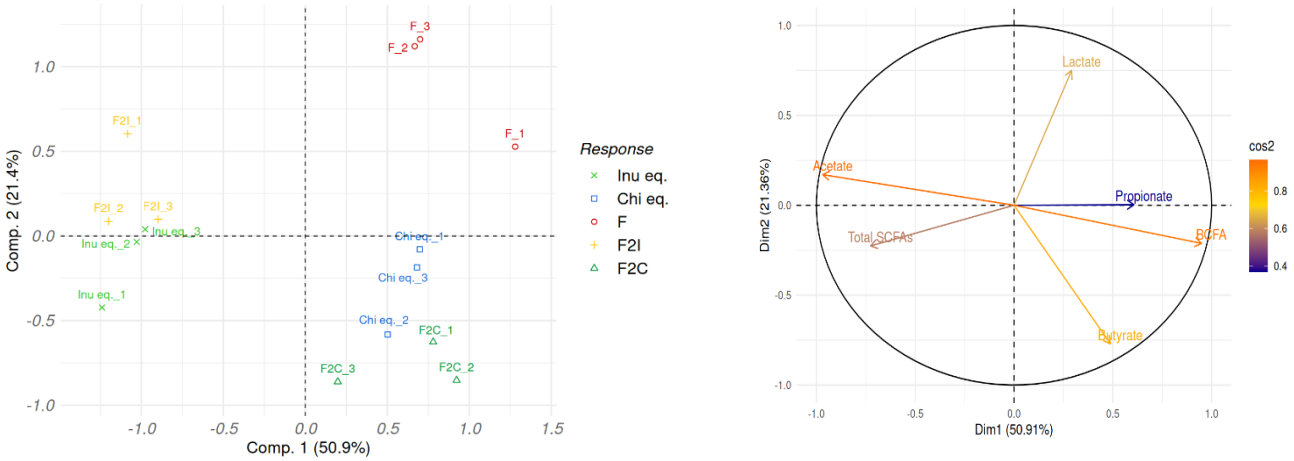

(B)

Figure 32. RGCCA individuals and variables plots for components 1 and 2

Individuals (left) and variables (right) plots from supervised RGCCA, displayed for components 1 and 2, considering the variables from (***A***) Gas Kinetics, and (***B***) Short Chain Fatty Acids from 12 h timepoint. Samples in the individuals plot are coloured by group similarly as PCA. In the variable plot, arrows colour and length are based on square cosine (cos^2), indicating the quality of variable representation by the first two components of RGCCA for a given block.

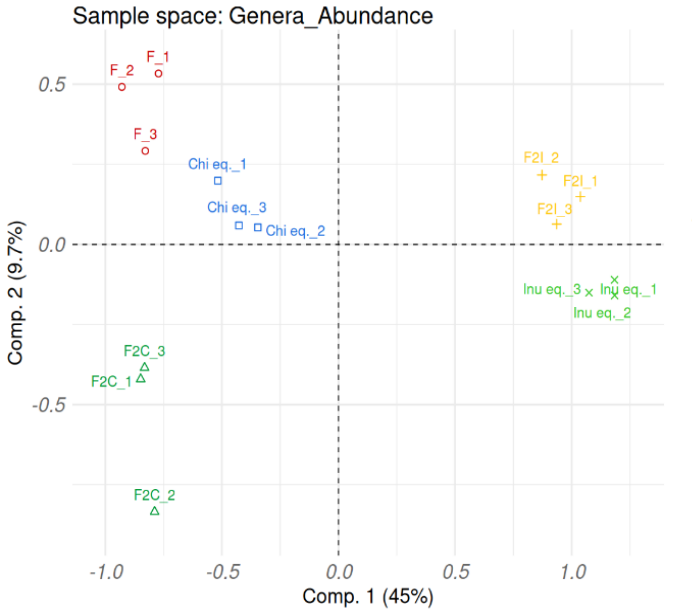

Microbiota	*R value*
Solobacterium	-0.948
Ruminococcus	-0.945
Lactobacillus	-0.925
nclassified Lachnospiraceae	-0.92
Butyrococcus	-0.92
Desulfovibrio	-0.912
Prevotella	-0.908
Streptococcus	-0.847
Bifidobacterium	-0.839
Fusobacterium	-0.823
Methanobrevibacter	-0.902
Acidaminococcus	-0.901
Mogibacterium	-0.869
Holdemanella	0.974
Catenisphaera	0.971
Prevotella	0.947
Blautia	0.921
Subdoligranulum	0.918
Sharpea	0.912
Faecalibacterium	0.88

Figure 33. Individuals plot from supervised RGCCA for genera abundance (>1%) at 12 h. (**A**) Individuals plot from supervised RGCCA, displayed for components 1 and 2, considering the variables from genera abundance >1% at the 12 h timepoint. Samples in the individuals plot are coloured by group similarly as PCA. (**B**) The table consist of Pearson correlation coefficients (r), which were adjusted using Bonferroni method (adjusted p-value < 0.001).

4.5. Discussion

This study introduced a multifaceted *in vitro* approach to evaluate the effects of crude chicory (Chi eq.), inulin (Inu eq.), and their combinations with feed (F, F2I, F2C) on microbial fermentation in the context of weaning piglet colonic physiology. To reflect the digestive environment more accurately, we applied sequential steps of *in vitro* digestion, absorption *via* dialysis, and batch fermentation. The molecular weight profiles of inulin and crude chicory fractions revealed key insights into how dialysis membrane size influences the retention or loss of specific molecular components. While inulin exhibited no significant differences across Mw, Mn, DPw, and DPn between the 3.5 kDa and 6–8 kDa dialyzed fractions, crude chicory showed a markedly different pattern. Dialysis through the 6–8 kDa membrane led to significantly higher average molecular weights and degrees of polymerization compared to both ND chicory and the 3.5 kDa dialyzed samples. This elevation in M_w suggests that smaller, lower molecular weight components—likely including simple sugars and short-chain oligosaccharides—were preferentially lost through the membrane, thereby shifting the molecular profile toward higher-weight polysaccharides. The similarity in PDI across treatments indicates that despite this shift, the overall distribution breadth remained consistent. These observations highlight the structural heterogeneity of crude chicory, which, unlike purified inulin, is more prone to dialysis-induced alterations. Such changes in polymer profile may have downstream implications on fermentation kinetics and metabolite production, as higher M_w fibers are typically fermented more slowly and can modulate microbial composition and SCFA production differently than smaller fractions.

Previous research indicates that factors such as higher insoluble fiber content, lower fructan availability, or high degrees of polymerization (DP) can slow fermentation rates (Pellikaan *et al.,* 2007; Shim *et al.,* 2007; Uerlings *et al.,* 2019). In our study, the fructan content was equated between treatments, with comparable average DPs for Inu (9–11) and Chi (13–15). Chi eq. exhibited slower and more prolonged fermentation kinetics compared to Inu eq., likely due to its higher content of insoluble fibers (ADF/NDF). This is consistent with findings from Ramasamy *et al*. (2024) and Uerlings *et al*. (2019), which show that insoluble fibers such as cellulose and lignin are fermented more slowly, often after soluble fibers are depleted. This may explain the higher B value observed for Chi eq. (Monro and Mishra, 2010; Hamaker and Tuncil, 2014). Additionally, the greater gas volume observed in digested-dialyzed (DD) samples compared to non-digested (ND) samples may be attributed to the swelling and increased viscosity of soluble fibers upon contact with digestive fluids, which can enhance microbial accessibility and activity. Interestingly, Chi eq. showed a higher B value and lower T_{max} in DD conditions compared to Inu eq., suggesting an earlier onset and more sustained fermentation without peak gas accumulation. This differential effect may be due to structural differences between crude chicory (with intact cell walls) and purified inulin (with less complex supramolecular structure), potentially influenced by viscosity, solubility, and fiber–microbe interactions (Capuano, 2017a; Mikkelsen *et al.,* 2011).

Greater gas production generally indicates higher microbial metabolic activity; however, this relationship was most evident in the digested–dialyzed (DD) samples, where Inu eq. yielded a higher total SCFA produced compared to Chi eq. A positive correlation was observed between total gas production and the abundance of major microbial genera, whereas a negative correlation was found between gas volume and total SCFA concentration ($r = –0.725$). This trend was particularly apparent when the first components (Comp. 1) of gas kinetics and microbial abundance datasets were examined using supervised RGCCA **(Figure 34A)**. Both Inu eq. and F2I displayed rapid fermentation with high gas production and were positively associated with microbial abundance. However, when gas kinetics were correlated with total SCFA levels **(Figure 34B)**, these treatments showed a strong inverse association, suggesting that high gas production may not always equate to efficient

SCFA output. This supports previous findings by Blümmel *et al.* (1999), who noted that gas volume and SCFA production are not always directly correlated during fiber fermentation.

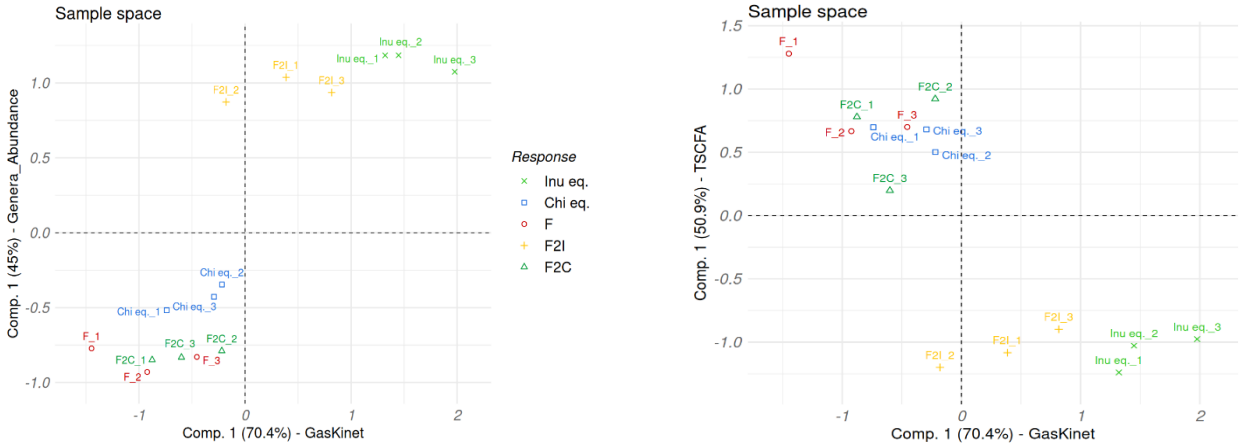

Figure 34. Individual biplots illustrating the correlation between the first components (Comp. 1) for block pairs in DD samples at 12 h using supervised RGCCA among (A) Gas Kinetics and Genera_Abundance blocks, (B) Gas Kinetics and TSCFA blocks. Samples are coloured by response.

In another observation of our study, DD samples showed higher SCFA levels at the 4 h mark compared to ND samples, suggesting that DD might accelerate microbial activity, contributing to increased gas production. As reviewed, differences in SCFA production across studies may result from variations in dose, source, chain length, inoculum, or metabolic status (Hughes *et al.,* 2021).

In many *in vitro* studies designed to mimic *in vivo* conditions, individual bioactive components are evaluated, often excluding feed, based on the assumption that feed composition is consistent across treatments and therefore not necessary to be included. Our findings, however, suggest otherwise, as F2C produced more butyrate and less acetate at 12 h than F2I—a difference not evident when comparing Inu eq. with Chi eq. This implies that the presence of feed's complex matrix can alter prebiotic fermentative effects, possibly by encouraging butyrate-producing microbes like *Lactobacillus*, *Butyricoccus*, and *Bifidobacterium* (Jung *et al.,* 2015; Kiernan *et al.,* 2023a; Xing *et al.,* 2020). Feed provides various substrates, including proteins, fats, and non-soluble fibers **(Table 7)**, which supports microbial communities that favour these substrates and influence overall microbial interdependencies. This effect of F2C could also be enhanced by other bioactives, such as dietary polyphenols and STLs from chicory, that are known to promote butyrate production in gut bacteria (Alves-Santos *et al.,* 2020; Pouille *et al.,* 2022b). Increased butyrate production might also be linked to reduced acetate levels through cross-feeding, where acetate serves as a precursor for butyrate synthesis (Hodgkinson *et al.,* 2023). This is further supported by RGCCA, which showed a significant (adj. $p < 0.001$) positive and negative correlation with Dimension 1 respectively between butyrate ($r = 0.488$) and acetate ($r = -0.968$).

In E2, Chi eq. and F2C demonstrated higher Shannon and Simpson indices than Inu eq. and F2I, consistent with prior studies linking a higher α-diversity to higher insoluble fiber intake (Aljuraiban *et al.,* 2023; Jiang *et al.,* 2020). This contrasts with a study on weaning piglets which showed higher α-diversity with soluble fibers; but this is likely due to differences in fiber composition between the studies (Chen *et al.,* 2019). Studies also suggest that butyrate production is positively associated with species richness and diversity in animal models (Hodgkinson *et al.,* 2023), and the higher butyrate levels in F2C versus F2I support this observation.

The aforementioned effect was significantly evident only in E2, with DD and ND samples showing differences in α-diversity, emphasizing the role of DD in shaping microbiota diversity. Such diversity differences may arise from variations in fermentation kinetics, SCFA production, environmental changes, and partial carbohydrate breakdown during digestion. ND samples, containing a broader nutrient profile, likely promote faster microbial activity due to simple sugars and amino acids. This accelerated fermentation leads to a rapid accumulation of fermentation byproducts, creating an environment that fosters the growth of specific bacterial groups. Studies suggest that simple sugars may reduce SCFA-producing species while promoting pathobionts (Wagenaar *et al.,* 2021), potentially disrupting microbiota and causing dysregulated immunometabolism (Arnone *et al.,* 2022; Zong *et al.,* 2024). In our study, Proteobacteria abundance was six times higher in ND than DD samples at 4 and 12 hr, reflecting its preference for simple sugars and its potential to foster a less beneficial microbial profile (Jamar *et al.,* 2021; Zong *et al.,* 2024). Additionally, ND samples also contained high level of crude proteins and undigested dietary proteins, promoting nitrogen-utilizing bacteria that produce toxic metabolites. This highlights the importance of including digestion steps in *in vitro* studies (Kiernan *et al.,* 2023b; Luise *et al.,* 2021; Rattigan *et al.,* 2020). Another possible effect could arise from the removal of buffering compounds during dialysis, which may modify pH dynamics and influences microbial metabolic pathways, thereby impacting microbiota composition. Regarding the β- diversity clustering, Inu eq. and F2I samples clustered separately from all other treatment groups. This finding aligns with *in vivo* studies which associate non-digestible polysaccharides and bioactive compounds, such as polyphenols and glucosinolates, with distinct microbial communities, further underscoring the influence of specific substrates on microbial structure (Jiang *et al.,* 2020; Shahinozzaman *et al.,* 2021).

At the phylum level, Firmicutes, Bacteroidota, and, to a lesser extent, Proteobacteria were dominant in both ND and DD conditions, aligning with findings from various *in vivo* (Kim and Isaacson, 2015; Niu *et al.,* 2015) and *in vitro* (Fleury *et al.,* 2017) studies. In the ND condition, Bacteroidota increased tenfold, while Firmicutes decreased by 20% after 12 h of fermentation, with a similar but milder trend observed in the DD condition. This shift suggests an increase in inflammation at 12 h, as a decreased Firmicutes/Bacteroidota (F/B) ratio is commonly associated with dysbiosis and inflammation. Additionally, Bacteroidota levels tend to be elevated in inflammatory bowel disease, where they contribute to disease progression (Stojanov *et al.,* 2020). Notably, Bacteroidota abundance was lower in F2C than in F2I at both timepoints, suggesting a possible anti-inflammatory effect. Although not statistically significant, a slight decrease in Bacteroidota was also observed in the Chi eq. group compared to Inu eq., potentially explaining the lower SCFA production observed in Chi eq., as Bacteroidota are known primary SCFA producers. Interestingly, polyphenols as found in Chi eq. have been reported to reduce Bacteroidota abundance in the colonic digesta of weaned pigs (Xu *et al.,* 2020). Inulin-treated groups (Inu eq. and F2I) showed significantly reduced growth of the Fusobacteriota and Proteobacteria, which may correlate with their lower α-diversity indices. However, Uerlings *et al.,* (2021b), on the contrary found a lower proportion of these two phyla in chicory root fermentation supernatant compared to that of an inulin fermentation. Both Proteobacteria and Fusobacteriota are associated with gut disorders, including inflammation and colon cancer (Hermann-Bank *et al.,* 2015; Tan *et al.,* 2019). The rapid fermentation of inulin may have suppressed the growth of these phyla more effectively, likely due to the SCFA produced, compared to the slower-fermenting chicory. However, since Firmicutes and Bacteroidota make up approximately 90% of the microbial community, changes observed in F2C could be more impactful than alterations in these lower-abundance phyla.

At the genus level, few genera significantly differed between Inu eq. and Chi eq. in ND samples. *Enterococcus* levels were two-fold higher in ND Inu eq. at 4 h, a genus that can act as either a commensal (Saillant *et al.,*

2021) or a pathogen (Crank and O'Driscoll, 2015; Krawczyk *et al.,* 2021). By 12 h, Chi eq. and Inu eq. had similar *Enterococcus* levels, reflecting the slower action of microbiota on insoluble fibers. Focusing on microbiota composition in E2, distinct differences emerged between the Inu eq. and Chi eq. treatments in terms of beneficial and potentially harmful microbial populations. Unclassified *Lachnospiraceae* and *Blautia,* both belonging to the *Lachnospiraceae* family and are known for strong hydrolytic activity (Vacca *et al.,* 2020), made up nearly 30% of all genera. Unclassified *Lachnospiraceae* which was abundant at 4 h in the DD Inu eq. group and at 12 h in the DD Chi eq. group, is a major butyrate producer and can convert lactate to butyrate (cross-feeding). Its decrease is linked with inflammation (Lobionda *et al.,* 2019; Louis and Flint, 2009).

Blautia, which responds well to inulin (Riva *et al.,* 2023) was more abundant in Inu eq., likely due to the higher soluble fiber content. This genus is positively correlated with acetate production, as observed in our results and those of previous studies (Chen *et al.,* 2019; Salonen *et al.,* 2014). This genus also contributes to immune modulation and inflammation control through butyrate production (Vacca *et al.,* 2020). *Lactobacillus* was the third most abundant genus, a higher abundance of which is also associated with the incorporation of mucin-covered microcosms in batch fermentation models as mucin is known to alter *Lactobacillus* growth due to their ability to thrive on mucus (Tran *et al.,* 2016a). *Lactobacillus* which had 2-3 times higher abundance in Chi eq. and F2C than in Inu eq. and F2I, is known for its anti-inflammatory effects and its role in enhancing gut health by upregulating barrier integrity genes, reducing pathogen load, and producing antimicrobial peptides (Lobionda *et al.,* 2019). Lower *Lactobacillus* levels are often associated with a weakened intestinal barrier (Xu, 2014). Both *Lactobacillus* and *Bifidobacterium*, although the latter accounts for less than 1% of the abundance, produce a variety of fatty acids beneficial for gut health (Kleessen *et al.,* 2007; Bastard *et al.,* 2020; Nilsson and Björck, 1988; Wang *et al.,* 2020). The presence of *Bifidobacterium,* found in higher amounts in Chi eq. and F2C, aligns with studies showing that inulin boosts *Lactobacillus* and *Bifidobacterium* levels while reducing inflammation by downregulating TNFα (Hiel *et al.,* 2020; Hino *et al.,* 2011). This inulin-associated increase in *Bifidobacterium* abundance has been observed in human as well as in *in vitro* studies (Baxter *et al.,* 2019; Le Bastard *et al.,* 2020; Trompette *et al.,* 2018; Uerlings *et al.,* 2019, Vandeputte *et al.,* 2017). Polyphenol (also found in crude chicory) has been shown to increase beneficial microbes such as *Lactobacillus*, *Bifidobacteria* and *Prevotella*, while reducing harmful *Streptococcus* and *Clostridium* (Kiernan *et al.,* 2023b). *Fecalibacterium,* another butyrate producer associated with anti-inflammatory effects, was higher in Inu eq., as seen in other inulin studies (Bastard *et al.,* 2020). Its reduced abundance in Chi eq. could be due to the genus's lower preference for insoluble fibers (Zhou *et al.,* 2018). Inu eq. may also contribute to anti-inflammatory effects through SCFA production and the long-chain fatty acid 3-hydroxyoctadecaenoic from *Holdemanella,* which was six times more abundant in Inu eq. *(Pujo et al., 2021)*. As observed in our study, inulin also promotes an increase in the abundance of other genera like *Phascolarctobacterium, Akkermansia* and *Ruminococcus* which are also responsible for SCFA modulation (Guo *et al.,* 2021; Yang *et al.,* 2023).

In our study, *Desulfovibrio* abundance significantly decreased in both Inu eq. and Chi eq., as well as in F2I and F2C, with the Inu-associated group showing the strongest reduction. This aligns with previous findings (Hiel *et al.,* 2020; Holscher *et al.,* 2015) and supports Sarmiento-Andrade *et al.,* (2022) who noted a positive correlation between inulin and butyrate production, alongside a negative correlation with *Desulfovibrionaceae* abundance. Similar observation was made in our study as significant negative correlation was found between butyrate (r=0.488) and *Desulfovibrio* (r=-0.912). In an *in vivo* study with piglets fed with soluble dietary fibers, a higher relative abundance of *Proteobacteria*, *Actinobacteria*, *Solobacterium*, and *Blautia* was observed, whereas insoluble fibers favoured *Bacteroides*, *Phascolarctobacterium* and *Prevotella* (Chen *et al.,* 2019). Interestingly in our study (RGCCA), Inu eq. and F2I were clustered on the positive side of Component 1 and

Prevotella (r=0.947) was found to be significantly positively correlated while *Solobacterium* (r=-0.948) was negatively correlated to Component 1. Despite using fecal inoculum from piglets of similar age, our results differed from those in these studies, except for *Blautia* and *Phascolarctobacterium*, highlighting that individual animal variation can influence microbiota composition. Therefore, it is critical to maintain consistency in fecal inoculum sources across *in vitro* experiments to allow for accurate comparisons. In our study, we ensured the use of the same inoculum pool across all ND and DD samples, controlling for variability.

This *in vitro* study, incorporating gastrointestinal digestion, dialysis, and fermentation, evaluated how inulin and crude chicory influence microbial fermentation under conditions mimicking the weaning piglet colon. While Inu eq. exhibited 2 times faster fermentation and greater gas production—particularly at 12 h in digested–dialyzed samples—Chi eq. and its feed-based counterpart F2C consistently supported higher microbial α-diversity indices and enriched several health-associated genera, including *Lactobacillus*, *Bifidobacterium*, unclassified *Lachnospiraceae*, and *Ruminococcus*. These microbial shifts, coupled with favourable SCFA profiles and a reduction in Bacteroidota, highlight crude chicory's potential to positively modulate gut microbiota. When included in a feed matrix, chicory (F2C) had higher (by 12-15%) inulin (F2I) in butyrate production and microbial richness, further emphasizing the role of substrate complexity in shaping fermentation outcomes. Overall, crude chicory appears to be at least as effective as inulin—and in some aspects, even superior—in supporting microbial diversity and fermentation quality. To further explore the functional relevance of these microbial shifts, the next chapter investigates how the fermentation supernatants from these treatments influence epithelial barrier integrity and inflammatory responses in a triple co-culture cell model.

5

Impact of fermented inulin and chicory supernatants on epithelial barrier integrity and inflammation in a triple cell culture model

Article II

Impact of fermented inulin and chicory supernatants on epithelial barrier integrity and inflammation in a triple cell culture model

Tushar Kulkarni[a,b], Pawel Siegien[a], Jimmy Vandel[e], Luke Comer[c], Benoit Cudennec[b], Sandy Theysgeur[b], Camille Dugardin[b], Anca Lucau-Danila[b,d], Nadia Everaert[c], Martine Schroyen[a,b,*] Rozenn Ravallec[b,*],

a. Precision Livestock and Nutrition Laboratory, TERRA Teaching and Research Centre, Gembloux Agro-Bio Tech, University of Liège, 5030 Gembloux, Belgium
b. UMR-T 1158, BioEcoAgro, University of Lille, University of Liege, 59650 Lille, France
c. Nutrition and Animal Microbiota EcoSystems lab, Division of A2H, Department of Biosystems, KU Leuven, 3001 Leuven, Belgium
d. Joint Laboratory CHIC41H University of Lille-Florimond - Desprez, Cité scientifique, 59655 Villeneuve d'Ascq, France
e. US 41 - UAR 2014 – PLBS – Bililleplatform, Univ. Lille, CNRS, Inserm, CHU Lille, Institut Pasteur de Lille, 59000 Lille, France

*Corresponding authors at : Université de Liège - Gembloux Agro-Bio Tech, Département AgroBioChem - Animal Sciences, Passage des Déportés, 2, 5030 Gembloux, Belgium; University of Lille - IUT A, Polytech Building, Lille, Scientific City, 59655 Villeneuve d'Ascq, France
Email adresses : rozenn.ravallec@univ-lille.fr (R. Ravallec) and martine.schroyen@uliege.be (M. Schroyen)

This chapter is adapted from the article submitted to Journal of Agricultural and Food Chemistry.

5.1. Abstract

Weaning induces significant stress in piglets, leading to intestinal inflammation, compromised barrier function, and increased epithelial permeability. Dietary fibers such as inulin and crude chicory have been shown to promote gut health by modulating the microbiota and generating beneficial fermentation metabolites. Therefore, this study aimed to compare the effects of fermentation supernatant of crude chicory (Chi) with inulin (Inu) and when associated with feed (F2I, F2C) (obtained in the Chapter 4) on a triple cell culture (Caco-2/HT-29-MTX/U937) model. To create a more comprehensive model, human cell lines were used, due to similarities between human and piglet GI physiology.

The experiment had 8 groups equated (eq.): RPMI (Non-stimulated), only LPS (Positive control), Dexamethasone (20 µM) and Indomethacin (100 µM) (Negative Control), Inu eq., Chi eq., F, F2I, and F2C. The triple cell culture model, developed with a physiologically relevant 90:10 Caco-2/HT-29-MTX ratio on apical, achieved optimum transepithelial electrical resistance (TEER ~806 $\Omega \cdot cm^2$) by 20 days, indicating an intact intestinal barrier. The differentiated U937 (macrophages) were placed in the basolateral compartment on day 21. Differentiated Caco-2/HT-29-MTX were pre-treated with LPS (-ctrl) 6 hr prior to and during incubation of fermentation supernatant for 24 h. Cytokine levels were analysed in the basolateral media with differentiated U937 (macrophages), gene expression was measured in the apical cells, and permeability by Lucifer Yellow after 24 h of treatment.

The fermentation supernatant at the 12-h timepoint demonstrated cell viability exceeding the 80% threshold for the triple cell co-culture starting at the higher concentration (C25). After 24 h FB treatment and LPS stimulation, Inu eq. and Chi eq. downregulated pro-inflammatory cytokines IL1β, IL8, TNFα and genes *MAPK14*, *MyD88*, *AKT1* ($p < 0.05$). Interestingly, F2C showed a more significant effect than F2I ($p < 0.05$). Chi eq. had a 3-fold increase in *MUC2*, while Inu eq. upregulated MUC*1* & *JAMB* expression ($p < 0.05$). F2I had a higher permeability than F2C ($p < 0.05$). In conclusion, cost-effective Chi eq. and F2C showed greater benefits in enhancing gut health.

Keywords: Chicory, Inulin, *in vitro*, fermentation, inflammation.

5.2. Introduction

Weaning is one of the most critical transitions in a piglet's early life, often associated with significant physiological and immunological stress. This abrupt separation from the sow typically occurs around 3–4 weeks of age, a period when the piglet's gastrointestinal (GI) and immune systems are still immature. The interruption of milk intake and the introduction of solid feed led to altered microbial colonization, intestinal inflammation, and compromised barrier function (Capaldo and Nusrat, 2009; Sido *et al.*, 2017; Stokes *et al.*, 2004; Zheng *et al.*, 2021a). Weaning stress activates both the innate and adaptive immune responses. It triggers the upregulation of pro-inflammatory cytokines such as TNFα, IL-1β, IL-6, IL-8, and IFNγ, which collectively disrupt tight junctions and increase intestinal permeability. These changes compromise mucosal integrity and contribute to short-term diarrhea and long-term immune dysregulation (Tang *et al.*, 2022; McCracken *et al.*, 1999; Spreeuwenberg *et al.*, 2001).

As a result of this stress-driven inflammation, strategies to support intestinal homeostasis during weaning are vital. Among them, dietary supplementation with fermentable fibers like inulin-type fructans has gained attention for its prebiotic effects. Crude chicory, a natural source of inulin and bioactives, have been shown to increase the abundance of beneficial bacteria and modulate immune responses. Several studies have reported that inulin can reduce the expression of pro-inflammatory cytokines (IL-1β, IL-6, TNFα) in animal models, including pigs, mice, and chickens (Babu *et al.*, 2012; Taranu *et al.*, 2012; Shukla *et al.*, 2016; Li *et al.*, 2018). Chicory, in addition to its inulin content, contains compounds such as chlorogenic and chicoric acid, which further contribute to its immunomodulatory potential. These bioactives are known to suppress inflammatory pathways by modulating NFκB and MAPK signaling, downregulating genes like CASP3 and TNFα (Alharthi, 2023; Cavaglieri *et al.*, 2009; Wang *et al.*, 2020).

Over the years, various *in vitro* models have been employed to investigate the effects of bioactives fibers during digestion, absorption, fermentation, and their impact on the intestinal epithelium. The intestinal epithelium primarily consists of enterocytes, responsible for nutrient absorption and goblet cells, which produce, store, and secrete mucin glycoproteins—the key components of mucus (Noah *et al.,* 2011). As there is no commercially available colonic cell line of porcine origin, IPEC-J2 cells isolated from the jejunum of a neonatal unsuckled piglet (Berschneider, 1989) are commonly used. However, MUC2, the key gel-forming mucin, is undetectable by RT-PCR in IPEC-J2 cells, indicating insufficient mucus production and highlighting the limitations of this monoculture in replicating the *in vivo* environment (Schierack *et al.,* 2006; Støy *et al.,* 2013; Verhoeckx *et al.,* 2015; Zakrzewski *et al.,* 2013). Mucus acts as a crucial physical and chemical barrier, separating the epithelial cell layer from luminal contents and playing a significant role in intestinal permeability (Behrens *et al.,* 2001; Johansson *et al.,* 2008). The HT-29-MTX human cell line, known for its mucus-secreting properties, has proven to be a valuable model for assessing the impact of food compounds and bacteria on mucus production in the gut (Verhoeckx *et al.,* 2015). Currently, no commercially available mucus-producing cell line exists for piglets comparable to the HT-29-MTX line, making it impossible to develop a coculture model using IPEC-J2 akin to the Caco-2/HT-29 MTX coculture.

Given these limitations, human-derived cell lines provide a robust alternative due to the anatomical and functional similarity between the porcine and human GI tracts (Deglaire and Moughan, 2012). In this study, we utilized a triple co-culture model composed of absorptive Caco-2 cells, mucus-secreting HT-29-MTX cells, and U937 monocytes differentiated into macrophage-like cells. This system more accurately simulates the intestinal epithelial environment by incorporating nutrient absorption, mucus barrier dynamics, and immune signaling pathways. It enables simultaneous measurement of cell viability, permeability, cytokine secretion, and gene expression under controlled inflammatory conditions, such as those induced by lipopolysaccharide (LPS).

Building upon the findings from Chapter 4, where *in vitro* digestion and fermentation using feces of weaned piglet of inulin and crude chicory demonstrated distinct microbial and metabolic outcomes, this chapter aims to investigate the functional consequences of these microbial metabolites on the intestinal epithelium. Fermentation supernatants from digested/dialyzed samples were applied to the triple co-culture model pre-treated with LPS to simulate an inflamed intestinal state. This approach allows for the assessment of whether fermentation-derived metabolites from crude chicory or inulin offer greater support for epithelial barrier integrity and immunomodulation under stress conditions. Through this, we seek to bridge microbial changes with host responses, providing a more holistic understanding of how dietary fibers may protect the intestinal mucosa during weaning.

5.3. Material and Methods

5.3.1. Triple Cell Culture Setup (Caco-2/HT-29-MTX/U937)

The triple cell culture model was established by culturing Caco-2 and HT-29-MTX cells on the apical side and differentiated U937 (macrophages) in the basolateral compartment. Caco-2, HT-29-MTX, and U937 cells, obtained from the European Collection of Cell Cultures (Salisbury, UK), were maintained separately at 37 °C in a humidified atmosphere of 5% CO_2 (Incubator, Thermo Scientific, Marietta, USA). Caco-2 and HT-29-MTX cells were grown in Dulbecco's Modified Eagle Medium (DMEM), while U937 cells were cultured in Roswell Park Memorial Institute (RPMI) medium. Both media were supplemented with 10% heat-inactivated fetal bovine serum (Gibco, Thermo Fisher Scientific), 100 U/mL penicillin, 1 mg/mL streptomycin (PanBiotech GmbH), 2 mM L-Glutamine (PanBiotech GmbH) and anti-mycoplasma treatment (MycoZap^{TM}, Lonza). For Caco-2 and HT-29 cultures, the medium was refreshed every 7 days, and cells were subcultured upon reaching 90% confluency using trypsin-EDTA (PanBiotech GmbH). U937 suspension cells had their medium changed every 2 days. Passage numbers were maintained between 20-35 for Caco-2, 15-30 for HT-29-MTX, and 10-20 for U937.

To differentiate U937 cells into macrophages, 14 million cells were seeded into a T75 flask along with 8.1nM phorbol 12-myristate 13-acetate (PMA, Sigma-Aldrich) in complete RPMI medium and incubated for 48 h. Following this incubation, the PMA-containing medium was replaced with RPMI without antibiotics, and the cells were incubated at 37 °C, 5% CO_2 for an additional 3 days. Differentiated U937 macrophages adhered to both the surface of the flask and to each other, exhibiting distinct morphological changes.

For the triple co-culture, Caco-2 and HT-29-MTX cells were seeded onto 12-well plate inserts (3µm) (BD Falcon, Ref 353292; Sacco SrL, Cadorago, Como, Italy) at a density of 2×10^4 cells/cm², maintaining a 90:10 ratio. The cells were cultured for 21 days, with DMEM replaced every 2-3 days in

both the apical and basolateral compartments. Starting from day 16, the DMEM in both compartments was substituted with RPMI to accommodate U937 cells. On day 20, differentiated U937 macrophages were detached and added to the basolateral compartment at a density of 2×10^6 cells/well, completing the triple co-culture system.

After 24 h of introducing macrophages to the basolateral compartment, the apical side of the triple cell culture was pre-treated for 6 h with RPMI (non-stimulated) and LPS (50 µg/mL) to simulate inflammation typical of weaning conditions before piglets are exposed to bioactive treatments. Following this 6 h inflammation period, the media were replaced, in order to have same LPS concentration (50 µg/mL) in the apical compartment even after different treatments, and the cultures were divided into the following treatment groups from E2: RPMI (Non-stimulated), only LPS (Positive control), Dexamethasone (20 µM) and Indomethacin (100 µM) (Negative Control), Inu eq., Chi eq., F, F2I, and F2C. Basolateral samples were collected at 6, 9, and 24 h, centrifuged, and stored at -20 °C. RNA was extracted from the coculture cells after 24 h.

5.3.2. Cell Viability Assessment

Cell viability was assessed using the CCK-8 (Tebu-bio, Le Perray-en-Yvelines, France) kit to determine the optimal concentration for Caco-2/ HT-29-MTX coculture. The compound 2-(2-methoxy-4-nitrophenyl)-3-(4-nitrophenyl)-5-(2,4-disulfophenyl)-2H-tetrazolium, monosodium salt (WST-8) is reduced intracellularly by electron carriers via the catalytic action of cellular dehydrogenases, producing a soluble orange formazan product. The amount of formazan generated is directly proportional to the number of viable cells. To evaluate the cytotoxic effects of fermentation supernatant on the Caco-2, HT-29-MTX and Caco-2/HT-29-MTX, cells were seeded in 96-well plates at a density of 2×10^4 cells/cm² with a 90:10 ratio. After 5 days of culture, LPS (50 µg/mL) and fermentation supernatant from 4h and 12 h timepoint diluted in antibiotic and serum free RPMI (50, 25, 12.5, 6.25, 3.125 and 1.5625 % [v/v]) were added to the cells in triplicates and incubated for 24 h at 37°C in a 5% CO_2 incubator (Thermo Scientific, Marietta, USA). WST-8 was then added at a final concentration of 5%, followed by a 2 h incubation at 37°C in the dark. A non-stimulated well was included in each test series in triplicates. The concentration of reduced WST-8 (formazan) was measured at 450 nm using a SpectraMax® iD3 spectrophotometer (Molecular Devices, San José, USA), with blanks containing all reagents except the cells. Results were expressed as a percentage of viability relative to the non-stimulated cells.

5.3.3. Barrier Integrity Evaluation (TEER and LY Assay)

Transepithelial electrical resistance (TEER) was measured using an ohmmeter (MERSSTX01, Millipore Millicell; Billerica, MA, USA) to evaluate the integrity of the barrier formed by the co-culture. Measurements were taken at each medium change, every other day from the second week onwards. The TEER values were corrected by subtracting the background resistance, then multiplied by the surface area of the filter (0.9 cm²) to obtain final values in Ohms per square centimetre ($\Omega \cdot cm^2$). Prior to measurement, the electrode was disinfected in 70% ethanol for 5 minutes and rinsed with 0.1M NaCl solution (Sigma Aldrich-Merck).

The permeability of the intestinal barrier was assessed by measuring the paracellular flux of the fluorescent dye lucifer yellow (LY; Sigma-Aldrich) across a Caco-2/HT-29-MTX monolayer. Caco-2/HT-29-MTX cells (90:10 ratio; 2×10^4 cells/cm²), cultured on inserts for 20 days until fully differentiated, were then treated with LPS (50 µg/mL, Sigma-Aldrich) and fermented supernatants in the apical compartment for 24 h. After treatment, the apical media was replaced with 1 mL of RPMI media (or HBSS solution) containing 100 µM LY, and 2mL of fresh medium was added to the basolateral compartment. Then monolayers were incubated at 37°C in the dark under 5% CO_2 for 90 minutes. Samples (80 µL) were collected from the basolateral chamber every 15 minutes. The fluorescence of the samples was analysed alongside a standard curve with concentrations ranging from 0.1953 µM to 100 µM. To achieve this, 80 µL of each sample or standard dilution was added to a 96-well plate, and fluorescence was measured using a fluorescence microplate reader (Xenius, Safas, Monaco) at an excitation wavelength of 485 nm and an emission wavelength of 530 nm, with a detector voltage set to 600 V.

The LY concentrations obtained in the basolateral samples using the LY range are plotted as a function of time for each condition, thus allowing the determination of the average apparent permeability of the Caco-2 cell monolayer. Apparent permeability (P_{app}) is calculated using the formula below:

$$P_{app} = (dQ/dt) \times (V/(A*C_0)$$

where dQ is the change in LY concentration in the basolateral compartment (µM), dt is the change in transport time (s), giving dQ/dt as the permeability rate determined by the slope of the linear regression of LY concentration in the basolateral supernatant over time. V represents the volume of the basolateral compartment (mL), A is the surface area of the insert (cm²) and C_0 is the initial LY concentration in the apical compartment (µM).

5.3.4. Cytokine Quantification

Samples from the basolateral compartment were collected at 6, 9, and 24 h and diluted in various proportions for cytokines analysis. The production of IL8, IL1β, IL10, and TNFα was quantified using ELISA kits from RandD Systems® (Minneapolis, USA). IL8was measured using the Quantikine™ IL8kit (D8000C), comparing optical densities to a standard curve of 31.3 to 2,000 pg/mL. IL1β was assessed using the Quantikine™ IL1β kit (DLB50), with a standard curve ranging from of 3.9 to 250 pg/mL. IL10 levels were determined using the Quantikine™ IL10 kit (D1000B), with a range of 7.8 to 5,000 pg/mL. TNFα was quantified using the Quantikine™ TNFα kit (DTA00D), with a standard curve ranging from of 7.8 to 5,000 pg/mL. All measurements were performed using a SpectraMax® iD3 microplate reader set at 450 nm.

5.3.5. Gene Expression Analysis

After 24 h, the inserts were rinsed three times with cold PBS, followed by carefully excision for RNA extraction using the ReliaPrep™ RNA Cell Miniprep System (Promega Corporation, Madison, WI). RNA concentration was measured using a Nanodrop spectrophotometer (Thermo Fisher Scientific, Waltham, MA), and the RNA was subsequently reverse transcribed

into cDNA using the Reverse Transcription Master Mix (Fluidigm Corporation, South San Francisco, CA). High-throughput quantitative PCR (qPCR) was performed, employing intron-spanning primer pairs (Kulkarni *et al.,* 2024) designed with Primer-BLAST (NCBI), following the methodology described by (Uerlings *et al.,* 2021a). Primer validation was confirmed via agarose gel electrophoresis and melting curve analysis.

The qPCR assays were run in 48×48 dynamic array-integrated fluidic circuits (Standard BioTools Inc., South San Francisco, CA, USA) using the following cycling conditions: an initial denaturation step of 60 seconds at 95 °C, followed by 30 amplification cycles of 5 seconds at 96 °C and 20 seconds at 60 °C. Quantification cycles (Cq) were determined with Fluidigm real-time PCR analysis software (version 3.0.2). Housekeeping genes were evaluated for stability, and the three most stable genes across treatments were identified using NormFinder (Andersen *et al.,* 2004). The standard curve method was used to compute the relative gene expression level for each target and housekeeping gene tested, and the geometrical mean of the relative expression of the three housekeeping genes was used to standardize all the samples.

5.3.6. Statistical Analysis

In this study, one way ANOVA with |Dunnett or Tukey's multiple range test to determine significant differences among treatment means using SAS Enterprise Guide 7.4 (SAS Institute Inc, Cary, NC). The bars labelled by different letters indicating significant differences within each cytokine at specific timepoints. Significance thresholds were established as follows: *$p < 0.05$ (significant), **$p < 0.01$ (highly significant), and ***$p < 0.001$ (very highly significant) based on the ANOVA. For microbiota analyses at each timepoint, the Kruskal-Wallis test followed by Dunn's test was performed. To uncover potential relationships among treatment groups, Principal Component Analysis (PCA) was performed on cytokine and gene expression datasets to identify patterns. Pearson correlation coefficients (r) were calculated, and p-values were adjusted for multiple comparisons using the Bonferroni correction to ensure statistical rigor. All analyses were conducted using R version 4.4.2 with the following packages: RGCCA (v3.0.3), factoextra (v1.0.7), FactoMineR (v2.9), ggplot2 (v3.5.1), corrplot (v0.92), corr (v0.4.4), dplyr (v1.1.4), and stringr (v1.5.1).

5.4. Results

5.4.1. Effect of fermentation supernatant on cell viability

The viability of Caco-2, HT-29-MTX, and Caco-2/HT-29-MTX cells was assessed, as these cells represent the apical compartment of the tri-cell culture model and are in direct contact with the fermentation supernatant and LPS (50 µg/mL) **(Figure 35)**. In E1, no significant differences were observed between the Inu eq. and Chi eq. groups at any timepoint, with cell viability remaining above the 80% threshold across all concentrations tested. However, in E2, at the 4 h timepoint, cell viability was markedly low for the Chi eq., F, and F2C groups, but increased gradually, surpassing the 80% threshold at the 6.25% (v/v) concentration (C6.25) **(Figure 35A)**. For the fermentation supernatant at the 12 h timepoint **(Figure 35B)**, cell viability exceeded the threshold starting from the higher concentration (C25). No significant differences in viability were observed between treatments at concentrations from C25 to C1.5625 at the 12 h timepoint.

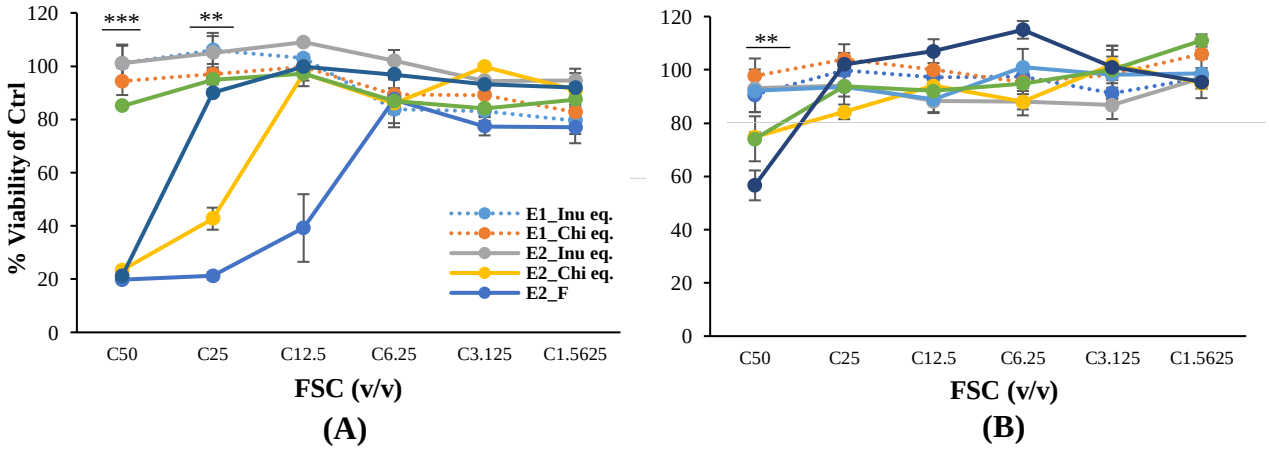

Figure 35. Impact of varying concentrations of Inu eq., Chi eq., F, F2I, and F2C along with LPS (50 µg/mL) on the viability of Caco-2/*HT-29*-MTX co-culture at (A) 4 *h* and (B) 12 *h* of E2.

Values are means ± SEM, n = 3 per treatment group. The dotted line at 80% viability represents the minimum threshold required to qualify for cytokine and gene expression studies. Statistical analysis ANOVA+ Tukey's test, * $p < 0.05$, ** $p < 0.01$, *** $p < 0.001$. No significant differences were found for E1, therefore significant differences mentioned are only for treatments within E2.

Notably, when the viability of HT-29-MTX cells was evaluated individually, it remained above the 80% threshold from C12.5 concentration across all treatment groups at the 12 h timepoint **(Figure 36D)**. In contrast, both Caco-2 and HT-29-MTX cells exhibited low viability at the 4 h timepoint when assessed individually **(Figure 36 A and B)**. Therefore, the use of fermentation supernatant from the 12 h timepoints at a concentration of 12.5% (v/v) was deemed more appropriate for evaluating immune modulation effects.

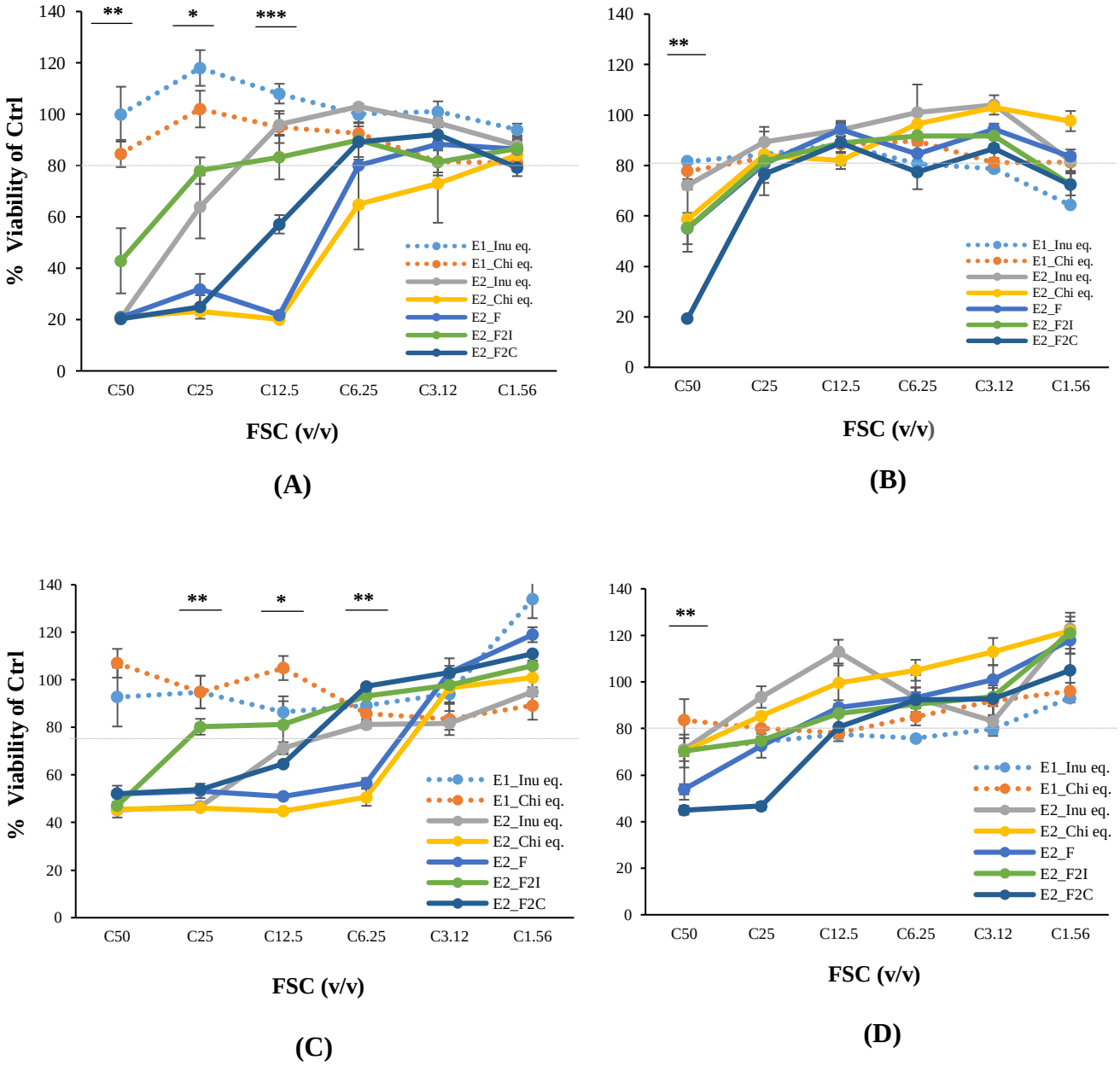

Figure 36. Impact of varying concentrations of Inu, Chi, F, F2I, and F2C along with LPS (50 µg/mL) on the viability of Caco-2 at 4 (A) and (B) 12 h and HT-29-MTX at (C) and 4 (D) 12 h.

Values are means ± SEM, n = 3 per treatment group. The dotted line at 80% viability represents the minimum threshold required to qualify for cytokine and gene expression studies. Statistical analysis ANOVA+ Tukey's test, * $p < 0.05$, ** $p < 0.01$, *** $p < 0.001$. No significant differences were found for E1, therefore significant differences mentioned are only for treatments within E2.

5.4.2. Effect of LPS and fermentation supernatant on permeability

The transepithelial electrical resistance (TEER) of the Caco-2/HT-29-MTX coculture reached values up to 806.6 ± 81.69 Ω.cm² by the end of the 20-day period. No significant differences were observed within the treatment groups on day 21 and 22 **(Figure 37)**.

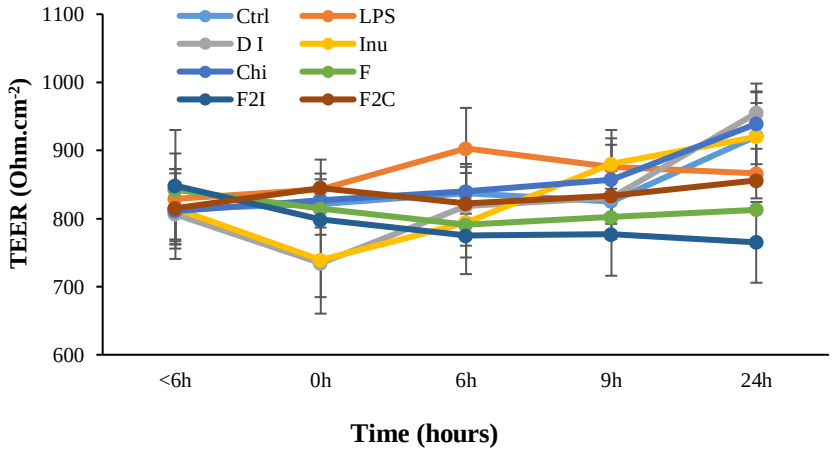

Figure 37. Measurement of the TEER on D20 at <6, 0, 6, 9 and 24 h through the Caco-2/HT-29-MTX co-culture for 24 h. Ctrl is non stimulated cells.
Values are means ± SEM, n = 9 per treatment group. The unlike a, b, c letters show the significance different ($p < 0.05$). Statistical analysis ANOVA+ Tukey's test, * $p < 0.05$, ** $p < 0.01$, *** $p < 0.001$.

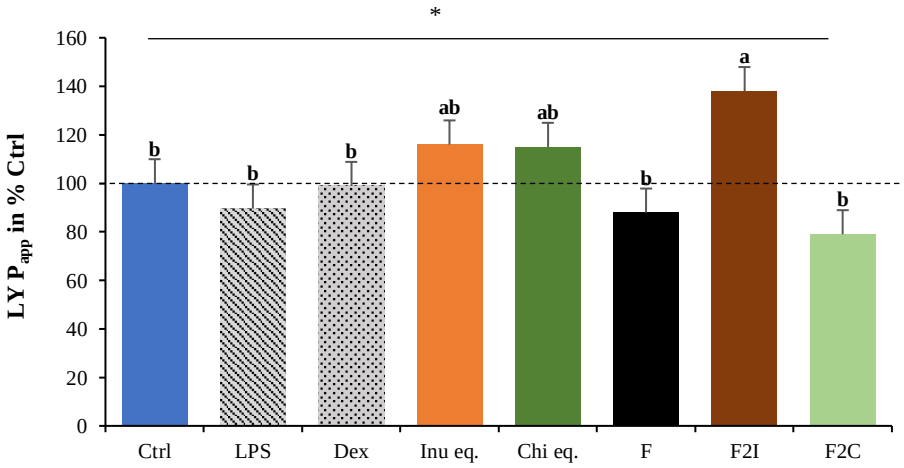

Figure 38. Measurement of permeability of LY from the apical compartment to the basolateral compartment through the Caco-2/HT-29-MTX co-culture monitored by spectrofluorescence at 24 h.
Ctrl represents non-stimulated cells. Collecting basolateral samples at different timepoints allowed for the calculation of the apparent permeability coefficient (P_{app}) of LY, which was normalized to the control (Ctrl P_{app}=2.4 x 10^{-6} ± 5.93 x 10^{-7} cm^{-1}). Values are means ± SEM (n = 9 per treatment group). Different letters (a, b, c) indicate significant differences ($p < 0.05$). One way ANOVA analysis (Tukey's test) was performed to calculate the significant differences, * $p < 0.05$.

The permeability coefficient (P_{app}) using LY was assessed after 24 h of treatment. Although no established reference value exists for this specific coculture model, we adopted a threshold of P_{app} = 4 x 10^{-6} cm/s, based on studies of LY permeability in colon tissues and existing coculture models

(Rozehnal *et al.,* 2012; Béduneau *et al.,* 2013; Ferraretto *et al.,* 2018; Verhoeckx *et al.,* 2015b). The P_{app} of LY was normalized to the non-stimulated control (NS Ctrl P_{app} = 2.4 x 10^{-6} ± 5.93 x 10^{-7} cm/s) **(Figure 38)**. Although all values were below the threshold, the F2I treatment showed a significantly higher P_{app} (138 ± 7.88%) compared to F2C (79 ± 0.756%) ($p < 0.05$). No significant differences were observed among the other treatments when compared to the Ctrl.

5.4.3. Effect of Inu and Chi on cytokines production

The effects of *in vitro* fermentation supernatant on LPS-stimulated cytokine production (IL1β, TNFα, IL10, and IL8) were quantified in the basolateral compartment, which contains macrophages. As expected, LPS-exposed cells showed significantly higher production of pro-inflammatory mediators, such as IL1β **(Figure 39A)**, TNFα **(Figure 39B)**, and IL8**(Figure 39D)** at 9 and 24 h compared to the non-stimulated control ($p < 0.01$). The production of these cytokines was significantly reduced ($p < 0.01$) at the corresponding timepoints when the cells were treated with the anti-inflammatory drugs (dexamethasone and indomethacin (D/I)) when compared to those cells that underwent LPS treatment. In contrast, IL10 production was significantly decreased in the LPS group compared to the D/I group at the 9 ($p < 0.01$) and 24 h ($p < 0.001$) timepoints.

At the 9 h timepoint, Chi eq. had significantly higher IL10 production than the LPS treatment alone ($p < 0.05$). At the 24 h timepoint, both Inu eq. ($p < 0.05$) and Chi eq. ($p < 0.01$) showed significantly higher IL10 production compared to the LPS treatment. F, F2I, and F2C exhibited significantly lower IL10 production ($p < 0.05$) than D/I group throughout the experiment. At 6 h, compared to the LPS treatment, Inu eq. and D/I group showed a decrease in IL1β production ($p < 0.05$), while only D/I showed a decrease in IL8 production. At the 9 and 24 h timepoints, like D/I group, Inu eq. and Chi eq. exhibited significantly lower IL1β, TNFα and IL8 (except at 9 h) levels than the LPS treatment ($p < 0.05$). However, at 24 h, F2I ($p < 0.001$) and F2C ($p < 0.05$) displayed significantly higher IL1β and TNFα than the D/I group. Notably, IL10 production was lower in F2I and F2C than in D/I group at 9 and 24 h ($p < 0.05$). Interestingly, at the 24 h timepoint, F2C exhibited lower levels of IL1β compared F2I, suggesting that F2C may have a stronger anti-inflammatory effect than F2I at later stages of inflammation.

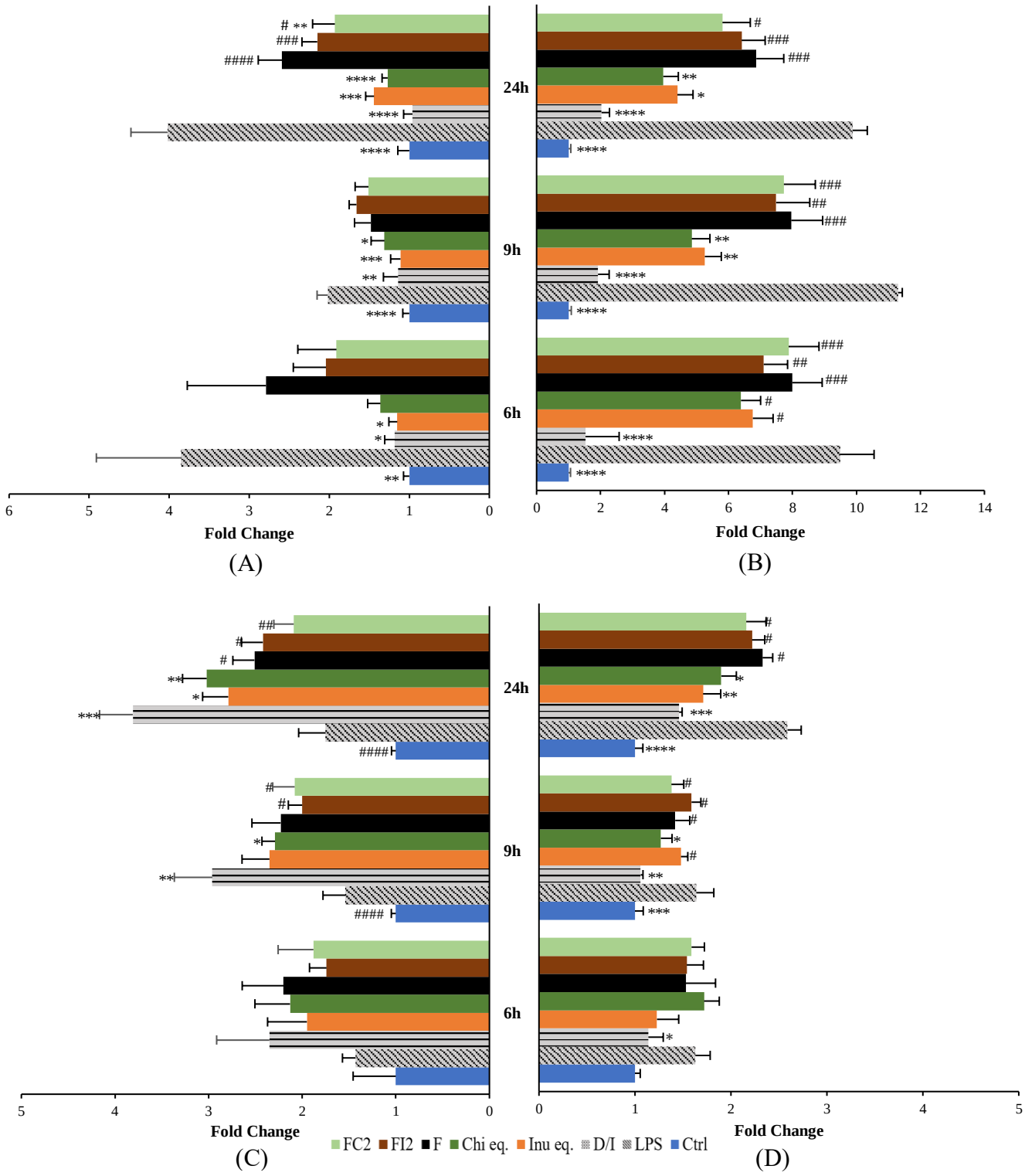

Figure 39. Effects of *in vitro* fermentation supernatant of E2 on the production of (A) IL1β, (B) TNFα, (C) IL10, and (D) IL8in the basolateral compartment of the tri-cell culture model (Caco-2/HT-29-MTX/U937) at 6, 9, and 24 h.

Cells were treated with LPS (50 µg/mL) to induce inflammation, starting 6 h prior to supernatant exposure, and continuing until the end of the experiment. The control (Ctrl) represents non-stimulated cells, while D/I serves as a negative control for inflammation inhibition ('D' = Dexamethasone, 20 µM; 'I' = Indomethacin, 100 µM). Cytokine levels are expressed as fold changes relative to non-stimulated Ctrl. Values are means (n=8) ± SEM. Statistical analysis was performed using one-way ANOVA and Dunnett's multiple comparisons test. * $p < 0.05$, ** $p < 0.01$, *** $p < 0.001$, using LPS; #$p < 0.05$; ## $p < 0.005$; ###$p < 0.001$ using D/I.

5.4.4. Gene Expression

The gene expression analysis was performed exclusively on the digested and dialyzed supernatant treated cells from apical side (E2) as shown in **Figure 40**. In the inflammation signalling pathway, *MAPK14* expression was significantly downregulated (adj. $p < 0.05$) in the Chi eq., F2C, and F2I groups compared to the LPS treatment, following a pattern like the D/I group. Inu eq. and Chi eq. also downregulated *MyD88* and *AKT1* expression in comparison with the LPS treatment, though to a lesser extent (adj. $p < 0.05$). Notably, Inu eq. led to a significant upregulation of the barrier integrity gene *JAMB* and *MUC1* compared to the LPS treatment, while Chi eq. showed a three-fold increase in *MUC2* expression (adj. $p < 0.01$). The pro-inflammatory genes *IL8* (adj. $p < 0.05$), *TNFα* (adj. $p < 0.01$) and *DEFB4α* (adj. $p < 0.05$) were significantly downregulated in the Inu eq. and Chi eq. groups relative to the LPS treatment. Interestingly, *TNFα* expression was also significantly downregulated in the F2C and F2I groups compared to the LPS treatment (adj. $p < 0.05$).

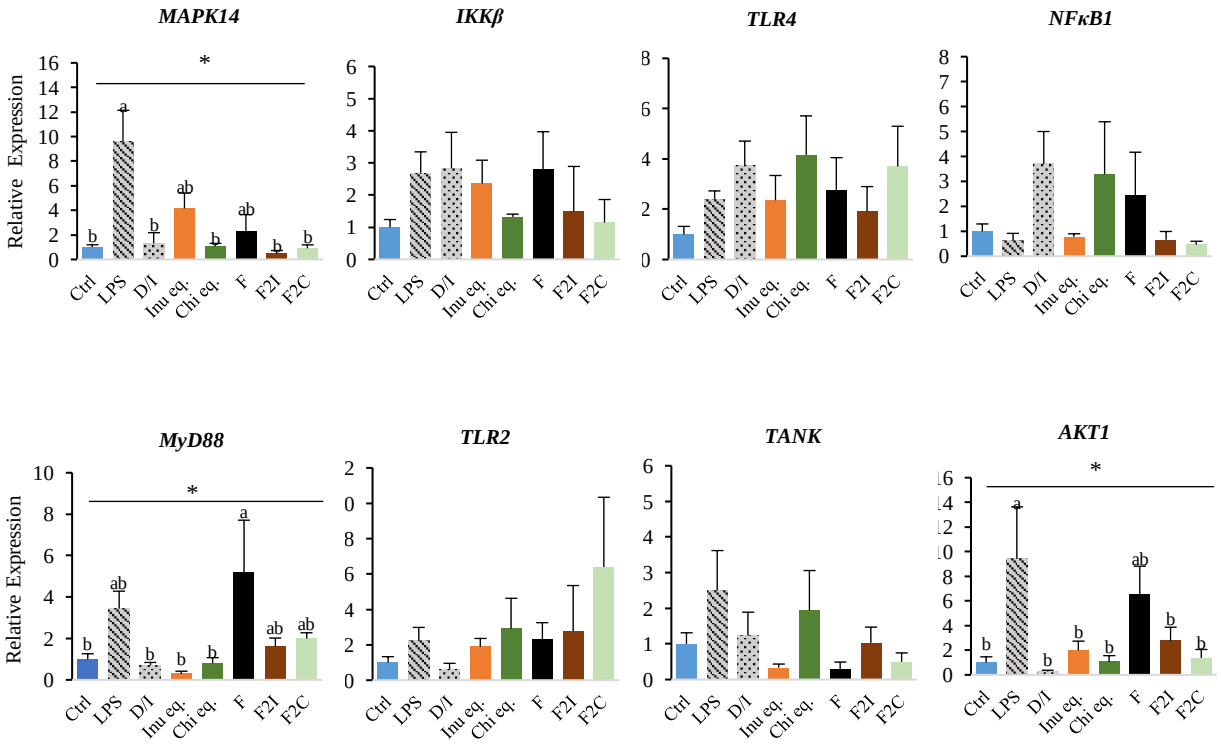

(A)

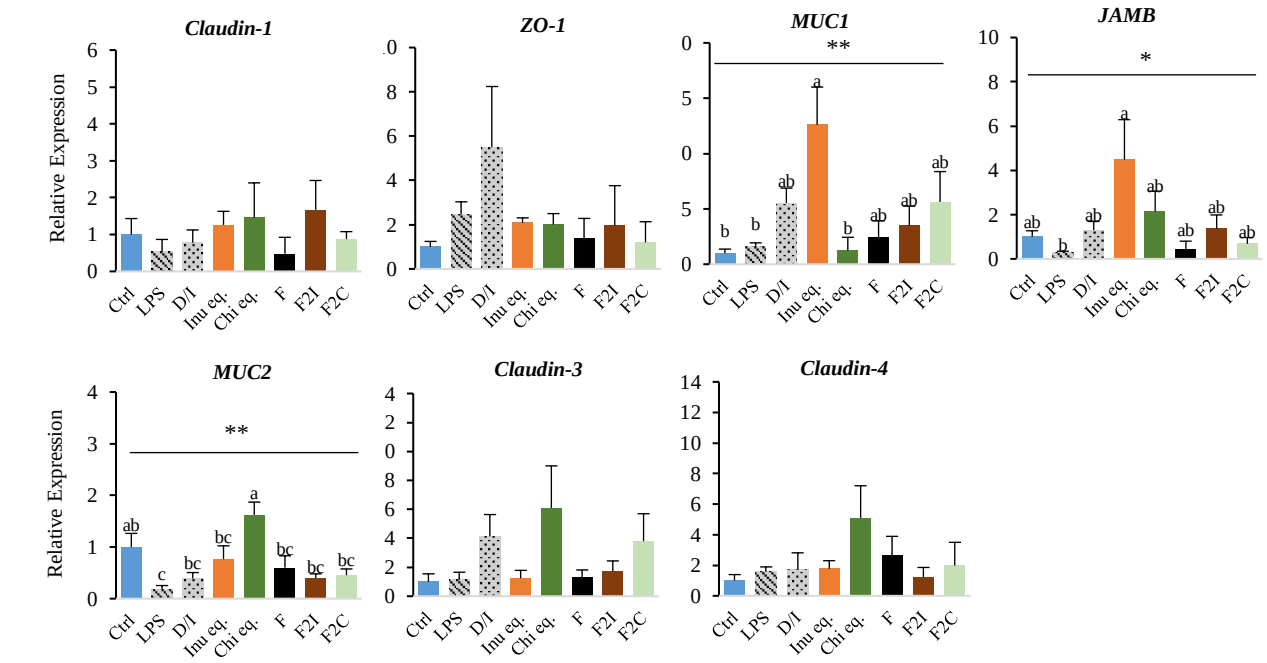

(B)

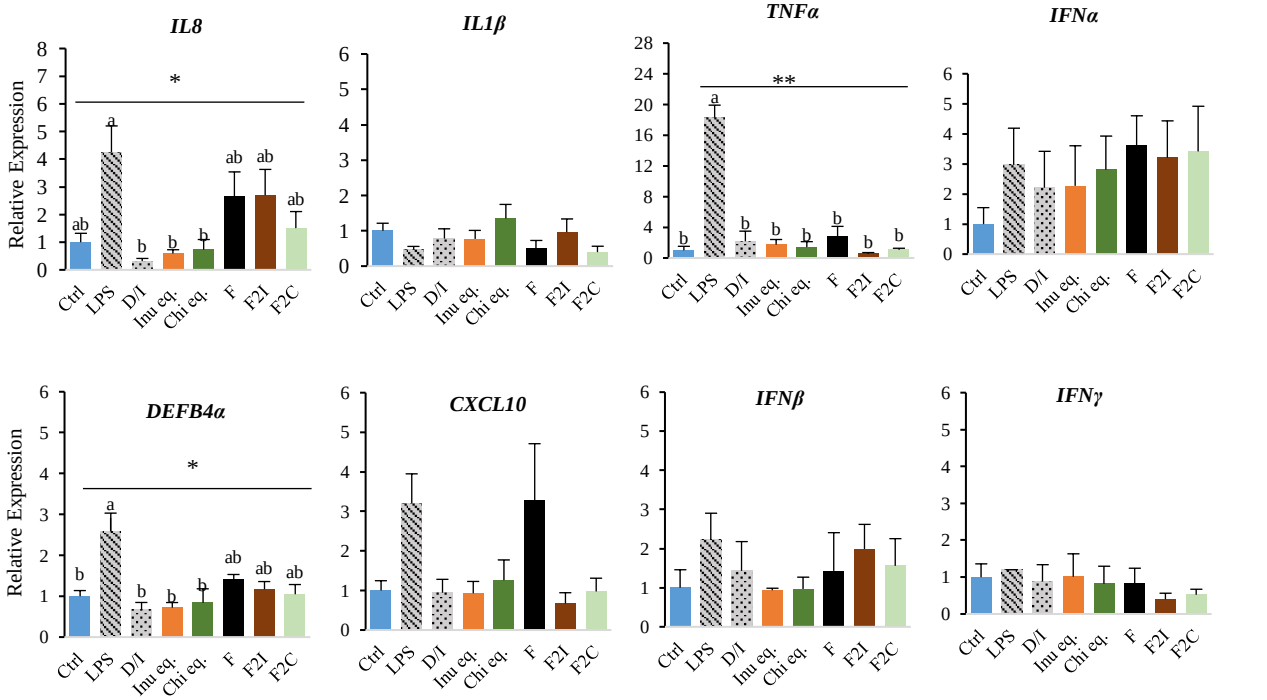

(C)

Figure 40. Effect of fermentation supernatant (E2) on expression of (A) Inflammation Signalling Pathway (B) Barrier Integrity and (C) Inflammatory Target genes as fold change relative to Ctrl.

Cells were treated with LPS (50 µg/mL) to induce inflammation, starting 6 h prior to supernatant exposure and continuing until the end of the experiment. The control (Ctrl) represents non-stimulated cells, while D/I serves as a positive control for inflammation inhibition (D/I = Dexamethasone, 20 µM; 'I' = Indomethacin, 100 µM). Values are means (n=9) ± SEM. Statistical analysis was performed using one way ANOVA followed by Tukey's test. Bars labelled with different letters indicate significant differences (* $p < 0.05$, ** $p < 0.01$).

5.4.5. Integration Analysis

The PCA biplot in the **Figure 41**, illustrates the relationships between treatment groups and cytokine expression. The first principal component (PC1), explaining 47.08% of the cytokine data variance, is primarily influenced by TNFα, IL1β, and IL10, which play a significant role in separating treatment groups such as Ctrl and LPS. In contrast, the second principal component (PC2), accounting for 25.48% of the variance, is dominated by IL8, which drives differentiation along this axis. Ctrl, D/I, and LPS are distinctly separated, reflecting divergent cytokine profiles, while Inu eq., and Chi eq. cluster close to the centre, showing overlapping responses. F, FI2, and FC2 are moderately distinct, with FC2 displaying tighter clustering after outlier removal. The biplot emphasizes the significant (adj.p < 0.01) pivotal roles of IL1β (r=0.939) and TNFα (r=0.932) in driving variability and treatment-specific cytokine expression patterns with respect to PC1.

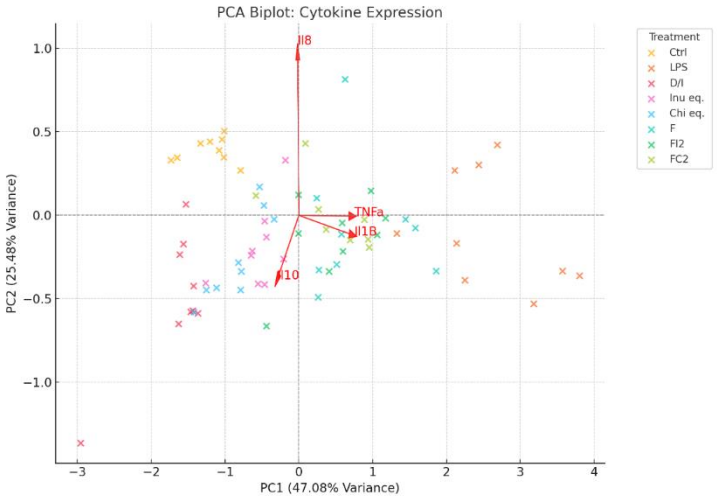

Figure 41. Principal Component Analysis (PCA) plots for cytokine expression. PCA plots (PC1 and PC2) with representation plots (Pearson correlation) for the variables IL8, TNFα, IL1β and IL10, in the cytokine expression block of the media collected from the basolateral side after 24 h of treatment exposure.

The PCA plot **(Figure 42)** for gene expression reveals distinct clustering among treatment groups. Ctrl, D/I, and LPS are clearly separated, indicating significant differences in gene expression profiles. However, D/I, Inu eq., and Chi eq. form partial clusters with some overlap, while FC2 shows moderate differentiation. The spread of data points reflects the variability in gene expression profiles between treatments. However, as shown in **Figure 42**, several genes were found to have significant positive or negative correlation with PC1.

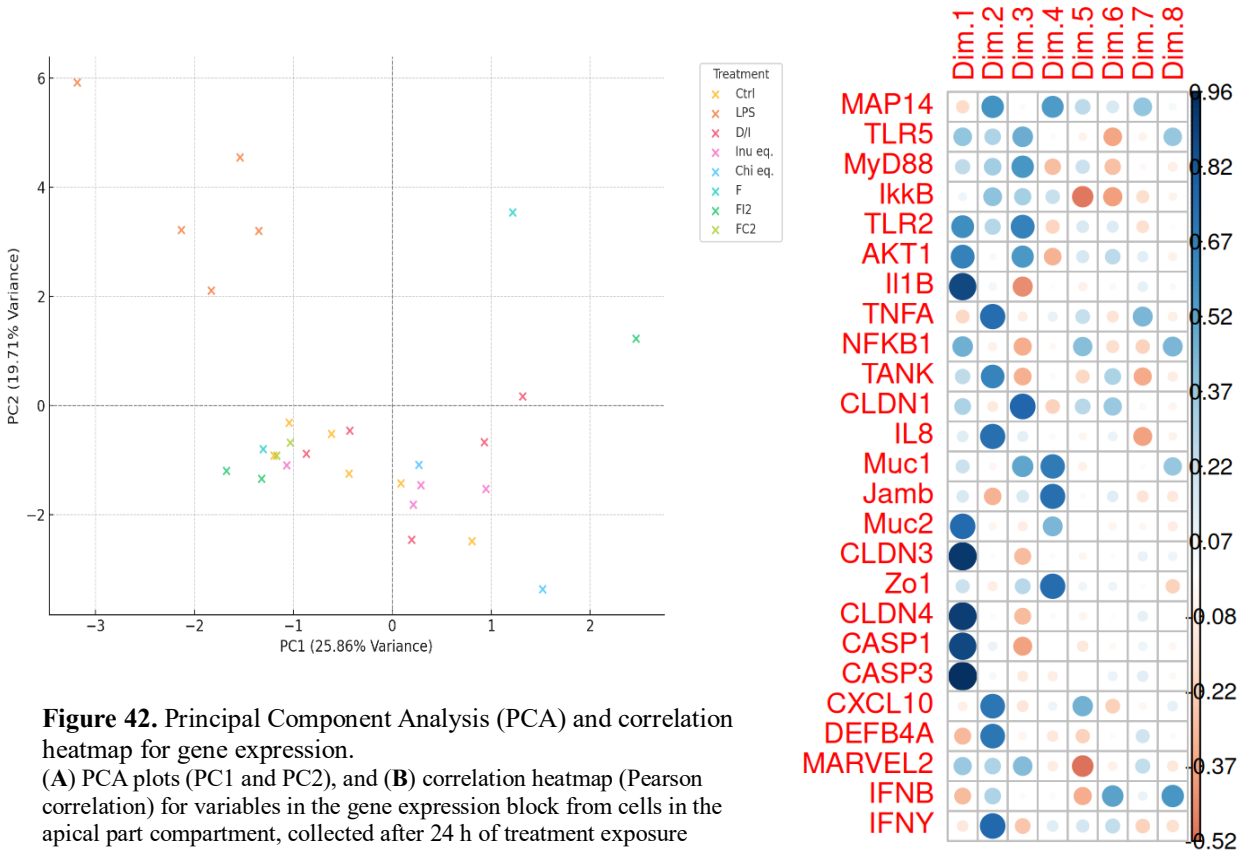

Figure 42. Principal Component Analysis (PCA) and correlation heatmap for gene expression.
(**A**) PCA plots (PC1 and PC2), and (**B**) correlation heatmap (Pearson correlation) for variables in the gene expression block from cells in the apical part compartment, collected after 24 h of treatment exposure

5.5. Discussion

This study introduced a multifaceted *in vitro* approach to assess the effects of Chi eq., Inu eq., and their combinations with feed (F, F2I, F2C) on colonic health in weaned piglets. By integrating *in vitro* digestion, dialysis, fermentation, and an advanced triple cell culture model, we aimed to simulate the complex interactions between dietary fibers, gut microbiota, and the intestinal epithelium under inflammatory conditions. This layered approach enabled us to move beyond microbiota composition and metabolite production, allowing functional validation of fermentation-derived effects on intestinal epithelial cells. Such a system is particularly valuable in the context of weaning, where barrier dysfunction and immune dysregulation are key challenges. Interestingly, the ND fermentation supernatant was not cytotoxic even at higher concentration (data not shown), which contrasts with the cytotoxicity observed in DD samples. These differences may be be due to traces of digestive components such as bile acids in DD supernatants which can influence cellular metabolism (Yi *et al.,* 2015). Despite dialysis, small bile acids may remain within the membrane due to their known ability to bind to dietary fibers, allowing them to bypass absorption in the small intestine (Capuano, 2017b; Phan *et al.,* 2015). ND samples, containing unprocessed substrates and higher simple sugar levels, prompt rapid, unbalanced microbial activity which fails to accurately simulate a digested diet. Therefore, due to the substantial effects of DD on gas production, microbial diversity, SCFA production, beneficial bacterial abundance, and their closer physiological relevance to *in vivo* condition unlike ND, we focused on DD fermentation samples for cell culture studies. A fermentation supernatant from 12 h timepoint, which showed better viability than the 4 h timepoint, was selected for cellular interactions under inflammatory conditions using LPS. Although C25 concentration supported coculture viability, individual viability assessments revealed that HT-29-MTX cells thrived only below C12.5, underscoring the need for individual cell viability testing.

In our study, we subjected the co-culture of Caco-2 and HT-29-MTX on the apical side to fermentation supernatant, while differentiated U937 macrophages were in close contact on the basolateral side. We ensured, through TEER and LY tests, that the membrane remained intact, preventing direct contact between the supernatant and macrophages. As such, this setup closely replicates the gut's inner wall, including its mucus-covered epithelial layer. We used 90:10 ratio of Caco-2 and HT-29-MTX, based on preliminary studies in the lab as well as existing literature; which as shown that is the most physiologically relevant ratio to mimic the intestinal barrier, maintaining a monolayer of cells while preserving a correct proportion and distribution of mucus (Chen *et al.,* 2010; Araújo and Sarmento, 2013). The coculture was maintained for 21 days, a timeframe shown by other studies to allow for full differentiation of intestinal cells, and confirmed by alkaline phosphatase activity (Kulthong *et al.,* 2020). Additionally, we used dexamethasone because glucocorticoids are commonly employed in inflammation treatment due to their anti-inflammatory effects, particularly through the reduction of pro-inflammatory cytokine gene expression (Medzhitov, 2010).

TEER values for Caco-2 monocultures and cocultures vary widely across studies due to differences in cell clones, passage numbers, multilayers, media, growth factors, and culture conditions, with reported values from 160 to 900 $\Omega \cdot cm^2$ (Araújo and Sarmento, 2013; Béduneau *et al.,* 2014a; Reale *et al.,* 2021; Schimpel *et al.,* 2014; Vital *et al.,* 2024). Our 20-day TEER measurements align closely with those from Ude *et al.* (2017), where Caco-2/HT-29-MTX cocultures at a 90:10 ratio reached approximately 861 $\Omega \cdot cm^2$ after 21 days. We found no significant TEER difference among treatments,

consistent with Kämpfer *et al.* (2017), who observed no TEER change with LPS treatment. However, propionate and acetate have been shown to increase TEER and reduce LY permeability in rat caecum, T84 human carcinoma cells, and Caco-2 monolayers (Suzuki *et al.,* 2008). As noted, TEER is widely used to assess permeability, but its accuracy is influenced by multiple experimental variables (e.g., temperature, medium formulation, cell passage), making inter-study comparisons challenging. To verify permeability changes beyond TEER measurements, additional methods such as LY assay can be helpful for evaluating integrity (Haddad *et al.,* 2023). Consequently, we performed the LY assay to further confirm tight junction efficacy. P_{app} is used to assess passive drug absorption by measuring permeability across the Caco-2/HT-29-MTX coculture. We applied a P_{app} threshold of 4×10^{-6} cm·s^{-1}, referencing LY permeability studies in colon tissues and similar cocultures (Rozehnal *et al.,* 2012; Béduneau *et al.,* 2013; Ferraretto *et al.,* 2018). While Caco-2 monolayers have a P_{app} threshold below 1×10^{-6}, HT-29-MTX cells are more porous so this value would not be ideal for the coculture (Béduneau *et al.,* 2014b; Fleury *et al.,* 2022). Since the values were below our threshold, this indicates that the membrane was intact, supporting our TEER observations. However, a significantly lower P_{app} value was recorded for F2C than F2I indicating lower permeability for F2C than F2I. This might be associated with higher butyrate levels in the fermentation supernatant of F2C. Butyrate supports intestinal epithelial integrity under stress by promoting tight junction reassembly and TEER restoration, reducing LPS-induced permeability, and inhibiting NLRP3 inflammasome activation while stimulating mucus production (Nielsen *et al.,* 2018; Siddiqui and Cresci, 2021; Elhaseen *et al.,* 2013; Zong *et al.,* 2024b; Rivière *et al.,* 2016). Dried chicory root has been found to play a protective role in reversing gut permeability induced by an apical stressor (Pham *et al.,* 2018). *Lactobacillus* which had 2-3 times higher abundance in Chi eq. and F2C than in Inu eq. and F2I, is known for its role in enhancing gut health by upregulating barrier integrity genes, reducing pathogen load, and producing antimicrobial peptides (Lobionda *et al.,* 2019). Lower *Lactobacillus* levels are often associated with a weakened intestinal barrier (Xu, 2014).

We prioritized the assessment of cytokines from the basolateral side of the media because, in preliminary tests, cytokine levels were undetectable or low on the apical side, which was in contact with the Caco-2/HT-29-MTX coculture, while they were significantly higher on the basolateral side, where macrophages were present. This pattern was also observed in previous studies (Kämpfer *et al.,* 2017; Grouls *et al.,* 2022; Leonard *et al.,* 2010; Matos *et al.,* 2024). These findings likely reflect the impact of stimulus placement and concentration, influenced by the distinct distribution of membrane receptors on the apical and basolateral surfaces of polarized epithelial cells. In this study, we applied LPS, a glycolipid from Gram-negative bacteria to the apical side of the Caco-2/HT-29-MTX cells to mimic intestinal lumen infection, consistent with how pathogenic bacteria deposit LPS on the intestinal epithelium. This process may lead to internalization, recycling, storage, or transcytosis of LPS to the basolateral side (Cario *et al.,* 2000), where it can activate the NFκB, MAPK, PI3K/Akt, and JAK-STAT pathways, resulting in cytokine production, such as TNFα, IL6, IL8, and IL1β (Meng *et al.,* 2024; Gupta *et al.,* 2010; Verhoeckx *et al.,* 2015). Both Chi eq. and Inu eq. had a positive impact on reducing pro-inflammatory IL8, a common biomarker of inflammation, after 24 hr (Yoshimura, 2015). Chi eq. demonstrated a more pronounced effect, showing this reduction at an earlier timepoint of 9 h. This pattern was also reflected in IL8 gene expression in the apical region of the coculture, with similar results observed for Chi eq. and Inu eq. Furthermore, in our study, IL8 production was positively correlated with other cytokines, such as TNFα and IL1β, possibly through NFκB and PI3K/Akt pathway activation, which is also supported by several studies (Osawa *et al.,* 2002; Leonard *et al.,* 2010; Lee *et*

al., 2005). The reduction in IL8 and TNFα levels may also relate to increases in beneficial bacteria, such as *Bifidobacteria* and *Lactobacilli*, which are negatively correlated with these cytokines (Li *et al.,* 2021; Liu *et al.,* 2016a). Notably, Bacteroidota abundance was lower in F2C than in F2I at both timepoints, suggesting a possible anti-inflammatory effect. A decreased Firmicutes/Bacteroidota (F/B) ratio is commonly associated with dysbiosis and inflammation. Additionally, Bacteroidota levels tend to be elevated in inflammatory bowel disease, where they contribute to disease progression (Stojanov *et al.,* 2020). Unclassified *Lachnospiraceae* which was abundant at 4 h in the DD Inu eq. group and at 12 h in the DD Chi eq. group, is a major butyrate producer and can convert lactate to butyrate. Its decrease is linked with inflammation (Lobionda *et al.,* 2019; Louis and Flint, 2009).

Chi eq. and Inu eq. demonstrated a TNFα lowering effect at both cytokine and gene expression level, whereas F2C and F2I showed an effect only at the gene expression level. TNFα activation on the apical side can initiate several signalling pathways, ultimately activating transcription factors like NFκB (Liu *et al.,* 2017). Increased levels of *Lactobacillus* (2-3 times higher abundance in Chi eq.), *Bifidobacterium* (higher in Chi eq.), *Holdemanella*, and *Fecalibacterium* (higher in Inu eq.) may also help modulate cytokine expression, favouring an anti-inflammatory profile (Sun *et al.,* 2016; Wan *et al.,* 2019; Schirmer *et al.,* 2016). The presence of *Bifidobacterium*, found in higher amounts in Chi eq. and F2C, aligns with studies showing that inulin boosts *Lactobacillus* and *Bifidobacterium* levels while reducing inflammation by downregulating TNFα (Hiel *et al.,* 2020; Hino *et al.,* 2011).

Moreover, Chen *et al.,* (2019) found that insoluble dietary fibers and a mixed dietary fiber diet (0.5% insoluble + 0.5% soluble fiber) decreased TNFα expression significantly ($p < 0.05$). This effect may be further enhanced by Chi bioactives such as caffeic acid, which is known for its antimicrobial and anti-inflammatory properties in macrophages by inhibiting the NFκB-dependent production of nitrite, TNFα, and prostaglandin E2 (PGE2) (Sorgi *et al.,* 2021). Additionally, Chi supplementation in mice has been shown to reduce TNFα, IL1β, and IL8 levels, with fructose, chlorogenic acid, and STLs as potential bio active compounds. Chlorogenic acid and STLs appeared to affect IL1β and IL8 levels the most, while fructose may be responsible for TNFα reduction (Pouille *et al.,* 2022a). IL10 is crucial for T_{reg} cells' anti-inflammatory effects (Round and Mazmanian, 2010). In our study, Inu eq. and Chi eq. treatments showed significantly higher IL10 production compared to the LPS group, highlighting their anti-inflammatory action. Chi eq. demonstrated a stronger effect at both 9 and 24 hr, suggesting sustained impact. Our results also connect with studies showing that *Lactobacillus* induces IL10 in T_{regs} (Jang *et al.,* 2019; Liu *et al.,* 2012), as the microbial changes in our treatments may support this IL10 elevation. Long-chain inulin-type fructans can promote $CD25^+$ $Foxp3^+$ $CD4^+$ T_{reg} cells and reduce $IL17A^+$ Th17 cells, thus suppressing inflammation (Chen *et al.,* 2017). Additionally, acetate's role in promoting IL10-producing B10 cells (Daïen *et al.,* 2021) and the effect of inulin (90%) on enhancing LPS-induced IL10 (Liu *et al.,* 2016; Pham *et al.,* 2018) support our findings that both Inu eq. and Chi eq. foster an anti-inflammatory response, comparable to other immune-modulating interventions. The effect on the release of TNFα, IL1β, and IL6, as well as IL10 may also be explained by the lower gene expression of MAPK14 (Qian *et al.,* 2015; Jia *et al.,* 2020). However, Uerlings *et al.* (2020) did not find a significant change in the regulation of pro-inflammatory cytokines (IL6, IL8, IL18) from chicory root supernatant, which was also the case in our study. Our slight, though not significant AKT1 downregulation with Chi eq. might be influenced by other Chi bioactives, as studies on chicory pulp

without inulin have also shown activation of pro-apoptotic targets *via* the PI3K-AKT pathway, indicated by reduced AKT1 expression (Uerlings *et al.,* 2020; Luo, 2005).

Our results showed a significant increase in MUC1 with Inu eq. and MUC2 with Chi eq., consistent with findings by Uerlings *et al.,* (2020) who observed similar effects on MUC1, Claudin-1, and Claudin-3 following exposure to inulin fermentation supernatant. The elevated MUC2 expression may relate to the combined effects of insoluble and soluble fibers (Chen *et al.,* 2019). Among the mucins secreted, MUC2 is typically the most abundant, though MUC3 and MUC5AC are also produced during parasitic or bacterial infections but we did not study them here (Haddad *et al.,* 2023). This also aligns with findings from Pham *et al.* (2018), where inulin and dried chicory root fiber supplementation restored gut barrier integrity in a HT-29-MTX cell model, likely due to butyrate (Pham *et al.,* 2018).

One limitation of our study is the potential loss of certain bioactive compounds during dialysis, although not all dialyzable compounds are entirely removed (absorbed). The unidirectional movement of the dialysis membrane in water led to the settling of digesta, which may have hindered the diffusion of smaller molecules. Another challenge is integrating gut microbiota with cell cultures, as differences in media composition and contamination risks complicate host-microbiota interactions, often limiting studies to short-term treatments. Additionally, the use of tumor-derived cell lines may influence responses to nutrients or stimuli, as these cells have altered glycosylation and proliferation behaviours (Brooks *et al.,* 2008). However, interestingly, our findings align well with several *in vivo* studies linking inulin and chicory bioactives with reduced pro-inflammatory cytokine expression and strengthened epithelial barrier function through microbial and signalling pathway modulation. Chi eq. shows greater effects, likely due to the bioactives bound to fiber, which remain intact during dialysis. Cellulose strongly binds to phenolic acids, possibly due to reduced electrostatic repulsion. These interactions are significant, as they facilitate the transport of certain bioactives to the lower gut, where they become available to microbiota and extend their effects beyond those of inulin (Capuano, 2017b; Phan *et al.,* 2015; Saura-Calixto, 2011; Crozier *et al.,* 2010).

5.6. Conclusion

This study applied a physiologically relevant triple cell culture model to evaluate the effects of fermentation supernatants from inulin and crude chicory on intestinal epithelial function under inflammatory conditions. Both Inu eq. and Chi eq. treatments significantly reduced (4-8-fold) key pro-inflammatory cytokines (IL1β, IL8, TNFα) and downregulated associated signalling genes (MAPK14, MyD88, AKT1), indicating robust anti-inflammatory activity. Notably, Chi eq. demonstrated stronger enhancement of mucus-related barrier function, with a 3-fold increase in MUC2 expression, while Inu eq. more effectively upregulated MUC1 and JAMB. Among feed-associated treatments, F2C outperformed F2I in reducing (18-20%) permeability and modulating inflammatory markers, highlighting the continued benefit of chicory even within a complex matrix. Taken together, these results suggest that fermentation-derived metabolites from crude chicory may offer greater potential than purified inulin in supporting epithelial integrity and immune modulation during weaning. This suggests that Chi may have a slightly more potent effect than Inu for promoting gut health and regulating inflammation.

6

General Discussion and Conclusion

6.1. General revision and objectives

The GI tract plays a vital role in piglet health, especially during the stressful weaning transition, which often leads to reduced feed intake, weight loss, and diarrhoea, compromising gut health and growth. This thesis effectively tackled these challenges through two complementary objectives. The first objective investigated the comparative effects of inulin and crude chicory flour on the intestinal health of weaning piglets, with a focus on permeability, inflammation, and microbiota composition. Special emphasis was placed on understanding if its only inulin or also other bioactive compounds in chicory which can contribute to reducing weaning-associated disturbances. The second objective focused on the development and integration of innovative *in vitro* methods, combining digestion, absorption, and fermentation with advanced cell culture models to simulate the intestinal environment. This approach aimed to reduce reliance on animal experimentation while ensuring physiological relevance and comparability to *in vivo* systems.

6.2. Inulin Vs Crude Chicory?

6.2.1. *In vivo*

We conducted two *in vivo* experiments to evaluate the impact of pure inulin (INU) and crude chicory (CHI) on gut health in weaning piglets. The first experiment utilized a low dosage of inulin based on a wide variation in doses reported in the literature, which yielded limited effects specifically on zootechnical parameters. In the second experiment (E2), we doubled the inulin dosage to better understand its impact, while ensuring that the inulin content between the INU and CHI treatments was equated.

A slightly lower Average Daily Feed Intake (ADFI) was observed in the CHI group during the initial two weeks of E2. Importantly, this did not affect the Average Daily Gain (ADG). By W3 of E2, however, CHI and INU supplementation resulted in significantly higher villus height and villus-to-crypt ratio in the ileum compared to the Ctrl, with CHI surpassing INU in villus height. Neither treatment significantly improved histomorphological parameters during the first two weeks, which may reflect the more gradual mode of action associated with bioactives, as opposed to the rapid anti-inflammatory or antimicrobial effects commonly seen with antibiotics or zinc oxide (ZnO) (Zhu *et al.,* 2016). Regarding permeability, by W3 CHI supplementation showed a non-significant trend toward reducing Lactulose: Mannitol ($p=0.057$) but achieved a remarkable 50% reduction in plasma lactulose concentration. Both CHI and INU treatments similarly decreased plasma D-xylose levels. Using a cocktail of sugars, lactulose, mannitol, and D-xylose, for a more comprehensive and reliable assessment of intestinal permeability. This approach was used as it minimizes the influence of individual metabolic pathways, which could confound measurements when relying on a single or limited set of permeability markers.

INU alone significantly elevated total SCFA concentrations in W1, showcasing its potent prebiotic effect. However, CHI had caught up by W3, illustrating again the gradual working mechanism of CHO. Interestingly, CHI demonstrated a more pronounced impact on gut microbiota composition, particularly in W3. CHI promoted the growth of health-benefiting genera while reducing harmful taxa such as shown in **Figure 43**. CHI caused a significant 8- to 10-fold reduction of *Streptococcus*, mostly due to bioactives chicoric acid, phenolics and sesquiterpene lactones.

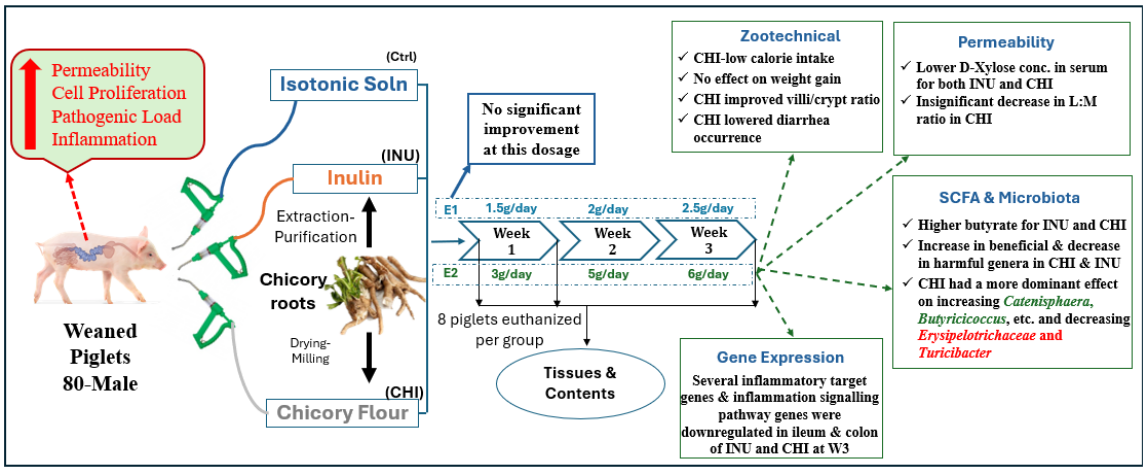

Figure 43. Schematic representation of *in vivo* experimentation setup and main results.

In the ileum and colon, both CHI and INU downregulated key inflammatory target genes (e.g., CXCL10, IL18, TNFα, MyD88, and NFκB1). RGCCA analysis confirmed a significant negative correlation between butyrate concentrations and inflammatory gene expression in the ileum (e.g., Il18, CXCL10) and colon (e.g., NFκB1, CASP1). The enhanced villus morphology, coupled with reduced inflammation, underscores the interplay between SCFA production, gut health, and host response. Additionally, RGCCA analysis demonstrated a positive correlation between ileum villus width (r=0.761) and colon butyrate concentrations, further supporting the role of SCFA in enhancing gut morphology. The elevated concentrations of lactate and SCFAs observed in the intestinal contents are most likely attributed to enhanced microbial fermentation activity rather than impaired epithelial absorption. This conclusion is supported by the upregulation of gut integrity-related genes, the proliferation-stimulating effects of fermentation supernatants *in vitro*, and the consistency of SCFA levels with previous studies. Together, these findings suggest that intestinal absorption mechanisms remained functional, while microbial production of beneficial metabolites was upregulated, reflecting an overall improvement in gut health. While inulin has long been recognised for its prebiotic properties, our findings suggest that crude chicory, with its diverse bioactive compounds, may offer superior benefits and cost-effective intervention for improving gut health in weaning piglets.

6.2.2. In vitro

The increasing scrutiny of animal use in research underscores the need for robust *in vitro* methods that closely mimic *in vivo* conditions, particularly for GI tract. Digestion and absorption are important processes in the GI tract of weaning piglets, yet our literature review highlighted inconsistencies in various *in vitro* studies regarding these steps and raosed questions about their usefulness in use of these steps prior to fermentation when evaluating the effects of bioactives on piglet gut health. To address this, we investigated the influence of *in vitro* digestion and absorption on fermentation patterns. Furthermore, we connected these processes to advanced triple cell culture model, thus creating, a more physiologically relevant system to evaluate the efficacy of crude chicory and inulin. Recognizing the similarity between pig's GI tract to the human GI system we used a complex cellular model (Caco-2/HT-29-MTX/U937) based on human origin cells. This approach aimed to bridge gaps, such as the lack of mucus secretion in observed commonly used IPEC-J2 cells.

Chi eq. demonstrated slower and more prolonged fermentation compared to Inu eq., producing significantly less gas (R_{max} and A value). This might be due to Chi eq.'s higher ADF/NDF content, which slows down

fermentation rates. Such slower fermentation can also be critical as it ensures the gradual release of fermentation products like SCFAs, allowing a sustained impact on colonic health. Chi eq. produced significantly higher butyrate at 4 hours in digested and dialyzed (DD) samples, but levels becoming comparable to Inu eq. at 24 hours. However, F2C produced more butyrate than F2I at 12 hours, showing the effect of inclusion of feed on F2I and F2C that were not observed in isolated Chi eq. and Inu eq. treatments. Thus, our observations question the practice of excluding feed when testing bioactives, as done in various studies. We also proved that when gas kinetics and SCFA datasets were correlated, Inu eq. and F2I displayed a positive correlation towards gas kinetics but showed a negative correlation with SCFA production. This demonstrates that higher gas production does not necessarily indicates higher SCFAs production.

Chi eq. had a more pronounced effect on microbial diversity and composition. A- diversity was higher for Chi eq. treatments compared to Inu eq. while β- diversity analysis showed significant treatment-specific clustering, indicating distinct microbial community structures. A decrease in the abundance of Firmicutes and a corresponding increase in Bacteroidota were observed after 12 h of fermentation compared to 4 h indicating timely sharp changes in microbiota abundances in static *in vitro* models. Chi eq. increased the abundance of several beneficial genera such as *Lactobacillus*, *Bifidobacterium*, and *Butyricicoccus*, which are known to promote gut health. This microbial modulation is critical, as it demonstrates Chi eq.'s ability to shift the microbiota composition in favour of a healthier gut environment. The Inu eq. treatment was also found to show some positive effects on beneficial microbiota and negative effects on harmful bacteria in general. The microbiota findings presented in this chapter are physiologically relevant because many of the observed taxonomic shifts are functionally linked to beneficial fermentation patterns and gut health in the context of weaning. For example, increased abundance of *Lactobacillus*, *Bifidobacterium*, and *Butyricicoccus*—particularly in chicory-treated groups—is associated with enhanced SCFA production, modulation of pH, and suppression of pathobionts, all of which support gut barrier stability *in vivo* (Kiernan *et al.,* 2023a; Xing *et al.,* 2020). Similarly, higher microbial α-diversity has been repeatedly linked to ecosystem resilience and improved resistance to post-weaning dysbiosis (Hodgkinson *et al.,* 2023). Additionally, the enrichment of acetate- and lactate-producing taxa, alongside known butyrate producers like *Ruminococcus* and unclassified *Lachnospiraceae*, suggests that chicory may foster cross-feeding networks that promote epithelial-supporting metabolites such as butyrate (Lobionda *et al.,* 2019). These changes provide a mechanistic basis for predicting how dietary fibres modulate host intestinal function—further explored in the following chapter using an epithelial cell model.

The fermentation supernatant at the 12-h timepoint demonstrated cell viability exceeding the 80% threshold for the triple cell co-culture starting at the higher concentration (C25). However, when HT-29-MTX cells were evaluated individually, viability was above 80% only at or below the concentration C12.5 across all treatment groups at the 12-h timepoint. This observation highlights the importance of viability testing of the individual cell when it's a multiple cell culture model. Based on these findings, fermentation supernatant from the 12-h timepoint at a concentration of 12.5% (v/v) was selected as the optimal condition for evaluating immune modulation effects.

The triple cell culture model, developed with a physiologically relevant 90:10 Caco-2/HT-29-MTX ratio, achieved optimum transepithelial electrical resistance (TEER ~806 $\Omega \cdot cm^2$) by 20 days, indicating an intact intestinal barrier. Using Lucifer Yellow (LY), we confirmed that the permeability coefficient (P_{app}) remained below the threshold of 4×10^{-6} $cm \cdot s^{-1}$, indicating an intact barrier. However, F2I showed slightly higher permeability than F2C. Both Chi eq. and Inu eq. treatments effectively reduced LPS-induced pro-inflammatory cytokines (IL1β, TNFα, IL8) and inflammatory pathway genes (*MAPK14*, *MyD88*, *AKT1*, $p < 0.05$). Notably,

CHI displayed a stronger anti-inflammatory effect, including a threefold upregulation of *MUC2*, which enhances mucus production and strengthens the epithelial defence barrier against pathogens. INU, on the other hand, increased *JAMB* expression, supporting tight junction integrity. Among feed treatments, F2C outperformed F2I in reducing intestinal permeability and inflammation, underscoring the importance of incorporating bioactives with feed for more physiologically relevant outcomes. PCA biplots of cytokine expression showed that crude chicory and inulin treatments clustered closely, reflecting overlapping yet distinct anti-inflammatory responses. The biplot emphasized the significant pivotal roles of IL1β (r=0.939) and TNFα (r=0.932) in driving variability and treatment-specific cytokine expression patterns. The integrated approach of combining digestion, absorption, and fermentation with a triple cell culture model provided a more physiologically relevant and comprehensive system for evaluating bioactives, bridging the gap between *in vitro* and *in vivo* studies.

6.3. Effect of digestion and dialysis on fermentation parameters

Digestion and dialysis (DD) (E2) introduced significant differences in fermentation outcomes compared to non-digested (ND) (E1) samples, underscoring their critical role in accurately simulating physiological conditions. DD samples exhibited significantly higher total gas production compared to ND samples, indicating enhanced microbial activity. In E1, Inu eq. fermented faster with a lower B value than Chi eq. However, after DD, Chi eq.'s B value increased and became comparable to Inu eq., suggesting that digestion modified substrate availability, slowing inulin fermentation while improving chicory fermentation rates. This highlights how digestion alters substrate characteristics, influencing fermentation gas kinetics.

DD and ND samples displayed contrasting SCFA profiles. In ND, Chi eq. had higher total SCFA production than Inu eq., but after DD, Inu eq. surpassed Chi eq. in SCFA production. This shift suggests that DD can impact the availability of fermentable components. Lactate production was consistently lower in DD samples compared to ND, reflecting the reduced availability of simple sugars in DD samples, which are the primary substrates for lactate-producing microbes. Microbial diversity was influenced by DD, with DD samples exhibiting a slightly higher α- diversity than ND samples, suggesting a broader microbial ecosystem resulting from substrate breakdown during digestion. Proteobacteria, a group associated with rapid fermentation of simple sugars and less beneficial microbial profiles, was six times more abundant in ND samples than DD samples, highlighting the role of digestion in reducing substrates that favour opportunistic microbes. ND samples also exhibited a tenfold increase in Bacteroidota and a 20% decrease in Firmicutes after 12 h, while DD samples showed a milder version of this trend. In E1, *Chi eq.* significantly reduced *Streptococcus* abundance at 12 h in ND, but in E2, after DD, *Chi eq.* and F2C showed higher *Streptococcus* abundance compared to *Inu eq.* and F2I, thus showing distinct genus-specific responses between treatments after digestion.

Another noteworthy observation was that ND fermentation supernatants were not cytotoxic even at higher concentrations, whereas DD supernatants exhibited cytotoxic effects, possibly due to bile acids retained during dialysis. ND samples, rich in unprocessed substrates and simple sugars, induced rapid but unbalanced microbial activity, while DD better reflected a digested diet, improving physiological relevance. The differences between ND and DD samples highlight the importance of incorporating digestion and dialysis in the *in vitro* studies.

6.4. Comparison of *in vivo* and *in vitro* models

Correlating *in vivo* and *in vitro* data provides valuable insights into gut health mechanisms but requires careful consideration of the inherent differences between the models. *In vitro* systems offer controlled conditions for studying specific processes, such as fermentation, immune modulation, and barrier function, but lack the complexity of whole-organism interactions observed *in vivo*, such as gut motility and systemic immune responses. Furthermore, differences in measurable markers, such as TEER, cytokine secretion, and gas kinetics *in vitro* versus zootechnical performance, histomorphology, and diarrhoea occurrences *in vivo*, limit direct comparisons. Instead, aligning trends and overlapping findings across both models bridges the gap, with *in vitro* experiments elucidating mechanisms and *in vivo* studies validating their physiological relevance. Among the common variables, SCFA production, α- diversity, microbiota composition, and gene expression were particularly relevant for comparison. Data from colonic content and tissue were deemed most logical to correlate, given that *in vitro* fermentation was conducted using fecal inoculum, closely representing the colonic environment.

Comparing SCFA concentrations across models yielded notable insights. Total SCFA levels from *in vivo* samples at W1 and W3 were comparable to those observed in 12 h *in vitro* fermentation supernatants, though SCFA profiles at 4 h *in vitro* were less aligned with *in vivo* results. Despite the dynamic nature of SCFA production and utilization in mucosa, both models showed treatment effects, particularly for molar ratios of individual SCFA. Although butyrate proportions were slightly lower *in vitro*, the F2C treatment consistently produced higher butyrate than F2I, paralleling the *in vivo* findings where CHI-fed piglets exhibited greater colonic butyrate levels than INU-fed piglets. Lactate proportions were lower *in vitro* compared to *in vivo* samples, reflecting differences in microbial activity across the models. α- diversity provided another point of comparison. Treatment-based differentiation was observed *in vitro* but not *in vivo*, however, the overall range of diversity indices was similar, indicating comparable microbial diversity trends. Analysis of individual genera revealed limited overlap, likely due to inherent natural variability in piglet microbiota composition. However, consistent treatment-related patterns emerged when broader microbial categories were compared. In the *in vivo* experiments, chicory increased beneficial genera, such as *Catenisphaera*, *Butyricicoccus*, and *Ruminococcus*, while reducing harmful genera like *Erysipelotrichaceae UCG-002*.

Similarly, in the *in vitro* studies, CHI fermentation increased beneficial genera, including *Lactobacillus*, *Lachnospira*, unclassified *Muribaculaceae*, and *Ruminococcus*, while reducing potentially harmful genera like *Faecalibacterium*. These analogies suggest that while specific microbial profiles may differ, the overall functional impact of the treatments is consistent across models.

Gene expression comparisons further demonstrated the parallel effects of inulin and chicory on barrier integrity and inflammation, although they operated through different genes. Both models showed treatment-driven upregulation of barrier integrity genes, such as *MUC1*, *MUC2*, and *JAMB*, alongside downregulation of inflammatory genes. For instance, *in vivo*, CHI and INU reduced pro-inflammatory genes, including IL8 and *TNFα*, while *in vitro*, CHI-equivalent treatments downregulated *CXCL10*, *IFNα*, and *NFκB1*. Although some gene-level differences arose due to the use of human cell lines *in vitro*, but the anti-inflammatory effects of both treatments were consistent. RGCCA analysis further supported these findings in both the models, linking butyrate to increased beneficial bacterial genera (e.g., *Blautia* and *Lactobacillus*) and reduced inflammatory markers, such as *TNFα* and *NFκB1*. Both models consistently clustered inulin and chicory treatments closely, distinct from control or LPS-only treatments, emphasizing their shared functional impact.

Permeability findings from *in vitro* and *in vivo* models also aligned. CHI-fed piglets showed a lower L:M ratio *in vivo*, indicating improved gut barrier function, while *in vitro*, F2C fermentation supernatants had lower lucifer yellow permeability compared to F2I. Despite methodological differences, both models consistently demonstrated the beneficial effects of chicory and inulin on enhancing intestinal barrier integrity.

In summary, while direct comparisons between *in vivo* and *in vitro* models are challenging due to their inherent differences, these studies revealed consistent trends in SCFA production, microbial diversity, gene expression, and intestinal permeability. *In vitro* models showed detailed differences between treatments, underscoring the complementary value of combining approaches such as digestion, absorption and fermentation with triple cell culture model in understanding the effects of chicory and inulin on gut health.

Table 20: Comparison between *in vivo* 2 and *in vitro* 2 (DD) results of permeability, SCFA, diversity, general abundance, and gene expression (Green: Similar; Red: Diff.; Black: No diff.) (NSD: No Signific. Diff.)

		In vivo		*In vitro*	
		***In vivo* W1**	***In vivo* W3**	***In vitro* 4h**	***In vitro* 12 h**
Permeability	**L:M** **D-Xylose**	NSD Inu and then Chi had ↓	**CHI fed piglets had ↓ L:M** Inu and Chi had ↓ than Ctrl	**NA**	**LY -F2C had lower than F2I** LY -NSD for Inu eq. and Chi eq.
SCFA	**Lactate(mmol/g)** **TSCFA (mg/g)** **Acetate (%)** **Propionate (%)** **Butyrate (%)** **BCFA (%)**	**(0.9-1.6) Inu ↑ than Chi** **(4.5-7.5) ↑ in Inu than Chi** **(**45-55) NSD (20-25) NSD **(15-20) ↑ in CHI and Inu** (5-7) NSD	**(0.8-1)** NSD **(6-8)** NSD **(45-55) ↓** in Inu and Chi than Ctrl (20-25) NSD **(15-20) ↑ in Chi, Inu than Ctrl** (5-7) NSD	**(0.02-0.5) Inu ↑ than Chi** (3.5-5) NSD (55-65)- ↑ in Inu than Chi (10-20%)- NSD (7-10%)- NSD (10-25% BCFA)- ↓ in Inu eq.	**(0.01-0.4)** NSD **(4- 8) ↑ in Inu than Chi** **(40-60)** ↑ in Inu and F2I than Chi and F2C (15-25) ↑ in Chi and F2C than Inu and F2I **(10-16%) ↑ in F2C than F2I** (4-8%) ↓ in Inu eq. and F2I
α diversity	**Chao1** **Shannon** **Simpson**	(289-504) NSD **(4.5-5.5)** NSD **(0.96-0.99)** NSD	(256-509) NSD (4.25-5.25) NSD **(0.965-0.99)** NSD	(270-356) NSD (4.07-4.73) ↑ for Chi and F2C **(0.951-0.980)** ↑ for Chi and F2C	(270-415) ↑ for Chi and F2C **(4.25-5.03)** ↑ for Chi and F2C **(0.964-0.988)** ↑ for Chi and F2C
Genera Abundance	*Lactobacillus* *Lachnospira* *Megasphaera* *Blautia* *Muribaculaceae* *Streptococcus* *Subdoligranulum* *Faecalibacterium* *Ruminococcus* *Holdemanella* *Sharpea* *Mitsuokella* *Fusobacterium*	**NSD** **NSD** **NSD** **NSD** **NSD** <1% abundance **NSD** NSD **NSD** **NSD** <1% abundance **NSD** **NSD**	**NSD** **NSD** **NSD** **NSD** **NSD** **↓ in Chi than Inu** **NSD** **NSD** **↑ in Chi than Inu** <1% abundance <1% abundance **NSD** **NSD**	↑ in Chi and F2C than Inu and F2I ↑ in Inu than Chi <1% abundance ↑ in Inu than Chi ↑ in Chi and F2C than Inu and F2I ↑ in F2C, Chi, F2I, Inu ↑ in Inu than Chi ↓ in Chi and F2C than Inu and F2I < 1% abundance ↑ in Inu, F2I than Chi, F2C < 1% abundance ↑ in Chi and F2C than Inu and F2I ↓ in Inu than Chi	↑ in Chi and F2C than Inu and F2I ↑ in Chi and F2C than Inu and F2I <1% abundance ↑ in Inu, F2I than Chi, F2C ↑ in Chi and F2C than Inu and F2I **↑ in Chi and F2C than Inu and F2I** ↑ in Inu, F2I than Chi, F2C ↓ in Chi and F2C than Inu and F2I **↑ in Chi than Inu** ↑ in Inu, F2I than Chi, F2C ↑ in Inu, F2I than Chi, F2C < 1% abundance ↓ in Inu and F2I than Chi and F2C
Gene Expression (Colon)	Barrier Integrity genes Inflammation Signally Pathway Genes Inflammatory Targets	**MUC2: ↑ in CHI but NS** **TANK:** ↓ in Inu than Chi **TLR2:** ↓ in Inu and Chi than Ctrl **CXCL10:** ↓ in Inu and Chi **IFNγ:** ↓ in Inu and Chi	**MUC1: ↑ in CHI than Inu** **NFκB1:** ↓ in Chi and Inu **TLR2:** ↓ in Inu and Chi than Ctrl **DEFB4α: ↓ in Inu/Chi than Ctrl** **IFNα:** ↓ in Chi than Inu	NA	**MUC1: ↑ in Inu, Chi than LPS** **MUC2: ↑ in Chi than Inu** **JAMB:** ↑ in Inu, Chi than LPS **MAPPK14:** ↓ in Chi than LPS **MyD88:** ↓ in Inu and Chi than LPS **AKT1:** ↓ in Inu and Chi than LPS **DEFB4α: ↓ in Inu and Chi** **IL8:** ↓ in Inu and Chi **TNFα:** ↓ in Inu, Chi, F2I and F2C

Note: When numbers/ values are also coloured, it means the similar range of the values for those molar ratios.

6.5. Methodological Discrepancies and Improvements: Perspectives

6.5.1. *In vivo* Methods

The present study extended the post-weaning experimental period to five weeks to assess the sustained effects of dietary fibre interventions. This design aimed to capture both acute and longer-term responses in gut health, microbial adaptation, and immune modulation. A critical methodological choice was the use of oral force-feeding over mixing fibres directly into the feed. This ensured precise, standardized dosing of inulin or crude chicory across all piglets, particularly important during the early post-weaning period, when feed intake is highly variable due to stress-induced anorexia. Force-feeding allowed for strict control over exposure to the test fibres and minimized confounding from unequal consumption, which would have been unavoidable with voluntary feed intake. While this approach may introduce transient stress and potentially reduce overall feed intake in some piglets—particularly in the chicory-fed group during Week 1 of E2—the effect was fully reversed by Week 2 and 3, with no significant difference in body weight compared to other groups. Moreover, although force-feeding does not fully mimic commercial feeding behaviour, it is essential for experimental reproducibility. Future studies may benefit from directly comparing force-feeding versus feed-mixed delivery to evaluate real-world applicability and dose-response consistency (Bus *et al.*, 2024).

The initial decrease in feed intake observed in chicory-fed piglets is likely attributable to the bitter taste and reduced palatability of crude chicory. However, advances in genetic modification, including CRISPR/Cas9 technology, have shown that bitterness in chicory can be significantly reduced, improving palatability while preserving bioactive content (Domont *et al.*, 2023). Such chicory variants merit further investigation in the context of early piglet feeding strategies. The basal diet used in this study was designed to be prebiotic-free to reduce background interference from other functional additives. Although it included fibrous components such as rice bran, spelled bran, and 30% barley—leading to relatively high NDF—it contained no added sugars, probiotics, or synthetic functional ingredients. While this diet posed nutritional challenges due to moderate protein and low digestible carbohydrate levels, particularly in newly weaned piglets, it created a controlled and physiologically relevant context in which the effects of fibre supplementation could be clearly distinguished. Future experiments should incorporate more balanced or commercially relevant diets to examine whether similar gut health outcomes can be achieved under standard production conditions.

Regarding the intestinal permeability test, the sugar cocktail dose was selected based on validated protocols in piglets and other large animal models. Although the dose may appear high compared to human studies on a per-kilogram basis, it was necessary to achieve detectable plasma concentrations within a short time window and to accommodate species-specific differences in gut transit, metabolism, and absorption kinetics. The sugar mixture was administered exactly one hour before euthanasia—a time point shown to capture differential permeability across paracellular and transcellular pathways. No signs of accelerated passage or abnormal stool consistency were observed, and plasma sugar concentrations fell within expected ranges reported in similar models. Nonetheless, future studies should consider using dose-response curves, alternative marker molecules such as L-rhamnose and bovine serum albumin, and timing modifications to refine the resolution of the assay. Parallel analysis of blood and urine samples from the same animal could also improve the accuracy of intestinal permeability assessments (Wijtten *et al.*, 2010).

Improvements in histomorphological analysis are also recommended. Advanced imaging tools like HistoMetriX could enable automated measurement of parameters such as villus height, width, crypt depth, and surface area, thereby reducing human error and observer bias associated with manual microscopy. Moreover, while fecal samples were used for both microbiota profiling and as inoculum for *in vitro* fermentation, they represent a complex and somewhat variable biological matrix. Parallel profiling of colonic content along with feces would enhance the resolution of microbial community shifts and improve correlations between microbial structure and functional fermentation output.

For SCFA analysis, the current study employed HPLC with an Aminex HPX-87H ion exclusion column and UV detection at 210 nm—a standard and widely used method. While effective, this approach lacks molecular specificity and may be susceptible to co-eluting compounds, particularly in complex matrices like feces and fermentation supernatant. Although retention times were matched to external standards and blanks were run to confirm peak identity, future work could integrate more selective and sensitive techniques such as gas chromatography–flame ionization detection (GC-FID) or HPLC–mass spectrometry (HPLC-MS) to enhance resolution and detection of short-chain and branched-chain fatty acids.

At the molecular level, evaluating the expression of genes involved in digestive enzyme production (e.g., sucrase-isomaltase, maltase-glucoamylase) could help determine whether dietary fibre interventions also modulate digestive functionality. This would provide insight beyond barrier integrity or inflammation markers and expand understanding of nutrient utilization efficiency (Shi *et al.*, 2022). Similarly, isolating and evaluating the effects of specific bioactive compounds from chicory—such as sesquiterpene lactones, chlorogenic acid, and caffeic acid—through both *in vitro* and *in vivo* models would help delineate their individual contributions to the observed anti-inflammatory and barrier-modulating effects (Pouille *et al.*, 2022).

Finally, comprehensive immune profiling, including measurements of serum cortisol, cytokine panels, immunoglobulin levels (especially IgA), and lymphocyte subset characterization, would significantly strengthen interpretation of systemic immune responses. These markers would help bridge the gap between mucosal and peripheral immunity and better contextualize *in vivo* findings within a broader immunological framework (Papatsiros *et al.*, 2024). Collectively, these methodological refinements and future directions aim to deepen the mechanistic understanding of dietary fibre effects on gut health, improve translational accuracy, and facilitate integration between *in vivo* and *in vitro* systems for early-life gut development research.

6.5.2. *In vitro* Methods

One limitation of the current *in vitro* digestion protocol lies in the use of a standardized digestive enzyme composition that may not accurately reflect the dynamic enzymatic profile of piglets during the weaning phase. During this critical period, the activity of digestive enzymes such as lipase and trypsin undergoes significant fluctuations. For instance, between 0 and 4 weeks of age, lipase and trypsin activities nearly double each week. However, these activities decline to one-third of pre-weaning levels within the first week after weaning, only recovering, or exceeding pre-weaning levels after approximately two weeks (Jiang *et al.*, 2019). Therefore, future *in vitro* digestion models should incorporate enzyme concentrations and activity curves tailored to the weaning stage to enhance physiological relevance and better reflect actual digestive capacity during this transition.

In addition to enzyme specificity, the use of static digestion protocols, while operationally straightforward, does not capture important physiological variables such as peristalsis, gastric emptying rates, and time-dependent enzyme secretion. Implementing dynamic digestion systems—such as those mimicking the piglet gastrointestinal tract—would allow for the continuous modulation of pH, flow, and enzyme release, thereby offering a more realistic simulation of gastrointestinal digestion (Kozu *et al.*, 2014; Wang *et al.*, 2019; Dupont *et al.*, 2019). These systems would also permit more precise timing and assessment of digestion and release kinetics for various substrates.

Furthermore, post-digestion monosaccharide profiling was not conducted in this study. The analysis of monosaccharide composition following digestion could yield valuable insights into the release and transformation of complex carbohydrates, and more accurately define substrate availability for microbial fermentation. Monitoring changes in sugar profiles before and after digestion could enhance interpretation of fermentation kinetics and metabolite profiles downstream.

Regarding the absorption simulation phase, the current study employed dialysis using a 3.5 kDa molecular weight cut-off membrane over 24 hours. While this step aims to remove absorbable nutrients and mimic small intestinal absorption, it may also inadvertently allow for the loss of low molecular weight fractions of fructooligosaccharides (FOS) and inulin. Future improvements could involve the use of smaller-pore dialysis membranes (e.g., 1 kDa) or dialysis device modifications that improve retention of bioactive oligosaccharides while better simulating intestinal nutrient absorption. Additionally, one limitation of this protocol was the absence of antimicrobial agents during the dialysis phase. This raises the potential risk of unintentional microbial fermentation within the dialysis solution, particularly given the presence of fermentable substrates. However, antibiotics were excluded intentionally to avoid residual antimicrobial compounds that could interfere with subsequent *in vitro* fermentation assays. Although digestion was carried out under sterile conditions, future studies could further optimize this step by employing shorter dialysis durations or pre-validating the microbial stability of the dialysate to reduce the risk of unintended microbial activity, while preserving downstream analytical integrity.

Another area for refinement is the standardization and timing of fecal inoculum collection. Fermentation dynamics can vary significantly depending on the source and timing of fecal sampling. Given that fecal microbial communities evolve rapidly in the post-weaning period, future studies should compare fermentation responses using inocula from different post-weaning timepoints (e.g., W1 vs. W3) and evaluate fresh versus frozen fecal samples to assess how microbial composition and activity are influenced by storage and developmental stage (Mao *et al.*, 2021).

The static fermentation model used in this study, although widely adopted, has limitations including substrate depletion and metabolite accumulation that can bias microbial activity over time. Integration of piglet-specific dynamic fermentation systems, such as the Baby Spime model, could improve simulation of colonic fermentation by incorporating flow, pH control, and continuous feeding. These models offer enhanced resolution of microbial succession and metabolite dynamics over time (Dufourny *et al.*, 2019).

Regarding the cell model, Caco-2 cells were used due to their well-established transport and barrier properties, and the absence of a commercially available mucus-producing porcine cell line. Although Caco-2 cells are human-derived and tumorigenic, they remain the most suitable option for developing complex co-culture

models until piglet-derived alternatives are developed. In contrast, IPEC-J2 cells—while non-tumorigenic and derived from neonatal piglet jejunum—lack MUC2 expression and do not form a physiologically relevant mucus layer, limiting their use in mimicking the intestinal epithelium (Schierack *et al.*, 2006; Støy *et al.*, 2013).

Nevertheless, the triple cell culture model employed here (Caco-2, HT-29-MTX, and U937) can be further enhanced. Incorporating additional immune components such as piglet-derived PBMCs, dendritic cells, THP-1 monocytes, or Raji B cells would allow more comprehensive modelling of epithelial–immune interactions. Additionally, the use of organoids derived from porcine stem cells offers a promising avenue to model complex tissue architecture and differentiation. New-generation systems like the 3D-Flipwell Co-Culture, as developed by Beamer *et al*. (2023), provide a stratified structure that includes epithelial cells, a semi-permeable mucus layer, and underlying immune components. These platforms more accurately reflect the native architecture of the gut and offer an advanced *in vitro* environment to study microbiota–epithelial–immune crosstalk under dynamic conditions.

6.6. Practical Applications and Relevance

- **Applications in Animal Health and Nutrition:** These studies provide effective strategies to improve gut health in weaning piglets, a critical phase marked by stress and intestinal dysfunction. Both inulin and crude chicory enhance intestinal barrier integrity, reduce inflammation, and promote beneficial microbial populations, helping alleviate post-weaning challenges. As a cheaper alternative to antibiotics and zinc oxide, chicory can support gut health more sustainable than extracted inulin.

- **Translational Relevance for Human Health:** The *in vitro* models, particularly the triple-cell culture system, offer insights into the effects of dietary fibres on gut health, relevant to conditions like inflammatory bowel disease and leaky gut syndrome in humans. Findings from chicory and inulin can inform the development of functional foods and prebiotic supplements. Chicory's additional bioactives enhance its potential for cost-effective, multifunctional prebiotic products for human health.

- **Methodological Advances:** The integration of *in vivo* and *in vitro* methods strengthens the findings. *In vitro* models provide controlled environments to explore fermentation and immune modulation, while *in vivo* studies validate physiological relevance. Together, they offer a comprehensive understanding of gut health mechanisms and serve as standardized tools for prebiotic evaluation before animal trials.

6.7. Final Conclusion

This manuscript provides comprehensive insights into the effects of crude chicory and inulin on gut health through the integration of *in vivo* and *in vitro* studies. Both approaches consistently demonstrated their potential as prebiotics to improve gut health by enhancing intestinal barrier integrity, modulating microbiota, and reducing inflammation. The *in vivo* study revealed significant improvements in gut morphology, such as increased villus height and reduced crypt depth, along with enhanced butyrate production, reduced permeability, and lower expression of pro-inflammatory genes in the ileum and colon of weaning piglets. Complementarily, the *in vitro* study offered mechanistic insights, showing that fermentation supernatants from crude chicory and inulin increased beneficial SCFA like butyrate, reduced pro-inflammatory cytokines, and supported the growth of beneficial microbial genera such as *Lactobacillus* and *Ruminicoccus*.

Crude chicory, with its additional bioactive compounds beyond inulin, demonstrated superior effects, including enhanced anti-inflammatory responses, better microbiota modulation, and improved intestinal barrier function, making it a cost-effective alternative to refined inulin. The clustering of inulin and chicory treatments in RGCCA analysis further highlighted their shared mechanisms in improving gut health.

This research highlights the importance of combining different *in vitro* methodologies like digestion and absorption (dialysis). Fermentation was combined with a novel triple cell culture model to bridge the gap between *in vitro* conditions and *in vivo* physiology. Together, these results support the potential of crude chicory and inulin as effective prebiotic alternatives to antibiotics and synthetic additives in livestock nutrition. By addressing critical challenges in gut health of weaning piglets, this work has significant implications for sustainable functional feed development and a more accurate *in vitro* evaluation of bioactives. It also paves the way for translational applications in human nutrition, offering innovative, natural strategies for improving gut health while addressing global challenges of antimicrobial resistance.

7

Bibliography

Abreu, M. T. (2010). Toll-like receptor signalling in the intestinal epithelium: how bacterial recognition shapes intestinal function. Nature Reviews Immunology, 10(2), 131–144. doi:10.1038/nri2707

Adhikari, B., Kim, S. W., and Kwon, Y. M. (2019). Characterization of Microbiota Associated with Digesta and Mucosa in Different Regions of Gastrointestinal Tract of Nursery Pigs. *International Journal of Molecular Sciences*, *20*(7), 1630. https://doi.org/10.3390/ijms20071630

Aguedo, M., Fougnies, C., Dermience, M., and Richel, A. (2014). Extraction by three processes of arabinoxylans from wheat bran and characterization of the fractions obtained. *Carbohydrate Polymers*, *105*, 317–324. https://doi.org/10.1016/j.carbpol.2014.01.096

Akbari, P., Fink-Gremmels, J., Willems, R. H. A. M., Difilippo, E., Schols, H. A., Schoterman, M. H. C., Garssen, J., and Braber, S. (2017). Characterizing microbiota-independent effects of oligosaccharides on intestinal epithelial cells: insight into the role of structure and size. *European Journal of Nutrition*, *56*(5), 1919–1930. https://doi.org/10.1007/s00394-016-1234-9

Alharthi, F. (2023). Chicoric acid enhances the antioxidative defence system and protects against inflammation and apoptosis associated with the colitis model induced by dextran sulfate sodium in rats. *Environmental Science and Pollution Research*, *30*(57), 119814–119824. https://doi.org/10.1007/s11356-023-30742-y

Aljuraiban, G. S., Algabsani, S. S., Sabico, S., AlShammari, S., Aljazairy, E. A., and AL-Musharaf, S. (2023). Types of fiber and gut microbiota composition and diversity among arab females. *Saudi Journal of Biological Sciences*, *30*(9), 103767. https://doi.org/10.1016/j.sjbs.2023.103767

Allaire, J. M., Crowley, S. M., Law, H. T., Chang, S.-Y., Ko, H.-J., and Vallance, B. A. (2018). The Intestinal Epithelium: Central Coordinator of Mucosal Immunity. *Trends in Immunology*, *39*(9), 677–696. https://doi.org/10.1016/j.it.2018.04.002

Allam-Ndoul, B., Castonguay-Paradis, S., and Veilleux, A. (2020). Gut Microbiota and Intestinal Trans-Epithelial Permeability. *International Journal of Molecular Sciences*, *21*(17), 6402. https://doi.org/10.3390/ijms21176402

Alminger, M., Aura, A. -M., Bohn, T., Dufour, C., El, S. N., Gomes, A., Karakaya, S., Martínez-Cuesta, M. C., McDougall, G. J., Requena, T., and Santos, C. N. (2014). *In vitro* Models for Studying Secondary Plant Metabolite Digestion and Bioaccessibility. *Comprehensive Reviews in Food Science and Food Safety*, *13*(4), 413–436. https://doi.org/10.1111/1541-4337.12081

Al-Sadi, R. (2009). Mechanism of cytokine modulation of epithelial tight junction barrier. *Frontiers in Bioscience*, *Volume*(14), 2765. https://doi.org/10.2741/3413

Al-Sadi, R., Guo, S., Ye, D., Rawat, M., and Ma, T. Y. (2016). TNFα Modulation of Intestinal Tight Junction Permeability Is Mediated by NIK/IKK-α Axis Activation of the Canonical NFκB Pathway. *The American Journal of Pathology*, *186*(5), 1151–1165. https://doi.org/10.1016/j.ajpath.2015.12.016

Alves-Santos, A. M., Sugizaki, C. S. A., Lima, G. C., and Naves, M. M. V. (2020). Prebiotic effect of dietary polyphenols: A systematic review. *Journal of Functional Foods*, *74*, 104169. https://doi.org/10.1016/j.jff.2020.104169

Ambrosio, C. M. S., de Alencar, S. M., de Sousa, R. L. M., Moreno, A. M., and Da Gloria, E. M. (2017). Antimicrobial activity of several essential oils on pathogenic and beneficial bacteria. *Industrial Crops and Products*, *97*, 128–136. https://doi.org/10.1016/j.indcrop.2016.11.045

Andersen, C. L., Jensen, J. L., and Ørntoft, T. F. (2004). Normalization of Real-Time Quantitative Reverse Transcription-PCR Data: A Model-Based Variance Estimation Approach to Identify Genes Suited for Normalization, Applied to Bladder and Colon Cancer Data Sets. *Cancer Research*, *64*(15), 5245–5250. https://doi.org/10.1158/0008-5472.CAN-04-0496

Apolinário, A. C., de Lima Damasceno, B. P. G., de Macêdo Beltrão, N. E., Pessoa, A., Converti, A., and da Silva, J. A. (2014). Inulin-type fructans: A review on different aspects of biochemical and pharmaceutical technology. *Carbohydrate Polymers*, *101*, 368–378. https://doi.org/10.1016/j.carbpol.2013.09.081

Apper, E., Meymerit, C., Bodin, J., Respondek, F., and Wagner, A. (2016a). Effect of Dietary Supplementation with Short-Chain Fructooligosaccharides in Lactating Sows and Newly Weaned Piglets on Reproductive Performance of Sows, Immune Response and Growth Performance of Piglets from Birth to Slaughter. *Journal of Animal Research and Nutrition*, *01*(04). https://doi.org/10.21767/2572-5459.100019

Apper, E., Meymerit, C., Bodin, J., Respondek, F., and Wagner, A. (2016b). Effect of Dietary Supplementation with Short-Chain Fructooligosaccharides in Lactating Sows and Newly Weaned Piglets on Reproductive Performance of Sows, Immune Response and Growth Performance of Piglets from Birth to Slaughter. *Journal of Animal Research and Nutrition*, *1*. https://doi.org/10.21767/2572-5459.100019

Araújo, F., and Sarmento, B. (2013). Towards the characterization of an *in vitro* triple co-culture intestine cell model for permeability studies. *International Journal of Pharmaceutics*, *458*(1), 128–134. https://doi.org/10.1016/j.ijpharm.2013.10.003

Argüello, H., Estellé, J., Zaldívar-López, S., Jiménez-Marín, Á., Carvajal, A., López-Bascón, M. A., Crispie, F., O'Sullivan, O., Cotter, P. D., Priego-Capote, F., Morera, L., and Garrido, J. J. (2018). Early Salmonella Typhimurium infection in pigs disrupts Microbiome composition and functionality principally at the ileum mucosa. *Scientific Reports*, *8*(1), 7788. https://doi.org/10.1038/s41598-018-26083-3

Arnone, D., Chabot, C., Heba, A.-C., Kökten, T., Caron, B., Hansmannel, F., Dreumont, N., Ananthakrishnan, A. N., Quilliot, D., and Peyrin-Biroulet, L. (2022). Sugars and Gastrointestinal Health. *Clinical Gastroenterology and Hepatology*, *20*(9), 1912-1924.e7. https://doi.org/10.1016/j.cgh.2021.12.011

Arrieta, M. C. (2006a). Alterations in intestinal permeability. *Gut*, *55*(10), 1512–1520. https://doi.org/10.1136/gut.2005.085373

Arrieta, M. C. (2006b). Alterations in intestinal permeability. *Gut*, *55*(10), 1512–1520. https://doi.org/10.1136/gut.2005.085373

Artis, D. (2008). Epithelial-cell recognition of commensal bacteria and maintenance of immune homeostasis in the gut. *Nature Reviews Immunology*, *8*(6), 411–420. https://doi.org/10.1038/nri2316

Artursson P, Palm K, Luthman K (2001) Caco-2 monolayers in experimental and theoretical predictions of drug transport. Adv Drug Deliv Rev 46:27–43

Awad, W. A., Ghareeb, K., Paßlack, N., and Zentek, J. (2013). Dietary inulin alters the intestinal absorptive and barrier function of piglet intestine after weaning. *Research in Veterinary Science*, *95*(1), 249–254. https://doi.org/10.1016/j.rvsc.2013.02.009

Ayuso, M., Michiels, J., Wuyts, S., Yan, H., Degroote, J., Lebeer, S., Le Bourgot, C., Apper, E., Majdeddin, M., Van Noten, N., Vanden Hole, C., Van Cruchten, S., Van Poucke, M., Peelman, L., and Van Ginneken, C. (2020a). Short-chain fructo-oligosaccharides supplementation to suckling piglets: Assessment of pre- and post-weaning performance and gut health. *PLOS ONE*, *15*(6), e0233910. https://doi.org/10.1371/journal.pone.0233910

Ayuso, M., Michiels, J., Wuyts, S., Yan, H., Degroote, J., Lebeer, S., Le Bourgot, C., Apper, E., Majdeddin, M., Van Noten, N., Vanden Hole, C., Van Cruchten, S., Van Poucke, M., Peelman, L., and Van Ginneken, C. (2020b). Short-chain fructo-oligosaccharides supplementation to suckling piglets: Assessment of pre- and post-weaning performance and gut health. *PLOS ONE*, *15*(6), e0233910. https://doi.org/10.1371/journal.pone.0233910

Bae, Y.-M., and Lee, S.-Y. (2017). Effect of salt addition on acid resistance response of Escherichia coli O157:H7 against acetic acid. *Food Microbiology*, *65*, 74–82. https://doi.org/10.1016/j.fm.2016.12.021

Bacon, James and Kitchel, Halie and Stutz, John and Chen, Jack Hua and Smith, Aaron and Van Horn, Robert D. and Moreland, Christopher and Abraham, Trent and Baker, Thomas and Aihara, Eitaro and Hillgren, Kathleen, Porcine Intestinal Organoids Cultured in an Organ-on-A-Chip Microphysiological System. http://dx.doi.org/10.2139/ssrn.5174434

Bailey, M., Haverson, K., Inman, C., Harris, C., Jones, P., Corfield, G., Miller, B., and Stokes, C. (2005). The development of the mucosal immune system pre- and post-weaning: balancing regulatory and effector function. *Proceedings of the Nutrition Society*, *64*(4), 451–457. https://doi.org/10.1079/PNS2005452

Bamigbade, G. B., Subhash, A. J., Kamal-Eldin, A., Nyström, L., and Ayyash, M. (2022). An Updated Review on Prebiotics: Insights on Potentials of Food Seeds Waste as Source of Potential Prebiotics. *Molecules*, *27*(18), 5947. https://doi.org/10.3390/molecules27185947

Bampidis, V., Azimonti, G., Bastos, M. de L., Christensen, H., Dusemund, B., Fašmon Durjava, M., Kouba, M., López-Alonso, M., López Puente, S., Marcon, F., Mayo, B., Pechová, A., Petkova, M., Ramos, F., Sanz, Y., Villa, R. E., Woutersen, R., Poiger, T., Tosti, L., … Tarrés-Call, J. (2023). Safety of a feed additive consisting of sodium saccharin for suckling and weaned piglets, fattening pigs, calves for rearing and for fattening (FEFANA asbl). *EFSA Journal*, *21*(1). https://doi.org/10.2903/j.efsa.2023.7710

Barcenilla, A., Pryde, S. E., Martin, J. C., Duncan, S. H., Stewart, C. S., Henderson, C., and Flint, H. J. (2000). Phylogenetic Relationships of Butyrate-Producing Bacteria from the Human Gut. *Applied and Environmental Microbiology*, *66*(4), 1654–1661. https://doi.org/10.1128/AEM.66.4.1654-1661.2000

Barreau, F., and Hugot, J. (2014). Intestinal barrier dysfunction triggered by invasive bacteria. *Current Opinion in Microbiology*, *17*, 91–98. https://doi.org/10.1016/j.mib.2013.12.003

Barroso, E., Cueva, C., Peláez, C., Martínez-Cuesta, M. C., and Requena, T. (2015). Development of human colonic microbiota in the computer-controlled dynamic SIMulator of the GastroIntestinal tract SIMGI. *LWT - Food Science and Technology*, *61*(2), 283–289. https://doi.org/10.1016/j.lwt.2014.12.014

Barszcz, M., Taciak, M., and Skomiał, J. (2016). The effects of inulin, dried Jerusalem artichoke tuber and a multispecies probiotic preparation on microbiota ecology and immune status of the large intestine in young pigs. *Archives of Animal Nutrition*, *70*(4), 278–292. https://doi.org/10.1080/1745039X.2016.1184368

Barszcz, M., Taciak, M., Tuśnio, A., Święch, E., Bachanek, I., Kowalczyk, P., Borkowski, A., and Skomiał, J. (2018). The effect of dietary level of two inulin types differing in chain length on biogenic amine concentration, oxidant-antioxidant balance and DNA repair in the colon of piglets. *PLOS ONE*, *13*, e0202799. https://doi.org/10.1371/journal.pone.0202799

Barszcz, M., Taciak, M., Tuśnio, A., Święch, E., and Skomiał, J. (2020). Dose-dependent effects of two inulin types differing in chain length on the small intestinal morphology, contractility and proinflammatory cytokine gene expression in piglets. *Archives of Animal Nutrition*, *74*(2), 107–120. https://doi.org/10.1080/1745039X.2019.1697140

Bauer, E. , W. B. A. , S. H. , V. M. W. , and M. R. (2006). Influence of the gastrointestinal microbiota on development of the immune system in young animals. *Current Issues in Intestinal Microbiology, 7*(2), 35–42.

Bäumler, A. J., and Sperandio, V. (2016). Interactions between the microbiota and pathogenic bacteria in the gut. *Nature*, *535*(7610), 85–93. https://doi.org/10.1038/nature18849

Bawish, B. M., Zahran, M. F. S., Ismael, E., Kamel, S., Ahmed, Y. H., Hamza, D., Attia, T., and Fahmy, K. N. E. (2023). Impact of buffered sodium butyrate as a partial or total dietary alternative to lincomycin on performance, IGF-1 and TLR4 genes expression, serum indices, intestinal histomorphometry, Clostridia, and litter hygiene of broiler chickens. *Acta Veterinaria Scandinavica*, *65*(1), 44. https://doi.org/10.1186/s13028-023-00704-y

Baxter, N. T., Schmidt, A. W., Venkataraman, A., Kim, K. S., Waldron, C., and Schmidt, T. M. (2019). Dynamics of Human Gut Microbiota and Short-Chain Fatty Acids in Response to Dietary Interventions with Three Fermentable Fibers. *MBio*, *10*(1). https://doi.org/10.1128/mBio.02566-18

Beamer, M.A., Zamora, C., Nestor-Kalinoski, A.L. *et al.* Novel 3D Flipwell system that models gut mucosal microenvironment for studying interactions between gut microbiota, epithelia and immunity. *Sci Rep* **13**, 870 (2023). https://doi.org/10.1038/s41598-023-28233-8

Beaumont, M., Paës, C., Mussard, E., Knudsen, C., Cauquil, L., Aymard, P., Barilly, C., Gabinaud, B., Zemb, O., Fourre, S., Gautier, R., Lencina, C., Eutamène, H., Theodorou, V., Canlet, C., and Combes, S. (2020). Gut microbiota derived metabolites contribute to intestinal barrier maturation at the suckling-to-weaning transition. *Gut Microbes*, *11*(5), 1268–1286. https://doi.org/10.1080/19490976.2020.1747335

Béduneau, A., Tempesta, C., Fimbel, S., Pellequer, Y., Jannin, V., Demarne, F., and Lamprecht, A. (2014a). A tunable Caco-2/HT-29-MTX co-culture model mimicking variable permeabilities of the human intestine obtained by an original seeding procedure. *European Journal of Pharmaceutics and Biopharmaceutics*, *87*(2), 290–298. https://doi.org/10.1016/j.ejpb.2014.03.017

Béduneau, A., Tempesta, C., Fimbel, S., Pellequer, Y., Jannin, V., Demarne, F., and Lamprecht, A. (2014b). A tunable Caco-2/HT-29-MTX co-culture model mimicking variable permeabilities of the human intestine obtained by an original seeding procedure. *European Journal of Pharmaceutics and Biopharmaceutics*, *87*(2), 290–298. https://doi.org/10.1016/j.ejpb.2014.03.017

Behrens, I., Stenberg, P., Artursson, P., and Kissel, T. (2001). Transport of lipophilic drug molecules in a new mucus-secreting cell culture model based on HT-29-MTX cells. *Pharmaceutical Research*, *18*(8), 1138–1145. https://doi.org/10.1023/A:1010974909998

Bellmann, S., Lelieveld, J., Gorissen, T., Minekus, M., and Havenaar, R. (2016). Development of an advanced *in vitro* model of the stomach and its evaluation versus human gastric physiology. *Food Research International*, *88*, 191–198. https://doi.org/10.1016/j.foodres.2016.01.030

Benoit, Y. D., Paré, F., Francoeur, C., Jean, D., Tremblay, E., Boudreau, F., Escaffit, F., and Beaulieu, J.-F. (2010). Cooperation between HNF-1α, Cdx2, and GATA-4 in initiating an enterocytic differentiation program in a normal human intestinal epithelial progenitor cell line. *American Journal of Physiology-Gastrointestinal and Liver Physiology*, *298*(4), G504–G517. https://doi.org/10.1152/ajpgi.00265.2009

Berghaus, L.J.; Moore, J.N.; Hurley, D.J.; Vandenplas, M.L.; Fortes, B.P.; Wolfert, M.A.; Boons, G.-J. Innate immune responses of primary murine macrophage-lineage cells and RAW 264.7 cells to ligands of toll-like receptors 2, 3, and 4. Comp. Immunol. Microbiol. Infect. Dis. 2010, 33, 443–454

Berkes, J. (2003). Intestinal epithelial responses to enteric pathogens: effects on the tight junction barrier, ion transport, and inflammation. *Gut*, *52*(3), 439–451. https://doi.org/10.1136/gut.52.3.439

Berschneider H.M. (1989). Abstracts of Papers Submitted to the American Gastroenterological Association. *Gastroenterology*, *96*(5), A1–A568. https://doi.org/10.1016/S0016-5085(89)80002-2

Bian, G., Ma, S., Zhu, Z., Su, Y., Zoetendal, E. G., Mackie, R., Liu, J., Mu, C., Huang, R., Smidt, H., and Zhu, W. (2016a). Age, introduction of solid feed and weaning are more important determinants of gut bacterial succession in piglets than breed and nursing mother as revealed by a reciprocal cross-fostering model. *Environmental Microbiology*, *18*(5), 1566–1577. https://doi.org/10.1111/1462-2920.13272

Bian, G., Ma, S., Zhu, Z., Su, Y., Zoetendal, E. G., Mackie, R., Liu, J., Mu, C., Huang, R., Smidt, H., and Zhu, W. (2016b). Age, introduction of solid feed and weaning are more important determinants of gut bacterial succession in piglets than breed and nursing mother as revealed by a reciprocal cross-fostering model. *Environmental Microbiology*, *18*(5), 1566–1577. https://doi.org/10.1111/1462-2920.13272

Biddle, A., Stewart, L., Blanchard, J., and Leschine, S. (2013). Untangling the Genetic Basis of Fibrolytic Specialization by Lachnospiraceae and Ruminococcaceae in Diverse Gut Communities. *Diversity*, *5*, 627–640. https://doi.org/10.3390/d5030627

Birchenough, G. M. H., Johansson, M. E., Gustafsson, J. K., Bergström, J. H., and Hansson, G. C. (2015). New developments in goblet cell mucus secretion and function. *Mucosal Immunology*, *8*(4), 712–719. https://doi.org/10.1038/mi.2015.32

Bischoff, S. C., Barbara, G., Buurman, W., Ockhuizen, T., Schulzke, J.-D., Serino, M., Tilg, H., Watson, A., and Wells, J. M. (2014). Intestinal permeability – a new target for disease prevention and therapy. *BMC Gastroenterology*, *14*(1), 189. https://doi.org/10.1186/s12876-014-0189-7

Bjarnason, I., Macpherson, A., and Hollander, D. (1995). Intestinal permeability: An overview. *Gastroenterology*, *108*(5), 1566–1581. https://doi.org/10.1016/0016-5085(95)90708-4

Blümmel, M., Aiple, K. -P., Steingaβ, H., and Becker, K. (1999). A note on the stoichiometrical relationship of short chain fatty acid production and gas formation *in vitro* in feedstuffs of widely differing quality. *Journal of Animal Physiology and Animal Nutrition*, *81*(3), 157–167. https://doi.org/10.1046/j.1439-0396.1999.813205.x

Bohn T, Carriere F, Day L, Deglaire A, Egger L, *et al.* 2018. Correlation between *in vitro* and *in vivo* data on food digestion. What can we predict with static *in vitro* digestion models? Crit. Rev. Food Sci. Nutr. 58:2239–61

Bolyen, E., Rideout, J. R., Dillon, M. R., Bokulich, N. A., Abnet, C. C., Al-Ghalith, G. A., Alexander, H., Alm, E. J., Arumugam, M., Asnicar, F., Bai, Y., Bisanz, J. E., Bittinger, K., Brejnrod, A., Brislawn, C. J., Brown, C. T., Callahan, B. J., Caraballo-Rodríguez, A. M., Chase, J., … Caporaso, J. G. (2019). Reproducible, interactive, scalable and extensible microbiome data science using QIIME 2. *Nature Biotechnology*, *37*(8), 852–857. https://doi.org/10.1038/s41587-019-0209-9

Bomba, L., Minuti, A., Moisá, S. J., Trevisi, E., Eufemi, E., Lizier, M., Chegdani, F., Lucchini, F., Rzepus, M., Prandini, A., Rossi, F., Mazza, R., Bertoni, G., Loor, J. J., and Ajmone-Marsan, P. (2014a). Gut response induced by weaning in piglet features marked changes in immune and inflammatory response. *Functional and Integrative Genomics*, *14*(4), 657–671. https://doi.org/10.1007/s10142-014-0396-x

Bomba, L., Minuti, A., Moisá, S. J., Trevisi, E., Eufemi, E., Lizier, M., Chegdani, F., Lucchini, F., Rzepus, M., Prandini, A., Rossi, F., Mazza, R., Bertoni, G., Loor, J. J., and Ajmone-Marsan, P. (2014b). Gut response induced by weaning in piglet features marked changes in immune and inflammatory response. *Functional and Integrative Genomics*, *14*(4), 657–671. https://doi.org/10.1007/s10142-014-0396-x

Bornhorst, G.M., Singh, R.P., 2012. Bolus formation and disintegration during digestion of food carbohydrates. Compr. Rev. Food Sci. Food Saf. 11 (2), 101–118. https:// doi.org/10.1111/j.1541-4337.2011.00172.x

Boudry, C., Poelaert, C., Portetelle, D., Thewis, A., and Bindelle, J. (2012). Discrepancies in microbiota composition along the pig gastrointestinal tract between *in vivo* observations and an *in vitro* batch fermentation model1. *Journal of Animal Science*, *90*(suppl_4), 393–396. https://doi.org/10.2527/jas.53906

Boudry, G., Guérin, S., and Malbert, C. H. (2004). Effect of an abrupt switch from a milk-based to a fibre-based diet on gastric emptying rates in pigs: difference between origins of fibre. *British Journal of Nutrition*, *92*(6), 913–920. https://doi.org/10.1079/BJN20041271

Boudry, G., Péron, V., Le Huërou-Luron, I., Lallès, J. P., and Sève, B. (2004). Weaning Induces Both Transient and Long-Lasting Modifications of Absorptive, Secretory, and Barrier Properties of Piglet Intestine. *The Journal of Nutrition*, *134*(9), 2256–2262. https://doi.org/10.1093/jn/134.9.2256

Brandtzaeg, P. (2007). Induction of secretory immunity and memory at mucosal surfaces. *Vaccine*, *25*(30), 5467–5484. https://doi.org/10.1016/j.vaccine.2006.12.001

Brodkorb A, Egger L, Alminger M, Alvito P, Assunção R, *et al.* 2019. INFOGEST static *in vitro* simulation of gastrointestinal food digestion. Nat. Protoc. 14:991–1014

Bron, P. A., van Baarlen, P., and Kleerebezem, M. (2012). Emerging molecular insights into the interaction between probiotics and the host intestinal mucosa. *Nature Reviews Microbiology*, *10*(1), 66–78. https://doi.org/10.1038/nrmicro2690

Brooks, P. H., Moran, C. A., Beal, J. D., Demeckova, V., Campbell, A., Varley, M. A., and Wiseman, J. (2001). *Liquid feeding for the young piglet.* https://api.semanticscholar.org/CorpusID:82386631

Brown, D. C., Maxwell, C. V., Erf, G. F., Davis, M. E., Singh, S., and Johnson, Z. B. (2006). The influence of different management systems and age on intestinal morphology, immune cell numbers and mucin production from goblet cells in post-weaning pigs. *Veterinary Immunology and Immunopathology*, *111*(3–4), 187–198. https://doi.org/10.1016/j.vetimm.2005.12.006

Brown, E. M., Clardy, J. and Xavier R.J. 2023. Gut microbiome lipid metabolism and its impact on host physiology. Cell Host & Microbe 31, https://doi.org/10.1016/j.chom.2023.01.009

Budiño, F. E. L., Thomaz, M. C., Kronka, R. N., Nakaghi, L. S. O., Tucci, F. M., Fraga, A. L., Scandolera, A. J., and Huaynate, R. A. R. (2005). Effect of probiotic and prebiotic inclusion in weaned piglet diets on structure and ultra-structure of small intestine. *Brazilian Archives of Biology and Technology*, *48*(6), 921–929. https://doi.org/10.1590/S1516-89132005000800008

Byrne, C. S., Chambers, E. S., Preston, T., Tedford, C., Brignardello, J., Garcia-Perez, I., Holmes, E., Wallis, G. A., Morrison, D. J., and Frost, G. S. (2019). Effects of Inulin Propionate Ester Incorporated into Palatable Food Products on Appetite and Resting Energy Expenditure: A Randomised Crossover Study. *Nutrients*, *11*(4), 861. https://doi.org/10.3390/nu11040861

C. H., X., Chen, X., Ji, C., Ma, Q., and Hao, K. (2005). Study of the Application of Fructooligosaccharides in Piglets. *Asian-Australasian Journal of Animal Sciences*, *18*. https://doi.org/10.5713/ajas.2005.1011

Cai, X., Zhu, L., Chen, X., Sheng, Y., Guo, Q., Bao, J., and Xu, J. (2016). X/XO or H2O2 induced IPEC-J2 cell as a new *in vitro* model for studying apoptosis in post-weaning piglets. *Cytotechnology*, *68*(4), 713–724. https://doi.org/10.1007/s10616-014-9823-z

Callahan, B. J., McMurdie, P. J., Rosen, M. J., Han, A. W., Johnson, A. J. A., and Holmes, S. P. (2016). DADA2: High-resolution sample inference from Illumina amplicon data. *Nature Methods*, *13*(7), 581–583. https://doi.org/10.1038/nmeth.3869

Calvani, R., Miccheli, A., Capuani, G., Tomassini Miccheli, A., Puccetti, C., Delfini, M., Iaconelli, A., Nanni, G., and Mingrone, G. (2010). Gut microbiome-derived metabolites characterize a peculiar obese urinary metabotype. *International Journal of Obesity*, *34*(6), 1095–1098. https://doi.org/10.1038/ijo.2010.44

Campbell, J. M., Crenshaw, J. D., and Polo, J. (2013). The biological stress of early weaned piglets. *Journal of Animal Science and Biotechnology*, *4*(1), 19. https://doi.org/10.1186/2049-1891-4-19

Cani, P. D., Possemiers, S., Van de Wiele, T., Guiot, Y., Everard, A., Rottier, O., Geurts, L., Naslain, D., Neyrinck, A., Lambert, D. M., Muccioli, G. G., and Delzenne, N. M. (2009). Changes in gut microbiota control inflammation in obese mice through a mechanism involving GLP-2-driven improvement of gut permeability. *Gut*, *58*(8), 1091–1103. https://doi.org/10.1136/gut.2008.165886

Cao, K. F., Zhang, H. H., Han, H. H., Song, Y., Bai, X. L., and Sun, H. (2016). Effect of dietary protein sources on the small intestine microbiome of weaned piglets based on high-throughput sequencing. *Letters in Applied Microbiology*, *62*(5), 392–398. https://doi.org/10.1111/lam.12559

Capaldo, C. T., and Nusrat, A. (2009). Cytokine regulation of tight junctions. *Biochimica et Biophysica Acta (BBA) - Biomembranes*, *1788*(4), 864–871. https://doi.org/10.1016/j.bbamem.2008.08.027

Capuano, E. (2017a). The behaviour of dietary fiber in the gastrointestinal tract determines its physiological effect. *Critical Reviews in Food Science and Nutrition*, *57*(16), 3543–3564. https://doi.org/10.1080/10408398.2016.1180501

Capuano, E. (2017b). The behaviour of dietary fiber in the gastrointestinal tract determines its physiological effect. *Critical Reviews in Food Science and Nutrition*, *57*(16), 3543–3564. https://doi.org/10.1080/10408398.2016.1180501

Carazzone, C., Mascherpa, D., Gazzani, G., and Papetti, A. (2013). Identification of phenolic constituents in red chicory salads (Cichorium intybus) by high-performance liquid chromatography with diode array detection and electrospray ionisation tandem mass spectrometry. *Food Chemistry*, *138*(2–3), 1062–1071. https://doi.org/10.1016/j.foodchem.2012.11.060

Cario, E., Rosenberg, I. M., Brandwein, S. L., Beck, P. L., Reinecker, H.-C., and Podolsky, D. K. (2000). Lipopolysaccharide Activates Distinct Signalling Pathways in Intestinal Epithelial Cell Lines Expressing Toll-Like Receptors. *The Journal of Immunology*, *164*(2), 966–972. https://doi.org/10.4049/jimmunol.164.2.966

Carlson, J., Erickson, J., Hess, J., Gould, T., and Slavin, J. (2017). Prebiotic Dietary Fiber and Gut Health: Comparing the *in vitro* Fermentations of B--Glucan, Inulin and Xylooligosaccharide. *Nutrients*, *9*, 1361. https://doi.org/10.3390/nu9121361

Caron, J., Domenger, D., Dhulster, P., Ravallec, R., and Cudennec, B. (2017). Protein Digestion-Derived Peptides and the Peripheral Regulation of Food Intake. *Frontiers in Endocrinology*, *8*. https://doi.org/10.3389/fendo.2017.00085

Castillo, M., Martín-Orúe, S. M., Nofrarías, M., Manzanilla, E. G., and Gasa, J. (2007). Changes in caecal microbiota and mucosal morphology of weaned pigs. *Veterinary Microbiology*, *124*(3–4), 239–247. https://doi.org/10.1016/j.vetmic.2007.04.026

Catalioto, R.-M., A. Maggi, C., and Giuliani, S. (2011). Intestinal Epithelial Barrier Dysfunction in Disease and Possible Therapeutical Interventions. *Current Medicinal Chemistry*, *18*(3), 398–426. https://doi.org/10.2174/092986711794839179

Cavaglieri, L., Orlando, J., and Etcheverry, M. (2009). Rhizosphere microbial community structure at different maize plant growth stages and root locations. *Microbiological Research*, *164*(4), 391–399. https://doi.org/10.1016/j.micres.2007.03.006

Cera, K. R., Mahan, D. C., and Reinhart, G. A. (1990). Effect of weaning, week postweaning and diet composition on pancreatic and small intestinal luminal lipase response in young swine. *Journal of Animal Science*, *68*(2), 384. https://doi.org/10.2527/1990.682384x

Ceuppens S, Uyttendaele M, Drieskens K, Heyndrickx M, Rajkovic A, Boon N *et al* (2012) Survival and germination of Bacillus cereus spores without outgrowth or enterotoxin production during *in vitro* simulation of gastrointestinal transit. Appl Environ Microbiol 78:7698–7705

Chang, M., Zhao, Y., Qin, G., and Zhang, X. (2018). Fructo-Oligosaccharide Alleviates Soybean-Induced Anaphylaxis in Piglets by Modulating Gut Microbes. *Frontiers in Microbiology*, *9*. https://doi.org/10.3389/fmicb.2018.02769

Chen, H., Zhang, S., and Kim, S. W. (2020). Effects of supplemental xylanase on health of the small intestine in nursery pigs fed diets with corn distillers' dried grains with solubles. *Journal of Animal Science*, *98*(6). https://doi.org/10.1093/jas/skaa185

Chen, J., Gaikwad, V., Holmes, M., Murray, B., Povey, M., Wang, Y., Zhang, Y., 2011. Development of a simple model device for *in vitro* gastric digestion investigation. Food and Function 2 (3–4), 174–182. https://doi.org/10.1039/c0fo00159g

Chen, K., Chen, H., Faas, M. M., de Haan, B. J., Li, J., Xiao, P., Zhang, H., Diana, J., de Vos, P., and Sun, J. (2017a). Specific inulin-type fructan fibers protect against autoimmune diabetes by modulating gut immunity, barrier function, and microbiota homeostasis. *Molecular Nutrition and Food Research*, *61*(8). https://doi.org/10.1002/mnfr.201601006

Chen, K., Chen, H., Faas, M. M., de Haan, B. J., Li, J., Xiao, P., Zhang, H., Diana, J., de Vos, P., and Sun, J. (2017b). Specific inulin-type fructan fibers protect against autoimmune diabetes by modulating gut immunity, barrier function, and microbiota homeostasis. *Molecular Nutrition and Food Research*, *61*(8). https://doi.org/10.1002/mnfr.201601006

Chen, L., Xu, Y., Chen, X., Fang, C., Zhao, L., and Chen, F. (2017). The Maturing Development of Gut Microbiota in Commercial Piglets during the Weaning Transition. *Frontiers in Microbiology*, *8*. https://doi.org/10.3389/fmicb.2017.01688

Chen, T., Chen, D., Tian, G., Zheng, P., Mao, X., Yu, J., He, J., Huang, Z., Luo, Y., Luo, J., and Yu, B. (2019). Soluble Fiber and Insoluble Fiber Regulate Colonic Microbiota and Barrier Function in a Piglet Model. *BioMed Research International*, *2019*, 1–12. https://doi.org/10.1155/2019/7809171

Chen, T., Chen, D., Tian, G., Zheng, P., Mao, X., Yu, J., He, J., Huang, Z., Luo, Y., Luo, J., and Yu, B. (2020). Effects of soluble and insoluble dietary fiber supplementation on growth performance, nutrient digestibility, intestinal microbe and barrier function in weaning piglet. *Animal Feed Science and Technology*, *260*, 114335. https://doi.org/10.1016/j.anifeedsci.2019.114335

Chen, W., Mi, J., Lv, N., Gao, J., Cheng, J., Wu, R., Ma, J., Lan, T., and Liao, X. (2018). Lactation Stage-Dependency of the Sow Milk Microbiota. *Frontiers in Microbiology*, *9*. https://doi.org/10.3389/fmicb.2018.00945

Chen, X.-M., Elisia, I., and Kitts, D. D. (2010). Defining conditions for the co-culture of Caco-2 and HT-29-MTX cells using Taguchi design. *Journal of Pharmacological and Toxicological Methods*, *61*(3), 334–342. https://doi.org/10.1016/j.vascn.2010.02.004

Cheng, H., and Leblond, C. P. (1974). Origin, differentiation and renewal of the four main epithelial cell types in the mouse small intestine I. Columnar cell. *American Journal of Anatomy*, *141*(4), 461–479. https://doi.org/10.1002/aja.1001410403

Chen Y, Yang B, Ross RP, Jin Y, Stanton C, Zhao J, Zhang H, Chen W. Orally administered CLA ameliorates DSS-induced colitis in mice via intestinal barrier improvement, oxidative stress reduction, and inflammatory cytokine and gut microbiota modulation. J Agric Food Chem 2019;67:13282–13298.

Chi, X., Huang, M., Tu, H., Zhang, B., Lin, X., Xu, H., Dong, C., and Hu, X. (2023). Innate and adaptive immune abnormalities underlying autoimmune diseases: the genetic connections. *Science China Life Sciences*, *66*(7), 1482–1517. https://doi.org/10.1007/s11427-021-2187-3

Christa Schimpel, Birgit Teubl, Markus Absenger, Claudia Meindl, Eleonore Fröhlich, Gerd Leitinger, Andreas Zimmer, and Eva Roblegg. 2014. Development of an Advanced Intestinal *in vitro* Triple Culture Permeability Model To Study Transport of Nanoparticles. *Molecular Pharmaceutics 11* (3), 808-818. DOI: 10.1021/mp400507g

Christensen, B., and Huber, L.-A. (2022). The effects of creep feed composition and form and nursery diet complexity on small intestinal morphology and jejunal mucosa-specific enzyme activities after weaning in pigs. *Journal of Animal Science*, *100*(5). https://doi.org/10.1093/jas/skac138

Cordonnier, C., Thévenot, J., Etienne-Mesmin, L., Denis, S., Alric, M., Livrelli, V., and Blanquet-Diot, S. (2015). Dynamic *In vitro* Models of the Human Gastrointestinal Tract as Relevant Tools to Assess the Survival of Probiotic Strains and Their Interactions with Gut Microbiota. *Microorganisms*, *3*(4), 725–745. https://doi.org/10.3390/microorganisms3040725

Corridoni, D.; Pastorelli, L.; Mattioli, B.; Locovei, S.; Ishikawa, D.; Arseneau, K.O.; Chieppa, M.; Cominelli, F.; Pizarro, T.T. Probiotic Bacteria Regulate Intestinal Epithelial Permeability in Experimental Ileitis by a TNF-Dependent Mechanism. PLoS ONE 2012, 7, e42067

Corr, S.; Hill, C.; Gahan, C.G.M. An *in vitro* cell-culture model demonstrates internalin- and hemolysin-independent translocation of Listeria monocytogenes across M-cells. Microb. Pathog. 2006, 41, 241–250

Corrêa-Oliveira, R., Fachi, J. L., Vieira, A., Sato, F. T., and Vinolo, M. A. R. (2016). Regulation of immune cell function by short-chain fatty acids. *Clinical and Translational Immunology*, *5*(4). https://doi.org/10.1038/cti.2016.17

Costabile, A., Fava, F., Röytiö, H., Forssten, S. D., Olli, K., Klievink, J., Rowland, I. R., Ouwehand, A. C., Rastall, R. A., Gibson, G. R., and Walton, G. E. (2012). Impact of polydextrose on the faecal microbiota: a double-blind, crossover, placebo-controlled feeding study in healthy human subjects. *British Journal of Nutrition*, *108*(3), 471–481. https://doi.org/10.1017/S0007114511005782

Crank, C., and O'Driscoll, T. (2015). Vancomycin-resistant enterococcal infections: epidemiology, clinical manifestations, and optimal management. *Infection and Drug Resistance*, 217. https://doi.org/10.2147/IDR.S54125

Cremonesi, P., Biscarini, F., Castiglioni, B., Sgoifo, C. A., Compiani, R., and Moroni, P. (2022). Gut microbiome modifications over time when removing in-feed antibiotics from the prophylaxis of post-weaning diarrhoea in piglets. *PLOS ONE*, *17*(3), e0262199. https://doi.org/10.1371/journal.pone.0262199

Crooks B., Stamataki N.S., McLaughlin J.T. 2021. Appetite, the enteroendocrine system, gastrointestinal disease and obesity. Proc Nutr Soc. 80(1):50-58. https://doi.org/10.1017/S0029665120006965

Crost, E. H., Coletto, E., Bell, A., and Juge, N. (2023). *Ruminococcus gnavus* : friend or foe for human health. *FEMS Microbiology Reviews*, *47*(2). https://doi.org/10.1093/femsre/fuad014

Cui, J., Lian, Y., Zhao, C., Du, H., Han, Y., Gao, W., Xiao, H., and Zheng, J. (2019). Dietary Fibers from Fruits and Vegetables and Their Health Benefits via Modulation of Gut Microbiota. *Comprehensive Reviews in Food Science and Food Safety*, *18*(5), 1514–1532. https://doi.org/10.1111/1541-4337.12489

Cummings, J. H., Pomare, E. W., Branch, W. J., Naylor, C. P., and Macfarlane, G. T. (1987). Short chain fatty acids in human large intestine, portal, hepatic and venous blood. *Gut*, *28*(10), 1221–1227. https://doi.org/10.1136/gut.28.10.1221

Cunningham, M., Vinderola, G., Charalampopoulos, D., Lebeer, S., Sanders, M. E., and Grimaldi, R. (2021). Applying probiotics and prebiotics in new delivery formats – is the clinical evidence transferable? *Trends in Food Science and Technology*, *112*, 495–506. https://doi.org/10.1016/j.tifs.2021.04.009

Dahiya, D. K., Renuka, Puniya, M., Shandilya, U. K., Dhewa, T., Kumar, N., Kumar, S., Puniya, A. K., and Shukla, P. (2017). Gut Microbiota Modulation and Its Relationship with Obesity Using Prebiotic Fibers and Probiotics: A Review. *Frontiers in Microbiology*, *8*. https://doi.org/10.3389/fmicb.2017.00563

Daïen, C. I., Tan, J., Audo, R., Mielle, J., Quek, L. E., Krycer, J. R., Angelatos, A., Duraes, M., Pinget, G., Ni, D., Robert, R., Alam, M. J., Amian, M. C. B., Sierro, F., Parmar, A., Perkins, G., Hoque, S., Gosby, A. K., Simpson, S. J., … Macia, L. (2021). Gut-derived acetate promotes B10 cells with antiinflammatory effects. *JCI Insight*, *6*(7). https://doi.org/10.1172/jci.insight.144156

Davani-Davari, D., Negahdaripour, M., Karimzadeh, I., Seifan, M., Mohkam, M., Masoumi, S., Berenjian, A., and Ghasemi, Y. (2019). Prebiotics: Definition, Types, Sources, Mechanisms, and Clinical Applications. *Foods*, *8*(3), 92. https://doi.org/10.3390/foods8030092

Davis, M. E., Sears, S. C., Apple, J. K., Maxwell, C. V., and Johnson, Z. B. (2006). Effect of weaning age and commingling after the nursery phase of pigs in a wean-to-finish facility on growth, and humoral and behavioural indicators of well-being1,2. *Journal of Animal Science*, *84*(3), 743–756. https://doi.org/10.2527/2006.843743x

de Greeff, A., Resink, J. W., van Hees, H. M. J., Ruuls, L., Klaassen, G. J., Rouwers, S. M. G., and Stockhofe-Zurwieden, N. (2016). Supplementation of piglets with nutrient-dense complex milk replacer improves intestinal development and microbial fermentation1. *Journal of Animal Science*, *94*(3), 1012–1019. https://doi.org/10.2527/jas.2015-9481

de Groot, N., Fariñas, F., Cabrera-Gómez, C. G., Pallares, F. J., and Ramis, G. (2021). Weaning causes a prolonged but transient change in immune gene expression in the intestine of piglets. *Journal of Animal Science*, *99*(4). https://doi.org/10.1093/jas/skab065

de Kivit S, van Hoffen E, Korthagen N *et al* (2011) Apical TLR ligation of intestinal epithelial cells drives a Th1-polarized regulatory or infl ammatory type effector response *in vitro*. Immunobiology 216:518–527

de La Pomélie, D., Santé-Lhoutellier, V., Sayd, T., Théron, L., and Gatellier, P. (2019). Using a dynamic artificial digestive system to investigate heme iron nitrosylation during gastro-intestinal transit. *Food Chemistry*, *281*, 231–235. https://doi.org/10.1016/j.foodchem.2018.12.094

de Lange, C. F. M., Pluske, J., Gong, J., and Nyachoti, C. M. (2010). Strategic use of feed ingredients and feed additives to stimulate gut health and development in young pigs. *Livestock Science*, *134*(1–3), 124–134. https://doi.org/10.1016/j.livsci.2010.06.117

Derricott, H.; Luu, L.; Fong, W.Y.; Hartley, C.S.; Johnston, L.J.; Armstrong, S.D.; Randle, N.; Duckworth, C.A.; Campbell, B.J.; Wastling, J.M.; *et al*. Developing a 3D intestinal epithelium model for livestock species. Cell Tissue Res. 2019, 375, 409–424.

De Vuyst, L., and Leroy, F. (2011). Cross-feeding between bifidobacteria and butyrate-producing colon bacteria explains bifdobacterial competitiveness, butyrate production, and gas production. *International Journal of Food Microbiology*, *149*(1), 73–80. https://doi.org/10.1016/j.ijfoodmicro.2011.03.003

De Vuyst, L., Moens, F., Selak, M., Rivière, A., and Leroy, F. (2014). Summer Meeting 2013: growth and physiology of bifidobacteria. *Journal of Applied Microbiology*, *116*(3), 477–491. https://doi.org/10.1111/jam.12415

Deglaire, A., and Moughan, P. J. (2012). Animal models for determining amino acid digestibility in humans – a review. *British Journal of Nutrition*, *108*(S2), S273–S281. https://doi.org/10.1017/S0007114512002346

Deplancke, B., and Gaskins, H. R. (2001). Microbial modulation of innate defence: goblet cells and the intestinal mucus layer. *The American Journal of Clinical Nutrition*, *73*(6), 1131S-1141S. https://doi.org/10.1093/ajcn/73.6.1131S

Dewulf, E. M., Cani, P. D., Claus, S. P., Fuentes, S., Puylaert, P. G., Neyrinck, A. M., Bindels, L. B., de Vos, W. M., Gibson, G. R., Thissen, J.-P., and Delzenne, N. M. (2013). Insight into the prebiotic concept: lessons from an exploratory, double blind intervention study with inulin-type fructans in obese women. *Gut*, *62*(8), 1112–1121. https://doi.org/10.1136/gutjnl-2012-303304

Diao, H., Jiao, A. R., Yu, B., Mao, X. B., and Chen, D. W. (2019). Gastric infusion of short-chain fatty acids can improve intestinal barrier function in weaned piglets. *Genes and Nutrition*, *14*(1), 4. https://doi.org/10.1186/s12263-019-0626-x

Dinh, D. M., Volpe, G. E., Duffalo, C., Bhalchandra, S., Tai, A. K., Kane, A. V., Wanke, C. A., and Ward, H. D. (2015). Intestinal Microbiota, Microbial Translocation, and Systemic Inflammation in Chronic HIV Infection. *Journal of Infectious Diseases*, *211*(1), 19–27. https://doi.org/10.1093/infdis/jiu409

Dinis, M., Plainvert, C., Kovarik, P., Longo, M., Fouet, A., and Poyart, C. (2014). The Innate Immune Response Elicited by Group A Streptococcus Is Highly Variable among Clinical Isolates and Correlates with the emm Type. *PLoS ONE*, *9*(7), e101464. https://doi.org/10.1371/journal.pone.0101464

Dodd, D., Mackie, R. I., and Cann, I. K. O. (2011). Xylan degradation, a metabolic property shared by rumen and human colonic Bacteroidetes. *Molecular Microbiology*, *79*(2), 292–304. https://doi.org/10.1111/j.1365-2958.2010.07473.x

Dominguez-Bello, M. G., Blaser, M. J., Ley, R. E., and Knight, R. (2011). Development of the Human Gastrointestinal Microbiota and Insights From High-Throughput Sequencing. *Gastroenterology*, *140*(6), 1713–1719. https://doi.org/10.1053/j.gastro.2011.02.011

Dou, S., Gadonna-Widehem, P., Rome, V., Hamoudi, D., Rhazi, L., Lakhal, L., Larcher, T., Bahi-Jaber, N., Pinon-Quintana, A., Guyonvarch, A., Huërou-Luron, I. L. E., and Abdennebi-Najar, L. (2017). Characterisation of Early-Life Fecal Microbiota in Susceptible and Healthy Pigs to Post-weaning Diarrhoea. *PLOS ONE*, *12*(1), e0169851. https://doi.org/10.1371/journal.pone.0169851

Duarte, M. E., Zhou, F. X., Dutra, W. M., and Kim, S. W. (2019). Dietary supplementation of xylanase and protease on growth performance, digesta viscosity, nutrient digestibility, immune and oxidative stress status, and gut health of newly weaned pigs. *Animal Nutrition*, *5*(4), 351–358. https://doi.org/10.1016/j.aninu.2019.04.005

Dupont, D., Alric, M., Blanquet-Diot, S., Bornhorst, G., Cueva, C., Deglaire, A., Denis, S., Ferrua, M., Havenaar, R., Lelieveld, J., Mackie, A. R., Marzorati, M., Menard, O., Minekus, M., Miralles, B., Recio, I., and Van den Abbeele, P. (2019). Can dynamic *in vitro* digestion systems mimic the physiological reality? *Critical Reviews in Food Science and Nutrition*, *59*(10), 1546–1562. https://doi.org/10.1080/10408398.2017.1421900

Durcan, C., Hossain, M., Chagnon, G., Perić, D., and Girard, E. (2024). Mechanical experimentation of the gastrointestinal tract: a systematic review. *Biomechanics and Modeling in Mechanobiology*, *23*(1), 23–59. https://doi.org/10.1007/s10237-023-01773-8

Eberhard, M., Hennig, U., Kuhla, S., Brunner, R. M., Kleessen, B., and Metges, C. C. (2007). Effect of inulin supplementation on selected gastric, duodenal, and caecal microbiota and short chain fatty acid pattern in growing piglets. *Archives of Animal Nutrition*, *61*(4), 235–246. https://doi.org/10.1080/17450390701431631

Egger L, Schlegel P, Baumann C, Stoffers H, Guggisberg D, *et al.* 2017. Physiological comparability of the harmonized INFOGEST *in vitro* digestion method to *in vivo* pig digestion. Food Res. Int. 102:567–74

Egger L, Ménard O, Baumann C, Duerr D, Schlegel P, *et al.* 2019. Digestion of milk proteins: comparing static and dynamic *in vitro* digestion systems with *in vivo* data. Food Res. Int. 118:32–39

EL Andaloussi, S., Mäger, I., Breakefield, X. O., and Wood, M. J. A. (2013). Extracellular vesicles: biology and emerging therapeutic opportunities. *Nature Reviews Drug Discovery*, *12*(5), 347–357. https://doi.org/10.1038/nrd3978

Elshahed, M. S., Miron, A., Aprotosoaie, A. C., and Farag, M. A. (2021). Pectin in diet: Interactions with the human microbiome, role in gut homeostasis, and nutrient-drug interactions. *Carbohydrate Polymers*, *255*, 117388. https://doi.org/10.1016/j.carbpol.2020.117388

Englyst, H. N., and Cummings, J. H. (1984). Simplified method for the measurement of total non-starch polysaccharides by gas-liquid chromatography of constituent sugars as alditol acetates. *Analyst*, *109*(7), 937–942. https://doi.org/10.1039/AN9840900937

Estrada, A., Drew, M., and Van Kessel, A. (2001). Effect of the dietary supplementation of fructooligosaccharides and Bifidobacterium longum to early-weaned pigs on performance and fecal bacterial populations. *Canadian Journal of Animal Science*, *81*, 141–148.

European Animal Research Association. (2024). *Pigs and biomedical research*. Https://Www.Eara.Eu/Pigs-and-Animal-Research. https://www.eara.eu/pigs-and-animal-research

European Commission. (2017). Commission Implementing Decision of 26.6.2017 Concerning, in the Framework of Article 35 of Directive 2001/82/EC of the European Parliament and of the Council, the Marketing Authorisations for Veterinary Medicinal Products Containing "Zinc Oxide" to be Ad; Official Journal of the European Union: Brussels, Belgium, 2017.

Everaert, N., Van Cruchten, S., Weström, B., Bailey, M., Van Ginneken, C., Thymann, T., and Pieper, R. (2017). A review on early gut maturation and colonization in pigs, including biological and dietary factors affecting gut homeostasis. *Animal Feed Science and Technology*, *233*, 89–103. https://doi.org/10.1016/j.anifeedsci.2017.06.011

Fairbrother, J. M., Nadeau, É., Bélanger, L., Tremblay, C.-L., Tremblay, D., Brunelle, M., Wolf, R., Hellmann, K., and Hidalgo, Á. (2017). Immunogenicity and protective efficacy of a single-dose live non-pathogenic Escherichia coli oral vaccine against F4-positive enterotoxigenic Escherichia coli challenge in pigs. *Vaccine*, *35*(2), 353–360. https://doi.org/10.1016/j.vaccine.2016.11.045

Feng, Y.; Bommer, G.T.; Zhao, J.; Green, M.; Sands, E.; Zhai, Y.; Brown, K.; Burberry, A.; Cho, K.R.; Fearon, E.R. Mutant Kras Promotes Hyperplasia and Alters Differentiation in the Colon Epithelium but Does Not Expand the Presumptive Stem Cell Pool. Gastroenterology 2011, 141, 1003–1013.

Ferioli, F., and D'Antuono, L. (2012). An update procedure for an effective and simultaneous extraction of sesquiterpene lactones and phenolics from chicory. *Food Chemistry*, *135*, 243–250. https://doi.org/10.1016/j.foodchem.2012.04.079

Fleury, L., Deracinois, B., Dugardin, C., Nongonierma, A. B., FitzGerald, R. J., Flahaut, C., Cudennec, B., and Ravallec, R. (2022). *In vivo* and *In vitro* Comparison of the DPP-IV Inhibitory Potential of Food Proteins from Different Origins after Gastrointestinal Digestion. *International Journal of Molecular Sciences*, *23*(15), 8365. https://doi.org/10.3390/ijms23158365

Fleury, M. A., Le Goff, O., Denis, S., Chaucheyras-Durand, F., Jouy, E., Kempf, I., Alric, M., and Blanquet-Diot, S. (2017). Development and validation of a new dynamic *in vitro* model of the piglet colon (PigutIVM): application to the study of probiotics. *Applied Microbiology and Biotechnology*, *101*(6), 2533–2547. https://doi.org/10.1007/s00253-017-8122-y

Flint, H. J., and Bayer, E. A. (2008). *Plant Cell Wall Breakdown by Anaerobic Microorganisms from the Mammalian Digestive Tract*. *Annals of the New York Academy of Sciences*, *1125*(1), 280–288. https://doi.org/10.1196/annals.1419.022

Forder, R. E. A., Howarth, G. S., Tivey, D. R., and Hughes, R. J. (2007). Bacterial Modulation of Small Intestinal Goblet Cells and Mucin Composition During Early Posthatch Development of Poultry. *Poultry Science*, *86*(11), 2396–2403. https://doi.org/10.3382/ps.2007-00222

Fouhse, J., Zijlstra, R. T., and Willing, B. (2016). The role of gut microbiota in the health and disease of pigs. *Animal Frontiers*, *6*, 30. https://doi.org/10.2527/af.2016-0031

Fouré, M., Dugardin, C., Foligné, B., Hance, P., Cadalen, T., Delcourt, A., Taminiau, B., Daube, G., Ravallec, R., Cudennec, B., Hilbert, J.-L., and Lucau-Danila, A. (2018). Chicory Roots for Prebiotics and Appetite Regulation: A Pilot Study in Mice. *Journal of Agricultural and Food Chemistry*, *66*(25), 6439–6449. https://doi.org/10.1021/acs.jafc.8b01055

Franck, A., and Leenheer, L. (2005). Inulin. In *Biopolymers online* (Vol. 6). https://doi.org/10.1002/3527600035.bpol6014

Frankič, T., Levart, A., and Salobir, J. (2010a). The effect of vitamin E and plant extract mixture composed of carvacrol, cinnamaldehyde and capsaicin on oxidative stress induced by high PUFA load in young pigs. *Animal*, *4*(4), 572–578. https://doi.org/10.1017/S1751731109991339

Frankič, T., Levart, A., and Salobir, J. (2010b). The effect of vitamin E and plant extract mixture composed of carvacrol, cinnamaldehyde and capsaicin on oxidative stress induced by high PUFA load in young pigs. *Animal*, *4*(4), 572–578. https://doi.org/10.1017/S1751731109991339

Frolova, L., Drastich, P., Rossmann, P., Klimesova, K., and Tlaskalova-Hogenova, H. (2008). Expression of Toll-like Receptor 2 (TLR2), TLR4, and CD14 in Biopsy Samples of Patients With Inflammatory Bowel Diseases: Upregulated Expression of TLR2 in Terminal Ileum of Patients With Ulcerative Colitis. *Journal of Histochemistry and Cytochemistry*, *56*(3), 267–274. https://doi.org/10.1369/jhc.7A7303.2007

García-Villalba, R., Vissenaekens, H., Pitart, J., Romo-Vaquero, M., Espín, J. C., Grootaert, C., Selma, M. V., Raes, K., Smagghe, G., Possemiers, S., Van Camp, J., and Tomas-Barberan, F. A. (2017). Gastrointestinal Simulation Model TWIN-SHIME Shows Differences between Human Urolithin-Metabotypes in Gut Microbiota Composition, Pomegranate Polyphenol Metabolism, and Transport along the Intestinal Tract. *Journal of Agricultural and Food Chemistry*, *65*(27), 5480–5493. https://doi.org/10.1021/acs.jafc.7b02049

Gautier, T.; Fahet, N.; Tamanai-Shacoori, Z.; Oliviero, N.; Blot, M.; Sauvager, A.; Burel, A.; Gall, S.D.-L.; Tomasi, S.; Blat, S.; *et al.* Roseburia intestinalis modulates PYY expression in a new a multicellular model including enteroendocrine cells. Microorganisms 2022, 10, 2263

Ge, P., Luo, Y., Okoye, C. S., Chen, H., Liu, J., Zhang, G., Xu, C., and Chen, H. (2020). Intestinal barrier damage, systemic inflammatory response syndrome, and acute lung injury: A troublesome trio for acute pancreatitis. *Biomedicine and Pharmacotherapy*, *132*, 110770. https://doi.org/10.1016/j.biopha.2020.110770

Ghosh Shweta, Caleb Samuel Whitley, Bodduluri Haribabu, and Venkatakrishna Rao Jala. 2017. Regulation of Intestinal Barrier Function by Microbial Metabolites. Cell Mol Gastroenterol Hepatol 2021; 11:1463–1482; https:// doi.org/10.1016/j.jcmgh.2021.02.007.

Gibson, G. R., Hutkins, R., Sanders, M. E., Prescott, S. L., Reimer, R. A., Salminen, S. J., Scott, K., Stanton, C., Swanson, K. S., Cani, P. D., Verbeke, K., and Reid, G. (2017). Expert consensus document: The International Scientific Association for Probiotics and Prebiotics (ISAPP) consensus statement on the definition and scope of prebiotics. *Nature Reviews Gastroenterology and Hepatology*, *14*(8), 491–502. https://doi.org/10.1038/nrgastro.2017.75

Goel, V., Chang, C., Slama, J. V, Barton, R., Bauer, R., Gahler, R., and Basu, T. K. (2002). Echinacea stimulates macrophage function in the lung and spleen of normal rats. *The Journal of Nutritional Biochemistry*, *13*(8), 487–492. https://doi.org/10.1016/S0955-2863(02)00190-0

Gong, J., Yu, H., Liu, T., Li, M., Si, W., de Lange, C. F. M., and Dewey, C. (2008). Characterization of ileal bacterial microbiota in newly-weaned pigs in response to feeding lincomycin, organic acids or herbal extract. *Livestock Science*, *116*(1–3), 318–322. https://doi.org/10.1016/j.livsci.2008.01.001

Gou, H.-Z., Zhang, Y.-L., Ren, L.-F., Li, Z.-J., and Zhang, L. (2022). How do intestinal probiotics restore the intestinal barrier? *Frontiers in Microbiology*, *13*. https://doi.org/10.3389/fmicb.2022.929346

Gresse, R., Chaucheyras-Durand, F., Denis, S., Beaumont, M., Van de Wiele, T., Forano, E., and Blanquet-Diot, S. (2021). Weaning-associated feed deprivation stress causes microbiota disruptions in a novel mucin-containing *in vitro* model of the piglet colon (MPigut-IVM). *Journal of Animal Science and Biotechnology*, *12*(1), 75. https://doi.org/10.1186/s40104-021-00584-0

Gresse, R., Chaucheyras-Durand, F., Fleury, M. A., Van de Wiele, T., Forano, E., and Blanquet-Diot, S. (2017a). Gut Microbiota Dysbiosis in Postweaning Piglets: Understanding the Keys to Health. *Trends in Microbiology*, *25*(10), 851–873. https://doi.org/10.1016/j.tim.2017.05.004

Gresse, R., Chaucheyras-Durand, F., Fleury, M. A., Van de Wiele, T., Forano, E., and Blanquet-Diot, S. (2017b). Gut Microbiota Dysbiosis in Postweaning Piglets: Understanding the Keys to Health. *Trends in Microbiology*, *25*(10), 851–873. https://doi.org/10.1016/j.tim.2017.05.004

Gribble, F. M., and Reimann, F. (2019). Function and mechanisms of enteroendocrine cells and gut hormones in metabolism. *Nature Reviews Endocrinology*, *15*(4), 226–237. https://doi.org/10.1038/s41574-019-0168-8

Groschwitz, K. R., and Hogan, S. P. (2009). Intestinal barrier function: Molecular regulation and disease pathogenesis. *Journal of Allergy and Clinical Immunology*, *124*(1), 3–20. https://doi.org/10.1016/j.jaci.2009.05.038

Gross, M. (2013). Antibiotics in crisis. *Current Biology*, *23*(24), R1063–R1065. https://doi.org/10.1016/j.cub.2013.11.057

Grouls, M., van der Zande, M., de Haan, L., and Bouwmeester, H. (2022). Responses of increasingly complex intestinal epithelium *in vitro* models to bacterial toll-like receptor agonists. *Toxicology in vitro*, *79*, 105280. https://doi.org/10.1016/j.tiv.2021.105280

Guerra, A., Denis, S., le Goff, O., Sicardi, V., François, O., Yao, A., Garrait, G., Manzi, A. P., Beyssac, E., Alric, M., and Blanquet-Diot, S. (2016). Development and validation of a new dynamic computer-controlled model of the human stomach and small intestine. *Biotechnology and Bioengineering*, *113*(6), 1325–1335. https://doi.org/10.1002/bit.25890

Guevarra, R. B., Hong, S. H., Cho, J. H., Kim, B.-R., Shin, J., Lee, J. H., Kang, B. N., Kim, Y. H., Wattanaphansak, S., Isaacson, R. E., Song, M., and Kim, H. B. (2018). The dynamics of the piglet gut microbiome during the weaning transition in association with health and nutrition. *Journal of Animal Science and Biotechnology*, *9*(1), 54. https://doi.org/10.1186/s40104-018-0269-6

Guevarra, R. B., Lee, J. H., Lee, S. H., Seok, M.-J., Kim, D. W., Kang, B. N., Johnson, T. J., Isaacson, R. E., and Kim, H. B. (2019). Piglet gut microbial shifts early in life: causes and effects. *Journal of Animal Science and Biotechnology*, *10*(1), 1. https://doi.org/10.1186/s40104-018-0308-3

Gullberg E, Leonard M, Karlsson J *et al* (2000) Expression of specifi c markers and particle transport in a new human intestinal M-cell model. Biochem Biophys Res Commun 279:808–813

Gullón, B., Gómez, B., Martínez-Sabajanes, M., Yáñez, R., Parajó, J. C., and Alonso, J. L. (2013). Pectic oligosaccharides: Manufacture and functional properties. *Trends in Food Science and Technology*, *30*(2), 153–161. https://doi.org/10.1016/j.tifs.2013.01.006

Guo, Y., Yu, Y., Li, H., Ding, X., Li, X., Jing, X., Chen, J., Liu, G., Lin, Y., Jiang, C., Liu, Z., He, Y., Li, C., and Tian, Z. (2021). Inulin supplementation ameliorates hyperuricemia and modulates gut microbiota in Uox-knockout mice. *European Journal of Nutrition*, *60*(4), 2217–2230. https://doi.org/10.1007/s00394-020-02414-x

Haddad, M. J., Sztupecki, W., Delayre-Orthez, C., Rhazi, L., Barbezier, N., Depeint, F., and Anton, P. M. (2023). Complexification of *In vitro* Models of Intestinal Barriers, A True Challenge for a More Accurate Alternative Approach. *International Journal of Molecular Sciences*, *24*(4), 3595. https://doi.org/10.3390/ijms24043595

Halas, D., Hansen, C. F., Hampson, D. J., Mullan, B. P., Kim, J. C., Wilson, R. H., and Pluske, J. R. (2010). Dietary supplementation with benzoic acid improves apparent ileal digestibility of total nitrogen and increases villous height and caecal microbial diversity in weaner pigs. *Animal Feed Science and Technology*, *160*(3–4), 137–147. https://doi.org/10.1016/j.anifeedsci.2010.07.001

Halas, D., Hansen, C. F., Hampson, D. J., Mullan, B. P., Wilson, R. H., and Pluske, J. R. (2009). Effect of dietary supplementation with inulin and/or benzoic acid on the incidence and severity of post-weaning diarrhoea in weaner pigs after experimental challenge with enterotoxigenic *Escherichia coli*. *Archives of Animal Nutrition*, *63*(4), 267–280. https://doi.org/10.1080/17450390903020414

HAMER, H. M., JONKERS, D., VENEMA, K., VANHOUTVIN, S., TROOST, F. J., and BRUMMER, R. -J. (2008). Review article: the role of butyrate on colonic function. *Alimentary Pharmacology and Therapeutics*, *27*(2), 104–119. https://doi.org/10.1111/j.1365-2036.2007.03562.x

HAMPSON, D. J. (1986). Alterations in piglet small intestinal structure at weaning. *Research in Veterinary Science*, *40*(1), 32–40. https://doi.org/10.1016/S0034-5288(18)30482-X

Hankel, J., Chuppava, B., Wilke, V., Hartung, C. B., Muthukumarasamy, U., Strowig, T., Knudsen, K., Kamphues, J., and Visscher, C. (2022). High Dietary Intake of Rye Affects Porcine Gut Microbiota in a Salmonella Typhimurium Infection Study. *Plants*, *11*, 2232. https://doi.org/10.3390/plants11172232

He, J., Xie, H., Chen, D., Yu, B., Huang, Z., Mao, X., Zheng, P., Luo, Y., Yu, J., Luo, J., and Yan, H. (2021). Synergetic responses of intestinal microbiota and epithelium to dietary inulin supplementation in pigs. *European Journal of Nutrition*, *60*(2), 715–727. https://doi.org/10.1007/s00394-020-02284-3

Hedemann, M. S., Højsgaard, S., and Jensen, B. B. (2003). Small intestinal morphology and activity of intestinal peptidases in piglets around weaning. *Journal of Animal Physiology and Animal Nutrition*, *87*(1–2), 32–41. https://doi.org/10.1046/j.1439-0396.2003.00405.x

Hedemann, M. S., Højsgaard, S., and Jensen, B. B. (2007). Lectin histochemical characterisation of the porcine small intestine around weaning. *Research in Veterinary Science*, *82*(2), 257–262. https://doi.org/10.1016/j.rvsc.2006.06.007

Heo, J. M., Opapeju, F. O., Pluske, J. R., Kim, J. C., Hampson, D. J., and Nyachoti, C. M. (2013). Gastrointestinal health and function in weaned pigs: a review of feeding strategies to control post-weaning diarrhoea without using in-feed antimicrobial compounds. *Journal of Animal Physiology and Animal Nutrition*, *97*(2), 207–237. https://doi.org/10.1111/j.1439-0396.2012.01284.x

Herfel, T. M., Jacobi, S. K., Lin, X., Fellner, V., Walker, D. C., Jouni, Z. E., and Odle, J. (2011). Polydextrose Enrichment of Infant Formula Demonstrates Prebiotic Characteristics by Altering Intestinal Microbiota, Organic Acid Concentrations, and Cytokine Expression in Suckling Piglets. *The Journal of Nutrition*, *141*(12), 2139–2145. https://doi.org/10.3945/jn.111.143727

Hermann-Bank, M. L., Skovgaard, K., Stockmarr, A., Strube, M. L., Larsen, N., Kongsted, H., Ingerslev, H.-C., Mølbak, L., and Boye, M. (2015). Characterization of the bacterial gut microbiota of piglets suffering from new neonatal porcine diarrhoea. *BMC Veterinary Research*, *11*(1), 139. https://doi.org/10.1186/s12917-015-0419-4

Hernandez, A., Hansen, C. F., Mullan, B. P., and Pluske, J. R. (2009). l-arginine supplementation of milk liquid or dry diets fed to pigs after weaning has a positive effect on production in the first three weeks after weaning at 21 days of age. *Animal Feed Science and Technology*, *154*(1–2), 102–111. https://doi.org/10.1016/j.anifeedsci.2009.08.007

Hernot, D. C., Boileau, T. W., Bauer, L. L., Middelbos, I. S., Murphy, M. R., Swanson, K. S., and Fahey, G. C. (2009). *In vitro* Fermentation Profiles, Gas Production Rates, and Microbiota Modulation as Affected by Certain Fructans, Galactooligosaccharides, and Polydextrose. *Journal of Agricultural and Food Chemistry*, *57*(4), 1354–1361. https://doi.org/10.1021/jf802484j

Herosimczyk, A., Lepczyński, A., Ożgo, M., Barszcz, M., Marynowska, M., Tuśnio, A., Taciak, M., Markulen, A., and Skomiał, J. (2018). Proteome changes in ileal mucosa of young pigs resulting from different levels of native chicory inulin in the diet. *Journal of Animal and Feed Sciences*, *27*(3), 229–237. https://doi.org/10.22358/jafs/93737/2018

Herosimczyk, A., Lepczyński, A., Ożgo, M., Tuśnio, A., Taciak, M., and Barszcz, M. (2020). Effect of dietary inclusion of 1% or 3% of native chicory inulin on the large intestinal mucosa proteome of growing pigs. *Animal*, *14*(8), 1647–1658. https://doi.org/10.1017/S1751731120000440

Herrera, P., Kwon, Y. M., and Ricke, S. C. (2009). Ecology and pathogenicity of gastrointestinal Streptococcus bovis. *Anaerobe*, *15*(1–2), 44–54. https://doi.org/10.1016/j.anaerobe.2008.11.003

Hidalgo IJ (1996) Cultured intestinal epithelial cell models. Pharm Biotechnol 8:35–50

Hiel, S., Gianfrancesco, M. A., Rodriguez, J., Portheault, D., Leyrolle, Q., Bindels, L. B., Gomes da Silveira Cauduro, C., Mulders, M. D. G. H., Zamariola, G., Azzi, A.-S., Kalala, G., Pachikian, B. D., Amadieu, C., Neyrinck, A. M., Loumaye, A., Cani, P. D., Lanthier, N., Trefois, P., Klein, O., … Delzenne, N. M. (2020). Link between gut microbiota and health outcomes in inulin -treated obese patients: Lessons from the Food4Gut multicentre randomized placebo-controlled trial. *Clinical Nutrition*, *39*(12), 3618–3628. https://doi.org/10.1016/j.clnu.2020.04.005

HINO, S., ITO, H., BITO, H., KAWAGISHI, H., and MORITA, T. (2011). Ameliorating Effects of Short-Chain Inulin-Like Fructans on the Healing Stage of Trinitrobenzene Sulfonic Acid-Induced Colitis in Rats. *Bioscience, Biotechnology, and Biochemistry*, *75*(11), 2169–2174. https://doi.org/10.1271/bbb.110460

Hodgkinson, K., El Abbar, F., Dobranowski, P., Manoogian, J., Butcher, J., Figeys, D., Mack, D., and Stintzi, A. (2023a). Butyrate's role in human health and the current progress towards its clinical application to treat gastrointestinal disease. *Clinical Nutrition*, *42*(2), 61–75. https://doi.org/10.1016/j.clnu.2022.10.024

Hodgkinson, K., El Abbar, F., Dobranowski, P., Manoogian, J., Butcher, J., Figeys, D., Mack, D., and Stintzi, A. (2023b). Butyrate's role in human health and the current progress towards its clinical application to treat gastrointestinal disease. *Clinical Nutrition*, *42*(2), 61–75. https://doi.org/10.1016/j.clnu.2022.10.024

Højberg, O., Canibe, N., Poulsen, H. D., Hedemann, M. S., and Jensen, B. B. (2005). Influence of Dietary Zinc Oxide and Copper Sulfate on the Gastrointestinal Ecosystem in Newly Weaned Piglets. *Applied and Environmental Microbiology*, *71*(5), 2267–2277. https://doi.org/10.1128/AEM.71.5.2267-2277.2005

Holscher, H. D. (2017). Dietary fiber and prebiotics and the gastrointestinal microbiota. *Gut Microbes*, *8*(2), 172–184. https://doi.org/10.1080/19490976.2017.1290756

Holscher, H. D., Bauer, L. L., Gourineni, V., Pelkman, C. L., Fahey, G. C., and Swanson, K. S. (2015). Agave Inulin Supplementation Affects the Fecal Microbiota of Healthy Adults Participating in a Randomized, Double-Blind, Placebo-Controlled, Crossover Trial1–3. *The Journal of Nutrition*, *145*(9), 2025–2032. https://doi.org/10.3945/jn.115.217331

Horwitz, W. , and L. G. W. (2010). *AOAC International, . Official methods of analysis of AOAC International (18th ed., 2005, revision 3). AOAC International.*

Horowitz, A., Chanez-Paredes, S.D., Haest, X. *et al.* Paracellular permeability and tight junction regulation in gut health and disease. *Nat Rev Gastroenterol Hepatol* **20**, 417–432 (2023). https://doi.org/10.1038/s41575-023-00766-3

Hossain, M. M., Park, J. W., and Kim, I. H. (2016). δ-Aminolevulinic acid, and lactulose supplements in weaned piglets diet: Effects on performance, fecal microbiota, and in-vitro noxious gas emissions. *Livestock Science*, *183*, 84–91. https://doi.org/10.1016/j.livsci.2015.11.021

Hou, L., Wang, J., Zhang, W., Quan, R., Wang, D., Zhu, S., Jiang, H., Wei, L., and Liu, J. (2020). Dynamic Alterations of Gut Microbiota in Porcine Circovirus Type 3-Infected Piglets. *Frontiers in Microbiology*, *11*. https://doi.org/10.3389/fmicb.2020.01360

Hu, C. H., Xiao, K., Luan, Z. S., and Song, J. (2013a). Early weaning increases intestinal permeability, alters expression of cytokine and tight junction proteins, and activates mitogen-activated protein kinases in pigs1. *Journal of Animal Science*, *91*(3), 1094–1101. https://doi.org/10.2527/jas.2012-5796

Hu, C. H., Xiao, K., Luan, Z. S., and Song, J. (2013b). Early weaning increases intestinal permeability, alters expression of cytokine and tight junction proteins, and activates mitogen-activated protein kinases in pigs1. *Journal of Animal Science*, *91*(3), 1094–1101. https://doi.org/10.2527/jas.2012-5796

Hu, S. X., Benner, C. P., and Fuller, T. E. (2023). Correlation of lactulose-to-mannitol ratios in plasma and urine for intestinal permeability assessment in pigs. *American Journal of Veterinary Research*, 1–7. https://doi.org/10.2460/ajvr.23.01.0002

Huang, C., Qiao, S., Li, D., Piao, X., and Ren, J. (2004). Effects of Lactobacilli on the Performance, Diarrhoea Incidence, VFA Concentration and Gastrointestinal Microbial Flora of Weaning Pigs. *Asian-Australasian Journal of Animal Sciences*, *17*(3), 401–409. https://doi.org/10.5713/ajas.2004.401

Hughes, R., Alvarado, D., Swanson, K., and Holscher, H. (2021). The Prebiotic Potential of Inulin-Type Fructans: A Systematic Review. *Advances in Nutrition (Bethesda, Md.)*, *13*. https://doi.org/10.1093/advances/nmab119

Huting, A. M. S., Middelkoop, A., Guan, X., and Molist, F. (2021). Using Nutritional Strategies to Shape the Gastro-Intestinal Tracts of Suckling and Weaned Piglets. *Animals*, *11*(2), 402. https://doi.org/10.3390/ani11020402

Isenring, J., Bircher, L., Geirnaert, A., and Lacroix, C. (2023). *In vitro* human gut microbiota fermentation models: opportunities, challenges, and pitfalls. *Microbiome Research Reports*, *2*(1), 2. https://doi.org/10.20517/mrr.2022.15

Ishimoto Y, Satsu H, Totsuka M *et al* (2011) IEX-1 suppresses apoptotic damage in human intestinal epithelial Caco-2 cells induced by co-culturing with macrophage-like THP-1 cells. Biosci Rep 31:345–351

Jacinta D. Bus, Iris J.M.M. Boumans, Dennis E. te Beest, Laura E. Webb, J. Elizabeth Bolhuis, Eddie A.M. Bokkers. 2024.Understanding the feeding strategies of growing-finishing pigs: Exploring links with pig characteristics and behaviour,Applied Animal Behaviour Science, Volume 272, 106208, ISSN 0168-1591, https://doi.org/10.1016/j.applanim.2024.106208.

Jamar, G., Ribeiro, D. A., and Pisani, L. P. (2021). High-fat or high-sugar diets as trigger inflammation in the microbiota-gut-brain axis. *Critical Reviews in Food Science and Nutrition*, *61*(5), 836–854. https://doi.org/10.1080/10408398.2020.1747046

Jang, K. B., and Kim, S. W. (2019). Supplemental effects of dietary nucleotides on intestinal health and growth performance of newly weaned pigs. *Journal of Animal Science*, *97*(12), 4875–4882. https://doi.org/10.1093/jas/skz334

Jang, S., Hyam, S. R., Jeong, J., Han, M. J., and Kim, D. (2013). Penta- O-galloyl- β- D-glucose ameliorates inflammation by inhibiting MyD88/ NFκB and MyD88/MAPK signalling pathways. *British Journal of Pharmacology*, *170*(5), 1078–1091. https://doi.org/10.1111/bph.12333

Jang, Y. J., Kim, W.-K., Han, D. H., Lee, K., and Ko, G. (2019). *Lactobacillus fermentum* species ameliorate dextran sulfate sodium-induced colitis by regulating the immune response and altering gut microbiota. *Gut Microbes*, *10*(6), 696–711. https://doi.org/10.1080/19490976.2019.1589281

Jensen, A. N., Mejer, H., Mølbak, L., Langkjær, M., Jensen, T. K., Angen, Ø., Martinussen, T., Klitgaard, K., Baggesen, D. L., Thamsborg, S. M., and Roepstorff, A. (2011). The effect of a diet with fructan-rich chicory roots on intestinal helminths and microbiota with special focus on Bifidobacteria and Campylobacter in piglets around weaning. *Animal*, *5*(6), 851–860. https://doi.org/10.1017/S175173111000251X

JENSEN, G., FRYDENDAHL, K., SVENDSEN, O., JORGENSEN, C., CIRERA, S., FREDHOLM, M., NIELSEN, J., and MOLLER, K. (2006). Experimental infection with Escherichia coli O149:F4ac in weaned piglets. *Veterinary Microbiology*, *115*(1–3), 243–249. https://doi.org/10.1016/j.vetmic.2006.01.002

Jensen-Waern, M., Melin, L., Lindberg, R., Johannisson, A., Petersson, L., and Wallgren, P. (1998). Dietary zinc oxide in weaned pigs — effects on performance, tissue concentrations, morphology, neutrophil functions and faecal microflora. *Research in Veterinary Science*, *64*(3), 225–231. https://doi.org/10.1016/S0034-5288(98)90130-8

Jha, R., and Berrocoso, J. F. D. (2016). Dietary fiber and protein fermentation in the intestine of swine and their interactive effects on gut health and on the environment: A review. *Animal Feed Science and Technology*, *212*, 18–26. https://doi.org/10.1016/j.anifeedsci.2015.12.002

Jia, L., Xue, K., Liu, J., Habotta, O. A., Hu, L., Abdel Moneim, A. E., and Caccamo, D. (2020). Anticolitic Effect of Berberine in Rat Experimental Model: Impact of PGE2/p38 MAPK Pathways. *Mediators of Inflammation*, *2020*, 1–12. https://doi.org/10.1155/2020/9419085

Jiang, Z.-F., Gou, X.-F., and Wang, T.-G. (2020). Role of the Complex Interface Between Bi $_2$ Sr $_2$ CaCu $_2$ O $_x$ Filaments and the Ag Matrix in the Mechanical and Electrical Behaviours of Composite Round Wires. *IEEE Transactions on Applied Superconductivity*, *30*(6), 1–11. https://doi.org/10.1109/TASC.2020.2989611

Johansson, M. E. V., and Hansson, G. C. (2011). Keeping Bacteria at a Distance. *Science*, *334*(6053), 182–183. https://doi.org/10.1126/science.1213909

Johansson, M. E. V., Phillipson, M., Petersson, J., Velcich, A., Holm, L., and Hansson, G. C. (2008). The inner of the two Muc2 mucin-dependent mucus layers in colon is devoid of bacteria. *Proceedings of the National Academy of Sciences*, *105*(39), 15064–15069. https://doi.org/10.1073/pnas.0803124105

Johansson, M. E. V., Sjövall, H., and Hansson, G. C. (2013). The gastrointestinal mucus system in health and disease. *Nature Reviews Gastroenterology and Hepatology*, *10*(6), 352–361. https://doi.org/10.1038/nrgastro.2013.35

Juhász, Á., Molnár-Nagy, V., Bata, Z., Tso, K.-H., Mayer, Z., and Posta, K. (2022). Alternative to ZnO to establish balanced intestinal microbiota for weaning piglets. *PLOS ONE*, *17*(3), e0265573. https://doi.org/10.1371/journal.pone.0265573

Jung, T.-H., Jeon, W.-M., and Han, K.-S. (2015). *In vitro* Effects of Dietary Inulin on Human Fecal Microbiota and Butyrate Production. *Journal of Microbiology and Biotechnology*, *25*(9), 1555–1558. https://doi.org/10.4014/jmb.1505.05078

Juśkiewicz, J., Zduńczyk, Z., Żary-Sikorska, E., Król, B., Milala, J., and Jurgoński, A. (2011). Effect of the dietary polyphenolic fraction of chicory root, peel, seed and leaf extracts on caecal fermentation and blood parameters in rats fed diets containing prebiotic fructans. *British Journal of Nutrition*, *105*(5), 710–720. https://doi.org/10.1017/S0007114510004344

Kaakoush, N. O. (2015a). Insights into the Role of Erysipelotrichaceae in the Human Host. *Frontiers in Cellular and Infection Microbiology*, *5*. https://doi.org/10.3389/fcimb.2015.00084

Kaakoush, N. O. (2015b). Insights into the Role of Erysipelotrichaceae in the Human Host. *Frontiers in Cellular and Infection Microbiology*, *5*. https://doi.org/10.3389/fcimb.2015.00084

Kämpfer, A. A. M., Urbán, P., Gioria, S., Kanase, N., Stone, V., and Kinsner-Ovaskainen, A. (2017). Development of an *in vitro* co-culture model to mimic the human intestine in healthy and diseased state. *Toxicology in vitro*, *45*, 31–43. https://doi.org/10.1016/j.tiv.2017.08.011

Karasova, D., Crhanova, M., Babak, V., Jerabek, M., Brzobohaty, L., Matesova, Z., and Rychlik, I. (2021). Development of piglet gut microbiota at the time of weaning influences development of postweaning diarrhoea – A field study. *Research in Veterinary Science*, *135*, 59–65. https://doi.org/10.1016/j.rvsc.2020.12.022

Karioti, A., Skaltsa, H., Zhang, X., Tonge, P. J., Perozzo, R., Kaiser, M., Franzblau, S. G., and Tasdemir, D. (2008). Inhibiting enoyl-ACP reductase (FabI) across pathogenic microorganisms by linear sesquiterpene lactones from Anthemis auriculata. *Phytomedicine: International Journal of Phytotherapy and Phytopharmacology*, *15*, 1125+. https://link.gale.com/apps/doc/A191955985/HRCA?u=anon~eff0976fandsid=googleScholarandxid=26bdd797

Kassab, R. B., Elbaz, M., Oyouni, A. A. A., Mufti, A. H., Theyab, A., Al-Brakati, A., Mohamed, H. A., Hebishy, A. M. S., Elmallah, M. I. Y., Abdelfattah, M. S., and Abdel Moneim, A. E. (2022). Anticolitic activity of prodigiosin loaded with selenium nanoparticles on acetic acid–induced colitis in rats. *Environmental Science and Pollution Research*, *29*(37), 55790–55802. https://doi.org/10.1007/s11356-022-19747-1

Kassinen, A., Krogius-Kurikka, L., Mäkivuokko, H., Rinttilä, T., Paulin, L., Corander, J., Malinen, E., Apajalahti, J., and Palva, A. (2007). The Fecal Microbiota of Irritable Bowel Syndrome Patients Differs Significantly From That of Healthy Subjects. *Gastroenterology*, *133*(1), 24–33. https://doi.org/10.1053/j.gastro.2007.04.005

Kayama, H., Okumura, R., and Takeda, K. (2020). Interaction Between the Microbiota, Epithelia, and Immune Cells in the Intestine. *Annual Review of Immunology*, *38*(1), 23–48. https://doi.org/10.1146/annurev-immunol-070119-115104

Kerneis S, Bogdanova A, Kraehenbuhl JP *et al* (1997) Conversion by Peyer's patch lymphocytes of human enterocytes into M cells that transport bacteria. Science 277:949–952

Kesisoglou, F.; Schmiedlin-Ren, P.; Fleisher, D.; Zimmermann, E.M. Adenoviral transduction of enterocytes and M-Cells using *in vitro* models based on Caco-2 cells: The Coxsackievirus and Adenovirus Receptor (CAR) mediates both apical and basolateral transduction. Mol. Pharm. 2010, 7, 619–629.

Khuenpet, K., Fukuoka, M., Jittanit, W., and Sirisansaneeyakul, S. (2017). Spray drying of inulin component extracted from Jerusalem artichoke tuber powder using conventional and ohmic-ultrasonic heating for extraction process. *Journal of Food Engineering*, *194*, 67–78. https://doi.org/10.1016/j.jfoodeng.2016.09.009

Kiernan, D. P., O'Doherty, J. V., and Sweeney, T. (2023a). The Effect of Prebiotic Supplements on the Gastrointestinal Microbiota and Associated Health Parameters in Pigs. *Animals*, *13*(19), 3012. https://doi.org/10.3390/ani13193012

Kiernan, D. P., O'Doherty, J. V., and Sweeney, T. (2023b). The Effect of Prebiotic Supplements on the Gastrointestinal Microbiota and Associated Health Parameters in Pigs. *Animals*, *13*(19), 3012. https://doi.org/10.3390/ani13193012

Kies, A. K., Kemme, P. A., Šebek, L. B. J., van Diepen, J. Th. M., and Jongbloed, A. W. (2006). Effect of graded doses and a high dose of microbial phytase on the digestibility of various minerals in weaner pigs1. *Journal of Animal Science*, *84*(5), 1169–1175. https://doi.org/10.2527/2006.8451169x

Kim, H. B., Borewicz, K., White, B. A., Singer, R. S., Sreevatsan, S., Tu, Z. J., and Isaacson, R. E. (2011). Longitudinal investigation of the age-related bacterial diversity in the faeces of commercial pigs. *Veterinary Microbiology*, *153*(1–2), 124–133. https://doi.org/10.1016/j.vetmic.2011.05.021

Kim, H. B., and Isaacson, R. E. (2015). The pig gut microbial diversity: Understanding the pig gut microbial ecology through the next generation high throughput sequencing. *Veterinary Microbiology*, *177*(3–4), 242–251. https://doi.org/10.1016/j.vetmic.2015.03.014

Kim, S. W., Holanda, D. M., Gao, X., Park, I., and Yiannikouris, A. (2019a). Efficacy of a Yeast Cell Wall Extract to Mitigate the Effect of Naturally Co-Occurring Mycotoxins Contaminating Feed Ingredients Fed to Young Pigs: Impact on Gut Health, Microbiome, and Growth. *Toxins*, *11*(11), 633. https://doi.org/10.3390/toxins11110633

Kim, S. W., van Heugten, E., Ji, F., Lee, C. H., and Mateo, R. D. (2010). Fermented soybean meal as a vegetable protein source for nursery pigs: I. Effects on growth performance of nursery pigs. *Journal of Animal Science*, *88*(1), 214–224. https://doi.org/10.2527/jas.2009-1993

Kim, Y. S., and Ho, S. B. (2010). Intestinal Goblet Cells and Mucins in Health and Disease: Recent Insights and Progress. *Current Gastroenterology Reports*, *12*(5), 319–330. https://doi.org/10.1007/s11894-010-0131-2

Kleessen, B., Schwarz, S., Boehm, A., Fuhrmann, H., Richter, A., Henle, T., and Krueger, M. (2007). Jerusalem artichoke and chicory inulin in bakery products affect faecal microbiota of healthy volunteers. *British Journal of Nutrition*, *98*(3), 540–549. https://doi.org/10.1017/S0007114507730751

Kocsis, I., Hagymási, K., Kéry, Á., Szoke, É., and Blázovics, A. (2003). Effects of chicory on pancreas status of rats in experimental dislipidemia. *Acta Biol Szeged*, *47*.

Kong, Fanbin, Singh, R.P., 2010. A human gastric simulator (HGS) to study food digestion in human stomach. J. Food Sci. 75 (9) https://doi.org/10.1111/j.1750- 3841.2010.01856.x

Konstantinov, S. (2003). Effect of fermentable carbohydrates on piglet faecal bacterial communities as revealed by denaturing gradient gel electrophoresis analysis of 16S ribosomal DNA. *FEMS Microbiology Ecology*, *43*(2), 225–235. https://doi.org/10.1016/S0168-6496(02)00430-0

Konstantinov, S. R., Awati, A. A., Williams, B. A., Miller, B. G., Jones, P., Stokes, C. R., Akkermans, A. D. L., Smidt, H., and De Vos, W. M. (2006a). Post-natal development of the porcine microbiota composition and activities. *Environmental Microbiology*, *8*(7), 1191–1199. https://doi.org/10.1111/j.1462-2920.2006.01009.x

Konstantinov, S. R., Awati, A. A., Williams, B. A., Miller, B. G., Jones, P., Stokes, C. R., Akkermans, A. D. L., Smidt, H., and De Vos, W. M. (2006b). Post-natal development of the porcine microbiota composition and activities. *Environmental Microbiology*, *8*(7), 1191–1199. https://doi.org/10.1111/j.1462-2920.2006.01009.x

Koo, B., Amarakoon, S. B., Jayaraman, B., Siow, Y. L., Prashar, S., Shang, Y., Karmin, O., and Nyachoti, C. M. (2021). Effects of dietary red-osier dogwood (*Cornus stolonifera*) on growth performance, blood profile, ileal morphology, and oxidative status in weaned pigs challenged with *Escherichia coli* K88 $^{+}$. *Canadian Journal of Animal Science*, *101*(1), 96–105. https://doi.org/10.1139/cjas-2019-0188

Kour, K., Bani, S., Sangwan, P. L., and Singh, A. (2016). Upregulation of Th1 Polarization by andlt;iandgt;Taraxacum officinaleandlt;/iandgt; in Normal and Immune Suppressed Mice. *Current Science*, *111*(4), 671. https://doi.org/10.18520/cs/v111/i4/671-685

Kozu, H., Nakata, Y., Nakajima, M., Neves, M. A., Uemura, K., Sato, S., Kobayashi, I., and Ichikawa, S. (2014). Development of a Human Gastric Digestion Simulator Equipped with Peristalsis Function for the Direct Observation and Analysis of the Food Digestion Process. *Food Science and Technology Research*, *20*(2), 225–233. https://doi.org/10.3136/fstr.20.225

Krawczyk, B., Wityk, P., Gałęcka, M., and Michalik, M. (2021). The Many Faces of Enterococcus spp.—Commensal, Probiotic and Opportunistic Pathogen. *Microorganisms*, *9*(9), 1900. https://doi.org/10.3390/microorganisms9091900

Kubasova, T., Davidova-Gerzova, L., Babak, V., Cejkova, D., Montagne, L., Le-Floc'h, N., and Rychlik, I. (2018). Effects of host genetics and environmental conditions on fecal microbiota composition of pigs. *PLOS ONE*, *13*(8), e0201901. https://doi.org/10.1371/journal.pone.0201901

Kucharzik, T., Maaser, C., Lügering, A., Kagnoff, M., Mayer, L., Targan, S., and Domschke, W. (2006). Recent understanding of IBD pathogenesis: Implications for future therapies. *Inflammatory Bowel Diseases*, *12*(11), 1068–1083. https://doi.org/10.1097/01.mib.0000235827.21778.d5

Kulkarni, T., Siegien, P., Comer, L., Vandel, J., Chataigne, G., Richel, A., Wavreille, J., Cudennec, B., Lucau, A., Everaert, N., Ravallec, R., and Schroyen, M. (2024). A comparative study of the effects of crude chicory and inulin on gut health in weaning piglets. *Journal of Functional Foods*, *123*, 106578. https://doi.org/10.1016/j.jff.2024.106578

Kulthong, K., Duivenvoorde, L., Sun, H., Confederat, S., Wu, J., Spenkelink, B., de Haan, L., Marin, V., van der Zande, M., and Bouwmeester, H. (2020). Microfluidic chip for culturing intestinal epithelial cell layers: Characterization and comparison of drug transport between dynamic and static models. *Toxicology in vitro*, *65*, 104815. https://doi.org/10.1016/j.tiv.2020.104815

Laforest-Lapointe, I., and Arrieta, M.-C. (2017). Patterns of Early-Life Gut Microbial Colonization during Human Immune Development: An Ecological Perspective. *Frontiers in Immunology*, *8*. https://doi.org/10.3389/fimmu.2017.00788

Lallès, J. P., Sève, B., Pié, S., Blazy, F., Laffitte, J., and Oswald, I. P. (2004a). Weaning Is Associated with an Upregulation of Expression of Inflammatory Cytokines in the Intestine of Piglets. *The Journal of Nutrition*, *134*(3), 641–647. https://doi.org/10.1093/jn/134.3.641

Lallès, J. P., Sève, B., Pié, S., Blazy, F., Laffitte, J., and Oswald, I. P. (2004b). Weaning Is Associated with an Upregulation of Expression of Inflammatory Cytokines in the Intestine of Piglets. *The Journal of Nutrition*, *134*(3), 641–647. https://doi.org/10.1093/jn/134.3.641

Lallès, J.-P., Bosi, P., Smidt, H., and Stokes, C. R. (2007). Nutritional management of gut health in pigs around weaning. *Proceedings of the Nutrition Society*, *66*(2), 260–268. https://doi.org/10.1017/S0029665107005484

Lalles, J.-P., Boudry, G., Favier, C., Floc'h, N., Le Huërou-Luron, I., Montagne, L., Oswald, I., Pié, S., Piel, C., and Sève, B. (2004). Gut function and dysfunction in young pigs: Physiology. *Http://Dx.Doi.Org/10.1051/Animres:2004018*, *53*. https://doi.org/10.1051/animres:2004018

LANG, A. (2004). Allicin inhibits spontaneous and TNF-? induced secretion of proinflammatory cytokines and chemokines from intestinal epithelial cells. *Clinical Nutrition*, *23*(5), 1199–1208. https://doi.org/10.1016/j.clnu.2004.03.011

Lawley, T. D., and Walker, A. W. (2013). Intestinal colonization resistance. *Immunology*, *138*(1), 1–11. https://doi.org/10.1111/j.1365-2567.2012.03616.x

Le Bastard, Q., Chapelet, G., Javaudin, F., Lepelletier, D., Batard, E., and Montassier, E. (2020). The effects of inulin on gut microbial composition: a systematic review of evidence from human studies. *European Journal of Clinical Microbiology and Infectious Diseases*, *39*(3), 403–413. https://doi.org/10.1007/s10096-019-03721-w

Le Sciellour, M., Labussière, E., Zemb, O., and Renaudeau, D. (2018). Effect of dietary fiber content on nutrient digestibility and fecal microbiota composition in growing-finishing pigs. *PLOS ONE*, *13*(10), e0206159. https://doi.org/10.1371/journal.pone.0206159

Leblois, J., Massart, S., Li, B., Wavreille, J., Bindelle, J., and Everaert, N. (2017). Modulation of piglets' microbiota: differential effects by a high wheat bran maternal diet during gestation and lactation. *Scientific Reports*, *7*(1), 7426. https://doi.org/10.1038/s41598-017-07228-2

Lehmann, MH, 1998. Recombinant human granulocyte-macrophage colony-stimulating factor triggers interleukin-10 expression in the monocytic cell line U937. Mol. Immunol. 35, 479–485. https://doi.org/ 10.1016/s0161-5890(98)00043-1

Leonard, F., Collnot, E.-M., and Lehr, C.-M. (2010). A Three-Dimensional Coculture of Enterocytes, Monocytes and Dendritic Cells To Model Inflamed Intestinal Mucosa *in vitro*. *Molecular Pharmaceutics*, *7*(6), 2103–2119. https://doi.org/10.1021/mp1000795

Levine, U. Y., Looft, T., Allen, H. K., and Stanton, T. B. (2013). Butyrate-Producing Bacteria, Including Mucin Degraders, from the Swine Intestinal Tract. *Applied and Environmental Microbiology*, *79*(12), 3879–3881. https://doi.org/10.1128/AEM.00589-13

Levy, M., Kolodziejczyk, A. A., Thaiss, C. A., and Elinav, E. (2017). Dysbiosis and the immune system. *Nature Reviews Immunology*, *17*(4), 219–232. https://doi.org/10.1038/nri.2017.7

Li, B., Schroyen, M., Leblois, J., Wavreille, J., Soyeurt, H., Bindelle, J., and Everaert, N. (2018). Effects of inulin supplementation to piglets in the suckling period on growth performance, postileal microbial and immunological traits in the suckling period and three weeks after weaning. *Archives of Animal Nutrition*, *72*(6), 425–442. https://doi.org/10.1080/1745039X.2018.1508975

Li, H., Ma, L., Zhang, L., Liu, N., Li, Z., Zhang, F., Liu, X., and Ma, X. (2021). Dietary Inulin Regulated Gut Microbiota and Improved Neonatal Health in a Pregnant Sow Model. *Frontiers in Nutrition*, *8*. https://doi.org/10.3389/fnut.2021.716723

Li, L., Yan, Q., Ma, N., Chen, X., Li, G., and Liu, M. (2021). Analysis of intestinal flora and inflammatory cytokine levels in children with non-infectious diarrhoea. *Translational Pediatrics*, *10*(5), 1340–1345. https://doi.org/10.21037/tp-21-168

Li, S., Zheng, J., Deng, K., Chen, L., Zhao, X. L., Jiang, X. M., Fang, Z. F., Che, L. Q., Xu, S. Y., Feng, B., li, J., Lin, Y., Wu, Y. Y., Han, Y. M., and Wu, D. (2018). Supplementation with organic acids showing different effects on growth performance, gut morphology and microbiota of weaned pigs fed with highly or less digestible diets. *Journal of Animal Science*. https://doi.org/10.1093/jas/sky197

Li, Y., Guo, Y., Wen, Z., Jiang, X., Ma, X., and Han, X. (2018). Weaning Stress Perturbs Gut Microbiome and Its Metabolic Profile in Piglets. *Scientific Reports*, *8*(1), 18068. https://doi.org/10.1038/s41598-018-33649-8

Li, Z., Feng, H., Han, L., Ding, L., Shen, B., Tian, Y., Zhao, L., Jin, M., Wang, Q., Qin, H., Cheng, J., and Liu, G. (2020). Chicoric acid ameliorate inflammation and oxidative stress in Lipopolysaccharide and <scp>d</scp> -galactosamine induced acute liver injury. *Journal of Cellular and Molecular Medicine*, *24*(5), 3022–3033. https://doi.org/10.1111/jcmm.14935

Lindemann, M. D., Cornelius, S. G., El Kandelgy, S. M., Moser, R. L., and Pettigrew, J. E. (1986). Effect of Age, Weaning and Diet on Digestive Enzyme Levels in the Piglet. *Journal of Animal Science*, *62*(5), 1298–1307. https://doi.org/10.2527/jas1986.6251298x

Lingyun, W., Jianhua, W., Xiaodong, Z., Da, T., Yalin, Y., Chenggang, C., Tianhua, F., and Fan, Z. (2007). Studies on the extracting technical conditions of inulin from Jerusalem artichoke tubers. *Journal of Food Engineering*, *79*(3), 1087–1093. https://doi.org/10.1016/j.jfoodeng.2006.03.028

Liu, F., Cottrell, J. J., Furness, J. B., Rivera, L. R., Kelly, F. W., Wijesiriwardana, U., Pustovit, R. V., Fothergill, L. J., Bravo, D. M., Celi, P., Leury, B. J., Gabler, N. K., and Dunshea, F. R. (2016). Selenium and vitamin E together improve intestinal epithelial barrier function and alleviate oxidative stress in heat-stressed pigs. *Experimental Physiology*, *101*(7), 801–810. https://doi.org/10.1113/EP085746

Liu, H., Ivarsson, E., Dicksved, J., Lundh, T., and Lindberg, J. (2012). Inclusion of Chicory (Cichorium intybus L.) in Pigs' Diets Affects the Intestinal Microenvironment and the Gut Microbiota. *Applied and Environmental Microbiology*, *78*, 4102–4109. https://doi.org/10.1128/AEM.07702-11

Liu, Q., Chen, Y., Shen, C., Xiao, Y., Wang, Y., Liu, Z., and Liu, X. (2017). Chicoric acid supplementation prevents systemic inflammation-induced memory impairment and amyloidogenesis via inhibition of NF-κB. *The FASEB Journal*, *31*(4), 1494–1507. https://doi.org/10.1096/fj.201601071R

Liu, T., Zhang, L., Joo, D., and Sun, S.-C. (2017). NFκB signalling in inflammation. *Signal Transduction and Targeted Therapy*, *2*(1), 17023. https://doi.org/10.1038/sigtrans.2017.23

Liu, T.-W., Cephas, K. D., Holscher, H. D., Kerr, K. R., Mangian, H. F., Tappenden, K. A., and Swanson, K. S. (2016). Nondigestible Fructans Alter Gastrointestinal Barrier Function, Gene Expression, Histomorphology, and the Microbiota Profiles of Diet-Induced Obese C57BL/6J Mice. *The Journal of Nutrition*, *146*(5), 949–956. https://doi.org/10.3945/jn.115.227504

Liu, W., Fu, D., Zhang, X., Chai, J., Tian, S., and Han, J. (2019). Development and validation of a new artificial gastric digestive system. *Food Research International*, *122*, 183–190. https://doi.org/10.1016/j.foodres.2019.04.015

Liu, W., Ye, A., Han, F., and Han, J. (2019). Advances and challenges in liposome digestion: Surface interaction, biological fate, and GIT modeling. *Advances in Colloid and Interface Science*, *263*, 52–67. https://doi.org/10.1016/j.cis.2018.11.007

Liu, Y., Fatheree, N. Y., Mangalat, N., and Rhoads, J. M. (2012). *Lactobacillus reuteri* strains reduce incidence and severity of experimental necrotizing enterocolitis via modulation of TLR4 and NFκB signalling in the intestine. *American Journal of Physiology-Gastrointestinal and Liver Physiology*, *302*(6), G608–G617. https://doi.org/10.1152/ajpgi.00266.2011

Liu, Y., Gibson, G. R., and Walton, G. E. (2016). An *In vitro* Approach to Study Effects of Prebiotics and Probiotics on the Faecal Microbiota and Selected Immune Parameters Relevant to the Elderly. *PLOS ONE*, *11*(9), e0162604. https://doi.org/10.1371/journal.pone.0162604

Liu, Y., Song, M., Che, T. M., Lee, J. J., Bravo, D., Maddox, C. W., and Pettigrew, J. E. (2014). Dietary plant extracts modulate gene expression profiles in ileal mucosa of weaned pigs after an Escherichia coli infection1. *Journal of Animal Science*, *92*(5), 2050–2062. https://doi.org/10.2527/jas.2013-6422

Liu L., Guo X., Rao J.N., Zou T., Xiao L, Yu T, Timmons JA, Turner DJ, Wang JY. Polyamines regulate E-cadherin transcription through c-Myc modulating intestinal epithelial barrier function. Am J Physiol Cell Physiol 2009;296:C801–C810.

Lo, S.-H., Chen, C.-Y., and Wang, H.-T. (2022). Three-step *in vitro* digestion model for evaluating and predicting fecal odor emission from growing pigs with different dietary protein intakes. *Animal Bioscience*, *35*(10), 1592–1605. https://doi.org/10.5713/ab.21.0498

Lobionda, S., Sittipo, P., Kwon, H. Y., and Lee, Y. K. (2019). The Role of Gut Microbiota in Intestinal Inflammation with Respect to Diet and Extrinsic Stressors. *Microorganisms*, *7*(8), 271. https://doi.org/10.3390/microorganisms7080271

Lodemann, U., Hübener, K., Jansen, N., and Martens, H. (2006). Effects of *Enterococcus faecium* NCIMB 10415 as probiotic supplement on intestinal transport and barrier function of piglets. *Archives of Animal Nutrition*, *60*(1), 35–48. https://doi.org/10.1080/17450390500468099

Loginova, K. V., Shynkaryk, M. V., Lebovka, N. I., and Vorobiev, E. (2010). Acceleration of soluble matter extraction from chicory with pulsed electric fields. *Journal of Food Engineering*, *96*(3), 374–379. https://doi.org/10.1016/j.jfoodeng.2009.08.009

Logtenberg, M. J., Akkerman, R., An, R., Hermes, G. D. A., de Haan, B. J., Faas, M. M., Zoetendal, E. G., Schols, H. A., and de Vos, P. (2020). Fermentation of Chicory Fructo-Oligosaccharides and Native Inulin by Infant Fecal Microbiota Attenuates Pro-Inflammatory Responses in Immature Dendritic Cells

in an Infant-Age-Dependent and Fructan-Specific Way. *Molecular Nutrition and Food Research*, *64*(13). https://doi.org/10.1002/mnfr.202000068

Loh, G., Eberhard, M., Brunner, R. M., Hennig, U., Kuhla, S., Kleessen, B., and Metges, C. C. (2006). Inulin Alters the Intestinal Microbiota and Short-Chain Fatty Acid Concentrations in Growing Pigs Regardless of Their Basal Diet. *The Journal of Nutrition*, *136*(5), 1198–1202. https://doi.org/10.1093/jn/136.5.1198

Long, S. F., Xu, Y. T., Pan, L., Wang, Q. Q., Wang, C. L., Wu, J. Y., Wu, Y. Y., Han, Y. M., Yun, C. H., and Piao, X. S. (2018). Mixed organic acids as antibiotic substitutes improve performance, serum immunity, intestinal morphology and microbiota for weaned piglets. *Animal Feed Science and Technology*, *235*, 23–32. https://doi.org/10.1016/j.anifeedsci.2017.08.018

Louis, P., and Flint, H. J. (2009). Diversity, metabolism and microbial ecology of butyrate-producing bacteria from the human large intestine. *FEMS Microbiology Letters*, *294*(1), 1–8. https://doi.org/10.1111/j.1574-6968.2009.01514.x

Louis, P., Flint, H. J., and Michel, C. (2016). *How to Manipulate the Microbiota: Prebiotics* (pp. 119–142). https://doi.org/10.1007/978-3-319-31248-4_9

Luise, D., Chalvon-Demersay, T., Lambert, W., Bosi, P., and Trevisi, P. (2021). Meta-analysis to evaluate the impact of the reduction of dietary crude protein on the gut health of post-weaning pigs. *Italian Journal of Animal Science*, *20*(1), 1386–1397. https://doi.org/10.1080/1828051X.2021.1952911

Luise, D., Le Sciellour, M., Buchet, A., Resmond, R., Clement, C., Rossignol, M.-N., Jardet, D., Zemb, O., Belloc, C., and Merlot, E. (2021). The fecal microbiota of piglets during weaning transition and its association with piglet growth across various farm environments. *PLOS ONE*, *16*(4), e0250655. https://doi.org/10.1371/journal.pone.0250655

Luissint, A.-C., Parkos, C. A., and Nusrat, A. (2016). Inflammation and the Intestinal Barrier: Leukocyte–Epithelial Cell Interactions, Cell Junction Remodeling, and Mucosal Repair. *Gastroenterology*, *151*(4), 616–632. https://doi.org/10.1053/j.gastro.2016.07.008

Ma, J., Rubin, B. K., and Voynow, J. A. (2018). Mucins, Mucus, and Goblet Cells. *Chest*, *154*(1), 169–176. https://doi.org/10.1016/j.chest.2017.11.008

Ma, P.; Fang, P.; Ren, T.; Fang, L.; Xiao, S. Porcine Intestinal Organoids: Overview of the State of the Art. Viruses 2022, 14, 1110. https://doi.org/10.3390/v14051110

Ma, X., Zhang, Y., Xu, T., Qian, M., Yang, Z., Zhan, X., and Han, X. (2021). Early-Life Intervention Using Exogenous Fecal Microbiota Alleviates Gut Injury and Reduce Inflammation Caused by Weaning Stress in Piglets. *Frontiers in Microbiology*, *12*. https://doi.org/10.3389/fmicb.2021.671683

Mabbott, N. A., Donaldson, D. S., Ohno, H., Williams, I. R., and Mahajan, A. (2013). Microfold (M) cells: important immunosurveillance posts in the intestinal epithelium. *Mucosal Immunology*, *6*(4), 666–677. https://doi.org/10.1038/mi.2013.30

MacDonald, V. E., and Howe, L. J. (2009). Histone acetylation: Where to go and how to get there. *Epigenetics*, *4*(3), 139–143. https://doi.org/10.4161/epi.4.3.8484

Macia, L., Tan, J., Vieira, A. T., Leach, K., Stanley, D., Luong, S., Maruya, M., Ian McKenzie, C., Hijikata, A., Wong, C., Binge, L., Thorburn, A. N., Chevalier, N., Ang, C., Marino, E., Robert, R., Offermanns, S., Teixeira, M. M., Moore, R. J., … Mackay, C. R. (2015). Metabolite-sensing receptors GPR43 and GPR109A facilitate dietary fibre-induced gut homeostasis through regulation of the inflammasome. *Nature Communications*, *6*(1), 6734. https://doi.org/10.1038/ncomms7734

Mackey, E., Ayyadurai, S., Pohl, C. S., D' Costa, S., Li, Y., and Moeser, A. J. (2016). Sexual dimorphism in the mast cell transcriptome and the pathophysiological responses to immunological and psychological stress. *Biology of Sex Differences*, *7*(1), 60. https://doi.org/10.1186/s13293-016-0113-7

Mackie, R. I., Sghir, A., and Gaskins, H. R. (1999). Developmental microbial ecology of the neonatal gastrointestinal tract. *The American Journal of Clinical Nutrition*, *69*(5), 1035S-1045S. https://doi.org/10.1093/ajcn/69.5.1035s

Macpherson, A. J., Geuking, M. B., and McCoy, K. D. (2005). Immune responses that adapt the intestinal mucosa to commensal intestinal bacteria. *Immunology*, *115*(2), 153–162. https://doi.org/10.1111/j.1365-2567.2005.02159.x

Mair, C., Plitzner, C., Domig, K. J., Schedle, K., and Windisch, W. (2010). Impact of inulin and a multispecies probiotic formulation on performance, microbial ecology and concomitant fermentation patterns in newly weaned piglets. *Journal of Animal Physiology and Animal Nutrition*, *94*(5), e164–e177. https://doi.org/10.1111/j.1439-0396.2010.01000.x

Manzanilla, E. G., Perez, J. F., Martin, M., Kamel, C., Baucells, F., and Gasa, J. (2004). Effect of plant extracts and formic acid on the intestinal equilibrium of early-weaned pigs1. *Journal of Animal Science*, *82*(11), 3210–3218. https://doi.org/10.2527/2004.82113210x

Marion, J., Biernat, M., Thomas, F., Savary, G., Le Breton, Y., Zabielski, R., Le Huërou-Luron, I., and Le Dividich, J. (2002). Small intestine growth and morphometry in piglets weaned at 7 days of age. Effects of level of energy intake. *Reproduction Nutrition Development*, *42*(4), 339–354. https://doi.org/10.1051/rnd:2002030

Marion, J., Petersen, Y. M., Romé, V., Thomas, F., Sangild, P. T., Dividich, J. Le, and Huërou-Luron, I. Le. (2005). Early Weaning Stimulates Intestinal Brush Border Enzyme Activities in Piglets, Mainly at the Posttranscriptional Level. *Journal of Pediatric Gastroenterology and Nutrition*, *41*(4), 401–410. https://doi.org/10.1097/01.mpg.0000177704.99786.07

Marzorati M, Vanhoecke B, De Ryck T, Sadaghian Sabadad M, Pinheiro I, Possemiers S *et al* (2014) The HMI module: a new *in vitro* tool to study the host microbiome interactions from the human gastrointestinal tract. BMC Microbiol 14:133

Maschmeyer, I., Hasenberg, T., Jaenicke, A., Lindner, M., Lorenz, A.K., Zech, J., Garbe, L. A., Sonntag, F., Hayden, P., Ayehunie, S., Lauster, R., Marx, U., Materne, E.M., 2015. Chip-based human liver–intestine and liver–skin co-cultures – a first step toward systemic repeated dose substance testing *in vitro*. Eur. J. Pharm. Biopharm. 95, 77–87. https://doi.org/10.1016/J.EJPB.2015.03.002

Mat DJL, Cattenoz T, Souchon I, Michon C, Le Feunteun S. 2018. Monitoring protein hydrolysis by pepsin using pH-stat: *in vitro* gastric digestions in static and dynamic pH conditions. Food Chem. 239:268–75

Matthias, A., Banbury, L., Stevenson, L. M., Bone, K. M., Leach, D. N., and Lehmann, R. P. (2007). Alkylamides from Echinacea Modulate Induced Immune Responses in Macrophages. *Immunological Investigations*, *36*(2), 117–130. https://doi.org/10.1080/08820130600745786

Matvieieva, N., Bessarabov, V., Khainakova, O., Duplij, V., Bohdanovych, T., Ratushnyak, Y., Kuzmina, G., Lisovyi, V., Zderko, N., and Kobylinska, N. (2023). Cichorium intybus L. "hairy" roots as a rich source of antioxidants and anti-inflammatory compounds. *Heliyon*, *9*(3), e14516. https://doi.org/10.1016/j.heliyon.2023.e14516

Mayer, E. A., Tillisch, K., and Gupta, A. (2015). Gut/brain axis and the microbiota. *Journal of Clinical Investigation*, *125*(3), 926–938. https://doi.org/10.1172/JCI76304

McCracken, B. A., Spurlock, M. E., Roos, M. A., Zuckermann, F. A., and Gaskins, H. R. (1999). Weaning Anorexia May Contribute to Local Inflammation in the Piglet Small Intestine. *The Journal of Nutrition*, *129*(3), 613–619. https://doi.org/10.1093/jn/129.3.613

McQuilken, S. A. (2021). Digestion and absorption. *Anaesthesia and Intensive Care Medicine*, *22*(5), 336–338. https://doi.org/10.1016/j.mpaic.2020.12.009

Mei, J., and Xu, R.-J. (2005). Transient changes of transforming growth factor-β expression in the small intestine of the pig in association with weaning. *British Journal of Nutrition*, *93*(1), 37–45. https://doi.org/10.1079/BJN20041302

Ménard, O., Cattenoz, T., Guillemin, H., Souchon, I., Deglaire, A., Dupont, D., and Picque, D. (2014). Validation of a new *in vitro* dynamic system to simulate infant digestion. *Food Chemistry*, *145*, 1039–1045. https://doi.org/10.1016/j.foodchem.2013.09.036

Meng, E. X., Verne, G. N., and Zhou, Q. (2024). Macrophages and Gut Barrier Function: Guardians of Gastrointestinal Health in Post-Inflammatory and Post-Infection Responses. *International Journal of Molecular Sciences*, *25*(17), 9422. https://doi.org/10.3390/ijms25179422

Menke, K. H. (1988). *Estimation of the energetic feed value obtained from chemical analysis and in vitro gas production using rumen fluid*. https://api.semanticscholar.org/CorpusID:91003801

Mensink, M. A., Frijlink, H. W., van der Voort Maarschalk, K., and Hinrichs, W. L. J. (2015). Inulin, a flexible oligosaccharide I: Review of its physicochemical characteristics. *Carbohydrate Polymers*, *130*, 405–419. https://doi.org/10.1016/j.carbpol.2015.05.026

Metzler-Zebeli, B. U., Ratriyanto, A., Jezierny, D., Sauer, N., Eklund, M., and Mosenthin, R. (2009). Effects of β-ine, organic acids and inulin as single feed additives or in combination on bacterial populations in the gastrointestinal tract of weaned pigs. *Archives of Animal Nutrition*, *63*(6), 427–441. https://doi.org/10.1080/17450390903299190

Michael AJ. Biosynthesis of polyamines and polyaminecontaining molecules. Biochem J 2016;473:2315–2329.

Mikkelsen, L., and Jensen, B. (2004). Effect of fructo-oligosaccharides on microbial populations and microbial activity in the gastrointestinal tract of piglets post-weaning. *Animal Feed Science and Technology - ANIM FEED SCI TECH*, *117*, 107–119. https://doi.org/10.1016/j.anifeedsci.2004.07.015

Millard, A. L., Mertes, P. M., Ittelet, D., Villard, F., Jeannesson, P., And Bernard, J. (2002). Butyrate affects differentiation, maturation and function of human monocyte-derived dendritic cells and macrophages. *Clinical and Experimental Immunology*, *130*(2), 245–255. https://doi.org/10.1046/j.0009-9104.2002.01977.x

Minekus, M., Alminger, M., Alvito, P., Ballance, S., Bohn, T., Bourlieu, C., Carrière, F., Boutrou, R., Corredig, M., Dupont, D., Dufour, C., Egger, L., Golding, M., Karakaya, S., Kirkhus, B., Le Feunteun, S., Lesmes, U., Macierzanka, A., Mackie, A., … Brodkorb, A. (2014). A standardised static *in vitro* digestion method suitable for food – an international consensus. *Food Funct.*, *5*(6), 1113–1124. https://doi.org/10.1039/C3FO60702J

Miralles, B., del Barrio, R., Cueva, C., Recio, I., and Amigo, L. (2018). Dynamic gastric digestion of a commercial whey protein concentrate†. *Journal of the Science of Food and Agriculture*, *98*(5), 1873–1879. https://doi.org/10.1002/jsfa.8668

Mizutani, T., Aboagye, S. Y., Ishizaka, A., Afum, T., Mensah, G. I., Asante-Poku, A., Asandem, D. A., Parbie, P. K., Abana, C. Z.-Y., Kushitor, D., Bonney, E. Y., Adachi, M., Hori, H., Ishikawa, K., Matano, T., Taniguchi, K., Opare, D., Arhin, D., Asiedu-Bekoe, F., … Kiyono, H. (2021). Gut microbiota signature of pathogen-dependent dysbiosis in viral gastroenteritis. *Scientific Reports*, *11*(1), 13945. https://doi.org/10.1038/s41598-021-93345-y

Modina, S. C., Aidos, L., Rossi, R., Pocar, P., Corino, C., and Di Giancamillo, A. (2021). Stages of Gut Development as a Useful Tool to Prevent Gut Alterations in Piglets. *Animals*, *11*(5), 1412. https://doi.org/10.3390/ani11051412

Modina, S. C., Polito, U., Rossi, R., Corino, C., and Di Giancamillo, A. (2019). Nutritional Regulation of Gut Barrier Integrity in Weaning Piglets. *Animals*, *9*(12), 1045. https://doi.org/10.3390/ani9121045

Moens, F., Verce, M., and De Vuyst, L. (2017). Lactate- and acetate-based cross-feeding interactions between selected strains of lactobacilli, bifidobacteria and colon bacteria in the presence of inulin-type fructans. *International Journal of Food Microbiology*, *241*, 225–236. https://doi.org/10.1016/j.ijfoodmicro.2016.10.019

Moeser, A. J., and Blikslager, A. T. (2007). Mechanisms of porcine diarrhoeal disease. *Journal of the American Veterinary Medical Association*, *231*(1), 56–67. https://doi.org/10.2460/javma.231.1.56

Moeser, A. J., Pohl, C. S., and Rajput, M. (2017a). Weaning stress and gastrointestinal barrier development: Implications for lifelong gut health in pigs. *Animal Nutrition*, *3*(4), 313–321. https://doi.org/10.1016/j.aninu.2017.06.003

Moeser, A. J., Pohl, C. S., and Rajput, M. (2017b). Weaning stress and gastrointestinal barrier development: Implications for lifelong gut health in pigs. *Animal Nutrition*, *3*(4), 313–321. https://doi.org/10.1016/j.aninu.2017.06.003

Moeser, A. J., Ryan, K. A., Nighot, P. K., and Blikslager, A. T. (2007). Gastrointestinal dysfunction induced by early weaning is attenuated by delayed weaning and mast cell blockade in pigs. *American Journal of Physiology-Gastrointestinal and Liver Physiology*, *293*(2), G413–G421. https://doi.org/10.1152/ajpgi.00304.2006

Molly, K., Vande Woestyne, M., and Verstraete, W. (1993). Development of a 5-step multi-chamber reactor as a simulation of the human intestinal microbial ecosystem. *Applied Microbiology and Biotechnology*, *39*(2), 254–258. https://doi.org/10.1007/BF00228615

Monro, J. A., and Mishra, S. (2010). Digestion-Resistant Remnants of Vegetable Vascular and Parenchyma Tissues Differ in Their Effects in the Large Bowel of Rats. *Food Digestion*, *1*(1–2), 47–56. https://doi.org/10.1007/s13228-010-0005-y

Montagne, L., Boudry, G., Favier, C., Huërou-Luron, I. Le, Lallès, J.-P., and Sève, B. (2007). Main intestinal markers associated with the changes in gut architecture and function in piglets after weaning. *British Journal of Nutrition*, *97*(1), 45–57. https://doi.org/10.1017/S000711450720580X

Morales, J., Cordero, G., Piñeiro, C., and Durosoy, S. (2012). Zinc oxide at low supplementation level improves productive performance and health status of piglets. *Journal of Animal Science*, *90*(suppl_4), 436–438. https://doi.org/10.2527/jas.53833

Morton, G. J., Cummings, D. E., Baskin, D. G., Barsh, G. S., and Schwartz, M. W. (2006). Central nervous system control of food intake and body weight. *Nature*, *443*(7109), 289–295. https://doi.org/10.1038/nature05026

Mu, Q., Kirby, J., Reilly, C. M., and Luo, X. M. (2017a). Leaky Gut As a Danger Signal for Autoimmune Diseases. *Frontiers in Immunology*, *8*. https://doi.org/10.3389/fimmu.2017.00598

Mu, Q., Kirby, J., Reilly, C. M., and Luo, X. M. (2017b). Leaky Gut As a Danger Signal for Autoimmune Diseases. *Frontiers in Immunology*, *8*. https://doi.org/10.3389/fimmu.2017.00598

Mulet-Cabero AI, Egger L, Portmann R, Ménard O, Marze S, *et al.* 2020a. A standardised semi-dynamic *in vitro* digestion method suitable for food: an international consensus. Food Funct. 11:1702–20

Nakayama, Y., Kawasaki, N., Tamiya, T., Anzai, S., Toyohara, K., Nishiyama, A., and Kitazono, E. (2020). Comparison of the prebiotic properties of native chicory and synthetic inulins using swine fecal cultures. *Bioscience, Biotechnology, and Biochemistry*, *84*(7), 1486–1496. https://doi.org/10.1080/09168451.2020.1749553

Nerio, L. S., Olivero-Verbel, J., and Stashenko, E. (2010). Repellent activity of essential oils: A review. *Bioresource Technology*, *101*(1), 372–378. https://doi.org/10.1016/j.biortech.2009.07.048

Neyrinck, A. M., Rodriguez, J., Zhang, Z., Seethaler, B., Sánchez, C. R., Roumain, M., Hiel, S., Bindels, L. B., Cani, P. D., Paquot, N., Cnop, M., Nazare, J.-A., Laville, M., Muccioli, G. G., Bischoff, S. C., Walter, J., Thissen, J.-P., and Delzenne, N. M. (2021). Prebiotic dietary fibre intervention improves fecal markers related to inflammation in obese patients: results from the Food4Gut randomized placebo-controlled trial. *European Journal of Nutrition*, *60*(6), 3159–3170. https://doi.org/10.1007/s00394-021-02484-5

Nielsen, D. S. G., Jensen, B. B., Theil, P. K., Nielsen, T. S., Knudsen, K. E. B., and Purup, S. (2018). Effect of butyrate and fermentation products on epithelial integrity in a mucus-secreting human colon cell line. *Journal of Functional Foods*, *40*, 9–17. https://doi.org/10.1016/j.jff.2017.10.023

Nielsen, T. S., Jensen, B. B., Purup, S., Jackson, S., Saarinen, M., Lyra, A., Sørensen, J. F., Theil, P. K., and Knudsen, K. E. B. (2016). A search for synbiotics: effects of enzymatically modified arabinoxylan and Butyrivibrio fibrisolvens on short-chain fatty acids in the cecum content and plasma of rats. *Food and Function*, *7*(4), 1839–1848. https://doi.org/10.1039/C6FO00114A

Nilsson, U., and Björck, I. (1988). Availability of Cereal Fructans and Inulin in the Rat Intestinal Tract. *The Journal of Nutrition*, *118*(12), 1482–1486. https://doi.org/10.1093/jn/118.12.2182

Niness, K. R. (1999a). Inulin and Oligofructose: What Are They? *The Journal of Nutrition*, *129*(7), 1402S-1406S. https://doi.org/10.1093/jn/129.7.1402S

Niness, K. R. (1999b). Inulin and Oligofructose: What Are They? *The Journal of Nutrition*, *129*(7), 1402S-1406S. https://doi.org/10.1093/jn/129.7.1402S

Niu, Q., Li, P., Hao, S., Zhang, Y., Kim, S. W., Li, H., Ma, X., Gao, S., He, L., Wu, W., Huang, X., Hua, J., Zhou, B., and Huang, R. (2015). Dynamic Distribution of the Gut Microbiota and the Relationship with Apparent Crude Fiber Digestibility and Growth Stages in Pigs. *Scientific Reports*, *5*(1), 9938. https://doi.org/10.1038/srep09938

Nyachoti, C. M., Omogbenigun, F. O., Rademacher, M., and Blank, G. (2006). Performance responses and indicators of gastrointestinal health in early-weaned pigs fed low-protein amino acid-supplemented diets1. *Journal of Animal Science*, *84*(1), 125–134. https://doi.org/10.2527/2006.841125x

O'Flaherty, S., Saulnier, D., Pot, B., and Versalovic, J. (2010). How can probiotics and prebiotics impact mucosal immunity? *Gut Microbes*, *1*(5), 293–300. https://doi.org/10.4161/gmic.1.5.12924

Oliphant, K., Ali, M., D'Souza, M., Hughes, P. D., Sulakhe, D., Wang, A. Z., Xie, B., Yeasin, R., Msall, M. E., Andrews, B., and Claud, E. C. (2021). *Bacteroidota* and *Lachnospiraceae* integration into the gut microbiome at key time points in early life are linked to infant neurodevelopment. *Gut Microbes*, *13*(1). https://doi.org/10.1080/19490976.2021.1997560

Ortega, A. D. S. V., and Szabó, C. (2021). Adverse Effects of Heat Stress on the Intestinal Integrity and Function of Pigs and the Mitigation Capacity of Dietary Antioxidants: A Review. *Animals*, *11*(4), 1135. https://doi.org/10.3390/ani11041135

Osawa, Y., Nagaki, M., Banno, Y., Brenner, D. A., Asano, T., Nozawa, Y., Moriwaki, H., and Nakashima, S. (2002). Tumor Necrosis Factor A--Induced Interleukin-8 Production via NFκB and Phosphatidylinositol 3-Kinase/Akt Pathways Inhibits Cell Apoptosis in Human Hepatocytes. *Infection and Immunity*, *70*(11), 6294–6301. https://doi.org/10.1128/IAI.70.11.6294-6301.2002

O'Sullivan, G., Kelly, P., O'Halloran, S., Collins, C., Collins, J., Dunne, C., and Shanahan, F. (2005). Probiotics: An Emerging Therapy. *Current Pharmaceutical Design*, *11*(1), 3–10. https://doi.org/10.2174/1381612053382368

Pácha, J. (2000). Development of Intestinal Transport Function in Mammals. *Physiological Reviews*, *80*(4), 1633–1667. https://doi.org/10.1152/physrev.2000.80.4.1633

Pahumunto, N., Dahlen, G., and Teanpaisan, R. (2023). Evaluation of Potential Probiotic Properties of Lactobacillus and Bacillus Strains Derived from Various Sources for Their Potential Use in Swine Feeding. *Probiotics and Antimicrobial Proteins*, *15*(3), 479–490. https://doi.org/10.1007/s12602-021-09861-w

Papatsiros, V. G., Maragkakis, G., & Papakonstantinou, G. I. (2024). Stress Biomarkers in Pigs: Current Insights and Clinical Application. *Veterinary Sciences*, *11*(12), 640. https://doi.org/10.3390/vetsci11120640

Panesar, P. S., Kaur, R., Singh, R. S., and Kennedy, J. F. (2018). Biocatalytic strategies in the production of galacto-oligosaccharides and its global status. *International Journal of Biological Macromolecules*, *111*, 667–679. https://doi.org/10.1016/j.ijbiomac.2018.01.062

Paone, P., and Cani, P. D. (2020). Mucus barrier, mucins and gut microbiota: the expected slimy partners? *Gut*, *69*(12), 2232–2243. https://doi.org/10.1136/gutjnl-2020-322260

Partanen, K. H., and Mroz, Z. (1999). Organic acids for performance enhancement in pig diets. *Nutrition Research Reviews*, *12*(1), 117–145. https://doi.org/10.1079/095442299108728884

Pastorelli L, De Salvo C, Mercado JR *et al* (2013) Central role of the gut epithelial barrier in the pathogenesis of chronic intestinal infl ammation: lessons learned from animal models and human genetics. Front Immunol 4:280

Peace, R. M., Campbell, J., Polo, J., Crenshaw, J., Russell, L., and Moeser, A. (2011). Spray-Dried Porcine Plasma Influences Intestinal Barrier Function, Inflammation,and Diarrhoea in Weaned Pigs. *The Journal of Nutrition*, *141*(7), 1312–1317. https://doi.org/10.3945/jn.110.136796

Pejsak, Z., Kaźmierczak, P., Butkiewicz, A. F., Wojciechowski, J., and Woźniakowski, G. (2023). Alternatives to zinc oxide in pig production. *Polish Journal of Veterinary Sciences*, 319–330. https://doi.org/10.24425/pjvs.2023.145033

Pellikaan, W. F., Verdonk, J. M. A. J., Shim, S. B., and Verstegen, M. W. A. (2007). Adaptive capacity of faecal microbiota from piglets receiving diets with different types of inulin-type fructans. *Livestock Science*, *108*(1–3), 178–181. https://doi.org/10.1016/j.livsci.2007.01.087

Peng, L., Li, Z.-R., Green, R. S., Holzmanr, I. R., and Lin, J. (2009). Butyrate Enhances the Intestinal Barrier by Facilitating Tight Junction Assembly via Activation of AMP-Activated Protein Kinase in Caco-2 Cell Monolayers. *The Journal of Nutrition*, *139*(9), 1619–1625. https://doi.org/10.3945/jn.109.104638

Pérez-Calvo, E., Wicaksono, A. N., Canet, E., Daulton, E., Ens, W., Hoeller, U., Verlhac, V., Celi, P., and Covington, J. A. (2019). The measurement of volatile organic compounds in faeces of piglets as a tool to assess gastrointestinal functionality. *Biosystems Engineering*, *184*, 122–129. https://doi.org/10.1016/j.biosystemseng.2019.06.005

Peron, G., Meroño, T., Gargari, G., Hidalgo-Liberona, N., Miñarro, A., Lozano, E. V., Castellano-Escuder, P., González-Domínguez, R., del Bo', C., Bernardi, S., Kroon, P. A., Cherubini, A., Riso, P., Guglielmetti, S., and Andrés-Lacueva, C. (2022). A Polyphenol-Rich Diet Increases the Gut Microbiota Metabolite Indole 3-Propionic Acid in Older Adults with Preserved Kidney Function. *Molecular Nutrition and Food Research*, *66*(21). https://doi.org/10.1002/mnfr.202100349

Pfaffl, M. W. (2001). A new mathematical model for relative quantification in real-time RT-PCR. *Nucleic Acids Research*, *29*(9), 45e–445. https://doi.org/10.1093/nar/29.9.e45

Pham, V. T., Seifert, N., Richard, N., Raederstorff, D., Steinert, R., Prudence, K., and Mohajeri, M. H. (2018). The effects of fermentation products of prebiotic fibres on gut barrier and immune functions *in vitro*. *PeerJ*, *6*, e5288. https://doi.org/10.7717/peerj.5288

Phan, A. D. T., Netzel, G., Wang, D., Flanagan, B. M., D'Arcy, B. R., and Gidley, M. J. (2015). Binding of dietary polyphenols to cellulose: Structural and nutritional aspects. *Food Chemistry*, *171*, 388–396. https://doi.org/10.1016/j.foodchem.2014.08.118

Pieper, R., Vahjen, W., and Zentek, J. (2015). Dietary fibre and crude protein: impact on gastrointestinal microbial fermentation characteristics and host response. *Animal Production Science*, *55*(12), 1367. https://doi.org/10.1071/AN15278

Pluske, J. R. (2016). Invited review: Aspects of gastrointestinal tract growth and maturation in the pre- and postweaning period of pigs. *Journal of Animal Science*, *94*(suppl_3), 399–411. https://doi.org/10.2527/jas.2015-9767

Pluske, J. R., Hampson, D. J., and Williams, I. H. (1997). Factors influencing the structure and function of the small intestine in the weaned pig: a review. *Livestock Production Science*, *51*(1–3), 215–236. https://doi.org/10.1016/S0301-6226(97)00057-2

Pluske, J. R., Turpin, D. L., and Kim, J.-C. (2018a). Gastrointestinal tract (gut) health in the young pig. *Animal Nutrition*, *4*(2), 187–196. https://doi.org/10.1016/j.aninu.2017.12.004

Poelaert, C., Nollevaux, G., Boudry, C., Taminiau, B., Nezer, C., Daube, G., Schneider, Y.-J., Portetelle, D., Théwis, A., and Bindelle, J. (2018). Reducing agent can be omitted in the incubation medium of the batch *in vitro* fermentation model of the pig intestines. *Animal*, *12*(6), 1154–1164. https://doi.org/10.1017/S1751731117002749

Pohl, C. S., Medland, J. E., Mackey, E., Edwards, L. L., Bagley, K. D., DeWilde, M. P., Williams, K. J., and Moeser, A. J. (2017). Early weaning stress induces chronic functional diarrhoea, intestinal barrier defects, and increased mast cell activity in a porcine model of early life adversity. *Neurogastroenterology and Motility*, *29*(11). https://doi.org/10.1111/nmo.13118

Pohl, C. S., Medland, J. E., and Moeser, A. J. (2015). Early-life stress origins of gastrointestinal disease: animal models, intestinal pathophysiology, and translational implications. *American Journal of Physiology-Gastrointestinal and Liver Physiology*, *309*(12), G927–G941. https://doi.org/10.1152/ajpgi.00206.2015

Pol, K., de Graaf, C., Meyer, D., and Mars, M. (2018). The efficacy of daily snack replacement with oligofructose-enriched granola bars in overweight and obese adults: a 12-week randomised controlled trial. *British Journal of Nutrition*, *119*(9), 1076–1086. https://doi.org/10.1017/S0007114518000211

Pouille, C. L., Ouaza, S., Roels, E., Behra, J., Tourret, M., Molinié, R., Fontaine, J.-X., Mathiron, D., Gagneul, D., Taminiau, B., Daube, G., Ravallec, R., Rambaud, C., Hilbert, J.-L., Cudennec, B., and Lucau-Danila, A. (2022a). Chicory: Understanding the Effects and Effectors of This Functional Food. *Nutrients*, *14*(5), 957. https://doi.org/10.3390/nu14050957

Pujo, J., Petitfils, C., Le Faouder, P., Eeckhaut, V., Payros, G., Maurel, S., Perez-Berezo, T., Van Hul, M., Barreau, F., Blanpied, C., Chavanas, S., Van Immerseel, F., Bertrand-Michel, J., Oswald, E., Knauf, C., Dietrich, G., Cani, P. D., and Cenac, N. (2021). Bacteria-derived long chain fatty acid exhibits anti-inflammatory properties in colitis. *Gut*, *70*(6), 1088–1097. https://doi.org/10.1136/gutjnl-2020-321173

Qian, Z., Wu, Z., Huang, L., Qiu, H., Wang, L., Li, L., Yao, L., Kang, K., Qu, J., Wu, Y., Luo, J., Liu, J. J., Yang, Y., Yang, W., and Gou, D. (2015a). Mulberry fruit prevents LPS-induced NFκB/pERK/MAPK signals in macrophages and suppresses acute colitis and colourectal tumorigenesis in mice. *Scientific Reports*, *5*(1), 17348. https://doi.org/10.1038/srep17348

Qiu, Y., Yang, J., Wang, L., Yang, X., Gao, K., Zhu, C., and Jiang, Z. (2021). Dietary resveratrol attenuation of intestinal inflammation and oxidative damage is linked to the alteration of gut microbiota and butyrate in piglets challenged with deoxynivalenol. *Journal of Animal Science and Biotechnology*, *12*(1), 71. https://doi.org/10.1186/s40104-021-00596-w

Quast, C., Pruesse, E., Yilmaz, P., Gerken, J., Schweer, T., Yarza, P., Peplies, J., and Glöckner, F. O. (2012). The SILVA ribosomal RNA gene database project: improved data processing and web-based tools. *Nucleic Acids Research*, *41*(D1), D590–D596. https://doi.org/10.1093/nar/gks1219

Quintero, M., Maldonado, M., Perez-Munoz, M., Jimenez, R., Fangman, T., Rupnow, J., Wittke, A., Russell, M., and Hutkins, R. (2011). Adherence Inhibition of Cronobacter sakazakii to Intestinal Epithelial Cells by Prebiotic Oligosaccharides. *Current Microbiology*, *62*(5), 1448–1454. https://doi.org/10.1007/s00284-011-9882-8

Ramasamy, U. S., Venema, K., Schols, H. A., and Gruppen, H. (2014). Effect of Soluble and Insoluble Fibers within the *in vitro* Fermentation of Chicory Root Pulp by Human Gut Bacteria. *Journal of Agricultural and Food Chemistry*, *62*(28), 6794–6802. https://doi.org/10.1021/jf501254z

Ramayo-Caldas, Y., Mach, N., Lepage, P., Levenez, F., Denis, C., Lemonnier, G., Leplat, J.-J., Billon, Y., Berri, M., Doré, J., Rogel-Gaillard, C., and Estellé, J. (2016). Phylogenetic network analysis applied to pig gut microbiota identifies an ecosystem structure linked with growth traits. *The ISME Journal*, *10*(12), 2973–2977. https://doi.org/10.1038/ismej.2016.77

Rattigan, R., Sweeney, T., Maher, S., Ryan, M. T., Thornton, K., and O'Doherty, J. V. (2020). Effects of reducing dietary crude protein concentration and supplementation with either laminarin or zinc oxide on the growth performance and intestinal health of newly weaned pigs. *Animal Feed Science and Technology*, *270*, 114693. https://doi.org/10.1016/j.anifeedsci.2020.114693

Reale, O., Huguet, A., and Fessard, V. (2021). Co-culture model of Caco-2/HT-29-MTX cells: A promising tool for investigation of phycotoxins toxicity on the intestinal barrier. *Chemosphere*, *273*, 128497. https://doi.org/10.1016/j.chemosphere.2020.128497

Redondo-Cuenca, A., Herrera-Vázquez, S. E., Condezo-Hoyos, L., Gómez-Ordóñez, E., and Rupérez, P. (2021). Inulin extraction from common inulin-containing plant sources. *Industrial Crops and Products*, *170*, 113726. https://doi.org/10.1016/j.indcrop.2021.113726

Reichardt, N., Duncan, S. H., Young, P., Belenguer, A., McWilliam Leitch, C., Scott, K. P., Flint, H. J., and Louis, P. (2014). Erratum: Phylogenetic distribution of three pathways for propionate production within the human gut microbiota. *The ISME Journal*, *8*(6), 1352–1352. https://doi.org/10.1038/ismej.2014.48

Reimer, R. A., Willis, H. J., Tunnicliffe, J. M., Park, H., Madsen, K. L., and Soto-Vaca, A. (2017). Inulin-type fructans and whey protein both modulate appetite but only fructans alter gut microbiota in adults with overweight/obesity: A randomized controlled trial. *Molecular Nutrition and Food Research*, *61*(11). https://doi.org/10.1002/mnfr.201700484

Rex Gaskins, H. (2000). Intestinal Bacteria and Their Influence on Swine Growth. In *Swine Nutrition, Second Edition*. CRC Press. https://doi.org/10.1201/9781420041842.ch26

Rios, D., Wood, M. B., Li, J., Chassaing, B., Gewirtz, A. T., and Williams, I. R. (2016). Antigen sampling by intestinal M cells is the principal pathway initiating mucosal IgA production to commensal enteric bacteria. *Mucosal Immunology*, *9*(4), 907–916. https://doi.org/10.1038/mi.2015.121

Rist, V. T. S., Weiss, E., Eklund, M., and Mosenthin, R. (2013). Impact of dietary protein on microbiota composition and activity in the gastrointestinal tract of piglets in relation to gut health: a review. *Animal*, *7*(7), 1067–1078. https://doi.org/10.1017/S1751731113000062

Riva, A., Rasoulimehrabani, H., Cruz-Rubio, J. M., Schnorr, S. L., von Baeckmann, C., Inan, D., Nikolov, G., Herbold, C. W., Hausmann, B., Pjevac, P., Schintlmeister, A., Spittler, A., Palatinszky, M., Kadunic, A., Hieger, N., Del Favero, G., von Bergen, M., Jehmlich, N., Watzka, M., … Berry, D. (2023). Identification of inulin-responsive bacteria in the gut microbiota via multi-modal activity-based sorting. *Nature Communications*, *14*(1), 8210. https://doi.org/10.1038/s41467-023-43448-z

Rivière, A., Selak, M., Lantin, D., Leroy, F., and De Vuyst, L. (2016). Bifidobacteria and Butyrate-Producing Colon Bacteria: Importance and Strategies for Their Stimulation in the Human Gut. *Frontiers in Microbiology*, *7*. https://doi.org/10.3389/fmicb.2016.00979

Roche H.M, Terres AM, Black IB, Gibney MJ, Kelleher D. Fatty acids and epithelial permeability: effect of conjugated linoleic acid in Caco-2 cells. Gut 2001; 48:797–802.

Rodriguez, J., Neyrinck, A. M., Van Kerckhoven, M., Gianfrancesco, M. A., Renguet, E., Bertrand, L., Cani, P. D., Lanthier, N., Cnop, M., Paquot, N., Thissen, J.-P., Bindels, L. B., and Delzenne, N. M. (2022). Physical activity enhances the improvement of body mass index and metabolism by inulin: a multicentre randomized placebo-controlled trial performed in obese individuals. *BMC Medicine*, *20*(1), 110. https://doi.org/10.1186/s12916-022-02299-z

Roh, S., Carroll, J. A., and Kim, S. W. (2015). Effects of fermented soybean meal on innate immunity-related gene expressions in nursery pigs acutely challenged with lipopolysaccharides. *Animal Science Journal*, *86*(5), 508–516. https://doi.org/10.1111/asj.12319

Rooks, M. G., Veiga, P., Wardwell-Scott, L. H., Tickle, T., Segata, N., Michaud, M., Gallini, C. A., Beal, C., van Hylckama-Vlieg, J. E. T., Ballal, S. A., Morgan, X. C., Glickman, J. N., Gevers, D., Huttenhower, C., and Garrett, W. S. (2014). Gut microbiome composition and function in experimental colitis during active disease and treatment-induced remission. *The ISME Journal*, *8*(7), 1403–1417. https://doi.org/10.1038/ismej.2014.3

Round, J. L., and Mazmanian, S. K. (2010). Inducible Foxp3 $^{+}$ regulatory T-cell development by a commensal bacterium of the intestinal microbiota. *Proceedings of the National Academy of Sciences*, *107*(27), 12204–12209. https://doi.org/10.1073/pnas.0909122107

Rubel, I. A., Pérez, E. E., Manrique, G. D., and Genovese, D. B. (2015). Fibre enrichment of wheat bread with Jerusalem artichoke inulin: Effect on dough rheology and bread quality. *Food Structure*, *3*, 21–29. https://doi.org/10.1016/j.foostr.2014.11.001

Ruiz-Aceituno, L., García-Sarrió, M. J., Alonso-Rodriguez, B., Ramos, L., and Sanz, M. L. (2016). Extraction of bioactive carbohydrates from artichoke (Cynara scolymus L.) external bracts using microwave assisted extraction and pressurized liquid extraction. *Food Chemistry*, *196*, 1156–1162. https://doi.org/10.1016/j.foodchem.2015.10.046

Sabater-Molina, M., Larqué, E., Torrella, F., Plaza, J., Ramis, G., and Zamora, S. (2011a). Effects of fructooligosaccharides on cecum polyamine concentration and gut maturation in early-weaned piglets. *Journal of Clinical Biochemistry and Nutrition*, *48*(3), 230–236. https://doi.org/10.3164/jcbn.10-100

Sabater-Molina, M., Larqué, E., Torrella, F., Plaza, J., Ramis, G., and Zamora, S. (2011b). Effects of fructooligosaccharides on cecum polyamine concentration and gut maturation in early-weaned piglets. *Journal of Clinical Biochemistry and Nutrition*, *48*(3), 230–236. https://doi.org/10.3164/jcbn.10-100

Saillant, V., Lipuma, D., Ostyn, E., Joubert, L., Boussac, A., Guerin, H., Brandelet, G., Arnoux, P., and Lechardeur, D. (2021). A Novel Enterococcus faecalis Heme Transport Regulator (FhtR) Senses

Host Heme To Control Its Intracellular Homeostasis. *MBio*, *12*(1). https://doi.org/10.1128/mBio.03392-20

Saladrigas-García, M., D'Angelo, M., Ko, H. L., Nolis, P., Ramayo-Caldas, Y., Folch, J. M., Llonch, P., Solà-Oriol, D., Pérez, J. F., and Martín-Orúe, S. M. (2021). Understanding host-microbiota interactions in the commercial piglet around weaning. *Scientific Reports*, *11*(1), 23488. https://doi.org/10.1038/s41598-021-02754-6

Salek, R. M., Maguire, M. L., Bentley, E., Rubtsov, D. V., Hough, T., Cheeseman, M., Nunez, D., Sweatman, B. C., Haselden, J. N., Cox, R. D., Connor, S. C., and Griffin, J. L. (2007). A metabolomic comparison of urinary changes in type 2 diabetes in mouse, rat, and human. *Physiological Genomics*, *29*(2), 99–108. https://doi.org/10.1152/physiolgenomics.00194.2006

Salonen, A., Lahti, L., Salojärvi, J., Holtrop, G., Korpela, K., Duncan, S. H., Date, P., Farquharson, F., Johnstone, A. M., Lobley, G. E., Louis, P., Flint, H. J., and de Vos, W. M. (2014). Impact of diet and individual variation on intestinal microbiota composition and fermentation products in obese men. *The ISME Journal*, *8*(11), 2218–2230. https://doi.org/10.1038/ismej.2014.63

San Andres, J. V, Mastromano, G. A., Li, Y., Tran, H., Bundy, J. W., Miller, P. S., and Burkey, T. E. (2019). The effects of prebiotics on growth performance and *in vitro* immune biomarkers in weaned pigs1. *Translational Animal Science*, *3*(4), 1315–1325. https://doi.org/10.1093/tas/txz129

Sangild, P. T., Fowden, A. L., and Trahair, J. F. (2000). How does the foetal gastrointestinal tract develop in preparation for enteral nutrition after birth? *Livestock Production Science*, *66*(2), 141–150. https://doi.org/10.1016/S0301-6226(00)00221-9

Sangild, P. T., Petersen, Y. M., Schmidt, M., Elnif, J., Petersen, T. K., Buddington, R. K., Greisen, G., Michaelsen, K. F., and Burrin, D. G. (2002). Preterm Birth Affects the Intestinal Response to Parenteral and Enteral Nutrition in Newborn Pigs. *The Journal of Nutrition*, *132*(9), 2673–2681. https://doi.org/10.1093/jn/132.9.2673

Sarmiento-Andrade, Y., Suárez, R., Quintero, B., Garrochamba, K., and Chapela, S. P. (2022). Gut microbiota and obesity: New insights. *Frontiers in Nutrition*, *9*. https://doi.org/10.3389/fnut.2022.1018212

Schierack, P., Nordhoff, M., Pollmann, M., Weyrauch, K. D., Amasheh, S., Lodemann, U., Jores, J., Tachu, B., Kleta, S., Blikslager, A., Tedin, K., and Wieler, L. H. (2006). Characterization of a porcine intestinal epithelial cell line for *in vitro* studies of microbial pathogenesis in swine. *Histochemistry and Cell Biology*, *125*(3), 293–305. https://doi.org/10.1007/s00418-005-0067-z

Schimek, K., Busek, M., Brincker, S., Groth, B., Hoffmann, S., Lauster, R., Lindner, G., Lorenz, A., Menzel, U., Sonntag, F., Walles, H., Marx, U., Horland, R., 2013. Integrating biological vasculature into a multi-organ-chip microsystem. Lab Chip 13, 3588–3598. https://doi.org/10.1039/C3LC50217A.

Schimpel, C., Teubl, B., Absenger, M., Meindl, C., Fröhlich, E., Leitinger, G., Zimmer, A., and Roblegg, E. (2014). Development of an Advanced Intestinal *in vitro* Triple Culture Permeability Model To Study Transport of Nanoparticles. *Molecular Pharmaceutics*, *11*(3), 808–818. https://doi.org/10.1021/mp400507g

Schoeler M, Caesar R. Dietary lipids, gut microbiota and lipid metabolism. Rev Endocr Metab Disord 2019; 20:461–472

Schokker, D., Fledderus, J., Jansen, R., Vastenhouw, S. A., de Bree, F. M., Smits, M. A., and Jansman, A. A. J. M. (2018a). Supplementation of fructooligosaccharides to suckling piglets affects intestinal microbiota colonization and immune development1. *Journal of Animal Science*, *96*(6), 2139–2153. https://doi.org/10.1093/jas/sky110

Schokker, D., Fledderus, J., Jansen, R., Vastenhouw, S. A., de Bree, F. M., Smits, M. A., and Jansman, A. A. J. M. (2018b). Supplementation of fructooligosaccharides to suckling piglets affects intestinal microbiota colonization and immune development1. *Journal of Animal Science*, *96*(6), 2139–2153. https://doi.org/10.1093/jas/sky110

Schumacher, E., Vigh, É., Molnár, V., Kenyeres, P., Fehér, G., Késmárky, G., Tóth, K., and Garai, J. (2011). Thrombosis Preventive Potential of Chicory Coffee Consumption: A Clinical Study. *Phytotherapy Research*, *25*(5), 744–748. https://doi.org/10.1002/ptr.3481

Segain, J.-P. (2000). Butyrate inhibits inflammatory responses through NFkappa B inhibition: implications for Crohn's disease. *Gut*, *47*(3), 397–403. https://doi.org/10.1136/gut.47.3.397

Segura E, Touzot M, Bohineust A *et al* (2013) Human infl ammatory dendritic cells induce Th17 cell differentiation. Immunity 38:336–348

Shah P, Jogani V, Bagchi T *et al* (2006) Role of Caco-2 cell monolayers in prediction of intestinal drug absorption. Biotechnol Prog 22:186–198

Shahinozzaman, M., Raychaudhuri, S., Fan, S., and Obanda, D. N. (2021). Kale Attenuates Inflammation and Modulates Gut Microbial Composition and Function in C57BL/6J Mice with Diet-Induced Obesity. *Microorganisms*, *9*(2), 238. https://doi.org/10.3390/microorganisms9020238

Sharpe, C., Thornton, D. J., and Grencis, R. K. (2018). A sticky end for gastrointestinal helminths; the role of the mucus barrier. *Parasite Immunology*, *40*(4). https://doi.org/10.1111/pim.12517

Shen, J., Zhang, B., Wei, H., Che, C., Ding, D., Hua, X., Bucheli, P., Wang, L., Li, Y., Pang, X., and Zhao, L. (2010). Assessment of the modulating effects of fructo-oligosaccharides on fecal microbiota using human flora–associated piglets. *Archives of Microbiology*, *192*(11), 959–968. https://doi.org/10.1007/s00203-010-0628-y

Shen, Y. B., Carroll, J. A., Yoon, I., Mateo, R. D., and Kim, S. W. (2011). Effects of supplementing Saccharomyces cerevisiae fermentation product in sow diets on performance of sows and nursing piglets1,2. *Journal of Animal Science*, *89*(8), 2462–2471. https://doi.org/10.2527/jas.2010-3642

Shetty, S. A., Marathe, N. P., Lanjekar, V., Ranade, D., and Shouche, Y. S. (2013). Comparative Genome Analysis of Megasphaera sp. Reveals Niche Specialization and Its Potential Role in the Human Gut. *PLoS ONE*, *8*(11), e79353. https://doi.org/10.1371/journal.pone.0079353

Shi, Z., Wang, T., Kang, J., Li, Y., Li, Y., & Xi, L. (2022). Effects of Weaning Modes on the Intestinal pH, Activity of Digestive Enzymes, and Intestinal Morphology of Piglets. *Animals*, *12*(17), 2200. https://doi.org/10.3390/ani12172200

Shi, C., Zhu, Y., Niu, Q., Wang, J., Wang, J., and Zhu, W. (2018). The Changes of Colonic Bacterial Composition and Bacterial Metabolism Induced by an Early Food Introduction in a Neonatal Porcine Model. *Current Microbiology*, *75*(6), 745–751. https://doi.org/10.1007/s00284-018-1442-z

Shim, S. B., Verdonk, J. M. A. J., Pellikaan, W. F., and Verstegen, M. W. A. (2007). Differences in Microbial Activities of Faeces from Weaned and Unweaned Pigs in Relation to *In vitro* Fermentation of Different Sources of Inulin-type Oligofructose and Pig Feed Ingredients. *Asian-Australasian Journal of Animal Sciences*, *20*(9), 1444–1452. https://doi.org/10.5713/ajas.2007.1444

Shimada Y, Kinoshita M, Harada K, Mizutani M, Masahata K, Kayama H, *et al*. 2013. Commensal Bacteria-Dependent Indole Production Enhances Epithelial Barrier Function in the Colon. PLoS ONE 8(11): e80604. https://doi.org/10.1371/journal.pone.0080604

Shoaib, M., Shehzad, A., Omar, M., Rakha, A., Raza, H., Sharif, H. R., Shakeel, A., Ansari, A., and Niazi, S. (2016). Inulin: Properties, health benefits and food applications. *Carbohydrate Polymers*, *147*, 444–454. https://doi.org/10.1016/j.carbpol.2016.04.020

Shu, C., Yan-Yan, Z., Hai, Z., Long-Kun, D., Yue, X., Man, Y., Chang, S., Liang, W., and Hao, H. (2022). Anti-inflammatory effects of NaB and NaPc in *Acinetobacter baumannii* -stimulated THP-1 cells *via* TLR2/NFκB/ROS/NLRP3 pathway. *Acta Pharmaceutica*, *72*(4), 615–628. https://doi.org/10.2478/acph-2022-0036

Sicard, J.-F., Le Bihan, G., Vogeleer, P., Jacques, M., and Harel, J. (2017). Interactions of Intestinal Bacteria with Components of the Intestinal Mucus. *Frontiers in Cellular and Infection Microbiology*, *7*. https://doi.org/10.3389/fcimb.2017.00387

Sido, A., Radhakrishnan, S., Kim, S. W., Eriksson, E., Shen, F., Li, Q., Bhat, V., Reddivari, L., and Vanamala, J. K. P. (2017). A food-based approach that targets interleukin-6, a key regulator of chronic intestinal inflammation and colon carcinogenesis. *The Journal of Nutritional Biochemistry*, *43*, 11–17. https://doi.org/10.1016/j.jnutbio.2017.01.012

Siggers, R. H., Thymann, T., Siggers, J. L., Schmidt, M., Hansen, A. K., and Sangild, P. T. (2007). Bacterial colonization affects early organ and gastrointestinal growth in the neonate. *Livestock Science*, *109*(1–3), 14–18. https://doi.org/10.1016/j.livsci.2007.01.025

Silva, M., Cueva, C., Alba, C., Rodriguez, J. M., de Pascual-Teresa, S., Jones, J., Caturla, N., Victoria Moreno-Arribas, M., and Bartolomé, B. (2022). Gut microbiome-modulating properties of a polyphenol-enriched dietary supplement comprised of hibiscus and lemon verbena extracts. Monitoring of phenolic metabolites. *Journal of Functional Foods*, *91*, 105016. https://doi.org/10.1016/j.jff.2022.105016

Skrzypek, T. H., Piedra, J. L. V., Skrzypek, H. W., Woliński, J., Kazimierczak, W., Szymańczyk, S., Pawłowska, M., and Zabielski, R. (2005). Light and scanning electron microscopy evaluation of the postnatal small intestinal mucosa development in pigs. *Journal of Physiology and Pharmacology : An Official Journal of the Polish Physiological Society*, *56 Suppl 3*, 71–87. https://api.semanticscholar.org/CorpusID:24774348

Slifierz, M. J., Friendship, R. M., and Weese, J. S. (2015). Longitudinal study of the early-life fecal and nasal microbiotas of the domestic pig. *BMC Microbiology*, *15*(1), 184. https://doi.org/10.1186/s12866-015-0512-7

Smith, B. N., Hannas, M., Orso, C., Martins, S. M. M. K., Wang, M., Donovan, S. M., and Dilger, R. N. (2020). Dietary osteopontin-enriched algal protein as nutritional support in weaned pigs infected with F18-fimbriated enterotoxigenic *Escherichia coli*. *Journal of Animal Science*, *98*(10). https://doi.org/10.1093/jas/skaa314

Smith, F., Clark, J. E., Overman, B. L., Tozel, C. C., Huang, J. H., Rivier, J. E. F., Blisklager, A. T., and Moeser, A. J. (2010). Early weaning stress impairs development of mucosal barrier function in the porcine intestine. *American Journal of Physiology-Gastrointestinal and Liver Physiology*, *298*(3), G352–G363. https://doi.org/10.1152/ajpgi.00081.2009

Snoeck, V., Huyghebaert, N., Cox, E., Vermeire, A., Saunders, J., Remon, J. P., Verschooten, F., and Goddeeris, B. M. (2004). Gastrointestinal transit time of nondisintegrating radio-opaque pellets in suckling and recently weaned piglets. *Journal of Controlled Release*, *94*(1), 143–153. https://doi.org/10.1016/j.jconrel.2003.09.015

Sorgi, C. A., de Campos Chaves Lamarque, G., Verri, M. P., Nelson-Filho, P., Faccioli, L. H., and Paula-Silva, F. W. G. (2021). Multifaceted effect of caffeic acid against Streptococcus mutans infection: microbicidal and immunomodulatory agent in macrophages. *Archives of Microbiology*, *203*(6), 2979–2987. https://doi.org/10.1007/s00203-021-02290-x

Souza, H. S. P., Tortori, C. J. A., Castelo-Branco, M. T. L., Carvalho, A. T. P., Margallo, V. S., Delgado, C. F. S., Dines, I., and Elia, C. C. S. (2005). Apoptosis in the intestinal mucosa of patients with inflammatory bowel disease: evidence of altered expression of FasL and perforin cytotoxic pathways. *International Journal of* Colour*ectal Disease*, *20*(3), 277–286. https://doi.org/10.1007/s00384-004-0639-8

Spees, A. M., Wangdi, T., Lopez, C. A., Kingsbury, D. D., Xavier, M. N., Winter, S. E., Tsolis, R. M., and Bäumler, A. J. (2013). Streptomycin-Induced Inflammation Enhances Escherichia coli Gut Colonization Through Nitrate Respiration. *MBio*, *4*(4). https://doi.org/10.1128/mBio.00430-13

Spreeuwenberg, M. A. M., Verdonk, J. M. A. J., Gaskins, H. R., and Verstegen, M. W. A. (2001). Small Intestine Epithelial Barrier Function Is Compromised in Pigs with Low Feed Intake at Weaning. *The Journal of Nutrition*, *131*(5), 1520–1527. https://doi.org/10.1093/jn/131.5.1520

Stojanov, S., Berlec, A., and Štrukelj, B. (2020). The Influence of Probiotics on the Firmicutes/Bacteroidetes Ratio in the Treatment of Obesity and Inflammatory Bowel disease. *Microorganisms*, *8*(11), 1715. https://doi.org/10.3390/microorganisms8111715

Stokes, C. R., Bailey, M., Haverson, K., Harris, C., Jones, P., Inman, C., Pié, S., Oswald, I. P., Williams, B. A., Akkermans, A. D. L., Sowa, E., Rothkötter, H.-J., and Miller, B. G. (2004). Postnatal development of intestinal immune system in piglets: implications for the process of weaning. *Animal Research*, *53*(4), 325–334. https://doi.org/10.1051/animres:2004020

Støy, A. C. F., Heegaard, P. M. H., Sangild, P. T., Østergaard, M. V., and Skovgaard, K. (2013). Gene Expression Analysis of the IPEC-J2 Cell Line: A Simple Model for the Inflammation-Sensitive Preterm Intestine. *ISRN Genomics*, *2013*, 1–7. https://doi.org/10.1155/2013/980651

Su, W., Gong, T., Jiang, Z., Lu, Z., and Wang, Y. (2022). The Role of Probiotics in Alleviating Postweaning Diarrhoea in Piglets From the Perspective of Intestinal Barriers. *Frontiers in Cellular and Infection Microbiology*, *12*. https://doi.org/10.3389/fcimb.2022.883107

Su, Y., Li, X., Li, D., and Sun, J. (2021). Fecal Microbiota Transplantation Shows Marked Shifts in the Multi-Omic Profiles of Porcine Post-weaning Diarrhoea. *Frontiers in Microbiology*, *12*. https://doi.org/10.3389/fmicb.2021.619460

Sumigray, K. D., Terwilliger, M., and Lechler, T. (2018). Morphogenesis and Compartmentalization of the Intestinal Crypt. *Developmental Cell*, *45*(2), 183-197.e5. https://doi.org/10.1016/j.devcel.2018.03.024

Sun, J., Du, L., Li, X., Zhong, H., Ding, Y., Liu, Z., and Ge, L. (2019). Identification of the core bacteria in rectums of diarrheic and non-diarrheic piglets. *Scientific Reports*, *9*(1), 18675. https://doi.org/10.1038/s41598-019-55328-y

Sun, J., Qiao, Y., Qi, C., Jiang, W., Xiao, H., Shi, Y., and Le, G. (2016). High-fat-diet–induced obesity is associated with decreased antiinflammatory Lactobacillus reuteri sensitive to oxidative stress in mouse Peyer's patches. *Nutrition*, *32*(2), 265–272. https://doi.org/10.1016/j.nut.2015.08.020

Susan Sungsoo Cho, P. S. (2009). *Fiber Ingredients* (S. S. Cho and P. Samuel, Eds.). CRC Press. https://doi.org/10.1201/9781420043853

Suzuki, T., Yoshida, S., and Hara, H. (2008). Physiological concentrations of short-chain fatty acids immediately suppress colonic epithelial permeability. *British Journal of Nutrition*, *100*(2), 297–305. https://doi.org/10.1017/S0007114508888733

Taciak, B.; Białasek, M.; Braniewska, A.; Sas, Z.; Sawicka, P.; Kiraga, Ł.; Rygiel, T.; Król, M. Evaluation of phenotypic and functional stability of RAW 264.7 cell line through serial passages. PLoS ONE 2018, 13, e0198943

Tactacan, G. B., Cho, S.-Y., Cho, J. H., and Kim, I. H. (2016). Performance Responses, Nutrient Digestibility, Blood Characteristics, and Measures of Gastrointestinal Health in Weanling Pigs Fed Protease Enzyme. *Asian-Australasian Journal of Animal Sciences*, *29*(7), 998–1003. https://doi.org/10.5713/ajas.15.0886

Takiishi, T., Fenero, C. I. M., and Câmara, N. O. S. (2017). Intestinal barrier and gut microbiota: Shaping our immune responses throughout life. *Tissue Barriers*, *5*(4), e1373208. https://doi.org/10.1080/21688370.2017.1373208

Tan, Z., Dong, W., Ding, Y., Ding, X., Zhang, Q., and Jiang, L. (2019). Porcine Epidemic Diarrhoea Altered Colonic Microbiota Communities in Suckling Piglets. *Genes*, *11*(1), 44. https://doi.org/10.3390/genes11010044

Tang, W., Liu, J., Ma, Y., Wei, Y., Liu, J., and Wang, H. (2021). Impairment of Intestinal Barrier Function Induced by Early Weaning via Autophagy and Apoptosis Associated With Gut Microbiome and Metabolites. *Frontiers in Immunology*, *12*. https://doi.org/10.3389/fimmu.2021.804870

Tang, W., Qian, Y., Yu, B., Zhang, T., Gao, J., He, J., Huang, Z., Zheng, P., Mao, X., Luo, J., Yu, J., and Chen, D. (2019). Effects of Bacillus subtilis DSM32315 supplementation and dietary crude protein level on performance, gut barrier function and microbiota profile in weaned piglets1. *Journal of Animal Science*, *97*(5), 2125–2138. https://doi.org/10.1093/jas/skz090

Tang, X., and Xiong, K. (2022). Intrauterine Growth Retardation Affects Intestinal Health of Suckling Piglets via Altering Intestinal Antioxidant Capacity, Glucose Uptake, Tight Junction, and Immune Responses. *Oxidative Medicine and Cellular Longevity*, *2022*, 1–12. https://doi.org/10.1155/2022/2644205

Tang, X., Xiong, K., Fang, R., and Li, M. (2022). Weaning stress and intestinal health of piglets: A review. *Frontiers in Immunology*, *13*. https://doi.org/10.3389/fimmu.2022.1042778

Tarini, J., and Wolever, T. M. S. (2010). The fermentable fibre inulin increases postprandial serum short-chain fatty acids and reduces free-fatty acids and ghrelin in healthy subjects. *Applied Physiology, Nutrition, and Metabolism*, *35*(1), 9–16. https://doi.org/10.1139/H09-119

Tawfick, M. M., Xie, H., Zhao, C., Shao, P., and Farag, M. A. (2022). Inulin fructans in diet: Role in gut homeostasis, immunity, health outcomes and potential therapeutics. *International Journal of Biological Macromolecules*, *208*, 948–961. https://doi.org/10.1016/j.ijbiomac.2022.03.218

Tedelind, S., Westberg, F., Kjerrulf, M., and Vidal, A. (2007). Anti-inflammatory properties of the short-chain fatty acids acetate and propionate: A study with relevance to inflammatory bowel disease. *World Journal of Gastroenterology*, *13*(20), 2826. https://doi.org/10.3748/wjg.v13.i20.2826

Tenenhaus, A., and Tenenhaus, M. (2011). Regularized Generalized Canonical Correlation Analysis. *Psychometrika*, *76*, 257–284. https://doi.org/10.1007/s11336-011-9206-8

Teresa Zelante, Rossana G. Iannitti, Cristina Cunha, Antonella De Luca, Gloria Giovannini, Giuseppe Pieraccini, Riccardo Zecchi, Carmen D'Angelo, Cristina Massi-Benedetti, Francesca Fallarino, Agostinho Carvalho, Paolo Puccetti, Luigina Romani. 2013. Tryptophan Catabolites from Microbiota Engage Aryl Hydrocarbon Receptor and Balance Mucosal Reactivity via Interleukin-22, Immunity, Volume 39, Issue 2, Pages 372-385. https://doi.org/10.1016/j.immuni.2013.08.003.

Tian, L., Bruggeman, G., van den Berg, M., Borewicz, K., Scheurink, A. J. W., Bruininx, E., de Vos, P., Smidt, H., Schols, H. A., and Gruppen, H. (2017). Effects of pectin on fermentation characteristics, carbohydrate utilization, and microbial community composition in the gastrointestinal tract of weaning pigs. *Molecular Nutrition and Food Research*, *61*(1). https://doi.org/10.1002/mnfr.201600186

Topping, D. L., and Clifton, P. M. (2001). Short-Chain Fatty Acids and Human Colonic Function: Roles of Resistant Starch and Nonstarch Polysaccharides. *Physiological Reviews*, *81*(3), 1031–1064. https://doi.org/10.1152/physrev.2001.81.3.1031

Tran Do, D.H., Kong, F., Penet, C., Winetzky, D., Gregory, K., 2016. Using a dynamic stomach model to study efficacy of supplemental enzymes during simulated digestion. LWT - Food Sci. Technol. (Lebensmittel-Wissenschaft -Technol.) 65, 580–588. https://doi.org/10.1016/j.lwt.2015.08.054

Tran, T. H. T., Boudry, C., Everaert, N., Théwis, A., Portetelle, D., Daube, G., Nezer, C., Taminiau, B., and Bindelle, J. (2016a). Adding mucins to an *in vitro* batch fermentation model of the large intestine induces changes in microbial population isolated from porcine faeces depending on the substrate. *FEMS Microbiology Ecology*, *92*(2), fiv165. https://doi.org/10.1093/femsec/fiv165

Tran, T. H. T., Everaert, N., and Bindelle, J. (2018). Review on the effects of potential prebiotics on controlling intestinal enteropathogens *Salmonella* and *Escherichia coli* in pig production. *Journal of Animal Physiology and Animal Nutrition*, *102*(1), 17–32. https://doi.org/10.1111/jpn.12666

Trevisi, P., De Filippi, S., Minieri, L., Mazzoni, M., Modesto, M., Biavati, B., and Bosi, P. (2008). Effect of fructo-oligosaccharides and different doses of Bifidobacterium animalis in a weaning diet on bacterial translocation and Toll-like receptor gene expression in pigs. *Nutrition*, *24*(10), 1023–1029. https://doi.org/10.1016/j.nut.2008.04.008

Trevisi, P., Merialdi, G., Mazzoni, M., Casini, L., Tittarelli, C., De Filippi, S., Minieri, L., Lalatta-Costerbosa, G., and Bosi, P. (2007). Effect of dietary addition of thymol on growth, salivary and gastric function, immune response, and excretion of Salmonella enterica serovar Typhimurium, in weaning pigs challenged with this microbe strain. *Italian Journal of Animal Science*, *6*(sup1), 374–376. https://doi.org/10.4081/ijas.2007.1s.374

Trompette, A., Gollwitzer, E. S., Pattaroni, C., Lopez-Mejia, I. C., Riva, E., Pernot, J., Ubags, N., Fajas, L., Nicod, L. P., and Marsland, B. J. (2018). Dietary Fiber Confers Protection against Flu by Shaping Ly6c− Patrolling Monocyte Hematopoiesis and CD8+ T Cell Metabolism. *Immunity*, *48*(5), 992-1005.e8. https://doi.org/10.1016/j.immuni.2018.04.022

TSUKAHARA, T., KISHINO, E., INOUE, R., NAKANISHI, N., NAKAYAMA, K., ITO, T., and USHIDA, K. (2013). Correlation between villous height and the disaccharidase activity in the small intestine of piglets from nursing to growing. *Animal Science Journal*, *84*(1), 54–59. https://doi.org/10.1111/j.1740-0929.2012.01039.x

Turner, J. R. (2009). Intestinal mucosal barrier function in health and disease. *Nature Reviews Immunology*, *9*(11), 799–809. https://doi.org/10.1038/nri2653

Tzounis, X., Rodriguez-Mateos, A., Vulevic, J., Gibson, G. R., Kwik-Uribe, C., and Spencer, J. P. (2011). Prebiotic evaluation of cocoa-derived flavanols in healthy humans by using a randomized, controlled, double-blind, crossover intervention study. *The American Journal of Clinical Nutrition*, *93*(1), 62–72. https://doi.org/10.3945/ajcn.110.000075

Uchiyama, K., Naito, Y., Takagi, T., Mizushima, K., Hirai, Y., Hayashi, N., Harusato, A., Inoue, K., Fukumoto, K., Yamada, S., Handa, O., Ishikawa, T., Yagi, N., Kokura, S., and Yoshikawa, T. (2012). Serpin B1 protects colonic epithelial cell via blockage of neutrophil elastase activity and its expression is enhanced in patients with ulcerative colitis. *American Journal of Physiology-Gastrointestinal and Liver Physiology*, *302*(10), G1163–G1170. https://doi.org/10.1152/ajpgi.00292.2011

Uerlings, J., Arévalo Sureda, E., Schroyen, M., Kroeske, K., Tanghe, S., Vos, M., Bruggeman, G., Wavreille, J., Bindelle, J., Purcaro, G., and Everaert, N. (2021). Impact of Citrus Pulp or Inulin on Intestinal Microbiota and Metabolites, Barrier, and Immune Function of Weaned Piglets. *Frontiers in Nutrition*, *8*. https://doi.org/10.3389/fnut.2021.650211

Uerlings, J., Bindelle, J., Schroyen, M., Richel, A., Bruggeman, G., Willems, E., and Everaert, N. (2019). Fermentation capacities of fructan- and pectin-rich by-products and purified fractions via an *in vitro* piglet faecal model. *Journal of the Science of Food and Agriculture*, *99*(13), 5720–5733. https://doi.org/10.1002/jsfa.9837

Uerlings, J., Schroyen, M., Bautil, A., Courtin, C., Richel, A., Sureda, E. A., Bruggeman, G., Tanghe, S., Willems, E., Bindelle, J., and Everaert, N. (2020). *In vitro* prebiotic potential of agricultural by-products on intestinal fermentation, gut barrier and inflammatory status of piglets. *British Journal of Nutrition*, *123*(3), 293–307. https://doi.org/10.1017/S0007114519002873

Uerlings, J., Schroyen, M., Bindelle, J., Bruggeman, G., and Everaert, N. (2021). Chicory root and inulin stimulate butyrate-producing bacterial communities in an *in vitro* model of the piglet's gastro-intestinal tract. *Bioactive Carbohydrates and Dietary Fibre*, *26*, 100269. https://doi.org/10.1016/j.bcdf.2021.100269

Uerlings, J., Schroyen, M., Willems, E., Tanghe, S., Bruggeman, G., Bindelle, J., and Everaert, N. (2020). Differential effects of inulin or its fermentation metabolites on gut barrier and immune function of porcine intestinal epithelial cells. *Journal of Functional Foods*, *67*, 103855. https://doi.org/10.1016/j.jff.2020.103855

Upadhaya, S.-D., and Kim, I.-H. (2021). The Impact of Weaning Stress on Gut Health and the Mechanistic Aspects of Several Feed Additives Contributing to Improved Gut Health Function in Weanling Piglets—A Review. *Animals*, *11*(8), 2418. https://doi.org/10.3390/ani11082418

Usuda, H., Okamoto, T., and Wada, K. (2021). Leaky Gut: Effect of Dietary Fiber and Fats on Microbiome and Intestinal Barrier. *International Journal of Molecular Sciences*, *22*(14), 7613. https://doi.org/10.3390/ijms22147613

Vacca, M., Celano, G., Calabrese, F. M., Portincasa, P., Gobbetti, M., and De Angelis, M. (2020). The Controversial Role of Human Gut Lachnospiraceae. *Microorganisms*, *8*(4), 573. https://doi.org/10.3390/microorganisms8040573

Van den Abbeele, P., Taminiau, B., Pinheiro, I., Duysburgh, C., Jacobs, H., Pijls, L., and Marzorati, M. (2018). Arabinoxylo-Oligosaccharides and Inulin Impact Inter-Individual Variation on Microbial Metabolism and Composition, Which Immunomodulates Human Cells. *Journal of Agricultural and Food Chemistry*, *66*(5), 1121–1130. https://doi.org/10.1021/acs.jafc.7b04611

Van den Abbeele, P., Venema, K., Van de Wiele, T., Verstraete, W., and Possemiers, S. (2013). Different Human Gut Models Reveal the Distinct Fermentation Patterns of Arabinoxylan versus Inulin. *Journal of Agricultural and Food Chemistry*, *61*(41), 9819–9827. https://doi.org/10.1021/jf4021784

van der Hee, B., Loonen, L. M. P., Taverne, N., Taverne-Thiele, J. J., Smidt, H., and Wells, J. M. (2018). Optimized procedures for generating an enhanced, near physiological 2D culture system from porcine intestinal organoids. *Stem Cell Research*, *28*, 165–171. https://doi.org/10.1016/j.scr.2018.02.013

van der Hee, B.; Madsen, O.; Vervoort, J.; Smidt, H.; Wells, J.M. 2020 Congruence of Transcription Programs in Adult Stem Cell-Derived Jejunum Organoids and Original Tissue During Long-Term Culture. Front. Cell Dev. Biol, 8, 375

Van Klinken, B.J.-W.; Oussoren, E.; Weenink, J.-J.; Strous, G.J.; Büller, H.A.; Dekker, J.; Einerhand, A.W.C. The human intestinal cell lines Caco-2 and LS174T as models to study cell-type specific mucin expression. Glycoconj. J. 1996, 13, 757–768.

Van Soest, P. J., Robertson, J. B., and Lewis, B. A. (1991). Methods for Dietary Fiber, Neutral Detergent Fiber, and Nonstarch Polysaccharides in Relation to Animal Nutrition. *Journal of Dairy Science*, *74*(10), 3583–3597. https://doi.org/10.3168/jds.S0022-0302(91)78551-2

Vancamelbeke, M., and Vermeire, S. (2017). The intestinal barrier: a fundamental role in health and disease. *Expert Review of Gastroenterology and Hepatology*, *11*(9), 821–834. https://doi.org/10.1080/17474124.2017.1343143

Vandeputte, D., Falony, G., Vieira-Silva, S., Wang, J., Sailer, M., Theis, S., Verbeke, K., and Raes, J. (2017). Prebiotic inulin-type fructans induce specific changes in the human gut microbiota. *Gut*, *66*(11), 1968–1974. https://doi.org/10.1136/gutjnl-2016-313271

Verdile, N., Mirmahmoudi, R., Brevini, T. A. L., and Gandolfi, F. (2019). Evolution of pig intestinal stem cells from birth to weaning. *Animal*, *13*(12), 2830–2839. https://doi.org/10.1017/S1751731119001319

Verdonk, J. M. A. J., Bruininx, E. M. A. M., van der Meulen, J., and Verstegen, M. W. A. (2007). Post-weaning feed intake level modulates gut morphology but not gut permeability in weaned piglets. *Livestock Science*, *108*(1–3), 146–149. https://doi.org/10.1016/j.livsci.2007.01.093

Verhoeckx, K., Cotter, P., López-Expósito, I., Kleiveland, C., Lea, T., Mackie, A., Requena, T., Swiatecka, D., and Wichers, H. (Eds.). (2015). *The Impact of Food Bioactives on Health*. Springer International Publishing. https://doi.org/10.1007/978-3-319-16104-4

Vinolo, M. A. R., Rodrigues, H. G., Nachbar, R. T., and Curi, R. (2011). Regulation of Inflammation by Short Chain Fatty Acids. *Nutrients*, *3*(10), 858–876. https://doi.org/10.3390/nu3100858

Vital, N., Gramacho, A. C., Silva, M., Cardoso, M., Alvito, P., Kranendonk, M., Silva, M. J., and Louro, H. (2024). Challenges of the Application of *In vitro* Digestion for Nanomaterials Safety Assessment. *Foods*, *13*(11). https://doi.org/10.3390/foods13111690

Vitetta, L., Llewellyn, H., and Oldfield, D. (2019). Gut Dysbiosis and the Intestinal Microbiome: Streptococcus thermophilus a Key Probiotic for Reducing Uremia. *Microorganisms*, *7*(8), 228. https://doi.org/10.3390/microorganisms7080228

Vogt, L., Meyer, D., Pullens, G., Faas, M., Smelt, M., Venema, K., Ramasamy, U., Schols, H. A., and De Vos, P. (2015). Immunological Properties of Inulin-Type Fructans. *Critical Reviews in Food Science and Nutrition*, *55*(3), 414–436. https://doi.org/10.1080/10408398.2012.656772

Wagenaar, C. A., van de Put, M., Bisschops, M., Walrabenstein, W., de Jonge, C. S., Herrema, H., and van Schaardenburg, D. (2021). The Effect of Dietary Interventions on Chronic Inflammatory Diseases in Relation to the Microbiome: A Systematic Review. *Nutrients*, *13*(9), 3208. https://doi.org/10.3390/nu13093208

Waldram, A., Holmes, E., Wang, Y., Rantalainen, M., Wilson, I. D., Tuohy, K. M., McCartney, A. L., Gibson, G. R., and Nicholson, J. K. (2009). Top-Down Systems Biology Modeling of Host Metabotype−Microbiome Associations in Obese Rodents. *Journal of Proteome Research*, *8*(5), 2361–2375. https://doi.org/10.1021/pr8009885

Walk, C. L., Wilcock, P., and Magowan, E. (2015). Evaluation of the effects of pharmacological zinc oxide and phosphorus source on weaned piglet growth performance, plasma minerals and mineral digestibility. *Animal*, *9*(7), 1145–1152. https://doi.org/10.1017/S175173111500035X

Walker, A. W., Ince, J., Duncan, S. H., Webster, L. M., Holtrop, G., Ze, X., Brown, D., Stares, M. D., Scott, P., Bergerat, A., Louis, P., McIntosh, F., Johnstone, A. M., Lobley, G. E., Parkhill, J., and Flint, H. J. (2011). Dominant and diet-responsive groups of bacteria within the human colonic microbiota. *The ISME Journal*, *5*(2), 220–230. https://doi.org/10.1038/ismej.2010.118

Walton, P. E., Dunshea, F. R., and Ballard, F. J. (1995). *In vivo* actions of IGF analogues with poor affinities for IGFBPs: Metabolic and growth effects in pigs of different ages and GH responsiveness. *Progress in Growth Factor Research*, *6*(2–4), 385–395. https://doi.org/10.1016/0955-2235(95)00007-0

Wan, X., Guo, H., Liang, Y., Zhou, C., Liu, Z., Li, K., Niu, F., Zhai, X., and Wang, L. (2020). The physiological functions and pharmaceutical applications of inulin: A review. *Carbohydrate Polymers*, *246*, 116589. https://doi.org/10.1016/j.carbpol.2020.116589

Wan, Y., Wang, F., Yuan, J., Li, J., Jiang, D., Zhang, J., Li, H., Wang, R., Tang, J., Huang, T., Zheng, J., Sinclair, A. J., Mann, J., and Li, D. (2019). Effects of dietary fat on gut microbiota and faecal metabolites, and their relationship with cardiometabolic risk factors: a 6-month randomised controlled-feeding trial. *Gut*, *68*(8), 1417–1429. https://doi.org/10.1136/gutjnl-2018-317609

Wang, J., Wu, P., Liu, M., Liao, Z., Wang, Y., Dong, Z., Chen, X.D., 2019. An advanced near real dynamic: *in vitro* human stomach system to study gastric digestion and emptying of beef stew and cooked rice. Food and Function 10 (5), 2914–2925. https://doi.org/10.1039/c8fo02586j.

Wang, D., Piao, X. S., Zeng, Z. K., Lu, T., Zhang, Q., Li, P. F., Xue, L. F., and Kim, S. W. (2011). Effects of Keratinase on Performance, Nutrient Utilization, Intestinal Morphology, Intestinal Ecology and Inflammatory Response of Weaned Piglets Fed Diets with Different Levels of Crude Protein. *Asian-Australasian Journal of Animal Sciences*, *24*(12), 1718–1728. https://doi.org/10.5713/ajas.2011.11132

Wang, H., Gu, J., Hou, X., Chen, J., Yang, N., Liu, Y., Wang, G., Du, M., Qiu, H., Luo, Y., Jiang, Z., and Feng, L. (2017). Anti-inflammatory effect of miltirone on inflammatory bowel disease via TLR4/NFκB/IQGAP2 signalling pathway. *Biomedicine and Pharmacotherapy*, *85*, 531–540. https://doi.org/10.1016/j.biopha.2016.11.061

Wang, J., Chen, L., Li, P., Li, X., Zhou, H., Wang, F., Li, D., Yin, Y., and Wu, G. (2008). Gene Expression Is Altered in Piglet Small Intestine by Weaning and Dietary Glutamine Supplementation3. *The Journal of Nutrition*, *138*(6), 1025–1032. https://doi.org/10.1093/jn/138.6.1025

Wang, J., Li, G. R., Tan, B. E., Xiong, X., Kong, X. F., Xiao, D. F., Xu, L. W., Wu, M. M., Huang, B., Kim, S. W., and Yin, Y. L. (2015). Oral administration of putrescine and proline during the suckling period improves epithelial restitution after early weaning in piglets1. *Journal of Animal Science*, *93*(4), 1679–1688. https://doi.org/10.2527/jas.2014-8230

Wang, J., Wang, S., Liu, H., Zhang, D., Wang, Y., and Ji, H. (2019). Effects of oligosaccharides on the growth and stress tolerance of Lactobacillus plantarum ZLP001 *in vitro*, and the potential synbiotic effects of L. plantarum ZLP001 and fructo-oligosaccharide in post-weaning piglets1. *Journal of Animal Science*, *97*(11), 4588–4597. https://doi.org/10.1093/jas/skz254

Wang, L. X., Zhu, F., Li, J. Z., Li, Y. L., Ding, X. Q., Yin, J., Xiong, X., and Yang, H. S. (2020). Epidermal growth factor promotes intestinal secretory cell differentiation in weaning piglets via Wnt/β-catenin signalling. *Animal*, *14*(4), 790–798. https://doi.org/10.1017/S1751731119002581

Wang, W., Chen, D., Yu, B., Huang, Z., Mao, X., Zheng, P., Luo, Y., Yu, J., Luo, J., Yan, H., and He, J. (2020). Effects of dietary inulin supplementation on growth performance, intestinal barrier integrity and microbial populations in weaned pigs. *British Journal of Nutrition*, *124*(3), 296–305. https://doi.org/10.1017/S0007114520001130

Weaver, A. C., and Kim, S. W. (2014). Supplemental nucleotides high in inosine 5′-monophosphate to improve the growth and health of nursery pigs1. *Journal of Animal Science*, *92*(2), 645–651. https://doi.org/10.2527/jas.2013-6564

Weedman, S. M., Rostagno, M. H., Patterson, J. A., Yoon, I., Fitzner, G., and Eicher, S. D. (2011). Yeast culture supplement during nursing and transport affects immunity and intestinal microbial ecology of weanling pigs1,2. *Journal of Animal Science*, *89*(6), 1908–1921. https://doi.org/10.2527/jas.2009-2539

Wei, X., Tsai, T., Knapp, J., Bottoms, K., Deng, F., Story, R., Maxwell, C., and Zhao, J. (2020). ZnO Modulates Swine Gut Microbiota and Improves Growth Performance of Nursery Pigs When Combined with Peptide Cocktail. *Microorganisms*, *8*(2), 146. https://doi.org/10.3390/microorganisms8020146

Weimer, P. J. (1996). Why Don't Ruminal Bacteria Digest Cellulose Faster? *Journal of Dairy Science*, *79*(8), 1496–1502. https://doi.org/10.3168/jds.S0022-0302(96)76509-8

Weitkunat, K., Schumann, S., Nickel, D., Hornemann, S., Petzke, K. J., Schulze, M. B., Pfeiffer, A. F., and Klaus, S. (2017). Odd-chain fatty acids as a biomarker for dietary fiber intake: a novel pathway for endogenous production from propionate ,. *The American Journal of Clinical Nutrition*, *105*(6), 1544–1551. https://doi.org/10.3945/ajcn.117.152702

Wells, J. M., Brummer, R. J., Derrien, M., MacDonald, T. T., Troost, F., Cani, P. D., Theodorou, V., Dekker, J., Méheust, A., de Vos, W. M., Mercenier, A., Nauta, A., and Garcia-Rodenas, C. L. (2017). Homeostasis of the gut barrier and potential biomarkers. *American Journal of Physiology-Gastrointestinal and Liver Physiology*, *312*(3), G171–G193. https://doi.org/10.1152/ajpgi.00048.2015

Wickham, M.J.S., Faulks, R.M., Mann, J., Mandalari, G., 2012. The design, operation, and application of a dynamic gastric model. Dissolution Technol. 19 (3), 15–22. https://doi.org/10.14227/DT190312P15

Wijtten, P. J. A., Meulen, J. van der, and Verstegen, M. W. A. (2011). Intestinal barrier function and absorption in pigs after weaning: a review. *British Journal of Nutrition*, *105*(7), 967–981. https://doi.org/10.1017/S0007114510005660

Winter, S. E., and Bäumler, A. J. (2014). Dysbiosis in the inflamed intestine. *Gut Microbes*, *5*(1), 71–73. https://doi.org/10.4161/gmic.27129

Winter, S. E., Winter, M. G., Xavier, M. N., Thiennimitr, P., Poon, V., Keestra, A. M., Laughlin, R. C., Gomez, G., Wu, J., Lawhon, S. D., Popova, I. E., Parikh, S. J., Adams, L. G., Tsolis, R. M., Stewart, V. J., and Bäumler, A. J. (2013a). Host-Derived Nitrate Boosts Growth of *E. coli* in the Inflamed Gut. *Science*, *339*(6120), 708–711. https://doi.org/10.1126/science.1232467

Winter, S. E., Winter, M. G., Xavier, M. N., Thiennimitr, P., Poon, V., Keestra, A. M., Laughlin, R. C., Gomez, G., Wu, J., Lawhon, S. D., Popova, I. E., Parikh, S. J., Adams, L. G., Tsolis, R. M., Stewart, V. J., and Bäumler, A. J. (2013b). Host-Derived Nitrate Boosts Growth of *E. coli* in the Inflamed Gut. *Science*, *339*(6120), 708–711. https://doi.org/10.1126/science.1232467

Wong, J., Piceno, Y. M., DeSantis, T. Z., Pahl, M., Andersen, G. L., and Vaziri, N. D. (2014). Expansion of Urease- and Uricase-Containing, Indole- and p-Cresol-Forming and Contraction of Short-Chain Fatty Acid-Producing Intestinal Microbiota in ESRD. *American Journal of Nephrology*, *39*(3), 230–237. https://doi.org/10.1159/000360010

Wong, W. M., and Wright, N. A. (1999). Cell proliferation in gastrointestinal mucosa. *Journal of Clinical Pathology*, *52*(5), 321–333. https://doi.org/10.1136/jcp.52.5.321

Wren, A. M., and Bloom, S. R. (2007). Gut Hormones and Appetite Control. *Gastroenterology*, *132*(6), 2116–2130. https://doi.org/10.1053/j.gastro.2007.03.048

Wu, F., Harper, B. J., and Harper, S. L. (2019). Comparative dissolution, uptake, and toxicity of zinc oxide particles in individual aquatic species and mixed populations. *Environmental Toxicology and Chemistry*, *38*(3), 591–602. https://doi.org/10.1002/etc.4349

Wu, Guoyao., Meier, S. A., and Knabe, D. A. (1996). Dietary Glutamine Supplementation Prevents Jejunal Atrophy in Weaned Pigs. *The Journal of Nutrition*, *126*(10), 2578–2584. https://doi.org/10.1093/jn/126.10.2578

Wu, H., Van Der Pol, W. J., Dubois, L. G., Morrow, C. D., and Tollefsbol, T. O. (2023). Dietary Supplementation of Inulin Contributes to the Prevention of Estrogen Receptor-Negative Mammary Cancer by Alteration of Gut Microbial Communities and Epigenetic Regulations. *International Journal of Molecular Sciences*, *24*(10), 9015. https://doi.org/10.3390/ijms24109015

Wu, W., Zhang, L., Xia, B., Tang, S., Liu, L., Xie, J., and Zhang, H. (2020). Bioregional Alterations in Gut Microbiome Contribute to the Plasma Metabolomic Changes in Pigs Fed with Inulin. *Microorganisms*, *8*(1), 111. https://doi.org/10.3390/microorganisms8010111

Wu, Y., Zhang, X., Han, D., Ye, H., Tao, S., Pi, Y., Zhao, J., Chen, L., and Wang, J. (2020). Short Administration of Combined Prebiotics Improved Microbial Colonization, Gut Barrier, and Growth Performance of Neonatal Piglets. *ACS Omega*, *5*(32), 20506–20516. https://doi.org/10.1021/acsomega.0c02667

Xiao, K., Song, Z.-H., Jiao, L.-F., Ke, Y.-L., and Hu, C.-H. (2014). Developmental Changes of TGF-β1 and Smads Signalling Pathway in Intestinal Adaption of Weaned Pigs. *PLoS ONE*, *9*(8), e104589. https://doi.org/10.1371/journal.pone.0104589

Xing, J. J., van Heugten, E., Li, D. F., Touchette, K. J., Coalson, J. A., Odgaard, R. L., and Odle, J. (2004). Effects of emulsification, fat encapsulation, and pelleting on weanling pig performance and nutrient digestibility1. *Journal of Animal Science*, *82*(9), 2601–2609. https://doi.org/10.2527/2004.8292601x

Xing, Y., Li, K., Xu, Y., Wu, Y., Shi, L., Guo, S., Yan, S., Jin, X., and Shi, B. (2020). Effects of galacto-oligosaccharide on growth performance, feacal microbiota, immune response and antioxidant capability in weaned piglets. *Journal of Applied Animal Research*, *48*(1), 63–69. https://doi.org/10.1080/09712119.2020.1732394

Xiong, X., Tan, B., Song, M., Ji, P., Kim, K., Yin, Y., and Liu, Y. (2019a). Nutritional Intervention for the Intestinal Development and Health of Weaned Pigs. *Frontiers in Veterinary Science*, *6*. https://doi.org/10.3389/fvets.2019.00046

Xiong, X., Tan, B., Song, M., Ji, P., Kim, K., Yin, Y., and Liu, Y. (2019b). Nutritional Intervention for the Intestinal Development and Health of Weaned Pigs. *Frontiers in Veterinary Science*, *6*. https://doi.org/10.3389/fvets.2019.00046

Xu, C., Chen, X., Ji, C., Ma, Q., and Hao, K. (2005). Study of the Application of Fructooligosaccharides in Piglets. *Asian-Australasian Journal of Animal Sciences*, *18*(7), 1011–1016. https://doi.org/10.5713/ajas.2005.1011

Xu, C.-L. (2014). Protective effect of glutamine on intestinal injury and bacterial community in rats exposed to hypobaric hypoxia environment. *World Journal of Gastroenterology*, *20*(16), 4662. https://doi.org/10.3748/wjg.v20.i16.4662

Xu, X., Hua, H., Wang, L., He, P., Zhang, L., Qin, Q., Yu, C., Wang, X., Zhang, G., and Liu, Y. (2020). Holly polyphenols alleviate intestinal inflammation and alter microbiota composition in lipopolysaccharide-challenged pigs. *British Journal of Nutrition*, *123*(8), 881–891. https://doi.org/10.1017/S0007114520000082

Yan, S., Long, L., Zong, E., Huang, P., Li, J., Li, Y., Ding, X., Xiong, X., Yin, Y., and Yang, H. (2018). Dietary sulfur amino acids affect jejunal cell proliferation and functions by affecting antioxidant capacity, Wnt/β-catenin, and the mechanistic target of rapamycin signalling pathways in weaning piglets1. *Journal of Animal Science*, *96*(12), 5124–5133. https://doi.org/10.1093/jas/sky349

Yang, C., Zhu, X., Liu, N., Chen, Y., Gan, H., Troy, F. A., and Wang, B. (2014). Lactoferrin up-regulates intestinal gene expression of brain-derived neurotrophic factors BDNF, UCHL1 and alkaline phosphatase activity to alleviate early weaning diarrhoea in postnatal piglets. *The Journal of Nutritional Biochemistry*, *25*(8), 834–842. https://doi.org/10.1016/j.jnutbio.2014.03.015

Yang, Q., Huang, X., Wang, P., Yan, Z., Sun, W., Zhao, S., and Gun, S. (2019). Longitudinal development of the gut microbiota in healthy and diarrheic piglets induced by age-related dietary changes. *MicrobiologyOpen*, *8*(12). https://doi.org/10.1002/mbo3.923

Yang, Q., Huang, X., Zhao, S., Sun, W., Yan, Z., Wang, P., Li, S., Huang, W., Zhang, S., Liu, L., and Gun, S. (2017). Structure and Function of the Fecal Microbiota in Diarrheic Neonatal Piglets. *Frontiers in Microbiology*, *8*. https://doi.org/10.3389/fmicb.2017.00502

Yang, Y., Jiang, X., Cai, X., Zhang, L., Li, W., Che, L., Fang, Z., Feng, B., Lin, Y., Xu, S., Li, J., Zhao, X., Wu, D., and Zhuo, Y. (2022). Deprivation of Dietary Fiber Enhances Susceptibility of Piglets to Lung Immune Stress. *Frontiers in Nutrition*, *9*. https://doi.org/10.3389/fnut.2022.827509

Yang, Z., Su, H., Lv, Y., Tao, H., Jiang, Y., Ni, Z., Peng, L., and Chen, X. (2023). Inulin intervention attenuates hepatic steatosis in rats via modulating gut microbiota and maintaining intestinal barrier function. *Food Research International*, *163*, 112309. https://doi.org/10.1016/j.foodres.2022.112309

Yi, J., Zhong, F., Zhang, Y., Yokoyama, W., and Zhao, L. (2015). Effects of Lipids on *in vitro* Release and Cellular Uptake of β-Carotene in Nanoemulsion-Based Delivery Systems. *Journal of Agricultural and Food Chemistry*, *63*(50), 10831–10837. https://doi.org/10.1021/acs.jafc.5b04789

Yin, Y. (2016). Differential proteome analysis along jejunal crypt-villus axis in piglets. *Frontiers in Bioscience*, *21*(2), 4392. https://doi.org/10.2741/4392

Yoshimura, T. (2015). Discovery of IL8/CXCL8 (The Story from Frederick). *Frontiers in Immunology*, *6*. https://doi.org/10.3389/fimmu.2015.00278

Yuan, D., Hussain, T., Tan, B., Liu, Y., Ji, P., and Yin, Y. (2017). The Evaluation of Antioxidant and Anti-Inflammatory Effects of *Eucommia ulmoides* Flavones Using Diquat-Challenged Piglet Models. *Oxidative Medicine and Cellular Longevity*, *2017*(1). https://doi.org/10.1155/2017/8140962

Yuan, L., Chang, J., Yin, Q., Lu, M., Di, Y., Wang, P., Wang, Z., Wang, E., and Lu, F. (2017). Fermented soybean meal improves the growth performance, nutrient digestibility, and microbial flora in piglets. *Animal Nutrition*, *3*(1), 19–24. https://doi.org/10.1016/j.aninu.2016.11.003

Zakrzewski, S. S., Richter, J. F., Krug, S. M., Jebautzke, B., Lee, I.-F. M., Rieger, J., Sachtleben, M., Bondzio, A., Schulzke, J. D., Fromm, M., and Günzel, D. (2013). Improved Cell Line IPEC-J2, Characterized as a Model for Porcine Jejunal Epithelium. *PLoS ONE*, *8*(11), e79643. https://doi.org/10.1371/journal.pone.0079643

Zeng, M. Y., Inohara, N., and Nuñez, G. (2017). Mechanisms of inflammation-driven bacterial dysbiosis in the gut. *Mucosal Immunology*, *10*(1), 18–26. https://doi.org/10.1038/mi.2016.75

Zenhom, M., Hyder, A., de Vrese, M., Heller, K. J., Roeder, T., and Schrezenmeir, J. (2011). Prebiotic Oligosaccharides Reduce Proinflammatory Cytokines in Intestinal Caco-2 Cells via Activation of PPARγ and Peptidoglycan Recognition Protein 31–3. *The Journal of Nutrition*, *141*(5), 971–977. https://doi.org/10.3945/jn.110.136176

Zhang, W., Zhu, Y.-H., Zhou, D., Wu, Q., Song, D., Dicksved, J., and Wang, J.-F. (2017). Oral Administration of a Select Mixture of Bacillus Probiotics Affects the Gut Microbiota and Goblet Cell Function following Escherichia coli Challenge in Newly Weaned Pigs. *Applied and Environmental Microbiology*, *83*(3). https://doi.org/10.1128/AEM.02747-16

Zhao, P. Y., Li, H. L., Hossain, M. M., and Kim, I. H. (2015). Effect of emulsifier (lysophospholipids) on growth performance, nutrient digestibility and blood profile in weanling pigs. *Animal Feed Science and Technology*, *207*, 190–195. https://doi.org/10.1016/j.anifeedsci.2015.06.007

Zhao, W., Wang, Y., Liu, S., Huang, J., Zhai, Z., He, C., Ding, J., Wang, J., Wang, H., Fan, W., Zhao, J., and Meng, H. (2015). The Dynamic Distribution of Porcine Microbiota across Different Ages and Gastrointestinal Tract Segments. *PLOS ONE*, *10*(2), e0117441. https://doi.org/10.1371/journal.pone.0117441

Zheng, L., Duarte, M. E., Sevarolli Loftus, A., and Kim, S. W. (2021a). Intestinal Health of Pigs Upon Weaning: Challenges and Nutritional Intervention. *Frontiers in Veterinary Science*, *8*. https://doi.org/10.3389/fvets.2021.628258

Zheng, L., Duarte, M. E., Sevarolli Loftus, A., and Kim, S. W. (2021b). Intestinal Health of Pigs Upon Weaning: Challenges and Nutritional Intervention. *Frontiers in Veterinary Science*, *8*. https://doi.org/10.3389/fvets.2021.628258

Zhong, X., Zhang, Z., Wang, S., Cao, L., Zhou, L., Sun, A., Zhong, Z., and Nabben, M. (2019). Microbial-Driven Butyrate Regulates Jejunal Homeostasis in Piglets During the Weaning Stage. *Frontiers in Microbiology*, *9*. https://doi.org/10.3389/fmicb.2018.03335

Zhou, L., Zhang, M., Wang, Y., Dorfman, R. G., Liu, H., Yu, T., Chen, X., Tang, D., Xu, L., Yin, Y., Pan, Y., Zhou, Q., Zhou, Y., and Yu, C. (2018). Faecalibacterium prausnitzii Produces Butyrate to Maintain Th17/Treg Balance and to Ameliorate Colourectal Colitis by Inhibiting Histone Deacetylase 1. *Inflammatory Bowel Diseases*, *24*(9), 1926–1940. https://doi.org/10.1093/ibd/izy182

Zhu, G., Hu, J., and Xi, R. (2021). The cellular niche for intestinal stem cells: a team effort. *Cell Regeneration*, *10*(1), 1. https://doi.org/10.1186/s13619-020-00061-5

Zhu, L. H., Xu, J. X., Zhu, S. W., Cai, X., Yang, S. F., Chen, X. L., and Guo, Q. (2014). Gene expression profiling analysis reveals weaning-induced cell cycle arrest and apoptosis in the small intestine of pigs1. *Journal of Animal Science*, *92*(3), 996–1006. https://doi.org/10.2527/jas.2013-7551

Zihni, C., Mills, C., Matter, K., and Balda, M. S. (2016). Tight junctions: from simple barriers to multifunctional molecular gates. *Nature Reviews Molecular Cell Biology*, *17*(9), 564–580. https://doi.org/10.1038/nrm.2016.80

Zimmerman, M. A., Singh, N., Martin, P. M., Thangaraju, M., Ganapathy, V., Waller, J. L., Shi, H., Robertson, K. D., Munn, D. H., and Liu, K. (2012). Butyrate suppresses colonic inflammation through HDAC1-dependent Fas upregulation and Fas-mediated apoptosis of T cells. *American Journal of Physiology-Gastrointestinal and Liver Physiology*, *302*(12), G1405–G1415. https://doi.org/10.1152/ajpgi.00543.2011

Zong, X., Luo, S., Liu, S., Deehan, E. C., Wang, Y., and Jin, M. (2024). Nondigestible carbohydrates and gut microbiota: A dynamic duo in host defence. *Animal Nutriomics*, *1*, e7. https://doi.org/10.1017/anr.2024.8

Zuo, J., Ling, B., Long, L., Li, T., Lahaye, L., Yang, C., and Feng, D. (2015). Effect of dietary supplementation with protease on growth performance, nutrient digestibility, intestinal morphology, digestive enzymes and gene expression of weaned piglets. *Animal Nutrition*, *1*(4), 276–282. https://doi.org/10.1016/j.aninu.2015.10.003

7

Publication and Conferences

Flash Oral Presentation

Tushar Kulkarni[a,b], Pawel Siegien[a], Luke Comer[c], Ester Arévalo Sureda[c], José Wavreille[d], Benoit Cudennec[b], Anca Lucau[b], Nadia Everaert[c], Rozenn Ravallec[b], Martine Schroyen[a]. 2024. A comparative study of effects of inulin and chicory on gut health in piglets during the weaning period. 4th International Conference on Food Bioactives and Health, September 18-21. Prague.

Oral presentation (Accepted)

Tushar Kulkarni[a,b], Pawel Siegien[a], Benoit Cudennec[b], Sandy Theysgeur[b], Camille Dugardin[b], Luke Comer[c], Anca Lucau[b,d], Nadia Everaert[c], Martine Schroyen[a,b*], Rozenn Ravallec[b*]. 2025. *In vitro* evaluation of chicory-induced modulation of intestinal health in weaning piglets: Approach combining *in vitro* digestion, dialysis, and fermentation with a triple cell culture model. 16th International Symposium on Digestive Physiology of Pigs on May 20th-24th Lake Geneva, WI , USA.

Poster Presentation

Tushar Kulkarni[a,b], Pawel Siegien[a], Pauline Lemal[a], Ester Arévalo Sureda[c], Jose Wavreille[d], Benoit Cudennec[b], Anca Lucau[b], Nadia Everaert[c], Rozenn Ravallec[b], Martine Schroyen[a]. 2024. Poster Presentation. ISAG-2023. 39th International Society for Animal Genetics Conference, Cape Town, South Africa

Publications

1. Tushar Kulkarni, Pawel Siegien, Luke Comer, Jimmy Vandel, Gabrielle Chataigne, Aurore Richel, José Wavreille, Benoit Cudennec, Anca Lucau, Nadia Everaert, Rozenn Ravallec, Martine Schroyen. 2024. A comparative study of the effects of crude chicory and inulin on gut health in weaning piglets. Journal of Functional Foods. Volume 123,106578, ISSN 1756-4646, https://doi.org/10.1016/j.jff.2024.106578.

2. Tushar Kulkarni[a,b], Pawel Siegien[a], Jimmy Vandel[e], Luke Comer[c], Benoit Cudennec[b], Sandy Theysgeur[b], Camille Dugardin[b], Aurore Richel[a], Anca Lucau[b,d], Nadia Everaert[c], Martine Schroyen[a,b,*] Rozenn Ravallec[b,*]. 2025. *In vitro* evaluation of effect of crude chicory on colonic health of a weaning piglet: Approach combining digestion, absorption and fermentation with a triple cell culture model (Submitted).

Evaluating inulin and chicory-induced gut health outcomes in weaning piglets via *in vivo* and complex *in vitro* models.

Abstract

The gastrointestinal (GI) tract is essential for nutrient absorption and serves as a barrier against harmful substances. However, weaning often disrupts this balance in piglets, leading to intestinal permeability, dysbiosis, and inflammation. Inulin, a prebiotic extracted from *Cichorium intybus*, promotes gut health but is costly to extract and during extraction bioactive compounds like polyphenols and sesquiterpene lactones are lost. To address these challenges, this study first aimed to compare the effects of purified inulin and crude chicory flour on intestinal permeability, inflammation, and microbiota in weaning piglets **(Chapter 3)**. Additionally, the study sought to develop advanced *in vitro* methods combining digestion, absorption, fermentation, and a triple cell culture model **(Chapter 4 & 5)** to evaluate the effects of these bioactives under physiologically relevant conditions.

Two sequential dose-dependent experiments (E1 and E2) were conducted, each involving 80 castrated male piglets weaned at 21 days of age and allocated to three groups with *ad libitum* feed: control (Ctrl), inulin (INU), and crude chicory flour (CHI). In E1, CHI exhibited a lower average daily calorie intake only at week 3 (W3), whereas in E2, it consistently remained lower than Ctrl and INU throughout the study. In E2, CHI supplementation resulted in an improved villus-to-crypt ratio and reduced diarrhoea incidence compared to Ctrl and INU. Both supplemented groups in E2 demonstrated higher butyrate production and reduced D-xylose permeability at W3 relative to Ctrl. Notably, CHI in E2 showed a greater impact on increasing the abundance of health-promoting genera such as *Catenisphaera* and *Butyricicoccus* while reducing harmful genera like *Erysipelotrichaceae_UCG-002* and *Turicibacter*. At W3, CHI and INU downregulated several inflammatory target genes (*CXCL10*, *IL18*, *TNFα*) and signalling pathway genes (*MyD88*, *NFκB1*) in the ileum. In the colon, both CHI and INU reduced the expression of inflammatory signalling and target genes (*NFκB1*, *DEFβ4A*, *TLR2*, and *IFNα*), highlighting their anti-inflammatory effects. These findings suggest that crude chicory flour, which is approximately three times less expensive than extracted inulin, may serve as a cost-effective alternative supplement to enhance gut health in weaned piglets.

To address ethical and economic concerns of *in vivo* research, an innovative *in vitro* approach was developed using digestion-dialysis-fermentation protocols and a triple cell culture model comprising Caco-2 (epithelial), HT-29-MTX (goblet), and U937 (immune) cells. To create a more comprehensive model, human cell lines were used, due to similarities between human and piglet GI physiology. The experiment had 5 groups: Inulin equated (Inu eq.), Chicory equated (Chi eq.), Feed (F), Feed+2% Chicory (F2C), Feed+2% Inulin (F2I). After digestion and 24-hour (h) dialysis, samples were fermented using a weaned piglet faeces inoculum. Gas volume was measured for 48 h, and fermentation broth (FB) collected at 12 h. Differentiated Caco-2/HT-29-MTX in the apical part were pre-treated with LPS (-ctrl), 6 hr prior to, and during incubation with FB from 12 h timepoint for 24 h. Cytokine levels were analysed in the basolateral media with differentiated U937 (macrophages), gene expression was measured in the apical cells, and permeability was assessed by Lucifer Yellow after 24 h of treatment. Inu eq. produced more gas and short chain fatty acids (SCFA) than Chi eq. while F2C had higher levels of butyrate than F2I. Chi eq. and F2C showed a higher α-diversity than Inu eq. and F2I. Compared to Inu eq., Chi eq. increased the abundance of beneficial microbiota such as *Lactobacillus*,

Bifidobacterium, *Butyricicoccus* & *Ruminococcus.* After 24 h exposure of LPS and fermentation supernatant, Inu eq. and Chi eq. downregulated pro-inflammatory cytokines IL1β, IL8, and TNFα (4-8-fold) as well as *MAPK14*, *MyD88*, and *AKT1* genes. Interestingly, F2C showed a more significant effect than F2I. Chi eq. had a 3-fold increase in *MUC2*, while Inu eq. upregulated *JAMB* expression. F2I had a higher permeability than F2C. In conclusion, cost-effective Chi eq. and F2C showed greater benefits in enhancing gut health.

Additionally, the study highlighted the critical impact of digestion and dialysis on fermentation outcomes. Digested-dialyzed (DD) samples displayed significantly altered fermentation patterns, including increased butyrate production, improved microbial diversity, and reduced substrates favouring opportunistic microbes compared to non-digested samples.

In conclusion, crude chicory flour, enriched with bioactives, demonstrated either similar or superior effects over inulin in improving gut health, offering a cost-effective and sustainable dietary supplement for weaning piglets. The integration of *in vitro* digestion, fermentation, and cell culture techniques provides a robust platform for studying bioactives' effects, bridging the gap between *in vivo* and *in vitro* approaches while addressing ethical and economic challenges in research.

Keywords: Weaning, chicory, inulin, inflammation, microbiota, permeability.

Évaluation des effets de l'Inuline et de la Chicorée sur la santé intestinale de porcelets en sevrage par l'utilisation de modèles *in vivo* et *in vitro*

RÉSUMÉ

Le tractus gastro-intestinal (GI) est essentiel pour l'absorption des nutriments et sert de barrière contre les substances nocives. Cependant, le sevrage perturbe souvent cet équilibre chez les porcelets, entraînant une perméabilité intestinale, une dysbiose et une inflammation. L'inuline, un prébiotique extrait de *Cichorium intybus*, favourise la santé intestinale, mais sa production est coûteuse et l'extraction entraîne la perte de composés bioactifs tels que les polyphénols et les lactones sesquiterpéniques. Pour relever ces défis, cette étude visait tout d'abord à comparer les effets de l'inuline purifiée et de la farine de chicorée brute sur la perméabilité intestinale, l'inflammation et le microbiote chez des porcelets en cours de sevrage **(Chapter 3)**. En outre, l'étude a cherché à développer des méthodes *in vitro* avancées combinant la digestion, l'absorption, la fermentation et un modèle de culture cellulaire triple **(Chapter 4 & 5)** afin d'évaluer les effets de ces bioactifs dans des conditions physiologiques pertinentes.

Deux expériences séquentielles dose-dépendantes (E1 et E2) ont été menées, chacune impliquant 80 porcelets mâles castrés sevrés à l'âge de 21 jours et répartis en trois groupes avec une alimentation *ad libitum* : contrôle (Ctrl), inuline (INU) et farine de chicorée brute (CHI). Dans le groupe E1, l'apport calorique quotidien moyen de la CHI n'a diminué qu'à la semaine 3 (W3), alors que dans le groupe E2, il est resté inférieur à celui du groupe Ctrl et de l'INU pendant toute la durée de l'étude. Dans l'étude E2, la supplémentation en CHI a permis d'améliorer le rapport villosités/cryptes et de réduire l'incidence de la diarrhée par rapport au Ctrl et à l'INU. Les deux groupes supplémentés en E2 ont montré une production plus élevée de butyrate et une réduction de la perméabilité au D-xylose à W3 par rapport au Ctrl. Notamment, CHI dans E2 a montré un impact plus important sur l'augmentation de l'abondance des genres favourables à la santé tels que *Catenisphaera* et *Butyricicoccus* tout en réduisant les genres nuisibles tels que *Erysipelotrichaceae_UCG-002* et *Turicibacter*. A W3, CHI et INU ont régulé à la baisse plusieurs gènes cibles inflammatoires (CXCL10, IL18, TNFα) et des gènes de signalisation (*MyD88, NFκB1*) dans l'iléon. Ces résultats suggèrent que la farine de chicorée brute peut servir de complément alternatif rentable pour améliorer la santé intestinale des porcelets sevrés.

Pour répondre aux préoccupations éthiques et économiques de la recherche *in vivo*, une approche *in vitro* innovante a été développée en utilisant des protocoles de digestion-dialyse-fermentation et un modèle de culture cellulaire triple comprenant des cellules Caco-2 (épithéliales), HT-29-MTX (gobelet) et U937 (immunitaires). Pour créer un modèle plus complet, des lignées cellulaires humaines ont été utilisées, en raison des similitudes entre la physiologie gastro-intestinale de l'homme et celle du porc. L'expérience comprenait 5 groupes Inulin equated (Inu eq.), Chicory equated (Chi eq.), Feed (F), Feed+2% Chicory (F2C), Feed+2% Inulin (F2I). Après digestion et dialyse de 24 h, les échantillons ont été fermentés en utilisant un inoculum de fèces de porcelets sevrés. Les Caco2/HT-29-MTX différenciés dans la partie apicale ont été prétraités avec du LPS (-ctrl), 6 heures avant, et pendant l'incubation avec 12 heures de FB pendant 24 heures. Inu eq. a induit la production de plus de gaz et d'acides gras à chaîne courte que Chi eq. mais F2C a permis d'obtenir des niveaux plus élevés de

butyrate qu'avec F2I. Les fermentations obtenues avec Chi eq. et F2C ont montré une plus grande diversité α que Inu eq. et F2I. Par rapport à Inu eq., Chi eq. a augmenté l'abondance d'un microbiote bénéfique tel que *Lactobacillus*, *Bifidobacterium*, *Butyricicoccus* et *Ruminococcus*. Après une exposition de 24 heures au LPS et au surnageant de fermentation, Inu eq. et Chi eq. ont régulé à la baisse les cytokines pro-inflammatoires IL1β, IL8, TNFα et les gènes *MAPK14, MyD88, AKT1*. Il est intéressant de noter que F2C a montré un effet plus significatif que F2I. Chi eq. a multiplié par 3 l'expression de MUC2, tandis que Inu eq. a augmenté l'expression de JAMB. La perméabilité cellulaire dans la condition F2I était plus élevée que celle avec F2C. En conclusion, Chi eq. et F2C se sont révélés plus bénéfiques pour la santé intestinale. En outre, l'étude a mis en évidence l'impact de la digestion et de la dialyse sur les résultats de la fermentation. Les échantillons digérés-dialysés (DD) ont présenté des schémas de fermentation significativement modifiés, notamment une production accrue de butyrate, une diversité microbienne améliorée et une réduction des substrats favourisant les microbes opportunistes par rapport aux échantillons non digérés.

En conclusion, la farine de chicorée brute, enrichie en bioactifs, a démontré une efficacité supérieure à celle de l'inuline dans l'amélioration de la santé intestinale, offrant un complément alimentaire rentable et durable pour les porcelets en cours de sevrage. L'intégration des techniques de digestion *in vitro*, de fermentation et de culture cellulaire fournit une plateforme solide pour étudier les effets des bioactifs, comblant ainsi le fossé entre les approches *in vivo* et *in vitro* tout en répondant aux défis éthiques et économiques de la recherche.

Mots-clés: Sevrage, chicorée, inuline, inflammation, microbiote, perméabilité